UNDERSTANDING AND ENGINEERING PHOTORESPONSES IN *ARABIDOPSIS THALIANA*

By

Martin W. Battle

Thesis submitted for the degree of Doctor of Philosophy

School of Biological Sciences

University of Essex

NOVEMBER, 2018

Abstract

Light is a remarkably versatile and precise tool, the prevalent nature of which has caused it to become a common stimulus in biological processes. Along with metabolic signals derived from photosynthesis, plants have evolved a suite of five known families of photoreceptor proteins which make up photoperception array of the organism. These photoreceptors are the red and far-red light sensitive phytochromes, the blue light sensitive cryptochromes, phototropins and zeitlupe family and the UV-B receptor UVR8.

The role of phototropins in the maintenance of circadian rhythms in the chloroplast has been recently identified, suggesting the potential for further involvement of phototropins in the circadian system of *Arabidopsis*. This study shows that in mutant plants lacking functional phototropins, the lack of phototropin function has little effect upon circadian rhythms of luciferase bioluminescence but is sufficient to induce loss of robustness in rhythms of chlorophyll fluorescence, indicating that phototropins are most likely indirectly involved in the regulation of circadian rhythms via the chloroplast and not directly involved in the regulation of the nuclear circadian clock.

No known plant photoreceptors have a peak of absorbance within the green range of the photosynthetically active spectrum. While plants are capable of developing to maturity in the absence of green light, this study examines some of the subtle ways in which plants respond to green light. Via observation of hypocotyl elongation in seedlings lacking specific photoreceptor functions we show that phytochromes and cryptochromes are required to induce de-etiolation in seedlings grown under green light. Additionally, luciferase bioluminescence imaging of mutants lacking cryptochrome function is used to show that cryptochromes are required to maintain circadian rhythms in *Arabidopsis* under certain green light spectra, although the presence of blue

wavelengths within the spectra of many green lights are sufficient to mask this response.

Finally, the subtlety of green light responses in plants has provided a non-invasive input for an optogenetic construct which allows for light controlled manipulation of gene expression *in planta*. In this study, we present the design and engineering of a green light sensitive optogenetic system for use within plants based upon a cyanobacterial photoreceptor. This prototype system is functional in transiently transformed *Nicotiana benthamiana* leaves but displays significant leakiness and requires further development before its uses can be developed upon. Additionally further development is required in order to better engineer the system for the production of stable transgenic lines in *Arabidopsis*.

The studies presented here seek to define and explore the roles of phototropins and green light within the circadian system and to design and engineer a green light sensitive optogenetic system for use in plants.

Acknowledgements

I would like to thank the University of Essex School of Biological Sciences and the Eastern Academic Research Consortium for providing funding for this research. Special thanks to Dr. Matthew A. Jones for facilitating this work, and for providing consistent training, support and input which have made my scientific education a pleasure and a privilege. Thanks also to Prof Philip M. Mullineaux, Prof Christine A. Raines, Prof Tracy Lawson, Dr Ulrike Bechtold, Dr Phillip A. Davey and Dr Lauren R. Headland for their valuable input throughout the course of this research. Thank you to all of the members of the Jones Lab, especially to Dr Suzanne Litthauer for all of your advice and support. Thank you to all of the members of Lab 5.36 and 6.23 at the University of Essex for your help and kindness, special thanks to Dr Patricia E. Lopez-Calcagno for your support and patience assisting with Golden Gate cloning and to Dr Marino Exposito-Rodriguez for all of your help working with *Nicotiana benthamiana*.

Final thanks to my friends and family outside of the lab. Special thanks to Mum, Dad and Nina for supporting me for these four years and always being willing to listen to my rambling, even if I have never been able to properly explain what I do at work. The culmination of this work is dedicated to my Nan, Ida Young, who was always equal parts proud and puzzled by my choice to stay in education for so long but would have only been proud to see its completion.

Publications

Components of this thesis have been published in the following journal articles:

Litthauer, S, Battle, MW and Jones, MA (2016) Phototropins do not alter accumulation of evening-phased circadian transcripts under blue light, *Plant Signalling and Behavior* **11**: e1126029

Litthauer, S, Battle, MW, Lawson, T and Jones, MA (2015) Phototropins maintain robust circadian oscillation of PSII operating efficiency under blue light, *The Plant Journal* **83**: 1034-1045

Contents

Chapter 2: Materials and Methods

Chapter 5: Engineering green-light specific photoresponses in plants

Chapter 6: General Discussion

List of Figures and Tables

Abbreviations

The following abbreviations are used during this thesis	
µE	µmol m-2 s-1
35S	Cauliflower mosaic virus 35S
ACT	ACTIN
ATP	Adenosine triphosphate
BRASS	Biological Rhythms Analysis Software System
BSA	Bovine serum albumin
CAM	Crassulacean acid metabolism
cB	Constant blue LED light
CCA1	CIRCADIAN CLOCK ASSOCIATED 1
CCD	Cold coupled device
CCR2	COLD CIRCADIAN REGULATED 2
cDNA	Complementary DNA
cfG	Constant green LED light filtered through a #312 canary filter
cG	Constant green LED light
Col	Columbia ecotype *Arabidopsis thaliana*
COP1	CONSTITUTIVELY PHOTOMORPHOGENIC 1
cpCK2a	HIGH HOMOLOGY TO CYTOSOLIC CASEIN KINASE 2 SUBUNIT A
cR	Constant red LED light
Cry	Cryptochrome
cry1cry2	*cry1-304 cry2-1*
CSK	Chloroplast sensor kinase
CT	Circadian Time

CTAB	Cetyltrimethyl ammonium bromide
DCMU	3-(3,4,-Dichlorophenyl)-1, 1-dimethylurea
DDT	Dichloropdiphenyltrichloroethane
DF	Delayed fluorescence
dH_2O	Distilled water
DMSO	Dimethyl sufoxide
DNA	Deoxyribonucleic acid
dNTPs	Deoxyribonucleotide triphosphates
EDTA	Ethylene diaminetetra-acetic acid
EE	Evening element
ELF	EARLY FLOWERING
FAD	Flavin adenine dinucleotide
Farn	*phot1phot2* mutant expressing farnesylated phot1-GFP fusion protein
FFT-NLLS	Fast Fourier Transform Non-Linear Least Squares
fGreen	Green LED light filtered through a #312 canary filter
FKF1	FLAVIN-BINDING, KELCH REPEAT, F-BOX 1
FMN	Flavin mononucleotide
FMV	FIGWORT MOSAIC VIRUS
F_q'/F_m'	PSII operating efficiency
FT	FLOWERING LOCUS T
gDNA	Genomic DNA
GFP	Green fluorescent protein
GI	GIGANTEA
GLA2	Second generation of GLASSys constructs

GLASSys	Green Light Activated Synthetic System
HY5	ELONGATED HYPOCOTYL 5
HYH	HY5 HOMOLOGUE
IRGA	Infra-red gas analyser
L0	Golden Gate Level 0 module
L1	Golden Gate Level 1 cassette
L2	Golden Gate Level 2 construct
LB	Luria-Bertani medium
LED	Light emitting diode
Ler	Landsberg erecta ecotype *Arabidopsis thaliana*
LHY	LATE ELONGATED HYPOCOTYL
LKP2	LOV KELCH PROTEIN 2
LNK	NIGHT LIGHT-INDUCIBLE AND CLOCK REGULATED GENE
LOV	Light oxygen voltage
LUC	LUCIFERASE
LUX	LUX ARRHYTHMO
MAS	MANNOPINE SYNTHASE
MCC	Microcentrifuge
MES	2-(N-morpholino)ethanesulfonic acid
mRNA	Messenger RNA
MS	Murashige and Skoog basal mineral salts
NLS	Nuclear localisation signal
nm	Nanometers
NTRC	NADPH-THIOREDOXIN REDUCTASE C

OD	Optical desnsity
p1p2	*phot1-5 phot2-1*
PAR	Photosynthetically active radiation
PCB	Phycocyanobilin
PCR	Polymerase chain reaction
PEP	Plastid encoded RNA polymerase
PF	Prompt fluorescence
P_{fr}	Far red light absorbing state of phytochrome
Phot	Phototropin
Phy	Phytochrome
PIF	Phytochrome interacting factor
PMSF	Phenylamethane sulfonyl fluoride
PΦB	Phytochromobilin tetrapyrrole chromophore
P_r	Red light absorbing state of phytochrome
PRR	PSEUDO-RESPONSE REGULATOR
Prx	Peroxiredoxin
PSI	Photosystem I
PSII	Photosystem II
PTK	Plastid transcription kinase
PVB	Phycoviolobilin
Q_A	Excited plastiquinone
Qo	Oxidised quinone
qRT-PCR	Real time quantitative reverse transcription PCR
RAE	Relative amplitude error

RNA	Ribonucleic acid
ROS	Reactive oxygen species
RVE	REVEILLE
SRX	SULFIREDOXIN
Taq	*Thermus aquaticus* DNA Polymerase I
TOC	TIMING OF CAB1
UBI	Ubiquitin
UV	Ultraviolet
UVR8	ULTRAVIOLET RESISTANCE LOCUS 8
v/v	Volume/volume
w/v	Weight/volume
Ws	Wassilewskija ecotype *Arabidopsis thaliana*
Y2H	Yeast two-hybrid
ZT	Zeitgeber time
ZTL	ZEITLUPE

Chapter 1- Native and engineered photoperception in plants

1.1. Photoperception and the clock in *Arabidopsis thaliana*

Light influences the behaviour and development of most living organism. To plants, light is not only an entraining signal but a ubiquitous source of energy, providing a stimulus that directs development, morphogenesis and physiology (Christie et al., 2015). Plants are exceptionally sensitive and responsive to light, able to detect a broad spectrum of light wavelengths, from UV-B to far-red (around 280-750 nm) (Galvao and Fankhauser, 2015, Wang and Folta, 2013). This range is granted by a suite of photoreceptive proteins and photosynthetic pigments, each of which influences the way in which plants interpret light cues for a wide range of processes, better allowing plants to react to changing light conditions and respond in a way which optimises photosynthetic activity (Galvao and Fankhauser, 2015, Devlin and Kay, 2001). As light is of such great importance to plants, it us unsurprising that the environmental light cycles of day and night are also of particular significance to plants. The circadian clock is an interconnected network of transcriptional feedback loops which allow plants to adapt to, interpret, and predict day-night and seasonal fluctuations (Hsu and Harmer, 2014). The circadian system not only allows plants to adapt and synchronise to the external stimuli provided by dawn and dusk but also allow for cell autonomous timekeeping independent of these stimuli (Hsu and Harmer, 2014). Overall the circadian clock acts to improve growth and fitness of the organism and reduce stress by synchronising individual components within the organism with each other and the environment (Dodd et al., 2005). This chapter will provide an overview of the mechanisms by which

light is interpreted by plants and interacts with the circadian clock as well as introducing methods by which novel forms of photoperception can be engineered.

1.2. Plant responses to light quality

As sessile organisms, plants have had to evolve mechanisms to cope with environmental light conditions. Many of these mechanisms are linked to photoreceptors and as such are specific to the light qualities which are detectable by these individual proteins, although some functions are redundant across many photoreceptors (Galvao and Fankhauser, 2015). The phytochromes recognise the red and far-red portions of the spectrum, whilst blue wavelengths are detected by phototropins, cryptochromes and the ZTL family of photoreceptors and UVR8 provides UV-B detection capabilities (Figure 1.1) (Sullivan and Deng, 2003, Franklin and Whitelam, 2004, Briggs et al., 2001, Liu et al., 2016, Kim et al., 2007, Christie et al., 2012a). Due to the nature of these photoreceptors, studies are often carried out under red or blue light in order to examine the effects of individual photoreceptors or photoreceptor groups (Ohgishi et al., 2004, Sullivan et al., 2016, Ito et al., 2007). Examination of plants with altered functionality in one or more photoreceptors under specific light qualities have allowed us to better understand the role of photoreceptors in plant development (Sullivan and Deng, 2003, Ohgishi et al., 2004). Similarly, due to the lack of a photoreceptor specifically responsive to green light, plant responses to this quality of light are less well understood than the responses to red and blue light (Smith et al., 2017). Furthermore, the model plant species *Arabidopsis thaliana* has been the primary source for much of the research in to plant responses to light qualities and some of the unusual qualities of this species, especially its long-day flowering nature, may have caused some of our understanding of

developmental responses to light quality to differ from what is found in other plant species (Mouradov et al., 2002). It should also be noted that natural light and white light conditions contain far-red, red, green, blue and UV wavelengths and will often trigger responses from more than one photoreceptor at once with the dominant photoreceptor being dependent upon the specific light conditions at the time (Whitelam et al., 1993, Maloof et al., 2001). These redundant functions across multiple photoreceptors are sometimes vital to plant development, such as seedling de-etiolation, the process by which seedlings develop from an immature, etiolated state, with long stems and small cotyledons, to a mature state where cotyledons develop into true leaves, which can be triggered by both red and blue light (Sullivan and Deng, 2003) and sometimes act to fine-tune development to the best conditions available and to outcompete neighbouring plants, such as in many low-light avoidance behaviours which can be triggered by very subtle variations in light conditions (Zhang et al., 2011, Casal, 2013). In this section I will discuss how different qualities of light are perceived in plants and how availability of each light quality influences plant development.

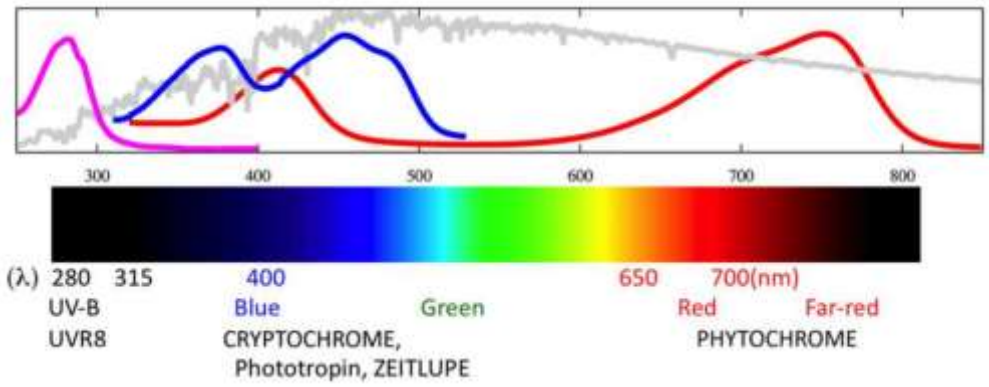

Figure 1.1. Absorption spectra of photoreceptors in *Arabidopsis thaliana*. Absorption spectra of red-light (PHYTOCHROMES; in red), blue-light (CRYPTOCHROMES, phototropins and ZEITLUPE family proteins; in blue) and UV-B (UVR8; in magenta) photoreceptors in *Arabidopsis*. Gray curve indicates approximate spectra of sunlight as measured on the surface of the earth. (Figure adapted from Yang et al., 2015; Figure 1).

1.2.1. Darkness and low-intensity white light

Due to the vital nature of light for plant development, it is not surprising that plants exhibit responses to the absence of light. Skotomorphogenesis is the most universal dark-avoidance response in plants, occurring during early seedling development. In *Arabidopsis,* before the formation of true leaves, seedlings follow etiolated development, with long hypocotyls and unexpanded cotyledons with an apical hook (Josse and Halliday, 2008 Alabadi et al., 2008). This process persists in the absence of light until light exposure, when de-etiolation occurs, allowing the plant to quickly grow in a negative-gravitropic fashion in search of light (Tepperman et al., 2006, Peschke and Kretsch, 2011, Su et al., 2015), allowing seedlings to reach through soil before development into a more optimal pattern for photosynthesis. Etiolation can also persist under very low levels of red, blue or green light (Wang and K, 2014, Lu et al., 2014), allowing for more suitable conditions for further development to be reached before de-etiolation begins. De-etiolation is a major developmental process and has been shown to result from a change of expression in around 30% of genes in the *Arabidopsis* genome (Ma et al., 2001, Tepperman et al., 2006). This has led to much of our understanding of events downstream of photoreceptors in the *Arabidopsis* genome being derived from the examination of de-etiolation of *Arabidopsis* seedlings (Quail, 2002, Folta et al., 2003, Tepperman et al., 2006, Lu et al., 2009a, Nusinow et al., 2011). These tests have shown that while each *Arabidopsis* photoreceptor has a wide range of distinct and overlapping functions and perceives a distinct range of light cues, all photoreceptors interact with and control the expression of a shared fraction of the genome (Ma et al., 2001).

In constant darkness the circadian clock is capable of sustaining rhythms although periodicity will increase over time and approach arrhythmicity after a long enough

period (Millar et al., 1995). As with darkness, low light is a condition which plants largely respond to with avoidance behaviours which can commonly be observed under natural conditions. Low light of all qualities triggers chloroplasts to accumulate at the upper surface of palisade mesophyll cells in order to maximise photosynthesis (Kasahara et al., 2002, Sakai et al., 2001, Briggs and Christie, 2002). Circadian period is also longer under low light, a phenotype which can be counteracted by the introduction of exogenous sucrose (Haydon et al., 2013b), indicating that this response is largely related to photosynthesis and not any one specific photoreceptor. The circadian clock in *Arabidopsis* roots has also been shown to be sensitive to low light intensities and respond differently to light exposure than the shoots (Bordage et al., 2016). Many low-light avoidance responses, including petiole elongation, upward leaf reorientation and leaf area reduction can be observed under low light of all qualities, as well as slightly higher intensities of green light (Zhang and Folta, 2012).

1.2.2. Red and far-red light

Red light is primarily detected by the phytochromes. Phytochromes are primarily red/far-red sensors, and are found in all land plants as well as many prokaryotes and some fungi (Bae and Choi, 2008, Purschwitz, et al. 2006). In plants, phytochromes are bilin binding dimers which convert between two forms, the inactive, red light absorbing P_r form and the active, far-red light absorbing P_{fr} form, in response to light exposure (Rockwell et al., 2006). The inactive P_r form of phytochromes localise to the cytoplasm while the active P_{fr} form of all phytochromes rapidly translocate to the nucleus (Montgomery and Lagarias, 2002, Klose et al., 2015). In *Arabidopsis* there are five phytochrome encoding genes *PHYA-E* each of which expresses a protein with a distinct,

but often partially overlapping function with the others of the family (Franklin and Quail, 2010). Primarily, phytochromes are involved in major developmental transitions during the *Arabidopsis* life cycle including germination, de-etiolation, floral transition and senescence, however they also play a role in low-light avoidance and notably, the circadian clock (Salter, et al. 2003).

Structurally, phytochromes consist of an N-terminal photosensory region binding a phytochromobilin tetrapyrrole chromophore (PϕB) and a C-terminal output region presumed to be involved in relaying photosignals (Costa Galvão and Fankhauser, 2015, Rockwell, 2006). This structure can convert rapidly between a biologically inactive (P_r), red light absorbing, form and a biologically active (P_{fr}) form, capable of absorbing far red light. Upon absorbing light of an appropriate wavelength, phytochromes will rapidly change configuration from one form to the other, however the active P_{fr} form will gradually revert to the inactive P_r form over time by thermal reversion, causing P_r to be the natural state in absence of red light (Galvao and Fankhauser, 2015). Additionally, upon photoconversion to the active Pfr form, phytochromes translocate from the cytoplasm to the nucleus, where they directly interact with a range of transcription factors, predominantly the Phytochrome-Interacting Factors (PIFs), PIF1-PIF8 (Xu et al., 2015). Interactions between phyB and the PIFs leads to the phosphorylation, ubiquitination and subsequent degradation of the PIFs via the 26S proteasome system (Xu et al., 2015).In this way etiolation, which the PIFs promote, is inhibited by photoactivation of the phytochromes, additionally leading to the promotion of photomorphogenesis (Ni et al., 2014, Zhu et al., 2016). Furthermore, negative feedback from the PIFs during this interaction also regulates phyB levels, serving to desensitise

cells to red light and fine-tune phytochrome switching behaviours (Ni et al., 2014, Zhu et al., 2016).

In *Arabidopsis* the dominant phytochrome, phyB, acts as the primary photoreceptor responsible for red light responses (Somers et al., 1998a), phyC, phyD and phyE play largely redundant roles (Franklin et al., 2003, Franklin and Quail, 2010). phyB, phyD and phyE form a discreet group based upon common evolutionary ancestry separate from phyA and phyC, which also share ancestry but seem to have more distinct functions due to the unique nature of phyA (Franklin and Whitelam, 2004).

phyA is responsible for sensing far-red light and mediating early responses to red light, it is abundant in etiolated seedlings and degrades rapidly upon illumination. The light-stable phytochromes, phyB-E, are dominant in light-grown plants and are predominantly involved in responses under sustained red or white light (Clough, 1997, Sharrock and Clack, 2002, Tepperman et al., 2006, Kami et al., 2010). Subsequent exposure to far-red light inhibits phyA degradation thereby inhibiting the progress of de-etiolation at this stage (Casal, 2013). In a *phyAphyB* double mutant, germination can still occur, with phyE mediating this process (Sullivan and Deng, 2003). As a part of the de-etiolation process, phyB plays a major role in the inhibition of hypocotyl elongation under red light, with phyA also contributing to this response and phyD taking a minor role (Aukerman et al., 1997). In a *phyAphyC* loss-of-function mutant, hypocotyl length under red light is significantly greater than that of wild type or the *phyA* or *phyC* single mutants (Franklin et al., 2003). Interestingly, the red light inhibition of hypocotyl elongation in *phyB* mutant seedlings is dependent upon the presence of either phyD or the blue light receptor CRY1 (Hennig et al., 1999). Additionally, *ztl* mutants have been shown to have short hypocotyls under red light but do not affect hypocotyl elongation

under blue light (Somers et al., 2000, Somers et al., 2004). Phytochromes also mediate negative phototropism in roots, aiding in proper alignment of roots and assisting in gravitropism (Robson and Smith, 1996).

In mature *Arabidopsis* plants, deficiency of phyB continues to have a noticeable effect. *phyB* mutants display an elongated growth habit, retarded leaf development, increased apical dominance, reduced number of stomata and early flowering (Robson et al., 1993, Halliday et al., 1994, Devlin et al., 1996, Boccalandro et al., 2009, Casson et al., 2009). These phenotypes resemble low-light avoidance responses (Whitelam, 1997) and suggest that red light perception is required to properly mediate the processes leading to proper development of each of these organs to maturity.

Red light is also involved in circadian control of flowering time, with *phyA* mutants being insensitive to day length with relation to time of flowering onset (Johnson et al., 1994). phyB, phyD and phyE act redundantly to repress flowering in high red and far red conditions (Halliday et al., 1994). *phyC* mutants also present early flowering in Columbia (Col) ecotype *Arabidopsis* when grown under short days (Monte et al., 2003), although this early flowering phenotype was not seen in the Wassilewskija (Ws) ecotype in which *phyC* is absent, suggesting that *phyC* is not wholly responsible for this phenotype (Franklin et al., 2003, Balasubramanian et al., 2006). This light dependant control of flowering time exhibited by phytochromes is largely mediated by CONSTANS, a protein which activates expression of the major activator of floral development, *FLOWERING LOCUS T* (*FT*). Under red light and during the mornings, CONSTANS is degraded by phyB, delaying flowering time. Additionally phyA stabilises CONSTANS under far-red light, promoting flowering (Jang et al., 2008, Wang and Wang, 2015).

1.2.3. Blue light

The majority of Arabidopsis photoreceptor proteins are blue light receptors, with three families of blue light photoreceptors identified; cryptochromes, phototropins and the ZEITLUPE family. As such blue light responses can be divided by which photoreceptor is primarily involved, although many roles are filled redundantly by multiple blue-light photoreceptors (Christie and Briggs, 2001, Galvao and Fankhauser, 2015). In addition to these primary blue light sensors, phyA, which is most commonly known as a far-red responsive photoreceptor, has been shown to be play a role in blue light responses, mediating both hypocotyl elongation and chloroplast gene transcription under blue light (Chun et al., 2001, Sullivan et al., 2016).

1.2.3.1. Cryptochromes

Cryptochromes are photoreceptors found in a wide range of organisms including bacteria, fungi, animals and plants (Cashmore et al., 1999, Chaves et al., 2011, Galvao and Fankhauser, 2015). In *Arabidopsis* the primary cryptochromes, cry1 and cry2, are UV-A/blue photoreceptors with some possible function under green light (Lin et al., 1995, Folta and Maruhnich, 2007, Sellaro et al., 2010, Liu et al., 2016). cry1 and cry2 largely localise to the nucleus (Selby and Sancar, 2006) and have partially overlapping functions in *Arabidopsis*. With cry1 mainly functioning during de-etiolation and cry2 functioning during flowering (Ahmad et al., 1998, Chen et al., 2004, Galvao and Fankhauser, 2015). cry1 and cry2 have been associated with entrainment of the clock, light regulated guard cell development and stomatal opening, magnetoreception, apoptosis, light regulation of root development, phototropism, gravitropism amongst

other minor possible functions (Yu et al., 2010, Oakenfull and Davis, 2017). Approximately 5–25% of the gene expression changes that occur during seedling de-etiolation under blue light can be attributed to the action of cry1 and cry2 in Arabidopsis (Folta and Spalding, 2001, Ma et al., 2001, Ohgishi et al., 2004). The third *Arabidopsis* cryptochrome, CRY3, is a CRY-DASH protein which localises to the mitochondria and chloroplasts (Selby and Sancar, 2006). Arabidopsis CRY3 and other CRY-DASH proteins may act as single-stranded DNA photolyases or dual-activity photoreceptors that have both photolyase and cryptochrome activities (Banerjee et al., 2007, Klar et al., 2007, Kleine et al., 2003). The physiological function of CRY3 is unknown but given its biochemical activity in repairing ssDNA, CRY3 is likely involved in protecting organellar genomes in Arabidopsis against UV damage (Kleine et al., 2003).

Cryptochromes share many structural similarities with their evolutionary ancestors, DNA photolyases, and CRY1 contains a flavin adenine dinucleotide (FAD) binding alpha domain and a dinucleotide binding alpha/beta domain (Brautigam et al., 2004, Chaves et al., 2011). The exact photochemistry of cryptochromes is not fully understood (Conrad et al., 2014), although the basic process is understood to involve blue light irradiation triggering reduction of the FAD chromophore to a 'signalling state' (Engelhard et al., 2014). This reduction of the chromophore triggers conformational changes allowing the cryptochrome to interact with signalling intermediates (Gyula et al., 2003, Liu et al., 2011).

It has been proposed that a grouping of three highly conserved tryptophan residues, termed the Trp-triad, serves as an electron donor in the photoreduction of FAD (Chaves et al., 2011, Liu et al., 2016). The Trp-triad exists in close proximity to the FAD within

the FAD binding pocket of both CRY1 and CRY2 and therefore may act as an electron relay from the cryptochrome to FAD (Chaves et al., 2011, Liu et al., 2016). Replacement of these tryptophan residues with structurally similar but redox-inert amino acids has been shown to be sufficient to abolish photoreduction of both CRY1 and CRY2 in vitro (Zeugner et al., 2005). In vivo however, the Trp-triad has proven controversial with evidence both for (Zeugner et al., 2005) and against (Li et al., 2011, Gao et al., 2015) its requirement for FAD reduction.

Through this pathway cryptochromes interact with upstream transcription factors of many genes including *FLOWERING LOCUS T* (*FT*) which leads to cryptochrome associated promotion of flowering in *Arabidopsis* (Liu et al., 2008, Song et al., 2013).

In early development, cryptochromes are required for blue light stimulated de-etiolation in *Arabidopsis* (Chen et al., 2004), affecting both hypocotyl elongation (Yu et al., 2010) and cotyledon expansion (Wu and Spalding, 2007), with cry1 playing a larger role than cry2 in this process (Lin et al., 1998). CRY1 and CRY2 also interact directly with PIF4 and PIF5, proteins more commonly associated with the phytochromes, in order to promote hypocotyl elongation under low-blue light conditions (Pedmale et al., 2016). Additionally, under high intensities of blue light the CRYs strongly repress expression of PIF4, inducing de-etiolation (Pedmale et al., 2016). Cryptochromes also mediate blue light stimulation of chloroplast development (Chen et al., 2004, Jiao et al., 2007). Interestingly, while cryptochromes are involved in the blue light mediated promotion of flowering, this process only requires the presence of at least two of cry1, cry2 and phyA, with double mutants of any combination of these expressing significantly late time of flowering onset (Mockler et al., 2003, Yu et al., 2010). The cryptochrome-interacting-basic-helix-loop-helix1 (CIB1) protein in *Arabidopsis*

thaliana, interacts with CRY2, resulting in a blue-light induced, CRY2-dependent floral initiation (Liu et al., 2008). Under these conditions CIB1 stimulates *FT* mRNA expression and further induces *FT* expression by binding to E-box elements within the promoter region of the *FT* gene (Liu et al., 2008).

1.2.3.2. Phototropins

Phototropins are found in cyanobacteria and plants (Christie, 2007, Montgomery, 2007). Phot1 and phot2 are the two phototropins found in *Arabidopsis*. Both are blue light receptors with overlapping functions which optimize photosynthetic efficiency and promote growth particularly under weak light conditions (Takemiya et al., 2005). phot1 and phot2 redundantly regulate hypocotyl and root phototropism (Sakai et al., 2001), chloroplast accumulation movement (Kagawa et al., 2001), stomatal opening (Kinoshita et al., 2001), leaf positioning and leaf flattening (Sakamoto and Briggs, 2002, Inoue et al., 2008b) and cotyledon expansion (Christie, 2007). phot1 specific responses have also been identified including the rapid inhibition of hypocotyl growth upon transfer of etiolated seedlings to light (Folta et al., 2003), transcript destabilization (Folta and Kaufman, 2003) and suppression of lateral root growth (Moni et al., 2015). Chloroplast avoidance movement is solely attributed to phot2 (Christie, 2007). While the phototropins may not have a role in the nuclear circadian clock (Litthauer et al., 2015, Litthauer et al., 2016), phototropins have been shown to be required for maintaining robust circadian rhythms in prompt Chlorophyll *a* Fluorescence (PF) in *Arabidopsis* (Litthauer et al., 2015).

Blue light is detected by phototropins via two flavin mononucleotide (FMN) chromophore-binding light oxygen voltage (LOV1 and LOV2) domains (Christie et al., 2002). In *Arabidopsis* phototropins are localised and attached to the intracellular side of the plasma membrane where their primary functions occur, phot1 re-localises primarily to the endoplasmic reticulum and phot2 re-localises to the Golgi apparatus when irradiated with blue light (Kong et al., 2013, Suetsugu and Wada, 2013, Zhang et al., 2013). However, lipid anchoring of phot1 to the plasma membrane has shown that internalisation of phot1 is not required to mediate blue light responses (Preuten et al., 2015). phot1 and phot2 can also localise to the outer membrane of the chloroplast, assisting in their role in regulating chloroplast photorelocation movements (Kong et al., 2013). All phototropins change conformation when photoactivated, activating a kinase domain and allowing phosphorylation of downstream signalling components (Gyula et al., 2003, Inoue et al., 2008a).

Phototropins are named for their involvement in the regulation of phototropism, with blue light regulating almost all phototropism responses in *Arabidopsis* (Sakai et al., 2001). Both phot1 and phot2, play a major role in this with phot1 operating under all light intensities and phot2 operating predominantly under high light conditions (Liscum and Briggs, 1995, Liscum et al., 2014, Christie et al., 1998). Interestingly, while red light is not sufficient to induce phototropism under most conditions, red light exposure 1-2 hours prior to directional blue light treatment has been shown to trigger phyA mediated enhancement of phototropism in *Arabidopsis* seedlings (Parks et al., 1996, Strasser et al., 2010, Goyal et al., 2013). Additionally, reduced hypocotyl curvature observed in *cry1cry2* double mutants indicates that cryptochromes may also be involved in the mediation of phototropism under blue light (Fankhauser and Christie, 2015). Other

functions of the phototropins include blue light regulated stomatal opening (Kinoshita et al., 2001, Briggs and Christie, 2002) and the mediation of chloroplast relocation into the lower region of cells in response to intense blue light (Jarillo et al., 2001b, Briggs and Christie, 2002, Kagawa and Wada, 2002, Kasahara et al., 2002).

1.2.3.3. ZEITLUPE proteins

The ZEITLUPE family of photoreceptors in *Arabidopsis* and many other higher plants contains the UV-A/blue light photoreceptors; ZEITLUPE (ZTL), FLAVIN-BINDING, KELCH REPEAT, F-BOX (FKF1) and LOV KELCH PROTEIN2 (LKP2) (Baudry et al., 2010, Kim et al., 2007, Ito et al., 2012). All ZEITLUPE family photoreceptors contain an FMN-binding LOV domain followed by an F-box and six Kelch repeats with any additional LOV domains associated with other output domains (Ito et al., 2012). Once photoactivated by blue light irradiation ZEITLUPEs remain in a stable signalling form for long periods (Galvao and Fankhauser, 2015, Kim et al., 2007, Kim et al., 2013).

The ZEITLUPE family are known for their interactions with circadian genes, especially GIGANTEA (GI), which binds to active ZEITLUPEs providing stability to both proteins or enhancing activity of binding domains (Baudry, 2010, Chen, et al. 2004, Kim, et al. 2007). ZTL and GI interact to regulate stability of the evening phased circadian clock proteins TOC1 and PRR5, degrading them in the presence of blue light (Baudry et al., 2010, Kim et al., 2007). TOC1 and PRR5 are two of the five PSEUDO-RESPONSE REGULATOR (PRR) circadian proteins found in *Arabidopsis thaliana* (Gendron et al., 2012). These PRRs (PRR9, PRR7, PRR5, PRR3 and then TOC1) are sequentially expressed from morning to night, assisting in regulation of circadian timing in

Arabidopsis (Gendron et al., 2012,). As a member of the central oscillator, TOC1 primarily acts to down-regulate expression of morning the phased circadian clock proteins CIRCADIAN CLOCK-ASSOCIATED 1 (CCA1) and LATE ELONGATED HYPOCOTYL (LHY), which in turn act to negatively regulate expression of TOC1, making TOC1 essential for regulation and maintenance of circadian rhythms throughout the day (Gendron et al., 2012). PRR5 also primarily acts as a transcriptional repressor, binding at a specific DNA motif, termed CCT, in order to regulate circadian expression of a wide range of genes, including many encoding transcription factors involved in flowering-time, hypocotyl elongation and cold-stress responses (Nakamichi et al., 2012)

LKP2 and FKF1 have a partially redundant function with ZTL in relation of maintenance of the circadian clock (Baudry et al., 2010, Wang et al., 2010). Arabidopsis mutants lacking ZTL lose circadian clock function (Somers et al., 2000), whereas *fkf1* mutants show alterations in flowering time (Imaizumi et al., 2003). Overexpression of LPK2 in Arabidopsis compromises both the clock and flowering times (Schultz et al., 2001), whilst lacking LKP2 has little effect on either of these processes (Baudry et al., 2010). The ZTL family are also known to help regulate the circadian system by mediating the degradation of the core circadian clock gene TOC1 (Mas et al., 2003, Kiba et al., 2007, Fujiwara et al., 2008).

1.2.4. Green light

Plants lack any known green light specific photoreceptor (Zhang and Folta, 2012). Additionally, although the green region of the spectrum is absorbed relatively effectively by plant leaves. the absorbance spectra of chlorophyll *a* and *b* are notably

lower in green regions of the Photosynthetically Active Radiation (PAR) spectrum than in red and blue regions (Smith et al., 2017). While carotenoids provide a greater level of green light absorbance for use in photosynthesis a noticeable absorbance trough still persists in the green-yellow region of the PAR spectrum (Smith et al., 2017). These factors all contribute to plant responses to green light being largely disregarded in many studies, and although green light responses have been observed the mechanisms regulating these responses are poorly understood (Smith et al., 2017, Wang et al., 2013, Wang and Folta, 2013, Folta, 2004, Lin et al., 1995).

Green light has been shown to trigger a range of responses in plants, from stomatal opening to low-light avoidance and hypocotyl elongation (Frechilla et al., 2000, Folta, 2004, Zhang et al., 2011). In *Vicia faba*, a 30 second pulse of green light has been shown to be sufficient to eliminate the stomatal opening signal which would typically be stimulated by an immediately preceding blue light pulse (Frechilla et al., 2000). Under low light conditions it has been shown that supplemental green light can inhibit or even reverse blue light responses in *Arabidopsis*, including flowering and stomatal opening (Wang and Folta, 2013, Zhang et al., 2011). While plants have no known photoreceptors specifically receptive to green light, the absorbance spectra of cryptochromes includes green wavelengths under certain conditions and cryptochromes have been linked a range of blue-green reversible responses in *Arabidopsis*, including the green-light induced reversal of blue-light induced inhibition of hypocotyl elongation and the green-light inhibition of blue-light induced flowering (Lin et al., 1995a, Wang et al., 2013, Zhang and Folta, 2012). Overexpression of CRY1 has also been linked to green light hypersensitivity in transgenic tobacco plants (Lin et al., 1995b). Green light also inhibits *FT* expression and *cry2* degradation under blue light (Zhang and Folta, 2012, Banerjee

et al., 2007). It has been suggested that these blue-green responses may occur in cryptochromes due to the accumulation of green-light absorbing flavin semiquinone radicals which may build up under blue light irradiation (Banerjee et al., 2007).

It should be noted however that at higher fluence rates, blue and red light responses can both override many green light responses (Wang and Folta, 2013, Zhang et al., 2011). Additionally, some green light responses have been shown to instead be caused by minor levels of blue light emitted by many green light sources (Wang et al., 2013) and plants have been shown to be far more sensitive to blue light than to green (Wang and Folta, 2013, Wang et al., 2013, Zhang et al., 2011). Plants are naturally less responsive to green light than to other wavelengths within the photosynthetically active spectrum (Folta and Maruhnich, 2007, Wang and Folta, 2013, Smith et al., 2017). Despite the relative lack of green-light sensitivity in photoreceptors and photosynthetic pigments, total leaf green-light absorbance is relatively high, comparable to that of blue-light absorbance in some plants (Smith et al., 2017). Improving green light utilisation may provide an opportunity to conveniently control plant gene expression.

Most of the energy in sunlight is found within the green region of the spectrum, photosynthetically active pigments however are less absorbent within this region than in red and blue regions of the spectrum (Smith et al., 2017). It has been suggested that these green-light absorbance troughs help to prevent photodamage under high light levels which would otherwise inhibit photosynthetic efficiency (Nishio, 2000). Interestingly, once absorbed by the leaf, green light is highly efficent at driving photosynthesis (Terashima et al., 2009), furthermore, it has been shown that green light plays a larger part in photosynthetic carbon fixation in cells the further they are from the leaf surface, where much of the energy has already been absorbed or reflected (Sun,

1998, Terashima et al., 2009). It has also been shown that some plant species are more able to absorb green light than others, typically those with darker leave (Nishio, 2000), although relatively little change in absorption of red or blue wavelengths have been observed in the same species (Inada, 1976, Nishio, 2000).

1.2.5. UV-B light

UVR8 is a UV-B photoreceptor protein found in many higher plants (Jiao et al., 2007). It is primarily involved in gene expression responses to UV-B leading to production of flavonols, protecting the plant from photodamage (Tilbrook et al., 2013). UVR8 also functions to control stomatal movement, phototropism and entrainment of the circadian clock under UV-B irradiation (Galvao and Fankhauser, 2015). No chromophore is bound by UVR8. Instead, UV-B light is detected by three tryptophan residues (W233, W285 and W337) (Christie et al., 2012a). In its inactive state UVR8 absorbs UV-B, photoactivating and changing conformation from a homodimer to a monomer (Wu et al., 2012). Monomeric UVR8 binds to CONSTITUTIVELY PHOTOMORPHOGENIC 1 (COP1), which is required for maintaining circadian rhythms under low-intensity UV-B irradiation, additionally, UVR8 associates with the promoter of ELONGATED HYPOCOTYL 5(*HY5*), regulating mRNA levels (Feher et al., 2011).

1.3. Photosynthesis mediated photoperception in plants

Plants are receptive to a wide range of light qualities, from UV-B to far red (Chen et al., 2004), a range which expands beyond that of photosynthetically active radiation (PAR) which ranges from around 400-700 nm (Nishio, 2000, Yang et al., 2015). Photosynthetic

light absorption occurs primarily in the chloroplast and is facilitated by photosynthetic antenna pigments, including Chlorophyll *a* and *b* along with carotenoids such as xanthrophylls (Hussain and Reigosa, 2015, Niyogi et al., 1998). These pigments are able to collectively absorb all PAR wavelengths, although plants are noticeably less able to absorb green light (around 500-600 nm) than other PAR wavelengths (Inada, 1976, Nishio, 2000, Smith et al., 2017).

Chloroplasts primarily transmit signals to other organelles via the nucleus in the form of retrograde signalling although interorganel communication can also occur without nuclear mediation (de Souza et al., 2017)**.** The most common forms of signalling from the chloroplast are metabolic signalling via photosynthetically derived carbohydrates (Dalchau et al., 2011, Haydon et al., 2013b) as well as stress signalling via Calcium ion (Ca^{2+}) and reactive oxygen species (ROS) signalling (de Souza et al., 2017).

In order to study interactions between photosynthesis and the circadian clock, photosynthesis is typically inhibited by either growing plants in CO_2 starved conditions or on media containing 3-(3,4-Dichlorophenyl)-1, 1-dimethlyurea (DCMU), an inhibitor of Photosystem II (Haydon et al., 2013b). The phenotype observed under either method can be reversed by re-supplying exogenous metabolic carbohydrates, typically sucrose, to photosynthesis-inhibited plants (Haydon et al., 2013b). Exogenous sucrose, glucose or fructose, but not mannitol or 3-0-methyl glucose, a non-metabolic glucose analogue, are sufficient to maintain circadian rhythms in continuous darkness, suggesting that circadian responses to exogenous sucrose represent a general response to metabolically active sugars (Haydon et al., 2013b).

1.4. Photosynthesis mediated regulation of the circadian clock

In cyanobacteria, chloroplast-encoded genes exhibit circadian rhythms independent of the nuclear circadian clock, however the nuclear clock acts to determine the period length of the chloroplast rhythms (Matsuo et al., 2006). The *Arabidopsis* circadian clock controls chloroplasts via anterograde signalling, allowing the clock to regulate growth by controlling the level of starch accumulation within the chloroplasts, limiting carbohydrate availability by favouring starch accumulation during the day and permitting peak growth by allowing greatest levels of starch degradation at the end of the night, when water availability is highest (Lu et al., 2005, Walter et al., 2009, Graf et al., 2010). Starch depletion during the night is linear and timed to allow around 95% of starch stored during the day to be depleted during the night (Smith and Stitt, 2007, Graf et al., 2010). In this way, the stresses which would be caused by carbohydrate depletion before the next dawn are also avoided. In turn, sugar signals from the chloroplast can entrain circadian rhythms in Arabidopsis by regulating circadian gene expression at dawn. Mutants lacking functional chloroplasts have been shown to have altered circadian rhythms (Hassidim et al., 2007), suggesting that retrograde signalling from the chloroplast is required to fine-tune the nuclear circadian clock and that photosynthesis acts as a light derived input for the circadian system.

1.5. The *Arabidopsis thaliana* circadian clock

Circadian rhythms are cyclic physiological and molecular patterns which are synchronised to and help to anticipate changes in light, heat and other common stressors throughout day-night cycles as well as yearly seasonal cycles (Harmer, 2009,

Hsu and Harmer, 2014). They are found in many organisms, from cyanobacteria to humans (Edgar et al., 2012). In higher plants, circadian rhythms arise from the circadian clock, an interconnected, autoregulatory network of transcription-translation feedback loops. The circadian clock cycles with a period of around 24 hours, independent of environmental cues, allowing it to continue to function for some time in complete darkness or constant light (Nagel and Kay, 2012, Hsu and Harmer, 2014). Under normal environmental conditions the clock is reset by specific entrainment stimuli, especially the transition to light at dawn and out of light at dusk, providing daily corrections to period and allowing better adjustment to changing conditions such as changing day lengths (Jones, 2009).

In *Arabidopsis*, the circadian clock regulates a vast range of processes, encompassing all stages of development within the plant life cycle (Hsu and Harmer, 2014, Jones, 2018). Circadian control of processes such as flowering, leaf movement, hypocotyl elongation and stomatal opening grant increased resistance to abiotic stress and improved photosynthetic efficiency (Dodd et al., 2005). Furthermore, transcription of around one third of genes in *Arabidopsis* (Covington et al., 2008) and 70% of the chloroplast genome (Noordally et al., 2013) have been shown to be regulated by the circadian clock. The *Arabidopsis* circadian clock controls not only gene transcription, but also has robust control over rate of translation of around one seventh of genes (Missra et al., 2015) by controlling the available transcript and level of ribosome binding (ribosome loading) in order to adjust speed of protein synthesis of a given transcript over the course of a light:dark cycle (Missra et al., 2015, Pal et al., 2013, Piques et al., 2009). The result of some circadian controlled processes, such as leaf movement, delayed fluorescence and

prompt fluorescence can be detected by imaging the plant over time, allowing accurate measurement of circadian rhythms *in planta* (Tindall et al., 2015, Litthauer et al., 2015).

While the circadian clock is primarily controlled by the nucleus, the highly-conserved nature of the circadian clock has led to a number of plant organelles containing a circadian-controlled genome partially independent from the nuclear circadian clock. Notably, the metabolic foci of the plant cell, the chloroplasts and the mitochondria, contain small genomes which are partially regulated by the nucleus (Timmis et al., 2004, Martin and Herrmann, 1998). While circadian rhythms in mitochondrial proteins appear to be largely regulated by the nucleus by anterograde pathways (Giraud et al., 2010), the chloroplast genome is strongly linked to the clock, interacting via both anterograde (nucleus-to-chloroplast) and retrograde (chloroplast-to-nucleus) signalling (de Souza et al., 2017). Chloroplasts are also capable of sensing environmental light signals and perceiving stress from these signals independently of the photoreceptor proteins commonly associated with the nuclear circadian clock (Mullineaux and Karpinski, 2002, Muller et al., 2001), meaning that the chloroplast circadian clock is both entrained by the nuclear circadian clock via transcriptional regulation and entrains the nuclear clock through metabolic regulation of photosynthetic sugar availability (Rugnone et al., 2013, Haydon et al., 2013b).

1.5.1. Characteristics of circadian rhythms

An external entraining signal provided to a circadian oscillator is referred to as a *zeitgeber* ("time-giver"). In plants these are typically provided by the appearance of light at dawn and its disappearance at dusk, with different organisms being more

attuned to one of these signals than the other (Haydon et al., 2013b). While temperature, metabollic sugar and many other signals can act as *zeitgebers*, light is the most important and universal *zeitgeber* in nature (McClung, 2006, Jones, 2009). The last *zeitgeber* observed by an organism is referred to as *zeitgeber time 0* (ZT0) (Mas et al., 2003). Under laboratory conditions, circadian rhythms are often entrained by cycles of light and dark with an overall period of 24h for several days before transfer to constant "free running" conditions after a specified ZT0 has been reached, usually dawn if being transferred to constant light or dusk when being transferred to constant darkness.

Circadian rhythms can be modelled as sinusoidal waves with a period, amplitude and phase (Figure1.2). Circadian rhythms can be separated from other oscillations by three major characteristics. Firstly, circadian rhythms cycle with an intrinsic periodicity of around 24 hours. Secondly, this rhythm can persist independently of environmental signals, such as in constant light or complete darkness. Finally, these rhythms are temperature compensated, adjusting for environmental temperature changes with little change to rhythmic periodicity (McClung, 2006, Jones, 2009).

Under laboratory conditions, after entrainment has occurred, circadian rhythms are often examined under constant conditions (Hsu and Harmer, 2014). While this method allows for observation of rhythms which reflect the dynamics and delays arising from interactions between the different components of the clock, they do not truly reflect the natural environment in which the clock usually functions. While many genes are controlled by the circadian clock, some genes cycle with a 24 hour rhythm independently from the clock due solely to the rhythmic cycles of environmental light and temperature. These non-circadian diurnal rhythms of transcription are likely to be

lost under constant laboratory conditions unlike circadian rhythms which will continue to cycle under constant conditions (Schaffer et al., 2001).

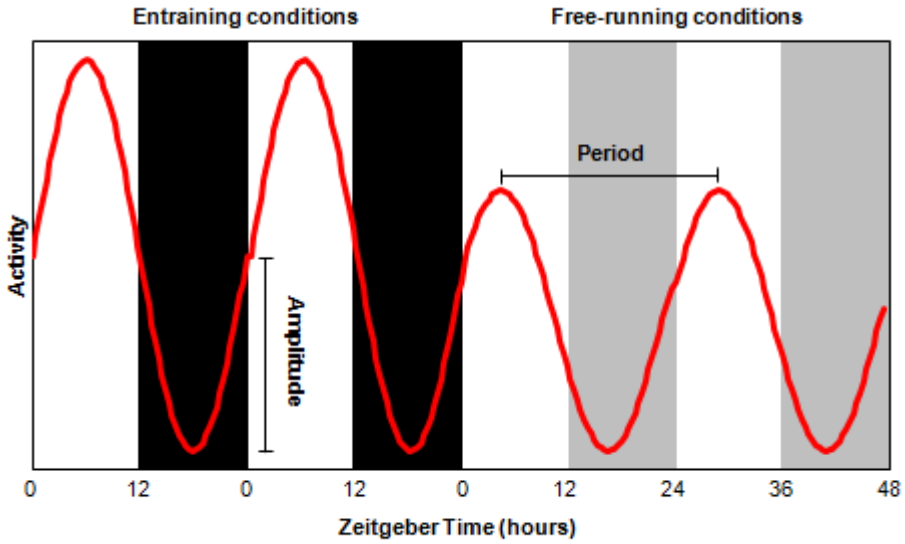

Figure 1.2. Basic properties of circadian clock outputs under laboratory conditions. A rhythmic circadian output represented by a sine wave with a period, amplitude and phase. Activity of the biological process is plotted on the y-axis. The Zeitgeber (ZT) Time; plotted on the x-axis, is measured in hours from the last onset of light. White bars indicate light, black bars indicate darkness and grey bars indicate subjective darkness under constant 'free-running' conditions. Under entraining conditions of 12h/12h light/dark cycles, the period of the rhythmic output corresponds to the 24 hour period of the Zeitgeber. The endogenous period oscillator maintains a period of approximately 24h under free-running conditions.

1.5.2. Transcriptional loops in the *Arabidopsis thaliana* circadian system

The circadian clock can be simplistically described as a biological network which cycles autonomously in constant conditions (Hsu and Harmer, 2014). In *Arabidopsis*, the clock is made up of a wide range of interconnected transcriptional feedback loops which can generally be divided into input and output loops which can in turn be subdivided by the phase at which their expression peaks (Hsu and Harmer, 2014, Millar, 2016, Jones, 2018).

The *Arabidopsis* circadian clock can be simplistically subdivided into four major groups of core clock genes, each of which is associated with genes peaking at specific times in a day/night (diel) period(Hsu and Harmer, 2014, Harmer, 2009). The morning-phased components; CIRCADIAN CLOCK ASSOCIATED 1 (CCA1) and LATE ELONGATED HYPOCOTYL (LHY) (Hsu and Harmer, 2014, Millar, 2016). The day-phased components, including the NIGHT LIGHT-INDUCIBLE AND CLOCK-REGULATED GENE (LNK) family genes, LNK1 and LNK2 along with two genes from the PSEUDO-RESPONSE REGULATOR (PRR) family (PRR7 and PRR9). The afternoon-phased components; REVEILLE8 (RVE8) and two of its close homologues RVE4 and RVE6. Finally, the evening-phased components; PRR5, TIMING OF CAB EXPRESSION 1 (TOC1), LUX ARRHYTHMO (LUX), EARLY FLOWERING 3 (ELF3) and ELF4 (Hsu and Harmer, 2014, Millar, 2016). The components of this system act in complexes grouped by phase, as each phase peaks in expression it in turn represses expression of the previously peaking complex. RVE8, along with LNK1 and LNK2 activate expression of most evening phased elements including PRR5, TOC1, LUX, ELF3 and ELF4 (Figure1.3) (Fogelmark and Troein, 2014, Hsu and Harmer, 2014). A major component of these interactions is the evening element (EE) a motif which recurs in the promoter region of many of the day, afternoon

and evening phased components. The EE acts as a nexus for the regulation of the circadian clock with CCA1 and LHY acting as repressors of the EE and RVE4, RVE6 and RVE8 acting as activators (Hsu and Harmer, 2014, Millar, 2016, Jones, 2018).

This grouping does not however include all known circadian clock genes in *Arabidopsis*, as a number of clock genes with multiple or unknown functions do not fit into this simplified model. For example, GIGANTEA (GI) regulates the clock gene Flowering Locus T (*FT*) to different levels when expressed in different tissues, with GI expressed in the mesophyll or vascular tissue increasing *FT* expression under short-days but not when expressed in the epidermis, shoot apical meristem or root (Sawa et al., 2007). GI also functions differently in the cytoplasm and the nucleus by binding to *FLOWERING LOCUS T* (*FT*) repressor proteins in the nucleus but not in the cytoplasm (Sawa et al., 2007). Additionally, while the circadian clocks of different tissues and cells interact to maintain rhythms throughout the organism, it has been shown that clocks exist independently in different plant tissues, with certain tissue clocks taking dominance over and regulating the clocks of other tissues under some conditions (Endo et al., 2014, Endo, 2016).

Many clock genes primarily function as transcription factors and additionally play a part in one or more feedback loops by repressing or promoting expression of other clock-related genes (Hsu and Harmer, 2014).

Additionally, many genes, such as phytochrome and cryptochrome photoreceptors, are both regulated by and regulate the circadian clock, providing further layers to the feedback system (Harmer et al., 2000, Toth et al., 2001). In addition to genetic transcriptional rhythms, metabolic rhythms of oxidation of peroxiredoxins (Prx) have been observed in the chloroplast (O'Neill et al., 2011). The mechanisms of Prx rhythms

are highly conserved throughout all circadian organisms and have been shown to interact with transcriptional rhythms in *Arabidopsis thaliana* (O'Neill et al., 2011, Edgar et al., 2012, van Ooijen and Millar, 2012).

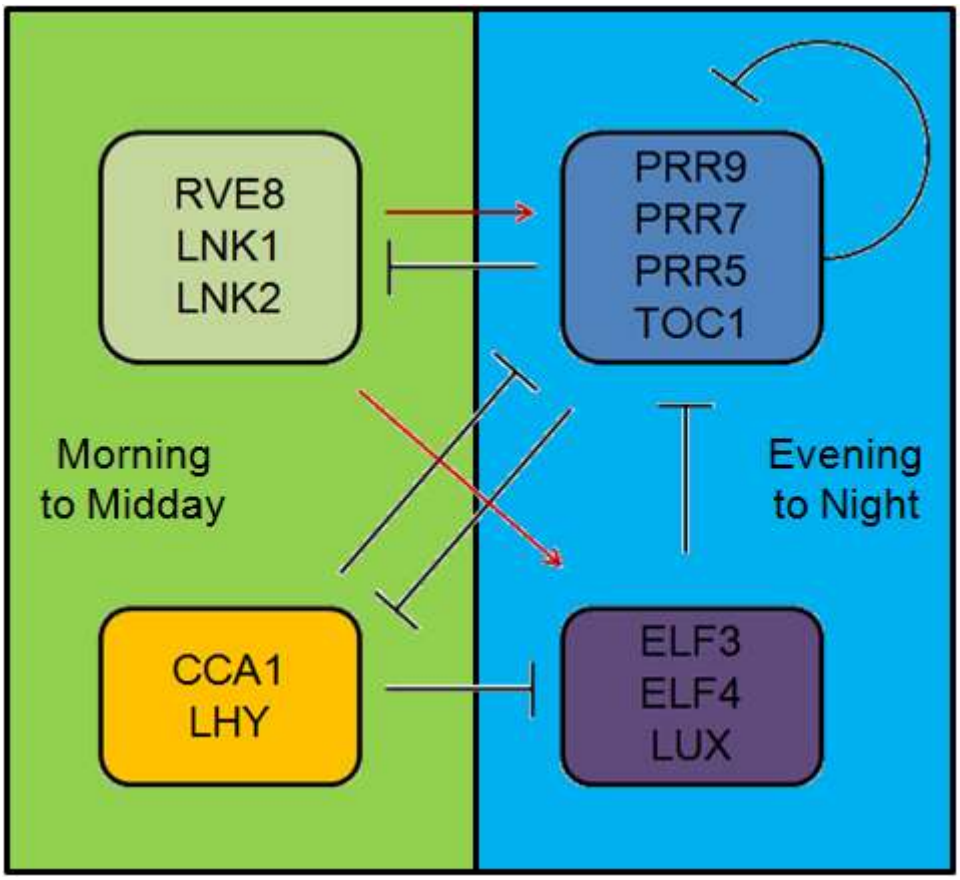

Figure 1.3. Simplified representation of the circadian clock in *Arabidopsis thaliana*. A simplified schematic of the *Arabidopsis* circadian system, simplified by the removal of numerous defined proteins and their interactions. Activation of one complex by another is indicated by red arrows while repression of one complex by another is indicated by black lines. Morning to midday phased genes are shown in the green section on the left whilst evening and night phased genes are shown in the blue section on the right. The system cycles by the repression of each component by the peaking of expression of the next in a continuous loop. RVE8 acts with LNK1 and LNK2 to activate transcription of evening-phased genes including ELF3, ELF4, LUX, TOC1 and PRR5. ELF3, ELF4 and LUX make up the Evening Complex which collectively represses expression of PRR7 and PRR9. TOC1 and PRR5 act along with PRR7 and PRR9 to repress expression of the morning phased CCA1 and LHY. until shortly before dawn. CCA1 and LHY then repress expression of all evening phased genes.

1.6. Methods for monitoring circadian rhythms in plants

1.6.1. Leaf Movement

In plants, although the term 'circadian' is relatively recent (coined by Franz Halberg in 1959), circadian rhythms have been known about for centuries (De Mairan, 1729, McClung, 2006). The earliest known method used to observe rhythmic changes in plant behaviour is to measure leaf movement over time (De Mairan, 1729, McClung, 2006). This method still proves to be an effective way of measuring circadian rhythms in plants (Muller and Jimenez-Gomez, 2016). Other methods, such as the rhythmic elongation of hypocotyls and petioles have been used to measure circadian rhythms through organ movement, although these produce less robust rhythms and are more difficult to measure than leaf movement (Tindall et al., 2015). Improvements in camera technology and computerised tracking and measuring software have driven down costs and improved the accuracy with which leaf movement can be measured in recent years (Tindall et al., 2015), providing a non-invasive, high throughput method with which to observe circadian rhythms *in planta* without the need for transgenic plants. A consumer level digital camera and open source tracking software are sufficient to measure circadian rhythms of leaf movement, making this method far cheaper than the cold coupled device (CCD) cameras and associated software required for lumino-fluorescent techniques of circadian rhythm measurement (Tindall et al., 2015). It should be noted however that this method is limited in that nyctinastic leaf movement cannot be observed in plant species with sessile leaves, including most monocots and all major crop species (Tindall et al., 2015), nor in mature *Arabidopsis thaliana* plants (Edwards and Millar, 2007).

1.6.2. Infra-red gas analysis

Infra-red gas analyser (IRGA) systems are another method by which circadian rhythms can be measured *in planta*. IRGA systems allow for measurement of CO_2 assimilation and stomatal conductance by growing whole or partial plants in a sealed chamber, containing a controlled atmosphere and analysing the composition of the resulting output air (Tindall et al., 2015). The IRGA can analyse this air at a high resolution multiple times per hour, producing a circadian timecourse of carbon assimilation over time (Tindall et al., 2015). IRGA systems have been used to measure circadian rhythms in crassulacean acid metabolism (CAM) plants (Bohn et al., 2001) and *Arabidopsis thaliana* (Somers et al., 1998b, Dodd et al., 2004). Newer designs of IRGA include field-portable models and large, multichannel models with large sealed chambers allowing for higher throughput of multiple plants at once (Dodd et al., 2004, Tindall et al., 2015). As with any indirect circadian assay, IRGA systems are limited in that they cannot be used to observe specific clock components, observing only the overall circadian system within a plant (Tindall et al., 2015).

1.6.3. Delayed chlorophyll fluorescence

Circadian regulation of light harvesting can be observed through fluorescent emissions of Photosystem II (PSII) which are expressed as delayed fluorescence and prompt fluorescence (Gould et al., 2009, Litthauer et al., 2015). Delayed fluorescence is the emission of light from a plant immediately following transfer from light to darkness (Tindall et al., 2015), resulting from the release of stored energy from the P680 light harvesting complex of PSII when returning to ground state from a high energy state

(Gould et al., 2009, Tindall et al., 2015). Delayed fluorescence is thought to occur during normal photosynthesis but cannot be measured under light as only 0.03% of absorbed solar energy is emitted in this way (Tindall et al., 2015). Imaging of delayed fluorescence requires a growth chamber with accurately controlled lighting systems in order to capture delayed fluorescence before its rapid and exponential decay can occur. A cold coupled device (CCD) camera set to an exposure of around 1 minute must be used to capture the image immediately after lights are turned off as delayed fluorescence decays after around 1 minute (Gould et al., 2009, Tindall et al., 2015). Delayed fluorescence intensity is controlled by the circadian clock in a nature which is not yet fully understood but is likely to be linked to the circadian control of the transcription of one or more of the many key genes which make up the light harvesting complexes within PSI and PSII (Tindall et al., 2015). Delayed fluorescence can be used to image circadian rhythms in non-transgenic plants. It has been used to image circadian rhythms in *Arabidopsis thaliana,* barley, wheat, maize, *Bryophyllum fedtschenkoi* (*Kalanchoe fedtschenkoi*) and Norway spruce (*Picea abies*) (Tindall et al., 2015, Malpas and Jones, 2016).

1.6.4. Prompt chlorophyll *a* fluorescence

Another form of chlorophyll fluorescence which can be used to measure circadian rhythms is prompt fluorescence. Although prompt fluorescence and delayed fluorescence are both emitted from PSII antenna complexes within the chloroplast, the signals provided and underlying mechanisms are different and each provides a different insight into the photosynthetic apparatus (Butler, 1978, Baker, 2008).

Prompt fluorescence imaging makes use of the energy dissipated from chlorophyll as fluorescence under specific conditions to calculate the quantum yield of PSII photochemistry (ϕ_{PSII}) under the constant actinic light of applied growth conditions. By applying a saturating pulse of light, the maximum fluorescence level (F_m') can be observed. The level of fluorescence under constant actinic light (F') is then compared to F_m', in order to calculate the fluorescent quenching occurring at a given time as a result of PSII photochemistry (F_m'-F'=F_q'). Finally, the equation F_q'/F_m' is used to calculate ϕ_{PSII} at the given fluence rate. ϕ_{PSII} is equivalent to the quantum yield of linear electron flux through the PSII reaction centres under the given conditions and as a result is used as a measure of PSII operating efficiency, i.e. the efficiency at which PSII is using energy from absorbed light to reduce the primary electron acceptor plastiquinone Q_A at a specific fluence rate (photon flux density; PPFD) (Baker, 2008). Prompt fluorescence has been used to provide insight into PSII photochemistry, linear electron flux and carbon assimilation in many different plant species (Goltsev et al., 2003, Baker, 2008) and into the circadian clock in *Kalanchoë daigremontiana* (Rascher et al., 2001, Wyka et al., 2005) and *Arabidopsis thaliana* (Litthauer et al., 2015). The mechanisms behind the circadian rhythms of prompt fluorescence are not yet well understood but it could provide a versatile, non-invasive method for the measurement of chloroplast circadian rhythms without the need for transformation.

1.6.5. Luciferase bioluminescence to measure gene expression

Transgenic luciferase reporters, fusion proteins combining the promoters of genes of interest with a luciferase gene (often firefly *photinus pyralis* luciferase or a modified, brighter derivative), are being used increasingly to probe the circadian clock for period

and robustness of specific clock genes (Tindall et al., 2015). *LUC+* and the enhanced, mammalian-codon optimised version of *LUC+* (*LUC2*) are modified, versions of firefly luciferase which are significantly brighter than the wild type gene and are commonly used when producing circadian promoter:LUC fusion proteins (luciferase reporters) (Toth et al., 2001, Mašek et al., 2013, Tindall et al., 2015). In *LUC2*, the number of consensus transcription factor binding sites found in *LUC+* was greatly reduced and codon sequences were optimised for use in mammalian cell lines, resulting in a greater than 4-fold increase in expression over *LUC+* in mammalian cell lines (pGL4.10[luc2] vector product Information #9PIE665, Promega Corporation) (Mašek et al., 2013). In order to observe luciferase bioluminescence, plants must first be saturated with luciferin. Luciferin undergoes enzyme-catalysed oxidation in the presence of luciferase, ATP and oxygen, emitting photons upon decaying to its ground state (Hastings, 1996, Tindall et al., 2015). Luciferase bioluminescence emissions are commonly measured using CCD camera connected to a light-tight chamber containing automated lighting systems and can also be measured using photo-multiplier tubes linked to a detector (Tindall et al., 2015). Bioluminescence is directly dependent upon the quantity of luciferase present and due to the nature of luciferase as an unstable enzyme this quantity is directly determined by the rate of luciferase expression (Tindall et al., 2015). Since this rate of expression is controlled by the circadian gene promoter in the luciferase reporter gene, luciferase bioluminescence can be observed to cycle in these reporters with a rhythm equivalent to the transcriptional rhythm of the circadian gene from which the promoter is derived (Harmer and Kay, 2005). For example, a luciferase reporter gene under the control of the morning phased clock gene *CCA1* (*CCA1:LUC*) will cycle with a circadian rhythm peaking in the morning (Harmer et al., 2000, Harmer and Kay, 2005). Luciferase reporter genes have been used to investigate the function of a

wide range of circadian clock genes and to investigate the effects of external stimuli upon the circadian rhythms of transcription of these genes (Millar et al., 1992, Millar et al., 1995, Toth et al., 2001, Harmer and Kay, 2005, Zhu et al., 2016). Oscillations of bioluminescence are highly robust, bright and stable but due to the requirement of excess ATP for luciferase activity oscillations of circadian reporters are very low or absent in continuous dark (Jones et al., 2015). They can however, be recovered with the application of exogenous sucrose to provide a source of carbohydrate in the absence of photosynthesis (Haydon et al., 2013a).

1.6.6. High resolution imaging techniques

Recently, novel circadian assays have been developed that allow the clock to be surveyed within individual tissues and even cells. CCA1 tagged with a Yellow Fluorescent Protein tag has been successfully used to identify the independence of the guard cell clock from the surrounding leaf (Yakir et al., 2009, Yakir et al., 2011). In plants, until recently the prevailing view was that circadian oscillators are locally-autonomous with a degree of cell type specialization (Wood et al., 2001, Thain et al., 2002, Dodd et al., 2004). Increasing evidence is emerging to suggest that inter-cellular communication between circadian clocks, such as between individual cells (James et al., 2008) and between different tissues (Wenden et al., 2011, Endo et al., 2014, Takahashi et al., 2015) is coordinated in phased waves of coordination from root to shoot (Fukuda et al., 2012, Takahashi et al., 2015). It has been demonstrated that significant communication occurs between the vascular and mesophyll tissue clocks with the vascular clock acting as the dominant coordinator (Endo et al., 2014, Takahashi et al., 2015). The required resolution for these techniques however is at the limit of current

detection capabilities but it seems likely that further inter-cellular coordination will be discovered as new technology makes higher resolution equipment available.

1.7. Interactions between the circadian clock and photoreceptors in *Arabidopsis thaliana*

Although plants are capable of detecting the presence or absence of light using photosynthesis alone, more specific responses to light quality and intensity are primarily regulated by the photoreceptors (Millar, 2003, Galvao and Fankhauser, 2015, Jones, 2018). As the circadian rhythms of all plants are closely linked to the light cycles of day and night, along with the changes in light quality which occur throughout the day, especially during sunrise and sunset, it is not unusual that most photoreceptors in *Arabidopsis* have been linked in some way to the regulation of the circadian clock (Millar, 2003, Hsu and Harmer, 2014).

Red light, through phytochromes plays a key part in the entrainment of the circadian clock with circadian phenotypes identified for each phytochrome in *Arabidopsis* excluding phyC (Somers et al., 1998a, Devlin and Kay, 2000). *phyA* mutants display long periods of *CAB:LUC* expression under low irradiances (<2 μmol m^{-2} s^{-1}) and *phyB* mutants show a similar phenotype under irradiances greater than 10 μmol m^{-2} s^{-1} (Somers et al., 1998a). *phyAphyB* double mutants show a long period phenotype under all light intensities (Devlin and Kay, 2000). *cry1* mutants have also been shown to have a similar phenotype to *phyA* mutants under low red irradiances, suggesting that both cry1 and phyA are required to maintain stable circadian rhythms under these conditions (Devlin and Kay, 2000). Studies in the *phyABCDE* quintuple mutant indicate that

phytochromes increase the pace of the clock in a light-independent manner (Hsu and Harmer, 2014). Additionally, phytochromes alter the clock in a fluence-rate dependent manner; accelerating pace under higher red light intensities and decreasing pace under lower red light intensities (Hsu and Harmer, 2014). Under far-red light, expression of evening phased clock genes is elevated and morning phased clock gene transcript levels are decreased (Wenden et al., 2011).

PHYB can interact with at least six clock components; CCA1, LHY, TOC1, GI, ELF3 and LUX although the nature of this interaction is dependent upon the light conditions, with phyB altering configuration depending upon whether red or far-red light have been absorbed (Liu et al., 2001, Yeom et al., 2014). It has been shown that LUX interacts more strongly with active, P_{fr} form of PHYB than the P_r form while CCA1 and TOC1 interact better with the P_r form (Yeom et al., 2014). While PHYB is the dominant phytochrome in *Arabidopsis,* PHYA acts as the primary sensor of far-red wavelengths (Somers et al., 1998a). The removal of one or more phytochromes in *Arabidopsis* results in a lengthening of circadian period under constant red light (Hu et al., 2013), it should be noted however that the *phyABCDE* quintuple mutant, lacking all phytochromes found in *Arabidopsis* has a shorter than normal circadian period under low levels of constant red or white light (Strasser et al., 2010, Hu et al., 2013).

Blue light is also of notable significance to the circadian clock with both the ZTL family and the cryptochromes having significant roles in regulation of the circadian system. ZTL, is a blue light photoreceptor largely associated with regulating the stability of the circadian clock protein TOC1 (Mas et al., 2003). As such, it is unsurprising that under blue light, *ztl* mutants present a long-period phenotype (Somers et al., 2004), unusually *ztl* mutants also express a long-period phenotype under red light, which might be

explained by physical interactions which have been observed between ZTL and portions of phyB (Jarillo et al., 2001a, Somers et al., 2004). While independently, CRY1 and CRY2 have only slight effects on circadian period under blue light (Somers et al., 1998a, Devlin and Kay, 2000), the *cry1cry2* double mutant has a pronounced long-period phenotype under blue light, indicating that both cryptochromes function semi-redundantly in controlling much of the blue-light input to the circadian clock (Somers et al., 1998a, Devlin and Kay, 2000).

Cryptochromes contribute to fluence rate dependent shortening of the period of the circadian clock under blue light, similarly to how phytochromes function under red light (Hsu and Harmer, 2014). No link between the nuclear clock and phototropins has been identified but under low intensities of blue light phototropins are required to maintain robust rhythms of prompt fluorescence in *Arabidiopsis* (Litthauer et al., 2015).

While photoreceptors clearly play a major role in the regulation of the circadian system under specific light qualities and conditions (Somers et al., 1998a, Mas et al., 2003, Feher et al., 2011), photoreceptor mutants lacking function of ztl, cry1, cry2, phyA or phyB and the double mutants *cry1cry2*, *phyAphyB* and *cry1phyA* along with the quintuple mutant *phyABCDE* mutant all have extended circadian periods but are not arrhythmic (Somers et al., 1998a, Somers et al., 2000, Fankhauser and Staiger, 2002, Jones et al., 2015). It has also been shown that cryptochromes and phytochromes, in spite of their significant roles as regulators of the circadian system, are not essential for circadian oscillations to occur in Arabidopsis (Devlin and Kay, 2000, Yanovsky and Kay, 2001). This is of particular note as mammalian cryptochromes form a core part of the circadian oscillator (Devlin and Kay, 2000).

1.8. Cyanobacteriochrome mediated green-light responses in cyanobacteria

Cyanobacteriochromes are a family of photoreceptors related to phytochromes and unique to cyanobacteria (Hirose et al., 2008). While structurally and functionally similar to phytochromes, cyanobacteriochromes are typically prokaryotic two component regulatory systems (Ikeuchi and Ishizuka, 2008). As such, they consist of an environmentally regulated histidine kinase which autophosphorylates under a specific stimulus, such as light, and a response regulator protein (Capra and Laub, 2012), usually a transcription factor (Galperin, 2010) rather than the single, hybrid protein found in eukaryotes (Hua et al., 1995, Stock et al., 2000). Furthermore, cyanobacteriochromes separate themselves significantly from phytochromes by absorbing a range of wavelengths shorter than, but with greater diversity than, the common red/far-red of phytochromes (Rockwell et al., 2012), from near-ultraviolet wavelengths (Song et al., 2011) to green wavelengths (Hirose et al., 2008). This characteristic makes cyanobacteriochromes particularly useful in the production of synthetic optogenetic light-switching systems as this wider diversity of absorbance spectra allows cyanobacteriochromes to trigger gene expression under wavelength ranges not found in other photoreceptors. These ranges likely evolved due to the aquatic habitat of cyanobacteria where light availability can vary significantly, for example red light is quickly absorbed by the marine habitat of many cyanobacteria and when unavailable alternative inputs must be utilised (Kehoe, 2010).

Cyanobacteriochromes can be roughly divided into two major types based on their chromophore: phycoviolobilin (PVB) or phycocyanobilin (PCB) (Narikawa et al., 2015b). PVB binding cyanobacteriochromes typically absorb under short wavelengths, from near-UV to green (Rockwell, et al. 2012). PCB binding cyanobacteriochromes

absorb longer wavelengths, typically from green to red light (Narikawa et al., 2014). Cyanobacteriochromes which absorb in the green region of the spectrum are of specific interest to optogenetics as they provide photoreceptors which absorb in a spectral range not found in plants. Of these green-light absorbing photoreceptors two major groups of PCB binding cyanobacteriochromes are well studied. Red/green type cyanobacteriochromes form a stable, red-light absorbing state and photoconvert to a less stable green-light absorbing state while green/red types are more stable in their green-light absorbing state and photoconvert to a red -light absorbing state (Song et al., 2015, Narikawa et al., 2015a).

The cyanobacteriochrome ccaS is a green/red type PCB-binding cyanobacteriochrome which has been found in two species of cyanobacteria, *Synechosystis* sp. PC6803 (Hirose et al., 2008) and *Nostic punctiforme* (Hirose et al., 2010). In *Synechocystis* sp. PCC 6803, the transcription factor ccaR forms a two component regulatory system with ccaS (Hirose et al., 2008). The naturally occuring *ccaS-ccaR-cpcG2* pathway allows green light to induce production of CpcG2, a phycobilisome protein which facilitates transfer of energy from green light to Photosystem I (PSI) (Hirose et al., 2008, Kondo et al., 2005, Kondo et al., 2007). The *ccaS-ccaR* gene cluster has been used to produce a synthetic light-switching mechanism in *Escherichia coli* and this system has been optimised by introducing alternative promoter and terminator sequences to *ccaS* and *ccaR* as well as producing a synthetic binding motif for ccaR to act as an inducible promoter for a targeted downstream gene (Schmidl et al., 2014). The gene cluster has also been introduced into *Synechococcus* sp. NKBG 15041c, successfully conferring green-light switching characteristics from a fresh-water cyanobacteria species to a marine species (Badary et al., 2015).

1.9. Optogenetic engineering of novel photoresponses

Modulating gene expression is a powerful tool in plant research allowing analysis of complexly connected systems and pathways as well as granting the chance to analyse genes which would be harmful to plant growth if expressed constitutively (Padidam, 2003). Synthetic biology is broadening the potential for control of gene expression *in planta*, improving on the efficiency of traditional inducible systems (Purnick and Weiss, 2009, Patron et al., 2015). The development of synthetic systems allowing for the protein-based switching of gene expression is quickly becoming more common, influencing a wide range of genes using an increasing range of input mechanisms (Kim and Lin, 2013, Stein and Alexandrov, 2014, Tischer and Weiner, 2014, Schmidt and Cho, 2015). Current systems used to control gene expression in plants often make use of invasive chemicals as trigger stimuli, making them useful as sensors for natural accumulation of these chemicals but less effective as dedicated switching mechanisms (Lu et al., 2009b, Rao, 2012, Liu and Stewart, 2016).

Protein-based switching mechanisms seek to make use of either biochemically inert ligands or light as an input, providing a non-invasive method of inducing gene expression without having a significant impact on the organism (Stein and Alexandrov, 2014). Optogenetic constructs are synthetic genetic systems designed to permit control of gene expression via photoreceptor proteins, using light as a triggering stimulus. Light is particularly valued as an input in these systems as it is cheap, can be supplied over a large area constantly for long periods of time, can be kept at a constant quantity and quality almost indefinitely, can be switched on and off instantly and, if used correctly, is non-invasive. In many prokaryotic organisms in which synthetic light switches are used, such as *E. coli*, light is largely unused by the natural processes within the cell, meaning

that no natural processes can be interfered with (Levskaya et al., 2005). In photosynthetically active organisms such as cyanobacteria and plants however, the choice of input wavelength can be highly important, reducing the impact which the trigger stimulus has upon the organism's natural processes.

Photoreceptors can be engineered to induce gene expression via a wide range of mechanisms specific to their structure and natural function (Kim and Lin, 2013, Tischer and Weiner, 2014). Some of the most commonly used photoreceptors in light-inducible gene expression systems are phytochromes, receptors that incorporate light-oxygen-voltage (LOV) motifs (commonly found in phototropins) and microbial rhodopsins (Christie et al., 2012b, Schmidt and Cho, 2015), of these three categories, phytochromes and LOV motif photoreceptors are commonly sourced from plants, although cyanobacteriochromes are becoming increasingly common. These phytochrome-like photoreceptors provide a diverse range of photosensitivities, with different cyanobacteriochromes providing absorbance spectra which include both longer and shorter absorbance ranges than are typically found in plant photoreceptors (Narikawa et al., 2015b). Optogenetic systems are particularly desirable due to the versatility and precision of light itself. Unlike other regulatory inputs, light can be accurately controlled to limit both quantity and quality over a large area for any required time, switching on and off almost instantaneously. Photoreceptor protein systems can reflect this, providing almost instantaneous gene expression once light is applied to systems using some photoreceptor proteins (Kralj et al., 2011). Furthermore light is a non-invasive input which can usually be controlled in such a way that it rarely causes stress or influences untargeted metabolic pathways in any organisms being stimulated by it,

unlike more common input effectors; chemicals such as ethanol or antibiotics (Gardner et al., 2000, Junker and Junker, 2012).

A large range of light-switching constructs have been produced to function within *Escherichia coli* (*E. coli*) (Moglich and Moffat, 2007, Ryu and Gomelsky, 2014, Tabor et al., 2011, Schmidl et al., 2014) providing a wide range of input wavelengths and output genes. Functional switches have been produced in cyanobacteria (Abe et al., 2014), mammalian cells (Muller and Weber, 2013), mice (Konermann et al., 2013), yeast (Milias-Argeitis et al., 2011), zebrafish (Beyer et al., 2015) and plants (Muller et al., 2014). However, as some of the main organisms from which photoreceptor proteins are sourced for light-switching systems, plants provide a challenge when implementing light-induced systems. The natural sensitivity of plants to, and dependence upon light, limits the range of input wavelengths which can be used without significantly influencing another, untargeted natural process within the organism (Carter and Knapp, 2001, Smith et al., 2017). The only synthetic, light-induced gene expression switches which have currently been produced for plants use plant photoreceptors such as Phytochrome B (Mayer and Heckel, 2006, Muller et al., 2014).

Early phytochrome based light-inducible two-component systems used the photoreceptive histidine kinase region of cyanobacterial phytochromes to produce chimeric proteins which function alongside bacterial response regulators, transcription factors which form two component systems with histidine kinases in prokaryotic histidine kinase complexes (Levskaya et al., 2005), producing a red-light switching mechanism. This system has been adapted and improved upon (Schmidl et al., 2014), simplifying the structure and improving the level of response to red light. This system

has been connected to a range of output genes (Bacchus and Fussenegger, 2012, Camsund et al., 2011, Gardner and Deiters, 2012).

The cyanobacteriochrome, CcaS has been used as part of its natural genomic cluster (*ccaS*-*ccaR*), along with the promoter for the naturally expressed antenna protein CpCG2, to produce a green-light switching mechanism for cyanobacteria (Abe et al., 2014) and *E. coli* (Tabor et al., 2011). This mechanism, like the PhyB chimera system has been optimised for *E. coli*, replacing the natural cyanobacterial promoters for both the *ccaS* and *ccaR* genes with constitutive *E. coli* promoters, which has been shown to improve expression of these genes when transgenically expressed in *E. coli*. Additionally, the removal of a constitutive promoter region from the downstream promoter for CpCG2 has been found to reduce leakiness of the output (Schmidl et al., 2014).

1.10. Conclusions and introduction to the study

Plants are acutely sensitive to light, able to detect changes in intensity, wavelength and periodicity and react appropriately. Furthermore, the circadian clock allows plants to anticipate cyclic changes in light conditions to prepare for stress and take advantage of predictable changes. Phototropins have been shown to have some involvement in maintaining robust circadian rhythms in the chloroplast under blue light, although no other circadian activity has been attributed to either *phot1* or *phot2* in *Arabidopsis.* Furthermore, while green light responses have been documented in plants they are poorly understood and the involvement of green light as an input into the circadian system has been largely ignored. Finally, optogenetics is a rapidly expanding field which

has just begun to incorporate plants into the organisms which have been manipulated, the incorporation of cyanobacteriochromes into optogenetic switching mechanisms could provide a method by which light wavelengths which are not already utilised by plant photoreceptors could be used as an input for a non-intrusive optogenetic system in plants.

This study aims to explore the interactions of plant photobiology with the circadian clock by defining and characterising the interactions between the phototropins and circadian rhythms and green light and the circadian system in *Arabidopsis.* We will also design, engineer and characterise the responsiveness of a green light controlled optogenetic construct for use in plants.

Chapter 2- Materials and methods

2.1. Materials and reagents

All chemicals were provided by Sigma-Aldrich Ltd (Poole, UK), Thermo Fisher Scientific UK (Southampton, UK) or Melford Laboratories Ltd (Ipswich, UK) unless stated otherwise.

Murashige and Skoog (MS) Basal Salt Mixture was supplied by either Duchefa Biochemie (Haarlem, Netherlands, cat# 0221) or Sigma-Aldrich Ltd (cat# D5758). Luria-Bertani (LB) media powder was provided by either Duchefa Biochemie (cat# L1703) or Melford Laboratories Ltd (cat# L1704).

QIA-quick® gel extraction kits (cat# 28704) and QIA-quick® PCR purification kits (cat# 28104) were supplied by Qiagen (UK). EZ-10 DNA Mini Spin Columns were sourced from NBS Biologicals (UK, cat# SD5005). BsaI type IIS restriction enzymes were provided by New England BioLabs Inc (Hitchin, UK, cat# R0535S). BpiI (BbsI) type IIS restriction enzymes (cat# ER1011) and T4 DNA ligase (cat# EL0011)were supplied by Thermo Fisher Scientific UK.

Light emitting diodes (LEDs) were sourced from Bright Technology Industrial Ltd (Shenzhen, China). Neutral density filters and #312 Canary Lighting Gel Sheet filters were supplied by Stage Depot Ltd (Bristol, UK). Shott Optical Glass OG515 filters were supplied by Schott Advanced Optics (Mainz, Germany) and Galvoptics Ltd (Basildon, UK).

2.2. Media and reagents prepared for use in this study

2.2.1. Murashige and Skoog media

Half-strength MS media (0.5x MS) agar was prepared for use in the growth of *Arabidopsis thaliana*. 2.15 g/l Murashige and Skoog Basal Salt Mixture was dissolved in dH_2O and pH adjusted to 5.7 using 1 M KOH solution (prepared in dH_2O). 0.8% (w/v) agar was added before sterilisation by autoclaving at 121 °C for 15 minutes. In some cases, 0.5x MS agar was prepared with 3% (w/v) sucrose, in these cases 100 µg/ml Carbenicilin (Fisher Bioreagents, cat# BP2648-1) was added after media sterilisation but before plate preparation.

2.2.2. Luria-Bertani media

Luria-Bertani media (LB) broth was prepared for use in the growth of *Escherichia coli* (*E. coli*) and *Agrobacterium tumefaciens* strain GV3101. 25 g/l LB media powder was dissolved in dH2O and pH adjusted to 7.2 using 1 M NaOH solution (prepared in dH2O) before sterilisation by autoclaving at 121 °C for 15 minutes. For agar plate production 1.6% (w/v) agar was added to LB broth before sterilisation.

2.2.3. Purification of Taq DNA Polymerase

Thermus aquaticus DNA Polymerase I (Taq) was purified according to (Pluthero, 1993) and used in PCR analysis. Glycerol stocks of *E. coli* Rosetta™ II strain previously

transformed with the pTaq recombinant plasmid (Engelke et al., 1990), in order to overproduce the Taq, were a gift from Prof S. Harmer (University of California, Davis, USA). Cells were recovered from glycerol stock by streaking on an LB agar plate (see Section 2.2.2) containing 100 µg/ml Ampicillin (Melford Laboratories Ltd, cat #A0104) and incubated overnight at 37 °C. An overnight culture was produced from a single colony and 100 µl of this culture was used to inoculate 1 l of LB broth containing 100 µg/ml Ampicillin. This 1 l culture was incubated at 37 °C with shaking until an optical density (OD_{600nm}) of 0.8 was reached (approximately 11 hours), at which point 128 mg/l Isopropyl β-D-1-thiogalactopyranoside (IPTG; Sigma-Aldrich, UK, cat# 16758) was added to induce protein expression. This final culture was incubated at 37 °C with shaking for 12 hours before cells were collected by centrifugation at 3000 rpm for 30 minutes at 4 °C and gently resuspended in 100 ml of Buffer A (50 mM Tris-HCl pH 7.9, 50 mM Dextrose, 1 mM ethylene diaminetetra-acetic acid (EDTA)). Cells were pelleted by centrifugation at 3000 rpm for 15 minutes and gently resuspended in 50 ml Buffer A with 4 mg/ml Lysozyme (Sigma-Aldrich, UK, cat# L6876). Mixtures were incubated at room temperature for 15 minutes before adding 50 ml Lysis Buffer (10 mM Tris-HCL pH 7.9, 50 mM KCl, 1 mM EDTA, 1 mM phenylmethane sulfonyl fluoride (PMSF), 0.5% Tween-20, 0.5% Nonidet P40) was added and incubated at 75 °C for 1 hour. Lysate was cleared by centrifugation at 10000 rpm for 15 mintues at 4 °C and transferred to a glass beaker. Protein was precipitated by adding 30 g ammonium sulphate to the cleared lysate over the course of 30 minutes with gentle stirring at room temperature. Solution was incubated with stirring at room temperature for 30 minutes and precipitated protein was collected by centrifugation at 10000 rpm for 15 minutes at 4 °C. Protein was resuspended in 20 ml Buffer A and dialysed against Storage Buffer (50 mM Tris-HCl pH 7.9, 50 mM KCl, 0.1 mM EDTA, 1 mM Dichlorodiphenyltrichloroethane (DDT), 50%

Glycerol, 0.5 mM phenylmethylsulfonyl fluoride (PMSF)) using Slide-A-Lyzer™ 20K MWCO 30 ml Dialysis Cassettes (Thermo Fisher Scientific, UK, cat# 66003) as per manufacturer's instructions. Initial dialysis was performed at 4 °C for 2 hours before replacement of Storage Buffer with fresh Storage Buffer for another 2 hours at 4 °C. Storage buffer was then replaced again with fresh Storage Buffer before dialysis was continued at 4 °C overnight. Protein was then diluted 1:1 with Storage Buffer.

Optimal Taq dilution was identified using a dilution series (1:0, 1:1, 1:3, 1:5, 1:7, 1:15, 1:31) using a sample of protein extract and Storage Buffer. Activity of this Taq dilution series was tested using PCR (see Section 2.4.2). Remaining protein extract was then diluted to the optimum dilution for PCR with Storage Buffer before being aliquoted and stored at -20 °C.

2.3. Plant material and growth conditions

2.3.1. Standard growth conditions for plants

Except where described otherwise, plants were grown in cool fluorescent white light under 12:12 light:dark photoperiod cycles at 60 μmol m^{-2} s^{-1} on half-concentration MS basal mineral salts (0.5x MS) agar plates in A1000 Adaptis chambers (Conviron Europe Ltd, Isleham, UK) prior to testing (later referred to as Standard Growth Conditions).

In experiments using coloured light emitting diodes (LEDs) (Bright Technology Industrial Limited, Shenzhen City, China), lights with the spectral peaks shown in (Figure 4.1.) were used. Spectra were measured using a SR9910-V7 Double Monochromator Spectroradiometer (Macam Photometrics Ltd, Livingston, UK).

2.3.2. *Arabidopsis thaliana* plant material

All wild type and transgenic *Arabidopsis thaliana* lines used in this study were in the *Arabidopsis thaliana* Columbia-0 (Col-0; Col) ecotype background. Single mutants *phot1-5* (*phot11; p1*) and *phot2-1*, deficient in PHOTOTROPIN 1 or PHOTOTROPIN 2 respectively and the *phot1-5 phot2-1* double mutant (*phot1phot2; p1p2*) have been previously described (Liscum and Briggs, 1995, Huala et al., 1997, Sakai et al., 2001) and were gifts from Prof John M. Christie (University of Glasgow, UK). *phot2-101*(*phot2; p2*) single mutants, also deficient in PHOTOTROPIN 2 have been previously described (Jarillo et al., 2001b, Cho et al., 2007) and were a gift from Prof John M. Christie (University of Glasgow, UK). *phot1 phot2* double mutants with an inserted *PHOT1* gene with a lipid anchoring farnesyl tag (*PHOT1 farn; farn*) have been previously described (Preuten et al., 2015) and were a gift from Prof John M. Christie (University of Glasgow, UK). The *cry1 cry2* (*cry1-304 cry2-1*; *c1c2*) double mutant deficient in both CRYPTOCHROME 1 and CRYPTOCHROME 2 is previously reported (Mockler et al., 1999) and were a gift from Prof John M. Christie (University of Glasgow, UK). *phyB-9* single mutants deficient in PHYTOCHROME B have been previously described (Jones et al., 2015) and was a gift from Prof S. Harmer (University of California, Davis, USA).

ntrc (SALK_012208C) and *srx* (SALK_015324C) single mutants deficient in NADPH-THIOREDOXIN REDUCTASE C (NTRC) and SULFIREDOXIN (SRX) respectively have been previously reported (Puerto-Galan et al., 2015) and were re-isolated from seed provided by the Nottingham *Arabidopsis* stock center (NASC) (Scholl et al., 2000). *cpck-2-A* (GABI-kat segregating set GK-615F11) is a knockout line for a previously described cytosolic casein kinase (CK2) chloroplast protein (cpCK2*a*) (Ogrzewalla et al., 2002) and was re-isolated from seed provided by NASC (Scholl et al., 2000). *cskA* (SALK_018074)

and *cskB* (SALK027360) are both alleles of knockout lines for CHLOROPLAST SENSOR KINASE, they have been previously described (Puthiyaveetil et al., 2008) and were re-isolated from seed provided by NASC (Scholl et al., 2000).

Col-0 luciferase reporter lines *CCR2::LUC* (Martin-Tryon et al., 2007) and *CCA1::LUC2* (Jones et al., 2015) used in this study have been previously reported, *CCR2::LUC* lines were gifts from Prof S. Harmer (University of California, Davis, USA). Mutant lines expressing the *CCA1::LUC2* reporter; *phot1-5 CCA1::LUC2, phot2-101 CCA1::LUC2, phot1-5 phot2-1 CCA1::LUC2* and *cry1 cry2 CCA1::LUC2* were generated by crossing the respective mutant lines to the *CCA1::LUC2* line (Jones et al., 2015). Col-0 luciferase reporter lines *CAB2::LUC, CCA1::LUC, GI::LUC, LHY::LUC* and *TOC1::LUC* (Tindall et al., 2015) were a kind gift from Prof Anthony Hall (University of Liverpool, UK).

2.3.3. Surface sterilisation of *Arabidopsis thaliana* seed

Seed was surface sterilised using chlorine gas exposure for 3 hours in a sealed glass desiccator jar. 20-200 seeds, as per experimental requirements, were gathered by genotype in open topped 1.5 ml microcentrifuge (MCC) tubes within a desiccator jar kept in a well-ventilated fume cupboard along with a beaker containing 50 ml of commercial bleach to which 3 ml of 37% HCl was added. The desiccator jar was then sealed and left for 3 hours to allow sterilization by chlorine fumes to occur. Seed was then removed and resuspended in 750 µl of sterile dH_2O and vernalised at 4 °C for 2-4 days before sowing.

2.3.4. Transformation of *Arabidopsis thaliana* to create transgenic lines

Prior to transformation with *Agrogbacterium tumefaciens* (strain GV3101), *Arabidopsis thaliana* seeds were sown on wet soil, vernalized in the dark at 4 °C for 3 days and germinated under standard growth conditions or long days (16h light: 8h dark) under cool white fluorescent lighting (60 µmol m^{-2} s^{-1}) and grown until the first signs of bolting.

Agrobacterium tumefaciens (strain GV3101) was transformed with a plasmid containing a desired plasmid using a freeze/thaw method. 250 µl competent GV3101 cells were thawed on ice before adding 20 µl of plasmid preparation (commonly Golden Gate Level 2 constructs; Section 2.4.4.). Cells were briefly mixed by gentle shaking before incubating on ice for 30 minutes, flash-freezing in liquid nitrogen for 5 minutes, and then incubating at 37 °C for 5 minutes. 1 ml LB media (Section 2.2.2.) was added before tubes were incubated in darkness at room temperature for 2-4 hours with gentle mixing. Cells were collected by centrifugation at 3000 rpm for 5 minutes and resuspended in 50 µl supernatant before transferring to two LB agar plates containing 150 µg/ml rifampicin (prepared in methanol; Melford Laboratories Ltd, cat# R0146) and 15 µl/ml gentamycin (prepared in dH_2O; Melford Laboratories Ltd, cat# G1914), along with any appropriate antibiotics for the expression plasmid. Cells were incubated at 28 °C for 2 days and overnight cultures were prepared in LB broth containing appropriate antibiotics.

Agrobacterium cultures were then used to transform bolting *Arabidopsis* plants or to infiltrate *Nicotiana benthamiana* leaves (see Section 2.3.6.). For *Arabidopsis,* a floral inoculation method as previously described (Narusaka et al., 2010) was used. Transformations were performed in late afternoon. After transformation, plants were

returned to original growth conditions and kept shaded to encourage *Agrobacterium* growth. Inoculation was repeated once every 3-4 days to treat newly emerging buds.

Seed harvested was sterilised (see Section 2.3.3.) and grown on 0.5x MS agar with appropriate antibiotics and herbicides. Positive transformants were selected from resistant seedlings.

2.3.5. *Nicotiana benthamiana* material and growth conditions

Nicotiana benthamiana seed used in this study was a gift from Prof Phill M. Mullineaux (University of Essex, UK). Seeds were grown individually on soil under standard growth conditions (Section 2.3.1.) for approximately six weeks, until just before flowering had occurred, before infiltration (Section 2.3.6.) and subsequent testing (commonly by luciferase imaging; see Section 2.6.2.). Any flowering plants were discarded and not used in testing.

2.3.6. Infiltration of *Nicotiana benthamiana* to produce transient gene expression

Mature *Nicotiana benthamiana* leaves from plants grown under standard conditions (see Section 2.3.5.) until just before flowering (around six weeks), were infiltrated using transformed *Agrobacterium* cell cultures (see Section 2.3.4.). Cells from 1 ml of culture were collected by centrifugation at 3000 rpm for 1 minute and resuspended in 30 µl infiltration media (10 mM MES buffer, 10 mM $MgCl_2$, 150 µg/ml acetosyringone). Optical density ($OD_{600\ nm}$) of the cell suspension was adjusted by dilution with infiltration media until an OD_{600} of 1.0 was achieved. A 1 ml needle-less syringe was

then used to inject cell suspension to the intercellular spaces of a tobacco leaf via the underside of the leaf. Plants were then returned to standard growth conditions for 4-8 days before testing (commonly by luciferase imaging; see Section 2.6.2.).

2.4. DNA preparation, cloning and manipulation

2.4.1. Agarose gel electrophoresis

Horizontal agarose gel electrophoresis was regularly used both for the identification of DNA fragments by molecular weight and to separate and purify such fragments. DNA samples were diluted to an appropriate concentration alongside 2 µl of electrophoresis loading buffer (30% (v/v) Glycerol, 30% (v/v) Ponceau S) and resolved by electrophoresis in 1.5xTAE buffer (40 mM Tris pH7.6, 1 mM EDTA, 20 mM acetic acid) at 100V. Agarose gels were made using 1.5% (w/v) agarose stained with 0.0006% (v/v) SafeView Nucleic Acid Stain (NBS Biologicals, Cambridgeshire, UK. cat# NBS-SV1). GeneRuler 1 kb DNA ladder (Thermo Fisher Scientific, cat# SM0313) was loaded alongside all samples to allow estimation of the molecular weight of fragments within the sample. Stained gels were visualised under blue light using GeneGenius Bioimaging system (Syngene, Synoptics Ltd., Cambridge, UK) per the manufacturer's instructions. If required, a QIAquick Gel Extraction Kit (Qiagen, UK) was then used to recover isolated fragments according to the manufacturer's protocol.

2.4.2. Polymerase chain reaction techniques

Polymerase chain reactions (PCR) were completed using an Applied Biosystems 2720 Thermal Cycler (Thermo Fisher Sicentific, UK). DNA oligonucleotides were designed *de novo* and checked using the programs Primer3Plus (Untergasser et al., 2007) or Benchling (http://benchling.com). For genotyping of Arabidopsis T-DNA insertion lines, the SALK T-DNA verification primer design online tool was used (http://signal.salk.edu/tdnaprimers.2.html). Specificity of designed primer sets was confirmed using Primer Blast (Ye et al., 2012). Primers used in this study can be found in Appendix Tables A1-A4.

PCR reactions were completed in the final volume of 20 µl. 0.2 µg of template DNA was added to a combination of 4 µl of 5X Phusion® HF Buffer (New England Biolabs, Hitchin, UK, cat# B0518S), 200 µM dNTPs (2.5 mM each, prepared in dH_2O, Thermo Scientific, cat# R0182), 1 µM each of forward and reverse primers and either 0.2 µl of Phusion® High-Fidelity DNA Polymerase (New England Biolabs, Hitchin, UK, cat# M05030S) for reactions used in Golden Gate cloning protocols (see section 2.4.4.) or 2 µl of purified Taq DNA polymerase (see Section 2.2.3.) for all other reactions. Amplification was performed using 40 cycles following an initial denaturation step of 2 min at 98 °C. A typical cycle consisted of an additional denaturation at 98 °C for 30 s, an annealing step at 60 °C for 1 min and an extension step at 72 °C for 1 min per Kb template. Modifications were made to this basic program when required by specific template DNA or primers.

2.4.3. Colony PCR

Individual colonies of transformed *E. coli* were transferred from a selective LB agar plate to a 200 µl PCR tube containing 5 µl dH_2O using a sterile pipette tip. A portion of each transferred colony was re-streaked onto a new selective LB agar plate and grown overnight at 37 °C. PCR was completed as described in Section 2.4.2. with an additional 10 minutes added to the initial denaturation step to ensure complete cell lysis. PCR samples were examined by agarose gel electrophoresis (Section 2.4.1.) and colonies containing the desired plasmid identified. Plasmid DNA was then isolated from appropriate new colonies taken from the re-streaked plates as described.

2.4.4. Golden Gate digestion-ligation reaction techniques

Golden Gate cloning (Engler et al., 2008, Engler et al., 2014, Werner et al., 2012) was used to assemble multigene constructs in three main stages. Level 0 (L0) modules (see Figure 5.2.), containing either promoters, coding sequences or terminators flanked by specifically coded overhangs containing binding sites for the type II restriction enzyme *BsaI* were sourced or produced. L0 modules were either sourced from existing glycerol stocks (kind gifts from Dr. Nicola J. Patron, Sainsbury Lab, Norwich, Dr. Patricia E. Lopez-Calcagno, University of Essex, Prof Christine Raines, University of Essex, Dr Marino Exposito-Rodriguez, University of Essex and Prof Phil M. Mullinauex, University of Essex) or produced. L0s were produced either by designing and synthesising whole sequences, or by adding the required overhangs to primers and cloning the desired sequences from existing plasmids or cDNA using PCR with Phusion® High-Fidelity DNA Polymerase (New England Biolabs, Hitchin, UK, cat# M05030S) as described in section

2.4.2. A list of L0 sequences produced can be found in Table 5.1. Synthesised sequences (L0-*ccaS*, L0-*ccaR* and L0-*pGLE*) were codon optimised for use in *Arabidopsis* and cloned into GeneArt pMK vectors (GeneArt kanamycin resistant standard cloning vector; GeneArt, Rosenburg, Germany). Sequences produced by PCR (*LUC*) cloned into pCR®8 vectors by TOPO cloning (Invitrogen Ltd, Paisley, UK) according to the manufacturer's protocol.

These modules were then assembled into Level 1 (L1) constructs (see Figure 5.3.). Each L1 construct contained three L0s; a promoter, a coding sequence and a terminator. L1s utilise a set of standardised cloning vectors, numbered F1-F7 (forward orientation) and R1-R7 (reverse orientation) which were used to designate the position and orientation of L1s in the assembly of Level 2 (L2) constructs. L0 overhangs are specific to promoters, coding sequences and terminators. When digested using *BsaI*, these overhangs produce 4 bp sticky ends which are designed to only allow specific ligation of promoter, coding sequence and terminator in order. Additionally the overhangs add ligation sites at the 3' end of the promoter sequence and 5' end of the terminator sequence to allow ligation into a L1 cloning vector. The *BsaI* binding sites on these overhangs are located so as to be removed from the desired sequence after digestion, meaning that once digested, correct ligation of three L0 modules into a L1 vector will result in a sequence lacking any *BsaI* binding sites, preventing re-digestion of correctly ligated sequences. In this way, L1 assembly is performed in a single tube by adding both *BsaI* restriction enzyme and T4 DNA ligase and cycling between incubation temperatures ideal to each enzyme (digestion-ligation cycles).

L2 constructs (see Figure 5.4.) were assembled from one or more L1 constructs. A standardised L2 cloning vector was used for all L2 assemblies. At each stage, assembled

plasmids were prepared by transforming into *E. coli*, screening and isolating as already described. L1 cloning vectors add flanking sequences to the assembled L1 construct which act similarly to the L0 overhangs. These sequences contain binding sites for a second type II restriction enzyme, *BpiI*, and add specific sticky ends which allow L1 constructs to be assembled by digestion-ligation cycles in order of position 1-7 as defined by the L1 vector used in cloning. Position 1 (F1 or R1) L1 vectors add a site which binds to the L2 cloning vector's acceptor site and an end linker element, specific to the last position L1 vector being used, completes the circularisation of the plasmid. L1 constructs used must begin with position 1 and be in sequence although, by using a mix of forward (F1-F7) and reverse (R1-R7) oriented vectors, the individual L1 sequences within the L2 construct can be designed with varying orientations.

2.4.5. Isolation of plasmid DNA from *Escherichia coli*

Newly ligated plasmids (Section 2.4.4.) were transformed into One Shot® TOP10 Chemically Competent *E. coli* (Thermo Fisher Scientific, cat # C404010). Cells were gently thawed on ice before plasmid was added and cells were incubated on ice for a further 30 minutes. Cells were then heat shocked at 42 °C for 45 seconds and returned to ice for another 5 minutes. 1 ml of iced Luria-Bertani (LB) broth (Section 2.2.2.) was then added and cells were incubated at 37 °C with shaking at 200 rpm for 1 hour. Transformed cells were then plated on LB media agar (Section 2.2.2.) with appropriate antibiotics and grown overnight at 37 °C.

A single colony was selected and cultured in 5ml LB broth overnight at 37 °C with shaking at 200 rpm. Cell culture was then pelleted by centrifugation at 3000 rpm for 15

minutes at 4 °C and supernatant was removed. This pellet was then processed using a QIAprep Spin Miniprep Kit (Qiagen, UK, cat# 27104). Plasmid DNA was resuspended in 50 µl dH_2O and tested for purity and quantity using a NanoDrop™ ND-1000 Spectrophotometer (Thermo Fisher Scientific, UK) with NanoDrop™ 1000 Operation Software as per the manufacturer's instructions. Absorbance of a 2 µl sample at 230 nm, 260 nm and 280 nm was determined. A 260/280 ratio of ~1.8 and a 260/230 ratio of 1.8-2.2 was regarded as indicated 'pure' plasmid or genomic DNA.

If required, Sanger Sequencing was performed on 'pure' prepared plasmid DNA. Sequencing was completed through the Sanger Sequencing Service from Source Bioscience (Nottingham, UK).

2.4.6. Isolation of genomic DNA from *Arabidopsis thaliana* tissue

Genomic DNA was extracted from *Arabidopsis thaliana* tissue using a modified version of the previously described cetyltrimethyl ammonium bromide (CTAB) protocol (Clarke, 2009). Plant leaf material, or 10-20 *Arabidopsis* seedlings were collected and stored in a 1.5 ml microcentrifuge (MCC) tube with two 2.0 mm diameter AISI stainless steel balls (Dejay Distribution Ltd, Cornwall, UK) and immediately frozen in liquid nitrogen. Tissue was then disrupted by shaking with a Qiagen Retsch MM300 Tissuelyser (Qiagen, UK), with metal plates chilled on ice prior to use, at 30 rpm for 1 minute. Tissue was refrozen using dry ice and tissue disruption was repeated if grinding was incomplete after a single cycle. Ground tissue was briefly centrifuged before adding 300 µl of CTAB buffer (2% CTAB, 1.4 M NaCl, 100 mM Tris-HCl pH 8, 20 mM EDTA) and incubating for 30 minutes at 65 °C and then allowing to cool to room temperature. 300

µl of chloroform was then added before centrifuging at 13,000 rpm and 4 °C for 15 minutes. Chloroform-extracted supernatant was then transferred to a clean tube containing 200 µl of Isopropanol before briefly vortexing and then pelleting DNA by centrifugation at 13,000 rpm and 4 °C for 15 minutes. DNA pellet was then washed three times by resuspending in 70% ethanol (prepared in dH_2O) and centrifuging at 13,000 rpm and 4 °C for 10 minutes. Pellets were then dried by incubating open MCC tubes at room temperature for 30 minutes before resuspension in 50 µl of sterile dH_2O by heating at 55 °C for 10 minutes. The quantity, purity and integrity of isolated DNA was assessed by 1.5% (w/v) agarose gel electrophoresis as described (Section 2.4.1.).

2.5. Physiological characterisation of *Arabidopsis thaliana* seedlings

2.5.1. Characterisation of phototropism in response to unilateral light exposure

Surface sterilised seed (Section 2.3.3.) were sown individually in horizontal lines onto square 0.5x MS agar (Section 2.2.1.) plates. These plates were then stored in darkness at 4 °C for 1 day prior to testing in order to stratify seeds prior to light exposure. These seeds were saturated under cool fluorescent white light at 60 µmol m^{-2} s^{-1} for 4 hours before being wrapped in aluminium foil and transferred to a sealed growth chamber in darkness and grown upright for 3 days. After this period, 0.5 µmol m^{-2} s^{-1} of light from blue LEDs was applied unilaterally to induce phototropism. Images of these plants were then taken using an Epson Perfection 3490 Photo scanner (Epson, Suwa, Japan) and processed using ImageJ (Schneider et al., 2012).

2.5.2. Characterisation of light regulated hypocotyl elongation

Surface sterilised seed (Section 2.3.3.) were sown individually in horizontal lines onto square 0.5x MS agar (Section 2.2.1.) plates. Plates were then incubated in darkness at 4 °C for up to 1 day. Seeds were saturated under cool fluorescent white light at 60 µmol m^{-2} s^{-1} for 4 hours before being moved to coloured LEDs as per experimental requirements and grown upright for 5 days. Images of these plants were then taken using an Epson Perfection 3490 Photo scanner (Epson, Suwa, Japan) and processed using ImageJ (Schneider et al., 2012).

2.6. Techniques for live imaging of circadian rhythms in plants

2.6.1. Entrainment and free running conditions for imaging of circadian rhythms

Before imaging, surface sterilised (see Section 2.3.3.) *Arabidopsis thaliana* seeds were sown on 0.5x MS agar (see Section 2.2.1.) plates with or without sucrose as per experimental requirements. Seeds were then germinated under standard growth conditions (see Section 2.3.1.) and entrained for 6, 10 or 12 days in 12 hours white light: 12 hours dark cycles (12h:12h) before moving to constant conditions.

For growth under free running conditions, entrained seedlings were moved to constant light conditions at subjective dawn. Free running conditions were at 22 °C under constant red LED light, blue LED light or green LED light (Bright Technologies Ltd, China; for LED emission spectra see Figure 4.1.), or a combination of these lighting conditions. Light conditions were adjusted for individual plates with or without

filtration by neutral density filters (Stage Depot, UK), or in the case of tests under green LED light, filtration with #312 canary filters (Stage Depot, UK) or OG515 filters (Scholl Advanced Optics, Germany).

2.6.2. Characterisation of circadian rhythms using luciferase imaging

For luciferase imaging, individual seedlings or groups of 5-15 were entrained for 6 days as described in section 2.6.1. Plants were sprayed with filter sterilised 3 mM D-luciferin dissolved in 0.01% Triton X-100 (diluted in sterile dH_2O) the day before imaging. Plants were then transferred to free-running conditions under red, green or blue LEDs or a combination of these (Section 2.6.1.) as per experimental requirements, and imaged for 5 days using an Andor iKon-M CCD camera controlled by μManager (Edelstein et al., 2010) as has been previously described (Jones et al., 2010). Imaging data was processed using ImageJ (Schneider et al., 2012). Patterns of luciferase activity were fitted to cosine waves using Fourier Fast Transform-Non-Linear Least Squares analysis (FFT-NLLS) (Plautz et al., 1997) to estimate circadian period length. RAE is a measure of rhythmic robustness, with a value of 0 indicating an exact fit to a cosine wave (Plautz et al., 1997).

If experiments required plants treated with DCMU, selected plants were sprayed with a solution of filter sterilised 20 mmol DCMU dissolved in dimethyl sulphoxide (DMSO) diluted 1:1000 in sterile dH_20 at the same period which D-luciferin treatments were applied. Negative control treatments of filter sterilised DMSO only diluted 1:1000 in sterile dH_20 were also applied to control plants for these experiments.

2.6.3. Analysis of circadian phase responses to light qualities

To produce a phase response curve, plants were entrained for 6 days on 0.5x MS agar with 3% supplemental sucrose (see Section 2.6.1.). Plants were sprayed with filter sterilised 3 mM D-luciferin dissolved in 0.01% Triton X-100 (diluted in sterile dH_2O) the day before imaging. Plants were then transferred to free-running conditions for imaging in constant darkness for 5 days from subjective dusk (ZT12) of day 6 using an Andor iKon-M CCD camera controlled by μManager (Edelstein et al., 2010) as has been previously described (Jones et al., 2010). From ZT 48 until ZT 72, at 2 hour intervals, samples were transferred from darkness to 20 μmol m^{-2} s^{-1} blue, green or filtered green light from blue LEDs, green LEDs (Bright Technologies Ltd, China) or green LEDs covered with a #312 Canary filter (Stage Depot, UK) for 1 hour before returning to free-running conditions in darkness. Data points were plotted over time starting from subjective dawn of the first day of imaging (ZT0). To estimate circadian periods, patterns of luciferase activity were fitted to cosine waves using Fourier Fast Transform-Non-Linear Least Squares (FFT-NLLS, Plautz, *et al*. 1997). Relative amplitude error (RAE) was also calculated and used to approximate robustness of circadian rhythms, an RAE value of 0 corresponds to the perfect fit of a pattern to a cosine wave (Plautz, *et al*. 1997). Peak times were estimated manually for each sample and compared to an untreated control.

2.6.4. Characterisation of circadian rhythms of delayed chlorophyll fluorescence

For delayed fluorescence imaging, groups of 15–20 seedlings were entrained for 12 days (see Section 2.6.1.) on 0.5 X MS media agar (see Section 2.2.1.) before transfer to

free-running conditions under 20 µmol m^{-2} s^{-1} blue LED light (Bright Technologies Ltd, China), with images being captured every hour (Gould et al., 2009). Imaging was completed over 5 days using an Andor iKon-M CCD camera controlled by µManager (Edelstein et al., 2010) as has been previously described (Jones et al., 2010) before data was processed using ImageJ (Schneider et al., 2012). Patterns of delayed fluorescence were fitted to cosine waves using FFT-NLLS analysis (Plautz et al., 1997) to estimate circadian period length. RAE is a measure of rhythmic robustness, with a value of 0 indicating an exact fit to a cosine wave (Plautz et al., 1997).

2.6.5. Simultaneous characterisation of circadian rhythms of prompt chlorophyll *a* fluorescence and leaf movement in *Arabidopsis thaliana*

Prompt chlorophyll *a* fluorescence parameters were recorded with a Fluorimager imaging system (Technologica Ltd, Colchester, UK) using automated camera control and image processing scripts provided by the manufacturer. Seed was surface sterilised (see Section 2.3.3.) and approximately 30 individually spaced seedlings were entrained for 12 days in 12:12 light:dark cycles on 0.5x MS agar (see Section 2.6.1.) before transfer to the imaging chamber. In the imaging chamber, plants were illuminated with 20 µmol m^{-2} s^{-1} blue light using blue LEDs (Technologica Ltd, Colchester, UK), with measuring pulses of 5713 µmol m^{-2} s^{-1} blue light for 800 msec once per hour. Chlorophyll fluorescence was imaged using a Dolphin camera (Allied Vision Technologies, UK) through a long pass filter to exclude the blue light from the LEDs. Images of chlorophyll fluorescence emission from light-adapted leaves (F') and maximal fluorescence emission from the light-adapted leaf following the saturating measuring pulse (F_m') were used to calculate Fq'/Fm' where $F_m' - F' = F_q'$ (Baker, 2008). Measurement of F_q'/F_v'

and F_v'/F_m' necessitated the inclusion of a dark adaptation step for 10 min before measurement to allow calculation of the minimal fluorescence from a light-adapted leaf (F_o') where $F_o' = F_o/[(F_v/F_m) + (F_o/F_m)]$ (Baker,2008). Patterns of F_q'/F_m' were fitted to cosine waves using FFT-NLLS analysis (Plautz et al., 1997) to estimate circadian period length and additional circadian parameters.

Using the images produced during this prompt chlorophyll *a* fluorescence imaging protocol, leaf area (mm^2) visible to the camera, detected using Fluorimager image processing scripts (Technologica Ltd, UK), were also used to estimate circadian rhythms of leaf movement. These rhythms of mm^2 were fitted to cosine waves using FFT-NLLS analysis (Plautz et al., 1997) to estimate circadian period length and additional circadian parameters.

2.6.6. Isolation of chlorophyll fluorescence rhythms from leaf movement in *Arabidopsis thaliana*

In order to isolate rhythms of leaf movement from those of chlorophyll fluorescence, leaf movement was restricted whilst imaging prompt chlorophyll *a* fluorescence and leaf movement (using a modified version of the protocol seen in Section 2.6.5.). In order to restrict leaf movement, seedlings were entrained under standard conditions for 16-20 days on shallow soil trays. These plants were then flattened using a thin wire mesh which was suspended just above the leaves during imaging, restricting the potential movement of the leaves. Images were recorded as with a Fluorimager imaging system (Technologica Ltd, Colchester, UK,) (see section 2.6.5.) and data for prompt chloropyll *a* fluorescence and visible leaf area was obtained. Patterns of prompt fluorescence and

visible leaf area were fitted to cosine waves using Fourier Fast Transform Non-Linear Least Squares analysis (FFT-NLLS) (Plautz et al., 1997) to estimate circadian period length and additional parameters.

Chapter 3- Investigating a Role for Phototropins within the Circadian System of *Arabidopsis thaliana*

3.1. Introduction

The phototropins are a family of flavoproteins which act as blue light activated photoreceptors in many higher plants (Christie et al., 1999). Phototropins are serine-threonine kinases consisting of an N-terminal photosensory region containing two Light-Oxygen-Voltage (LOV) domains and a C-terminal protein kinase domain (Jones and Christie, 2008). Phototropins are known to mediate a range of photoresponses in plants including phototropism, stomatal opening, chloroplast movement and leaf positioning (Kinoshita et al., 2001, Inoue et al., 2008b, Liscum et al., 2014, Christie et al., 2015). *Arabidopsis thaliana* contains two phototropins (phot1 and phot2), which perform a range of overlapping and distinct functions (Takemiya et al., 2005). phot1 governs responses over a range of light intensities of light whilst phot2 predominantly regulates responses to higher fluence rates (Kagawa et al., 2001, Sakai et al., 2001). When exposed to light, phototropins autophosphorylate and re-locate from the cell membrane to intracellular locations including the cytosol, endoplasmic reticulum and Golgi apparatus (Sakamoto and Briggs, 2002, Kaiserli et al., 2009, Preuten et al., 2015). The phototropins are unique amongst plant photoreceptors in that they are not known to act as a light input into the circadian clock, a factor which we have examined in more detail after the recent discovery that phototropins are required to maintain rhythms of prompt chlorophyll fluorescence in *Arabidopsis* under blue light (Litthauer et al., 2015, Litthauer et al., 2016). In this chapter, the interactions between phototropins and the

circadian clock in *Arabidopsis* are investigated and some potential causes of prompt chlorophyll *a* fluorescence rhythms are examined.

3.2. Results

3.2.1. Imaging circadian rhythms in *Arabidopsis thaliana*

In order to understand the circadian clock, accurate measurement of circadian rhythms is essential. As such, a range of imaging techniques have been developed, each with its own strengths and limitations. In *Arabidopsis thaliana*, circadian rhythms can be measured *in planta* by analysing a range of circadian controlled processes. While subtle processes such as gene transcription can be analysed directly using methods such as real-time quantitative PCR (qRT-PCR) (Litthauer et al., 2015), methods utilizing cameras are particularly useful as they allow for higher throughput analyses (Tindall et al., 2015). Four major processes utilized to analyse circadian rhythms in *Arabidopsis* are; luciferase bioluminescence, delayed chlorophyll fluorescence, prompt chlorophyll fluorescence and leaf movement (Millar et al., 1992, Gould et al., 2009, Tindall et al., 2015, Litthauer et al., 2015). Each of these process allows measurement of the rhythms of the circadian clock via a different output pathway, providing a different degree of robustness and stability of measured rhythms and permitting more accurate measurement under different circumstances (Tindall et al., 2015). In order to provide a thorough analysis of these methods we used each to measure circadian rhythms in wild type *Arabidopsis* seedlings or wild type seedlings expressing circadian luciferase reporters and compared the accuracy and robustness of data produced using each of these methods.

3.2.1.1. Luciferase bioluminescence

Luciferase bioluminescence imaging is one of the most commonly used methods for assessing circadian rhythms in *Arabidopsis thaliana*, as it provides clear, accurate rhythms linked directly to the transcription of a targeted gene in a transgenic plant. Transgenic plants expressing a 'reporter construct' formed from the promoter region of a circadian clock regulated gene bound to a luciferase protein are used to produce rhythmic expression of luciferase bioluminescence aligned with rhythms of transcription of the circadian gene from which the promoter region was taken, which can then be used to measure circadian rhythms by imaging at specific timepoints (Millar et al., 1992).

Firstly, we measured rhythms of luciferase bioluminescence using a range of different circadian luciferase reporter constructs available from previous studies (see section 2.3.2.). Much of the original work using luciferase reporters to monitor circadian rhythms used sucrose as a media supplement to increase bioluminescence (Millar et al., 1995). More recently, work has demonstrated that exogenous sucrose acts as an input to the circadian system (Webb and Satake, 2015). We therefore sought to determine how previously reported circadian reporter lines behaved in the absence of sucrose.

Transgenic seedlings expressing either a *CCR2::LUC* (Figure 3.1.A.) or a *CCA1::LUC2* (Figure 3.1.B.) luciferase reporter construct were grown for 6 days under standard growth conditions (see Methods section 2.3.1.). *CCR2::LUC* seedlings were grown in groups of 5-10 seedlings while *CCA1::LUC2* seedlings were grown individually due to the greater brightness of their *LUC2* luciferase reporter. After entrainment (see Methods section 2.6.1.) under standard growth conditions, seedlings were transferred to free running conditions under 20 μmol m^{-2} s^{-1} of blue LED light for luciferase imaging (see

Methods section 2.6.2.). Waveforms of rhythms of luciferase bioluminescence from each test were collated and periods were estimated by FFT-NLLS using BRASS. Both *CCR2::LUC* and *CCA1::LUC2* seedlings produced rhythms with a circadian period of around 23.75h and with an RAE of around 0.2 (Figure 3.1.F.) although, as previously reported rhythms of *CCR2::LUC* peak at around dusk (CT14) (Kreps and Simon, 1997, Martin-Tryon et al., 2007) whilst *CCA1::LUC2* seedlings peak at around dawn (CT0) (Alabadi et al., 2001).

3.2.1.2. Delayed fluorescence

Delayed fluorescence, the process by which light excitation of photosystem II (PSII) leads to the subsequent emission of a photon (Gould et al., 2009) can also be used to assess circadian rhythms in *Arabidopsis* and many other plants. These emissions can be measured at regular intervals allowing for an estimation of the circadian period of the examined plant. In many plants, including *Arabidopsis thaliana* (Gould et al., 2009), delayed fluorescence emissions are present in wild type plants without need for genetic manipulation, making this process of measurement of circadian rhythms widely applicable.

Delayed fluorescence was measured in wild type plants arranged in groups of 5-10 seedlings were entrained for 12 days under standard growing conditions (see Methods section 2.3.1.) before transferring to a light box and imaging for delayed fluorescence under 20 μmol m^{-2} s^{-1} of blue LED light for delayed fluorescence imaging (see Methods section 2.6.4.). Rhythms of delayed fluorescence from each group of seedlings were collated and, using Biological Rhythms Analysis Software System (BRASS) (Millar et al., 2010), were normalised and baseline detrended before periods were estimated by Fast Fourier Transform with Non-Linear Least Squares (FFT-NLLS; Figure 3.1.C.). As

previously reported (Gould et al., 2009), rhythms obtained from delayed fluorescence under these conditions show a period of around 23h with a relative amplitude error (RAE) of around 0.4 (Figure 3.1.F). This demonstrates that delayed fluorescence can be monitored using our equipment, although the necessity of normalization to generate high amplitude rhythms suggested that the method required further optimization.

3.2.1.3. Prompt fluorescence

Rhythms can also be measured in wild type plants using prompt fluorescence imaging (see Methods section 2.6.5.). This method has been previously used to observe rhythms in the crassulacean acid metabolism (CAM) plant *Kalanchoë daigremontiana* (Malpas and Jones, 2016) and more recently has been applied to *Arabidopsis thaliana* (Litthauer et al., 2015). Using this method, rhythms of the operating efficiency of PSII (*Fq'/Fm'*, ϕ_{PSII}), can be observed to cycle with a circadian rhythm. The precise method by which this rhythm occurs is as of yet unknown but clear rhythms can be observed in individual *Arabidopsis* seedlings grown and entrained for 12-18 days under standard conditions (see methods section 2.3.1.) before being imaged under 20 μmol m^{-2} s^{-1} of blue light.

We evaluated circadian rhythms using prompt fluorescence in individual seedlings entrained under standard growth conditions for 12 days (Figure 3.1.D.). These plants were then imaged under 20 μmol m^{-2} s^{-1} of blue light by prompt fluorescence imaging (see Methods section 2.6.5.). Rhythms of *Fq'/Fm'* from each plant were collated and, using BRASS, were baseline detrended, before periods were estimated by FFT-NLLS. Rhythms of *Fq'/Fm'* measured under these conditions show a period of around 24.5h with an RAE of around 0.13 (Figure 3.1.F.).

3.2.1.4. Leaf movement

Although not applicable to monocots or other species with sessile leaves, rhythms of leaf movement are widely prevalent in plants (Tindall et al., 2015). Regardless of the method by which leaf movement occurs, rhythms of leaf movement are usually linked to the circadian clock (Tindall et al., 2015). While leaf movement has been a useful tool for measuring circadian rhythms for centuries (De Mairan, 1729, McClung, 2006), digital cameras and automatic tracking and measurement software has increased the accuracy by which rhythms of leaf movement can be measured, increasing throughput and making it a useful tool by which circadian rhythms can be measured in wild type plants (Tindall et al., 2015). In *Arabidopsis thaliana*, circadian controlled leaf movement ceases to occur in mature plants (Edwards and Millar, 2007), meaning that only young seedlings can be accurately measured using this method.

Commonly, leaf movement is measured using cameras held laterally to the leaves of the plant allowing for measurement of leaf angle and assessment of rhythms over time using movement tracking software (Edwards and Millar, 2007, Tindall et al., 2015, Muller and Jimenez-Gomez, 2016). We instead measured rhythms of leaf movement using cameras held vertically above the leaves, as with all other imaging methods described here, allowing for leaf movement to be estimated by measuring the area of the leaf visible to the camera at each time point. While this method does not allow for measurement of leaf angle over time, it does allow leaf movement to be analysed alongside other imaging methods simultaneously as we did alongside prompt fluorescence. As such, when assessing rhythms of leaf movement Individual plants were grown for 12 days under standard growth conditions and imaged under 20 µmol m^{-2} s^{-1} of blue light by prompt fluorescence imaging (see Methods section 2.6.6.). Waveforms of

visible leaf area rhythms (Figure3.1.E.) were then collated and grouped in the same way as described with rhythms of *Fq'/Fm'* and BRASS was used to baseline detrend and estimate periods by FFT-NLLS. Under these conditions, leaf movement cycles with a period of around 22.3h with an RAE of around 0.37 (Figure 3.1.F.).

Each of these methods (Figure 3.1.) was used to measure circadian rhythms in wild type *Arabidopsis* seedlings under 20 μmol m^{-2} s^{-1} of constant blue LED light and whilst all methods produced a circadian rhythm of around 24h each yielded rhythms with a slightly different period and robustness. The brightest, most robust rhythms were observed by luciferase imaging. Using both the *CCR2::LUC* (Figure 3.1.A.) and the *CCA1::LUC2* (Figure 3.1.B.) reporter produced similar measurements with a period of around 23.75h and an RAE of 0.2. The *CCA1::LUC2* reporter however should also be noted to produce much brighter luciferase bioluminescence than the *CCR2::LUC* reporter, which makes measurement of rhythms clearer in individual seedlings without the need for grouping seedlings together to increase total brightness per datapoint. By comparison, delayed fluorescence (Figure3.1.C.) produces a fairly short period of around 23h and has very poor robustness with an RAE of around 0.4, while prompt fluorescence (Figure 3.1.D.) produces a long but robust period of 24.5h with an RAE of around 0.13. Circadian period measurements derived from leaf movement reported a short circadian period of approximately 22.3h with an RAE of around 0.37 (Figure3.1.E), it should be noted however that the reliability of these data are limited by the low amplitude of rhythms observed.

Furthermore, it should be noted that luciferase imaging allows for analysis of the circadian rhythms of transcription of the individual gene to which the luciferase reporter being used is associated, whereas delayed fluorescence, prompt fluorescence

and leaf movement all allow an assessment of the rhythms of the whole circadian system rather than the rhythms of a specific gene. Additionally, leaf movement and delayed and prompt chlorophyll fluorescence imaging methods do benefit over luciferase imaging in that transgenic plants expressing luciferase reporters are not required for measurements to be made. However, given the low amplitude of leaf movement and delayed fluorescence we decided to utilise prompt fluorescence and luciferase imaging to examine circadian behaviour.

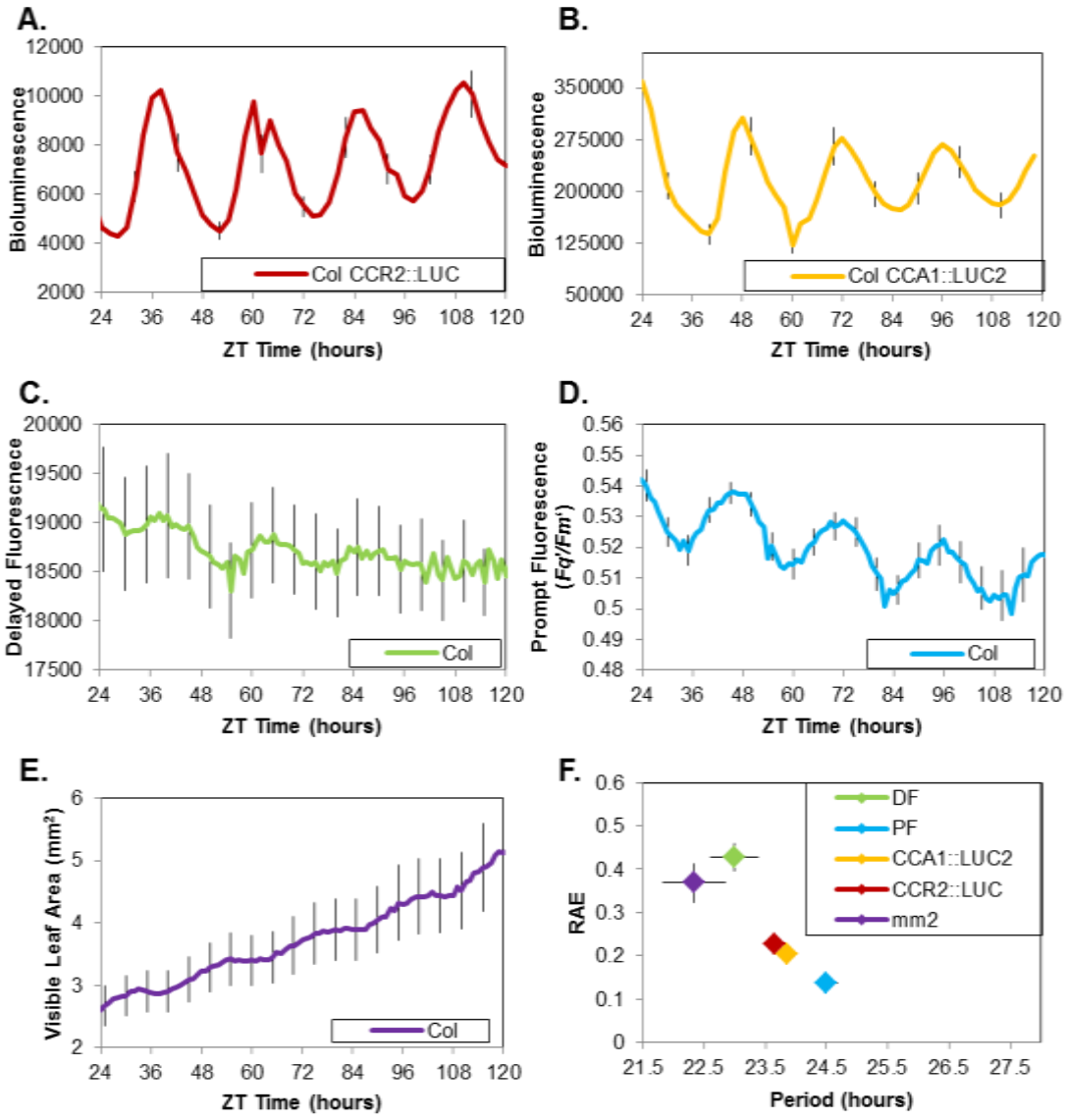

Figure 3.1. Comparison of methods for live imaging of circadian rhythms in *Arabidopsis thaliana.* Waveforms of luciferase activity in 6 day old Col-0 seedlings expressing either a (**A**) *CCR2::LUC* or (**B**) *CCA1::LUC2* luciferase reporter in constant blue light. (**C**) Delayed fluorescence waveform in 12 day old Col-0 seedlings in constant blue light. (**D**) Waveforms of PSII operating efficiency (F_q'/F_m') calculated from prompt chlorophyll fluorescence imaging of 12 day old Col-0 seedlings under blue light. (**E**) Waveforms of leaf movement visualised as visible leaf area (mm^2) from prompt chlorophyll fluorescence imaging of 12 day old Col-0 seedlings under blue light. (**F**) Circadian period estimates of Col-0 seedlings plotted against Relative Amplitude Error (RAE) determined for each imaging method shown previously (**A-E**). Error bars indicate standard error of the mean with n=10-23. Waveforms are an average of time series data for seedlings used in analysis, with error bars shown every 5-10 hours for clarity. Data from one of three independent experiments are shown.

3.2.2. Rhythms of F_q'/F_m' in *Arabidopsis thaliana* are independent of leaf movement

Utilization of prompt fluorescence to measure circadian rhythms is a recent innovation (Litthauer et al., 2015, Malpas and Jones, 2016), and so we sought to understand the mechanisms underlying rhythms of prompt fluorescence. Due to the subtle nature of rhythms of *Fq'/Fm'*, it was considered that these rhythms may have been derived from the angle of leaves to the camera caused by rhythms of leaf movement rather than a true circadian controlled change in the operating efficiency of PSII. In order to assess this possibility, the leaves of seedlings imaged using prompt fluorescence imaging (Methods 5.6.5.) were restrained and the visible area of these leaves were also measured (Methods 5.6.6.) over time in order to simultaneously measure rhythms of leaf movement in order to confirm that the leaves were properly restrained (Figure 3.2.A.).

Individual seedlings entrained on soil for 18 days under standard conditions (Methods 2.3.1.) were positioned under a restraining wire mesh and imaged under 20 μmol m^{-2} s^{-1} of blue light by prompt fluorescence imaging (Methods 2.6.6., Figure 3.2.A.). Rhythms of *Fq'/Fm'* and visible leaf area (mm^2) were collated and periods of *Fq'/Fm'* were estimated by FFT-NLS using BRASS. No circadian period could be calculated for leaf movement in restrained leaves as no rhythmic change in visible leaf area could be observed (Figure 3.2.A., Figure 3.2.D.). However, rhythms of *Fq'/Fm'* in restrained leaves cycled with a period of around 24.5h and an RAE of around 0.16 (Figure 3.2.A., Figure 3.2.D.).

We next determined whether restriction of leaf movement altered rhythms of Fq'/Fm'. Unrestrained seedlings were grown for 12 days under standard conditions (Methods 2.3.1.) and imaged simultaneously under constant blue light for rhythms of F_q'/F_m'

(Figure 3.2.B.) and leaf movement (Figure 3.2.C.). Circadian period estimates (Figure 3.2.D.) for F_q'/F_m' and leaf movement were calculated and plotted against RAE alongside the period of F_q'/F_m' in restrained leaves. Unrestrained rhythms of F_q'/F_m' cycled with a period of approximately 23.1h and an RAE of around 0.15 and unrestrained rhythms of leaf movement cycled with an approximately 22.3h period and an RAE of around 0.37. There was no significant difference in circadian period length between restrained and unrestrained rhythms of F_q'/F_m' (p= 0.725). Additionally, there was no significant difference in circadian period length between unrestrained rhythms of F_q'/F_m' and leaf area (p= 0.992). These data demonstrate that while rhythms of F_q'/F_m' cycle with a similar period to rhythms of leaf movement, they are not directly caused by leaf movement and are a distinct physiological process in *Arabidopsis thaliana*.

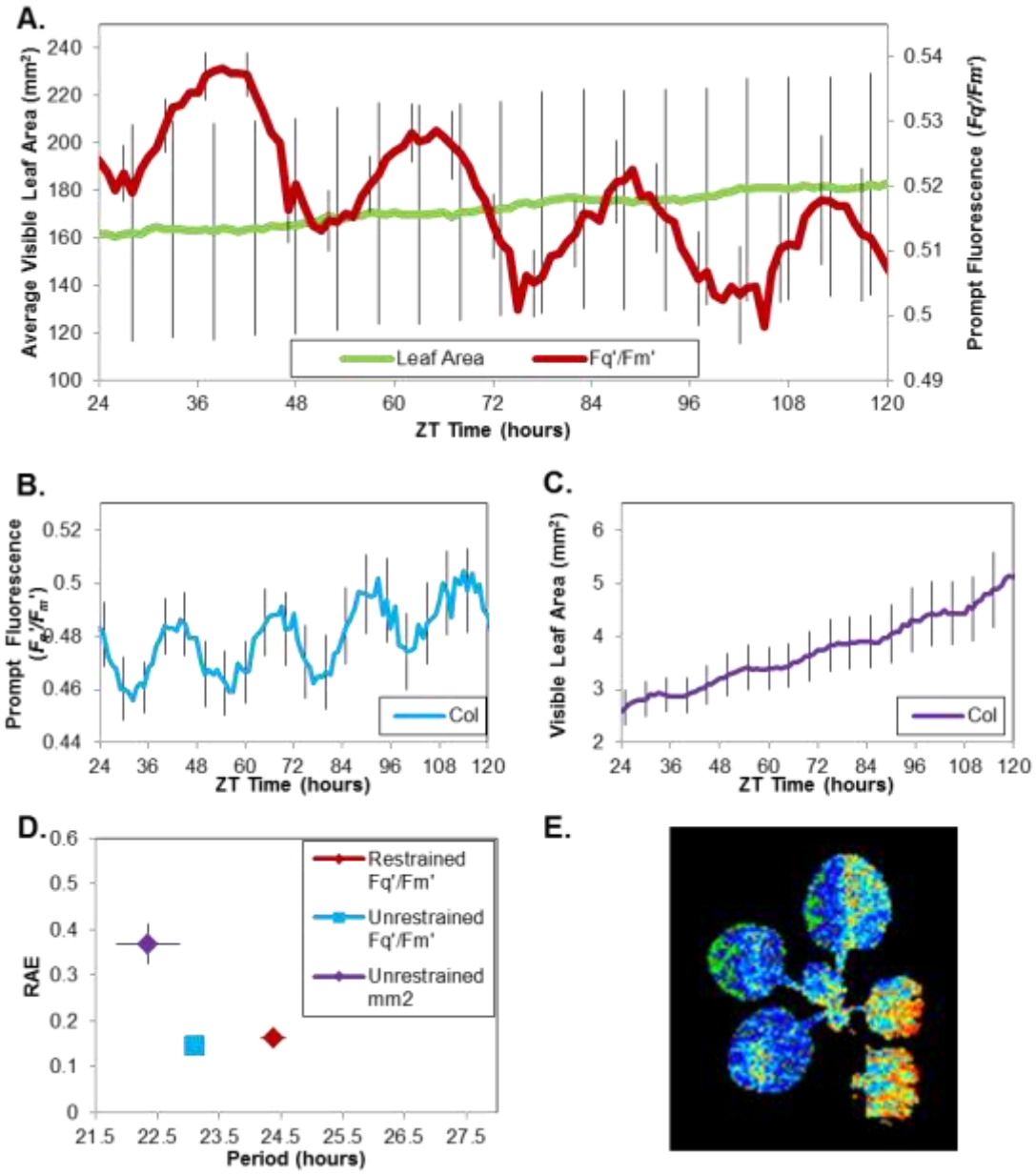

Figure 3.2. Prompt chlorophyll fluorescence rhythms imaged simultaneously with leaf movement. (**A**) Waveforms from seedlings restrained under a wire mesh showing rhythms of prompt chlorophyll fluorescence (F_q'/F_m'; red) and leaf movement measured from visible leaf area from above (mm^2; green). Seedlings were grown for 18 days on soil and entrained under 12:12 light:dark cycles under 60 µmol m^{-2} s^{-1} white light before imaging under 20 µmol m^{-2} s^{-1} constant blue light. (**B**, **C**) Waveforms from unrestrained seedlings sowing rhythms of (**B**) prompt chlorophyll fluorescence (F_q'/F_m'; blue) and (**C**) leaf movement measured from visible leaf area from above (mm^2; purple) in 12 day old seedlings grown on 0.5x MS agar and entrained under 12:12 light:dark cycles under 60 µmol m^{-2} s^{-1} white light before imaging under 20 µmol m^{-2} s^{-1} constant blue light. (**D**) Circadian period estimates of waveforms from restrained (**A**) and unrestrained (**B**, **C**) seedlings showing leaf movement (green, purple) and F_q'/F_m' (red, blue) rhythms. Error bars indicate standard error of the mean. (**E**) Prompt fluorescence image of an 18 day old seedling restrained by wire mesh.

3.2.3. Exogenous oxidised quinone inhibits circadian rhythms of F_q'/F_m' in *Arabidopsis thaliana*

The circadian clock in *Arabidopsis* includes numerous rhythmic pathways which occur independantly of transcription. Amongst these are the rhythms of peroxiredoxin (PRX) reduction which cycle in the chloroplast in absence of rhythmic nuclear transcription (Edgar et al., 2012). The cyanobacterial circadian clock has been demonstrated to be directly influenced by oxidation state, resetting to a dusk phase with the application of exogenous oxidised quinone (Qo) (Kim et al., 2012, Hosokawa et al., 2013). Due to the highly conserved nature of the cyanobacterial clock (Edgar et al., 2012) and the ancestral similarities between cyanobacteria and plant chloroplasts (Arabidopsis Genome, 2000, Martin et al., 2002, Raven and Allen, 2003, Mittag et al., 2005), it was hypothesised that altering the redox state in *Arabidopsis* chloroplasts might influence circadian rhythms of PRX within the chloroplast which may be connected to rhythms of F_q'/F_m'.

In order to test this hypothesis, seedlings entrained for 12 days under standard conditions (Methods 2.3.1.) were imaged using prompt chlorophyll fluorescence imaging techniques (Methods 2.6.5.). A spray treatment of Qo dissolved in DMSO or a control treatment of DMSO only was then applied to the seedlings during imaging at ZT24. Waveforms of F_q'/F_m' (Figure 3.3.A.) show a loss of amplitude and rhythmicity immediately after treatment with Qo, this effect upon rhythmicity lasts throughout the test period although amplitude begins to recover around 48h after Qo treatment. Little to no effect upon rhythms of F_q'/F_m' was observed in seedlings treated with the control spray of DMSO. Circadian period estimates calclulated from waveforms of F_q'/F_m' after treatment with Qo or DMSO were plotted against RAE of F_q'/F_m' (Figure 3.3.B.) showing

the control treated seedlings to have a period of around 25h and an RAE of around 0.25 while the Qo treated seedlings have a significantly increased period of around 26.4h (p= 0.00342**) and an RAE of around 0.5. These data indicate that while circadian rhythms of F_q'/F_m' in *Arabidopsis* are not reset to a dusk state with the application of Qo as has been seen in cyanobacteria, they are disrupted significantly by exogenous Qo.

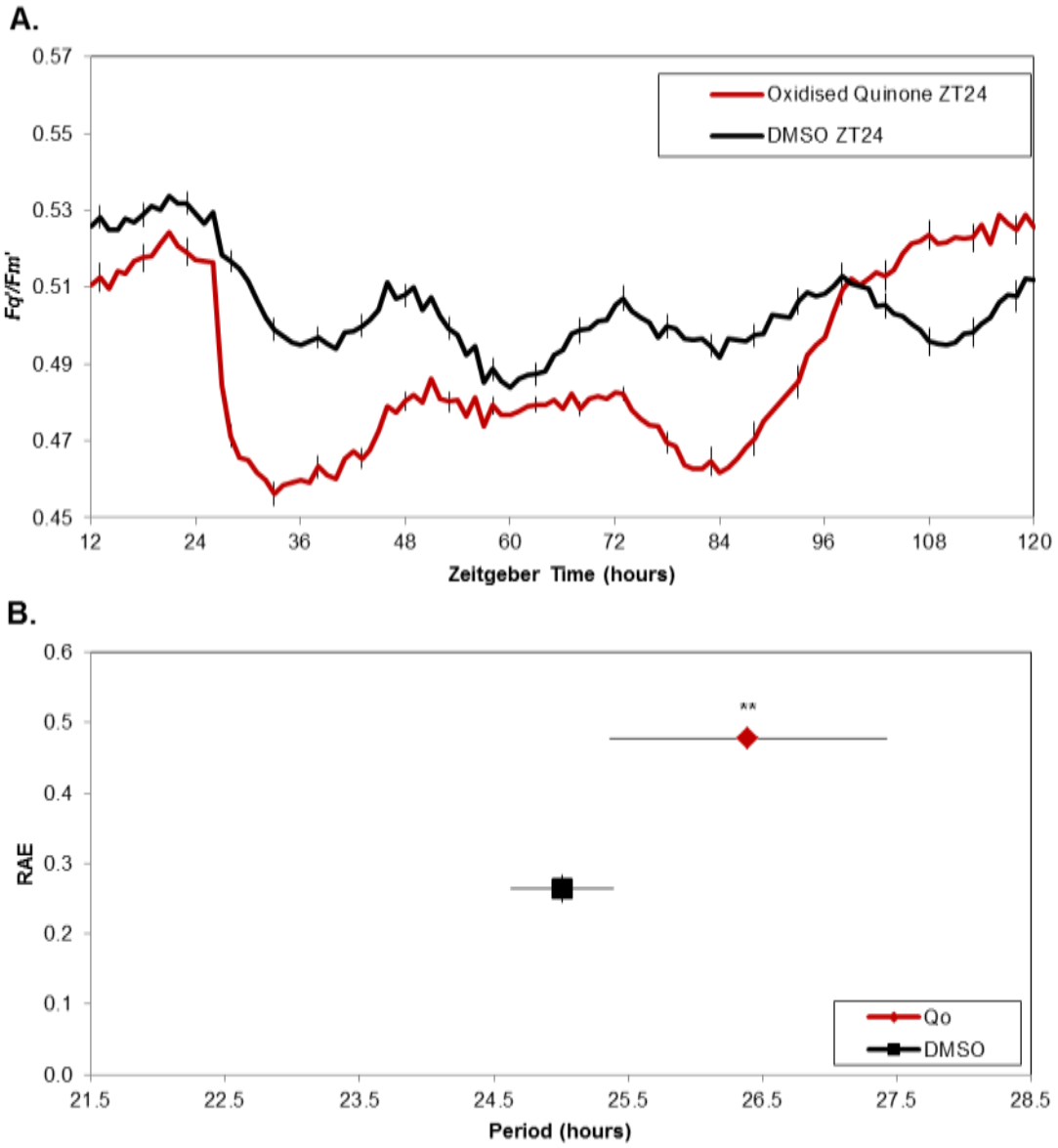

Figure 3.3. Exogenous oxidised quinone inhibits rhythms of F_q'/F_m' in *Arabidopsis thaliana*. (**A**) Waveforms of F_q'/F_m' rhythms in Col-0 seedlings treated at ZT24 with either oxidised quinone (Qo; dissolved in DMSO; shown in red) or control treatments of DMSO only (shown in black). (B) Circadian period estimates of Col-0 seedlings treated with either Qo (red) or control treatments of DMSO only (black). Seedlings were grown for 12 days on 0.5x MS agar plates and entrained in 12h:12h light:dark cycles under 60 µmol m^{-2} s^{-1} white light before imaging under 20 µmol m^{-2} s^{-1} constant blue light. Error bars indicate standard error of the mean with n=8-11. For waveforms, error bars are shown every 5 hours for clarity. Data from one of three independent experiments are shown. Asterisks indicates statistically significant difference in period compared to DMSO treated control (p<0.001; students T test)

3.2.4. Loss of function in a range of redox related chloroplast proteins have little effect on rhythms of F_q'/F_m' in *Arabidopsis thaliana*

In order to try to better understand the process by which rhythms of F_q'/F_m' occur in *Arabidopsis* and to better determine whether these rhythms are dependent upon the redox state of the chloroplast, prompt fluorescence imaging was used to analyse F_q'/F_m' rhythms in a range of mutants lacking function of one of a group of proteins associated with redox regulation in the chloroplast.

cpCK2α is a chloroplast protein named for its high homology to the α subunit of cystolic casein kinase (CK2) (Ogrzewalla et al., 2002). In mustard (*Sinapis alba*) cpCK2α functions similarly to plastid transcription kinase (PTK), a serine-specific protein kinase associated with the plastid encoded RNA polymerase (PEP), PEP-A, a major, redox-regulated, photosynthesis-related protein in the chloroplast (Ogrzewalla et al., 2002, Diaz et al., 2018). cpCK2α has also been shown to phosphorylate components of the plastid transcription apparatus of the chloroplast (Ogrzewalla et al., 2002, Jeong et al., 2004).

Chloroplast sensor kinase (CSK) senses and regulates the plastiquinone redox state within both photosystems (PSI and PSII) through both transcriptional regulation of PSI and PSII reaction centre genes and phosphorylation of the light-harvesting complexes of PSI and PSII (Puthiyaveetil et al., 2008, Allen et al., 2011, Puthiyaveetil et al., 2013).

NADPH thioredoxin reductase C (NTRC) and sulfiredoxin (SRX) are a pair of proteins involved in the maintenance and regulation of 2-Cys peroxiredoxins (2-Cys PRXs), an enzyme which is highly abundant within the chloroplast and acts to regulate hydrogen peroxide levels and oxidation cycles within the chloroplast (Edgar et al., 2012, Puerto-

Galan et al., 2015). Under oxidising conditions, 2-Cys PRXs can become overoxidised and thereby inactivated. NTRC regulates this state by reducing a disulphide bridge in 2-Cys PRX, allowing overoxidation to occur (Puerto-Galan et al., 2015). SRX acts to counteract this activity by reverting overoxidated 2-Cys PRX to its active state (Puerto-Galan et al., 2015). While the activity of NTRC and SRX have been shown to cycle alongside the peroxidatic catalytic cycle of 2-Cys PRXs, it has been proposed that the transcription of these genes is not circadian controlled and that 2-Cys PRX peroxidation in the chloroplast is rather a light dependant cyclic activity (Puerto-Galan et al., 2015).

Waveforms of F_q'/F_m' rhythms in 12 day old Col-0 knockout mutant seedlings for each of these chloroplast proteins; (Figure 3.4.A.) cpCK2*α* (*cpck-2-A*) and CSK (*cskA* and *cskB*), along with (Figure 3.4.C.) NTRC (*ntrc*) and SRX (*srx*), were imaged using prompt fluorescence imaging under 20 μmol m^{-2} s^{-1} blue light (Methods 2.6.5.) and circadian periods calculated from these waveforms were plotted against RAE of F_q'/F_m' (Figures 3.4.B. and 3.4.D.). All plants tested presented a circadian period of F_q'/F_m' rhythms of around 22-23 hours with no significant difference in circadian period between Col-0 wild type and any of the knockout mutants tested (*p values*: *cpck-2-A*= 0.8482, *cskA*=0.7999, *cskB*=0.9718, *ntrc* = 0.4771, *srx* =0.0161).

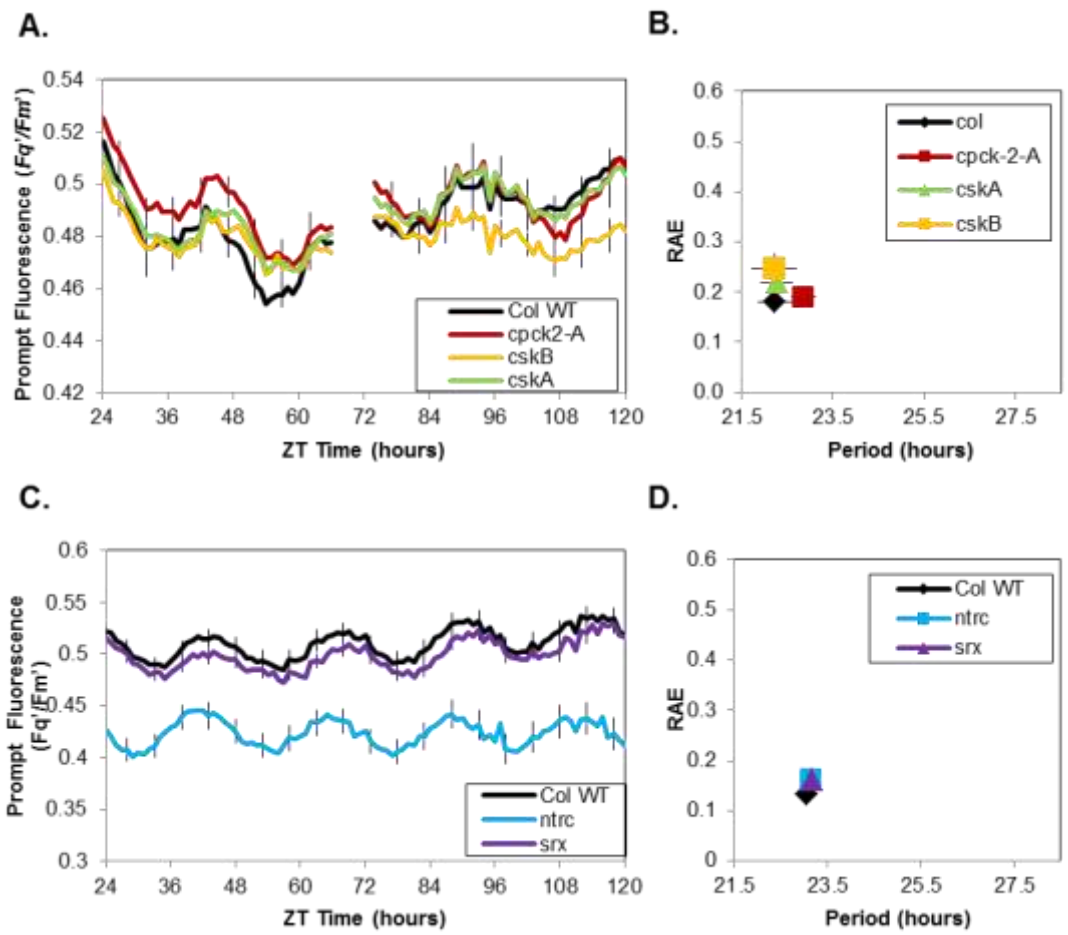

Figure 3.4. F_q'/F_m' rhythms in chloroplast protein mutants under blue light. (**A**, **C**) Waveforms and (**B**, **D**) circadian period estimates plotted against Relative Amplitude Error (RAE) of F_q'/F_m' rhythms in Col-0 (black) and (**A**, **B**) *cpck-2-A* (red), *cskA* (green) and *cskB* (yellow) or (**C**, **D**) *ntrc* (blue) and *srx* (purple) chloroplast protein mutant seedlings. Seedlings were grown for 12 days on 0.5x MS agar plates and entrained in 12h:12h light:dark cycles under 60 µmol m^{-2} s^{-1} white light before imaging under 20 µmol m^{-2} s^{-1} constant blue light. Error bars indicate standard error of the mean with n=7-26. For waveforms, error bars are shown every 5 hours for clarity. Data from one of three independent experiments are shown.

3.2.5. Inhibiting internalisation of phototropins does not inhibit circadian rhythms of F_q'/F_m' in *Arabidopsis thaliana*

It has been shown that phototropins are required to maintain rhythms of F_q'/F_m' (Litthauer et al., 2015), although the mechanism causing this to occur is currently unknown. The phototropins regulate chloroplast subcellular localisation in response to blue light exposure (Jarillo et al., 2001b, Kagawa et al., 2001, Sakai et al., 2001, Preuten et al., 2015) and, it was hypothesised may, through this process, indirectly mediate rhythms of F_q'/F_m'.

In order to test this hypothesis, mutants in which phot1 internalisation has been prevented via the addition of a lipid anchoring farnesyl group (*farn*) were utilised (Preuten et al., 2015). *farn* mutants are *phot1 phot2* double mutants containing an insertional, modified phot1- green fluorescent protein (GFP) fusion protein in which the *GFP* tag has an added C-terminal farnesyl group. This farnesyl group acts as a lipid anchor for the new fusion protein, binding it to the cell membrane and preventing internalisation of the phot1 protein. It has been shown that in these mutants, phototropism and light-mediated turnover of phot1 are not inhibited, suggesting that internalisation is not involved in this function (Preuten et al., 2015). Additionally, *farn* mutants show little phenotypic difference from Col-0 wild type (Figure 3.5.A.).

Col-0 seedlings, along with *phot1 phot2* double mutants *farn* mutants were entrained for 12 days under standard conditions (Methods 2.6.1.) and imaged using prompt fluorescence imaging (Methods 2.6.5.). Waveforms of F_q'/F_m' rhythms were measured and used to estimate circadian periods, which were plotted against RAE of F_q'/F_m' (Figures 3.5.B and 3.5.C.). Circadian periods of *phot1-5 phot2-1* (*phot1 phot2*) and *farn* mutants were not significantly different from the periods of wild type seedlings tested

(*p values*: *phot1phot2*= 0.9224, *farn*= 0.4972) with all periods of F_q'/F_m' rhythms being around 24h. However, as has been previously reported (Litthauer et al., 2015), *phot1 phot2* mutants presented a significant loss of rhythmicity with an RAE of around 0.24 (*p* <0.001) compared to around 0.16 seen in Col-0, this phenotype is recovered in the *farn* mutant lines (RAE of around 0.12; *p*= 0.935).

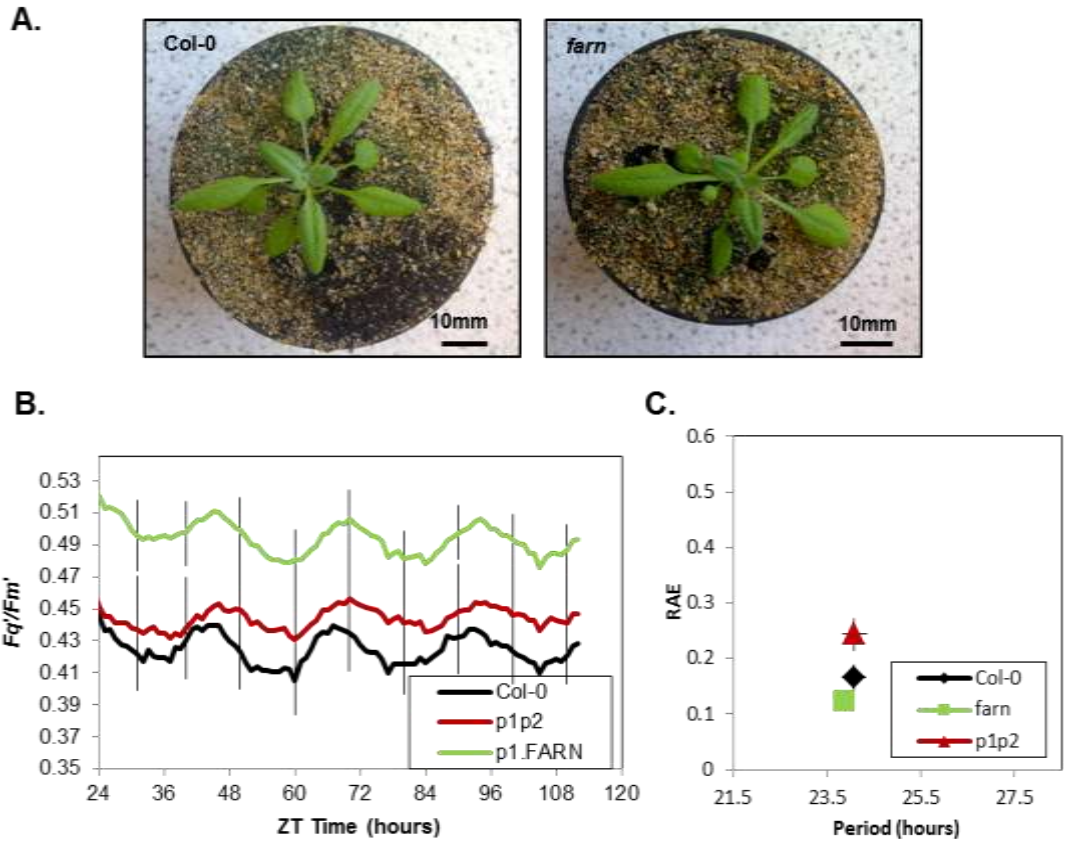

Figure 3.5. F_q'/F_m' rhythms in mutants with lipid anchored phototropin 1. (**A**) Morphology of Col-0 and *farn* seedlings after 4 weeks of growth on soil under 12:12 light:dark photoperiod cycles under 60 µmol m^{-2} s^{-1} cool white fluorescent light. (**B**) Waveforms and (**C**) circadian period estimates plotted against Relative Amplitude Error (RAE) of F_q'/F_m' in Col-0 (black), *phot1phot2* double phototropin mutants (*p1p2*; red) and *phot1.farn* (*farn*; green) lipid anchored phototropin mutants entrained for 12 days under 12h:12h light:dark cycles under 60 µmol m^{-2} s^{-1} white light before imaging under 20 µmol m^{-2} s^{-1} constant blue light. Error bars indicate standard error of the mean with n=9-11. For waveforms, error bars are shown every 5 hours for clarity. Data from one of two independent experiments are shown.

3.2.6. The effects of different circadian luciferase reporters upon measured rhythms of luciferase bioluminescence

In order to better assess what effects phototropins may be having upon circadian rhythms in *Arabidopsis*, we planned to produce phototropin loss of function mutant lines containing circadian luciferase reporter constructs. Before this was undertaken however, we assessed the rhythmicity, robustness and brightness of a range of luciferase reporter constructs in wild type in order to judge which would be best for use in our phototropin mutants.

The circadian clock controls expression of a wide range of genes in *Arabidopsis* (Hsu and Harmer, 2014) and as such, the promoter regions of many clock associated genes can be used to produce luciferase reporter fusion proteins in order to observe circadian rhythms of transcription of these genes using luciferase imaging. Differently controlled circadian genes cycle with different phases, peaking at different points in the circadian cycle. As such, wild type plants expressing different circadian reporter genes should generally present the same circadian period but may have a wide range of phases. Additionally, the expression levels of the gene from which the promoter region is taken will control the level of luciferase bioluminescence and as such, genes under more robust circadian control will present clearer rhythms of luciferase bioluminescence (Introduction 1.6.5.).

In order to assess the different circadian reporter genes available to us, Col-0 wild type seedlings expressing a range (*TOC1:LUC, LHY::LUC, CAB::LUC, GI::LUC, CCR2::LUC* and *CCA1::LUC2*) of circadian reporter constructs were entrained for 6 days under standard growth conditions. All plants were grown in clumps of 5-10 seedlings except those expressing the *CCA1::LUC2* reporter which were grown individually due to the increased

brightness of the *LUC2* reporter over the *LUC* reporter in each other line. Entrained seedlings were imaged under 20 μmol m^{-2} s^{-1} of blue LED light by luciferase imaging (Methods 2.6.2.). Waveforms of luciferase bioluminescence (Figure 3.6.A.) from each group of plants were collated and circadian period estimates, plotted against RAE (Figure 3.6.B.) of these waveforms were measured. Rhythms of luciferase bioluminescence in each reporter line measured under these conditions show a period of around 25h with no significant difference between the periods of any of these reporter lines (*p values*= >0.2). It should be noted that while the periods of each of these luciferase reporter lines is similar, the phase of these waveforms (Figure 3.6.A.) vary depending upon the phase of the reporter gene with genes such as *CCA1* peaking in the morning and *TOC1* peaking in the evening. Additionally, while the *CAB::LUC* was brighter than all other *LUC* reporters tested, it should be noted that *CCA1::LUC2* lines were measured individually rather than in groups of 5-10 seedlings, showing that the *CCA1::LUC2* reporter may be brighter per seedling than the *CAB::LUC* reporter. Due to the robustness and clarity of rhythms seen in individual seedlings here, and due to the nature of *CCA1* as a core circadian clock gene, the *CCA1::LUC2* reporter was chosen for production of our phototropin knockout luciferase reporter lines.

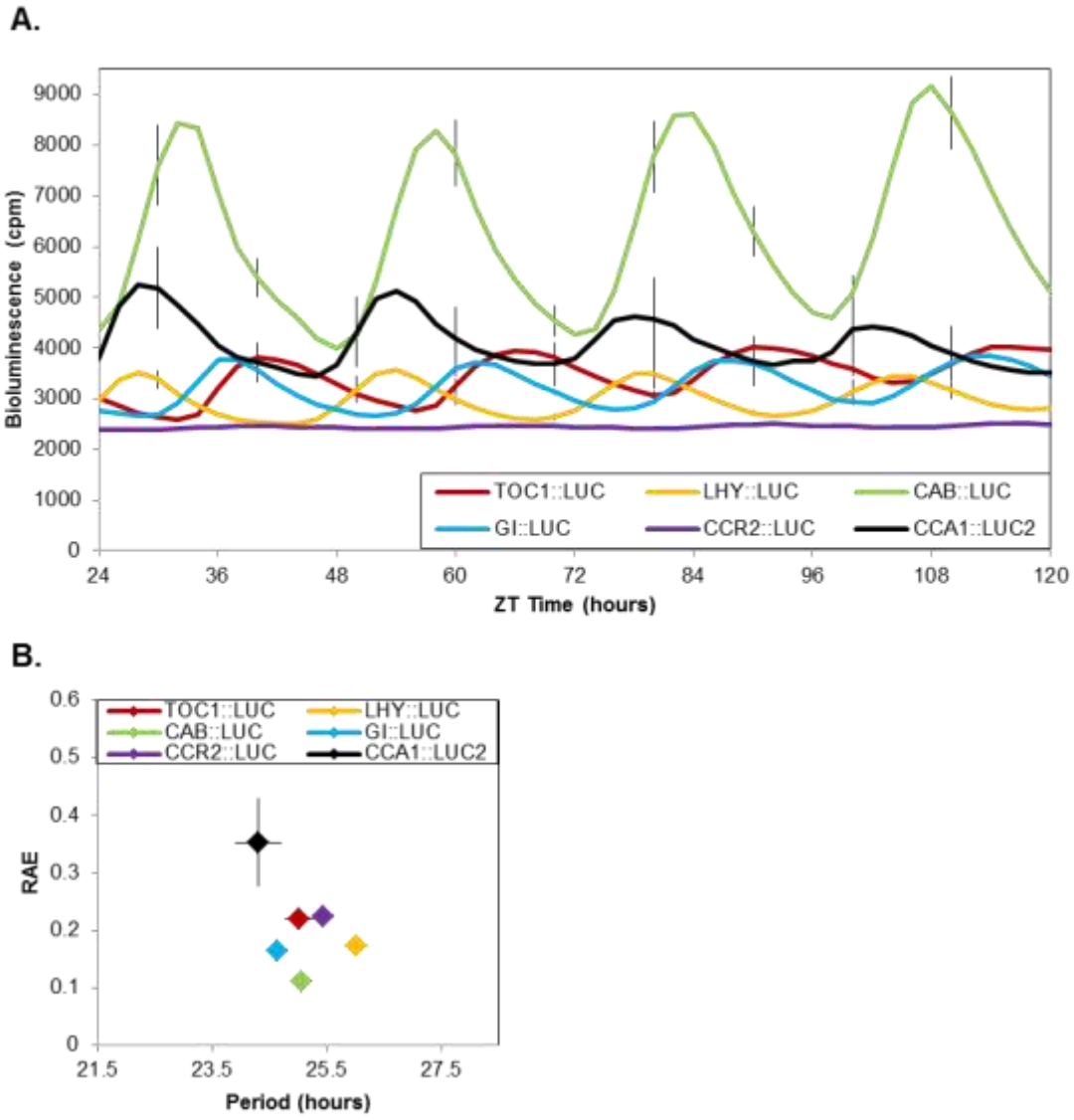

Figure 3.6. Measuring circadian rhythms using luciferase bioluminescence driven by a range of reporter constructs. (**A**) Waveforms and (**B**) circadian period estimates plotted against Relative Amplitude Error (RAE) of luciferase bioluminescence in Col-0 seedlings expressing the luciferase reporter constructs; *TOC1::LUC* (red), *LHY::LUC* (yellow), *CAB::LUC* (green), *GI::LUC* (blue), *CCR2::LUC* (purple) or *CCA1::LUC2* (black). Excluding seedlings expressing *CCA1::LUC2* which were grown individually, seedlings were grown in groups of 5-10 on 0.5x MS agar plates. Seedlings were entrained for 6 days under 12h:12h light:dark cycles under 60 µmol m^{-2} s^{-1} white light before imaging under 20 µmol m^{-2} s^{-1} constant blue light. Error bars indicate standard error of the mean with n=4-10. For waveforms, error bars are shown every 5 hours for clarity. Data from one of two independent experiments are shown.

3.2.7. Identifying phototropin single and double knockout mutant lines

It has been shown phototropins are required to maintain robustness of rhythms of *Fq'/Fm'* under blue light and so we were curious whether phototropins were also necessary to maintain circadian rhythms in the nucleus (Litthauer et al., 2015). In order to assess any further influence phototropins upon circadian rhythms in *Arabidopsis* we produced transgenic circadian reporter lines expressing a *CCA1::LUC2* reporter gene in *Arabidopsis* phototropin knockout mutant lines. The previously described single mutant lines for phot1 (*phot1-5*) and phot2 (*phot2-101*) as well as the double mutant *phot1-5phot2-1* (*phot1phot2, p1p2*) were crossed with a wild type line expressing a *CCA1::LUC2* circadian reporter gene and F3 hybrid lines expressing this reporter were identified using the kanamycin resistance associated with this reporter line.

In order to ensure that these reporter lines were knockouts for the appropriate phototropins, genotyping using appropriate primers (Appendix Table A1) was performed on the *phot1-5* (Figure 3.7.B.) and *phot2-101* (Figure 3.7.C.) single mutant lines. Primers for the identification of the *phot2-1* allele proved to be ineffective, and as such the double mutant *phot1-5 phot2-1* lines could not be properly identified using genotyping. As such these seedlings were instead screened by phenotypes found in *phot1 phot2* double mutants; a loss of phototropism (Methods 2.5.1, Figure 3.7.A.) and pronounced leaf folding (Figure 3.7.D.). Lines found to include only plants with these phenotypes in tests of around 20 seedlings were identified and seed from these plants were used for further testing of the *p1p2 CCA1::LUC2* reporter mutant.

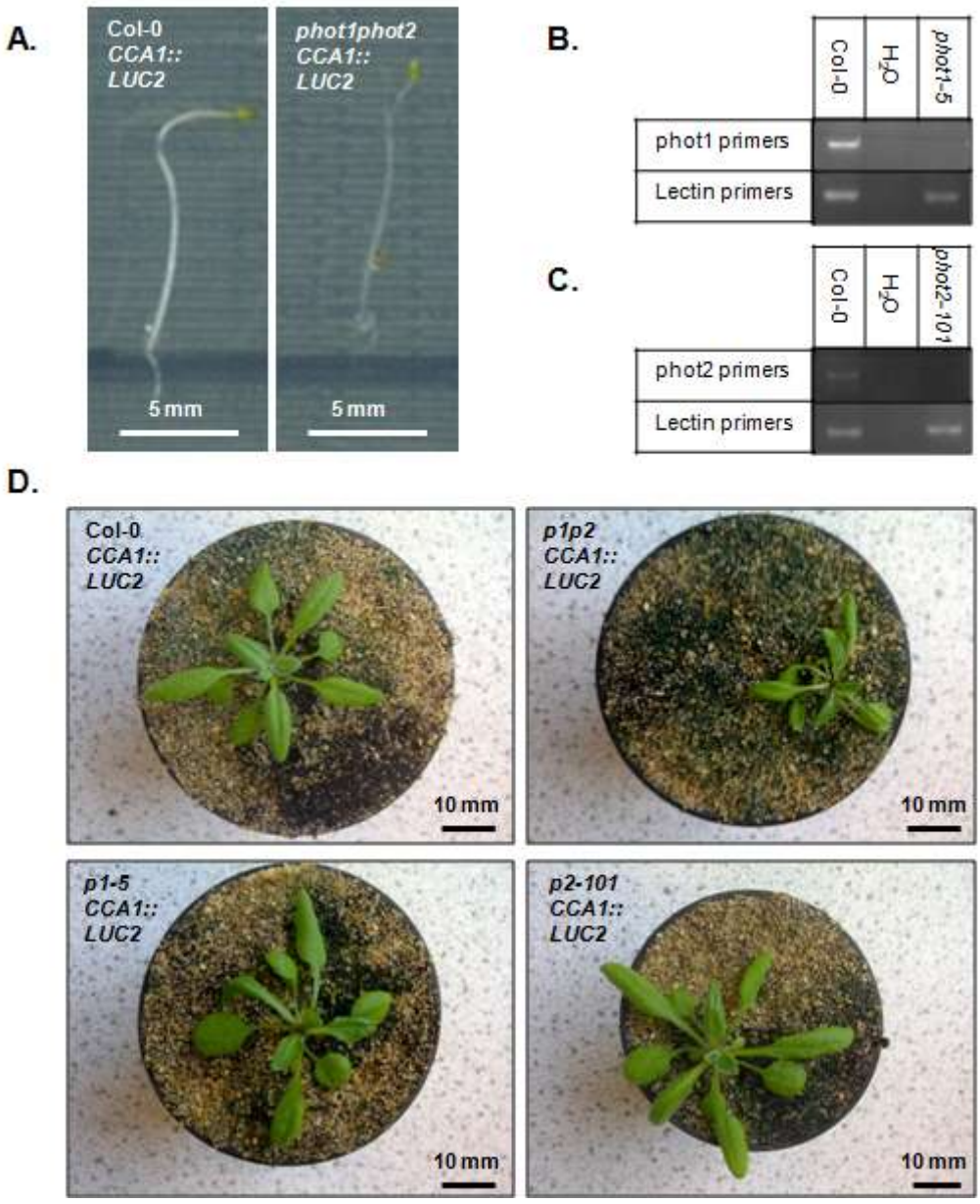

Figure 3.7. Phototropin loss of function mutants expressing luciferase reporter constructs in *Arabidopsis thaliana*. Before further testing, plants containing the *CCA1::LUC2* reporter were identified by screening with kanamycin. (**A**) Morphology of Col-0 *CCA1::LUC2* and *phot1phot2 CCA1::LUC2* double mutant seedlings 4 days after germination showing non-phototropic phenotype of *phot1phot2* mutants. Seedlings were grown for 3 days in constant darkness on 0.5x MS agar plates before exposure to 0.5 µmol m^{-2} s^{-1} unilateral blue light for 24 hours in order to induce phototropism. (**B**, **C**) Gel electrophoresis from genotyping PCR of (**B**) *phot1-5 CCA1::LUC2* and (**C**) *phot2-101 CCA1::LUC2* genomic DNA using primers specific to the phot1 or phot2 gene respectively in order to identify knockout mutant lines, as well as a positive control screen using primers specific to lectin. (**D**) Morphology of Col-0 *CCA1::LUC2*, *phot1phot2* (*p1p2*) *CCA1::LUC2*, *phot1-5* (*p1-5*) *CCA1::LUC2* and *phot2-101* (*p2-101*) *CCA1::LUC2* seedlings grown for 4 weeks on soil.

3.2.8. Imaging circadian rhythms in phototropin loss of function mutants

In order to identify any irregularities in the circadian clocks of phototropin mutants, circadian rhythms of phototropin mutants were assessed using prompt fluorescence imaging, delayed fluorescence imaging and luciferase imaging. Prompt and delayed chlorophyll fluorescence provide insight into the effects upon the circadian clock in the chloroplast via two distinct pathways whilst luciferase bioluminescence imaging allows evaluation of the rhythms of nuclear transcription of a specific gene, in this case *CCA1*.

For prompt fluorescence imaging, individual Col-0, *phot1*, *phot2* and *phot1 phot2* seedlings grown on 0.5x MS agar plates and entrained (Methods 2.6.1.) for 12 days under standard (Methods 2.3.1.) conditions were imaged under 20 µmol m^{-2} s^{-1} of blue light by prompt fluorescence imaging (Methods 2.6.5.). Waveforms of F_q'/F_m' rhythms (Figure 3.8.A.) were produced and used to calculate circadian period estimates which were plotted against RAE of F_q'/F_m' rhythms (Figure 3.8.B.). Collection of this data was cut short at 4 days rather than a compete test period of 5 days, as such the expected loss of F_q'/F_m' rhythmicity of *phot1 phot2* (Litthauer et al., 2015) mutants, which is most apparent on day 5, was not observed. F_q'/F_m' rhythms under these conditions showed a period of around 25h in all genotypes with no significant difference between the periodicity of Col-0 wild type and any of the phot single or double mutant lines (*p values*= >0.3). Rhythms were robust with an RAE of around 0.3 in wild type and 0.2 in all *phot* mutant lines.

For delayed fluorescence imaging, groups of 5-10 Col-0, *phot1, phot2* or *phot1 phot2* seedlings grown on0.5x MS agar plates and entrained (Methods 2.6.1.) for 12 days under standard (Methods 2.3.1.) conditions were imaged under 20 µmol m^{-2} s^{-1} of blue light by delayed fluorescence imaging (Methods 2.6.4.). Waveforms of delayed

fluorescence rhythms (Figure 3.8.C.) were produced and used to calculate circadian period estimates which were plotted against RAE of delayed fluorescence rhythms (Figure 3.8.D.). Rhythms of delayed fluorescence measured under these conditions show a period of around 23h in wild type, 23.8h in *phot1phot2*, 25h in *phot1* and 26.6h in *phot2*. Due partly to the lack of robustness of these rhythms, with all RAE values in wild type and *phot2* of around 0.4 and at around 0.3 and 0.35 in *phot1phot2* and *phot1* respectively, no significant difference in period between wild type and either of the *phot* single mutants or the *phot1phot2* double mutant could be observed (*p value*= >0.1).

For luciferase bioluminescence imaging, groups of 5-10 Col-0 *CCA1::LUC2*, *phot1 CCA1::LUC2, phot2 CCA1::LUC2* or *phot1 phot2 CCA1::LUC2* seedlings grown on0.5x MS agar plates and entrained (Methods 2.6.1.) for 6 days under standard conditions were imaged under 20 μmol m^{-2} s^{-1} of blue light by luciferase bioluminescence imaging (Methods 2.6.2.). Waveforms of luciferase bioluminescence rhythms (Figure 3.8.E.) were produced and used to calculate circadian period estimates which were plotted against RAE of luciferase bioluminescence rhythms (Figure 3.8.F.). Rhythms of luciferase bioluminescence measured under these conditions show a period of around 24h in wild type and each mutant line and an RAE of around 0.2 in all lines. No significant difference was observed between wild type periods and the periods of either of the phototropin single mutants or the *phot1phot2* double mutant (*p values*= >0.03).

These data suggest that under 20 μmol m^{-2} s^{-1} of blue light, phototropins have little or no effect on circadian rhythms in *Arabidopsis* either in the chloroplast, as shown by prompt and delayed chlorophyll fluorescence imaging, or in the nuclear transcription of the core circadian clock gene *CCA1*. However, as the previously observed phototropin mediated maintenance of rhythms of F_q'/F_m' were primarily observed from day 5 of

constant conditions onward (Litthauer et al., 2015), it is possible that there are some subtle effects which were not observed in these testing protocols.

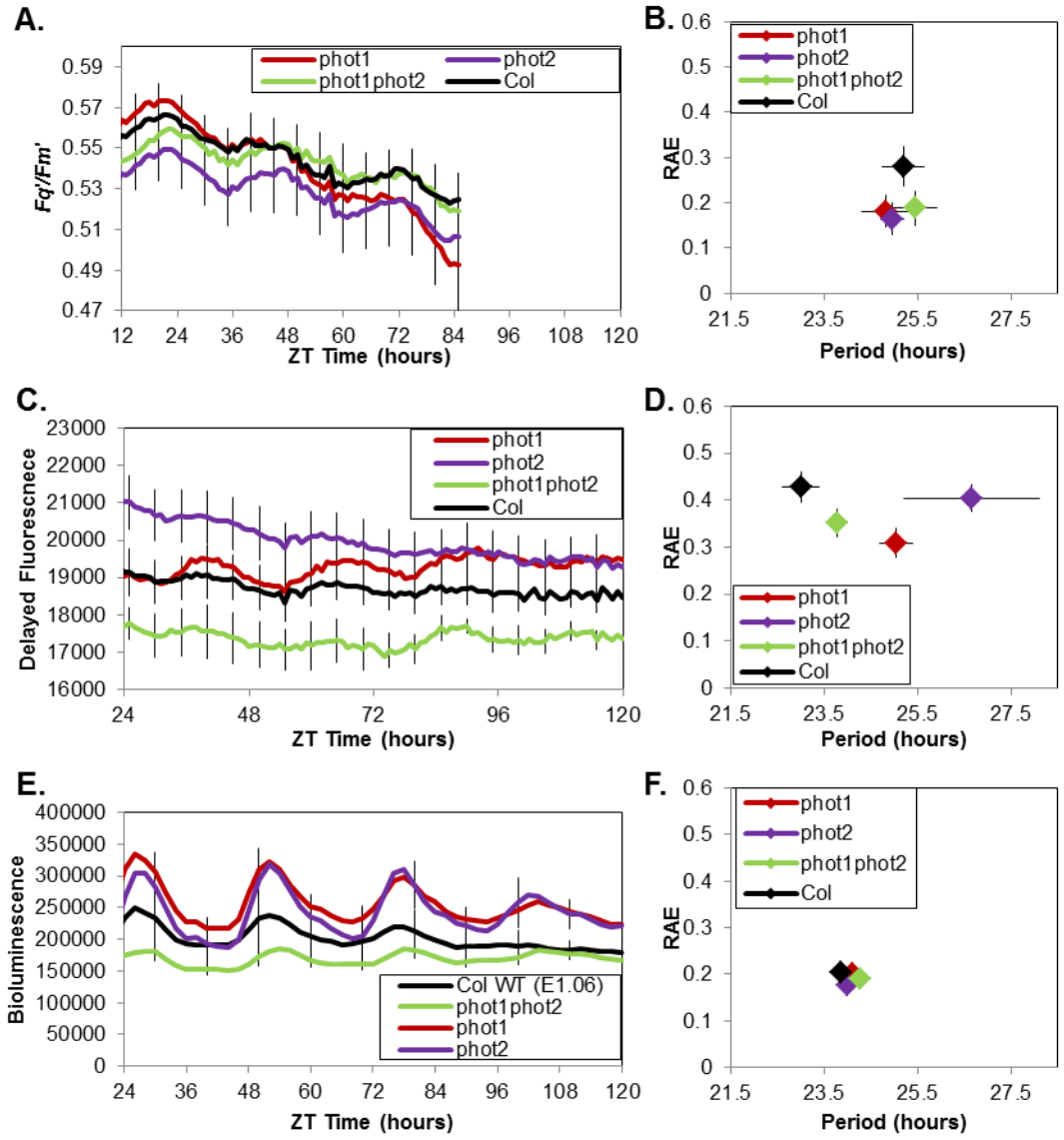

Figure 3.8. Live imaging of circadian rhythms in *Arabidopsis thaliana* phototropin knockout mutants. (**A**) Waveforms of PSII operating efficiency (F_q'/F_m') and (**B**) circadian period estimates plotted against Relative amplitude Error (RAE) calculated from prompt chlorophyll fluorescence imaging of individual 12 day old Col-0 (black) seedlings, *phot1-5* (*phot1*; red) or *phot2-101* (*phot2*; purple) phototropin single mutant seedlings or *phot1-5 phot2-1* (*phot1phot2*; green) double mutant seedlings under blue light. (**C**) Delayed fluorescence waveforms and (**D**) derived circadian period estimates plotted against RAE in groups of 5-10, 12 day old Col-0 seedlings, *phot1* or *phot2* phototropin mutant seedlings or *phot1phot2* double mutant seedlings in constant blue light. (**E**) Waveforms of luciferase bioluminescence and (F) derived circadian period estimates plotted against RAE in individual 6 day old Col-0 seedlings, *phot1* or *phot2* phototropin mutant seedlings or *phot1phot2* double mutant seedlings each expressing a *CCA1::LUC2* luciferase reporter and imaged in constant blue light. Seedlings were grown under 12:12 light:dark cycles of 60 µmol m^{-2} s^{-1} white light before imaging and were imaged under 20 µmol m^{-2} s^{-1} constant blue light. Error bars indicate standard error of the mean with n=2-23. Waveforms are an average of time series data for seedlings used in analysis, with error bars shown every 5-10 hours for clarity. Data from one of 3-4 independent experiments are shown.

3.2.9. Effects of light intensity and quality upon circadian rhythms in *Arabidopsis thaliana* phototropin mutants

In *Arabidopsis* all known photoreceptors, other than phototropins, act as a light input for the circadian clock (Hsu and Harmer, 2014). Previous work in our lab has shown that under 20 μmol m^{-2} s^{-1} constant blue light, phototropins contribute to the maintenance of prompt fluorescence rhythms while at 50 μmol m^{-2} s^{-1} these rhythms can maintain robustness even in the *phot1phot2* double mutant (Litthauer et al., 2015). In order to test whether the loss of F_q'/F_m' rhythms seen in the chloroplast in *phot1 phot2* double mutants was sufficient to alter nuclear rhythms,, *phot* mutants were tested under a range of blue light intensities from 7 μmol m^{-2} s^{-1} to 40 μmol m^{-2} s^{-1}. Plants were also imaged under red light of the same intensity to assess whether light intensity, rather than quality was causing any effects seen under very low blue light. Individual Col-0 *CCA1::LUC2,phot1 CCA1::LUC2*, *phot2 CCA1::LUC2* or *phot1 phot2 CCA1::LUC2* seedlings were entrained (Methods 2.6.1.) for 6 days under standard (Methods 2.3.1.) before being transferred to red (Figure 3.9.A. and 3.9.B.) or blue (Figure 3.9.C. and 3.9.D.) light of either 7, 15, 25 or 40 μmol m^{-2} s^{-1} for luciferase imaging (Methods 2.6.2.). Waveforms of luciferase bioluminescence rhythms (Figure 3.9.A. and 3.9.C.) were produced and used to calculate circadian period estimates which were plotted against RAE of luciferase bioluminescence rhythms (Figure 3.9.B. and 3.9.D.).

Under red light, as fluence rate increases, circadian period shortens; under 7 μmol m^{-2} s^{-1} of red light, each line had a rhythm with a period of around 26.5h, this reduced to 25.5h under 15 μmol m^{-2} s^{-1}, 25h under 25 μmol m^{-2} s^{-1} and 24h under 40 μmol m^{-2} s^{-1} (Figure 3.9.B.). As such, an increase of red light fluence led to an increase in pace of

circadian rhythms. The fluence rate response to red light was not shown to be significantly different in *phot* mutants than in wild type (*p value* = >0.1).

Blue light also causes an increase in circadian pace as fluence rate increases. In general, wild type and *phot1* mutants have similar circadian periods, while *phot2* mutants and the *phot1 phot2* double mutant have a similar (*p value*= >0.5) but slightly longer period (around 0.5h longer than wild type at all fluence rates) (Figure 3.9.C. and 3.9.D.). Under 40 μmol m^{-2} s^{-1} of blue light, wild type and *phot1* plants have a period of around 25.1h, at this same fluence rate, *phot2* single mutants and *phot1 phot2* double mutant plants have a slightly longer period at around 25.5h. At this fluence rate there is no significant difference in period between wild type and any *phot* mutants (*p value* = >0.87). The RAE of both mutants and wild type is around 0.15 at this fluence rate. When the blue light intensity is reduced to 25 μmol m^{-2} s^{-1}, wild type and *phot1* plants reduce their circadian pace to around 25.5h which is still slightly faster than *phot2* and *phot1 phot2* which have a period of around 26.0h (circadian periods of all mutants are not significantly different from wild type; *p* >0.29; Dunnet's test). The RAE of all lines at 25 μmol m^{-2} s^{-1} is around 0.15, similar to that seen under 40 μmol m^{-2} s^{-1} of blue light. At 15μmol m^{-2} s^{-1} of blue light, wild type, *phot1* and *phot2* all have a period of around 26.1h (*p values* of *phot* single mutants = >0.9), around 0.5h longer than under 25μmol m^{-2} s^{-1} of blue light. *phot1phot2* double mutants are still not significantly different to wild type with a period of 26.5h (*p value*= 0.737). The RAE at 15μmol m^{-2} s^{-1} of blue light remains at around 0.15 for all lines. Under 7μmol m^{-2} s^{-1} of blue light wild type and *phot1* plants have a period of around 26.6h, *phot2* and *phot1phot2* mutants have a period of around 27.2h which is still not significantly different from wild type (*p value* = >0.9). The RAE of all lines under 7 μmol m^{-2} s^{-1} of blue light for all lines has increased to around 0.3 (Figure

3.8.D) showing that some rhythmic stability has begun to be lost at this low fluence rate. Overall, this leads to the rate at which circadian pace is changed by fluence rate of blue in wild type when compared to *phot1*and *phot2* single mutants (*p value*= >0.9) and in *phot1phot2* double mutants (*p value*= 0.584) to be statistically similar to the change in circadian period relative to fluence rate seen in wild type.

These data suggest that phototropins have little effect upon circadian rhythms of *CCA1* transcription in the nucleus. This is consistent with the current understanding that phototropins do not regulate the circadian clock in *Arabidopsis*. Overall, this suggests that any phototropin related disruption to rhythms of photosynthesis in the chloroplast are insufficient to feed back into the nuclear circadian system

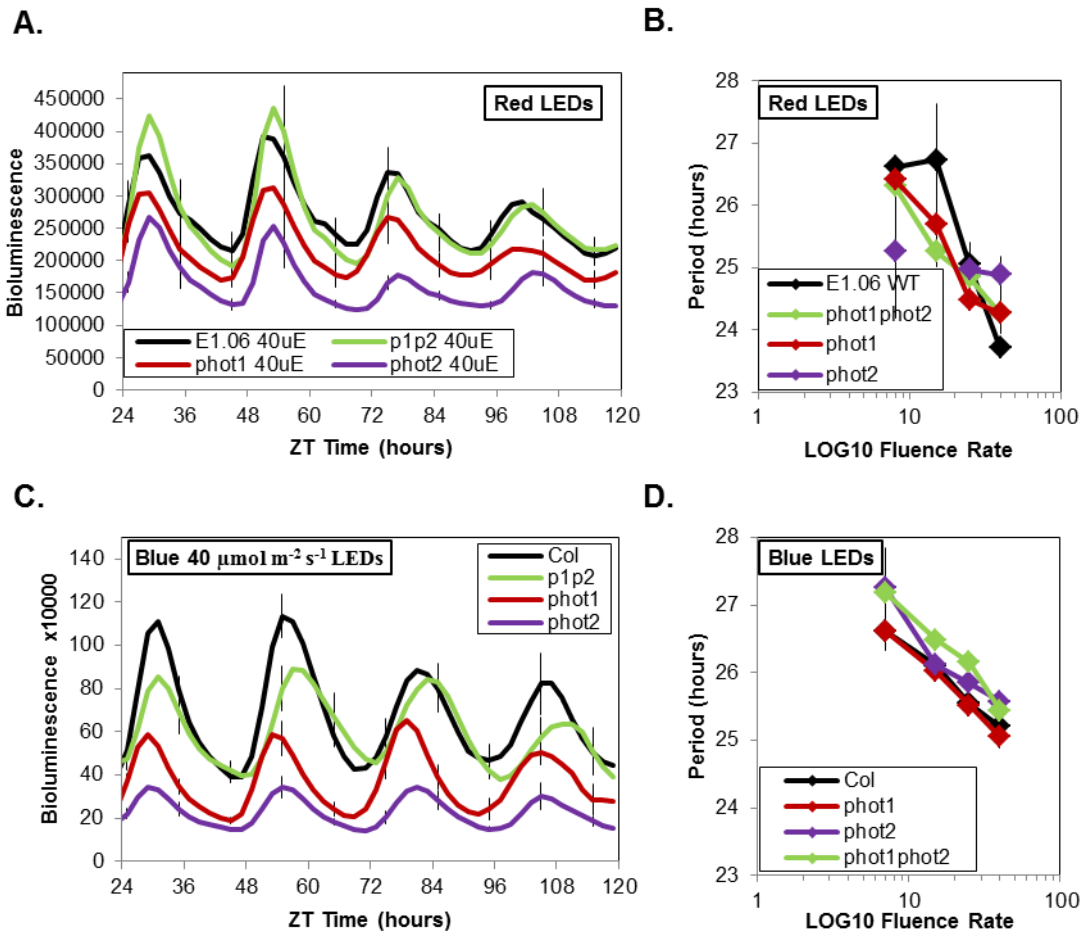

Figure 3.9. Circadian rhythms in phototropin mutants under different fluence rates and qualities of light. (**A**, **C**) Waveforms of luciferase bioluminescence rhythms and (**B**, **D**) circadian period estimates plotted against fluence rate of light treatment in Col-0 *CCA1::LUC2* (black) and *phot1-5 CCA1::LUC2 (phot1*; red), *phot2-101 CCA1::LUC2* (*phot2*; purple) and *phot1-5 phot2-1 CCA1::LUC2* (*phot1phot2*; green). Seedlings were grown for 6 days on 0.5x MS agar plates and entrained in 12h:12h light:dark cycles under 60 µmol m^{-2} s^{-1} white light before imaging under 40 µmol m^{-2} s^{-1} (**B**, **D**) or 7, 15, 25 or 40 µmol m^{-2} s^{-1} constant red (**A**, **B**) or blue (**C**, **D**) light. Error bars indicate standard error of the mean with n=8-22. For waveforms, error bars are shown every 10 hours for clarity.

3.3. Discussion

3.3.1. Prompt fluorescence imaging as a tool for examining circadian rhythms in the *Arabidopsis thaliana* chloroplast

Chlorophyll *a* fluorescence has been used as a tool for the measurement of circadian rhythms in *Arabidopsis* plants for some time in the form of delayed fluorescence (Gould et al., 2009). While prompt fluorescence is a form of chlorophyll *a* fluorescence, it is distinct from delayed fluorescence and is not produced by the same mechanisms (Baker, 2008, Barber, 2009). Delayed fluorescence is caused by charge recombination between excited plastiquinone (Q_A) and P680 within PSII, which causes photons to be emitted from chlorophyll *a* post illumination (Gould et al., 2009). Circadian rhythms of delayed fluorescence can be measured using a CCD camera and allow for a high throughput, non-invasive method to measure circadian rhythms in non-transgenic plants. Prompt fluorescence has been extensively studied in the crassulacean acid metabolism (CAM) plant, *Kalanchoë daigremontiana* (*Kalanchoe*), and as such is a relatively well defined process caused by the emission of excess energy from PSII in the form of photochemical quenching (Goltsev et al., 2003, Baker, 2008, Barber, 2009). Circadian rhythms of prompt fluorescence have been observed in *Kalanchoe* leaves (Wyka et al., 2005) and have recently been described in *Arabidopsis* (Litthauer et al., 2015, Malpas and Jones, 2016). Furthermore, we have found measurements of prompt fluorescence can be clearer and more robust than measurements of delayed fluorescence (Figure 3.1), potentially providing more accurate measurement chloroplast circadian rhythms in non-transgenic than were previously possible.

Additionally, we have shown that prompt fluorescence rhythms are independent of leaf movement (Figure 3.2.) and continue when leaves are restrained beneath a wire mesh

(Figure 3.2.A). By measuring the leaf area visible to the camera from above, we were able to measure rhythms of leaf movement from the change in visible leaf area as leaf angle rhythmically adjusts over the course of a circadian period, allowing for the simultaneous measurement of prompt fluorescence rhythms and leaf movement rhythms using a single camera (Figure 3.2.B. and 3.2.C.). Using this method we have also demonstrated that while rhythms of leaf movement are not the cause of rhythms of F_q'/F_m', they are out of phase with these rhythms (Figure 3.3.B and 3.3.C) with rhythms of F_q'/F_m' peaking at around circadian time (CT) 21 in whilst rhythms of visible leaf area peak at around CT 9 in 12 day old seedlings. Once the mechanism behind prompt fluorescence rhythms is better understood this method could provide insight into the interaction between the chloroplast circadian clock and the organismal circadian clock as a whole by allowing simultaneous measurement of these differently controlled rhythms.

Additionally, we have demonstrated that rhythms of F_q'/F_m' are disrupted when exogenous Qo is introduced to the plant (Figure 3.3.). However, it should be noted, that while a clear and significant effect has been caused, additional work will be required to understand how the application of exogenous Qo alters the redox status of the quinone pool in the chloroplast. Currently, no mechanistic link between the application of Qo and F_q'/F_m' rhythms can be drawn. However, as we have observed both this disruption of these rhythms linked to the redox status of the chloroplast and it has previously been observed in our lab that phototropins, which are also associated with redox sensing (Huala et al., 1997), are required to maintain rhythms of F_q'/F_m' (Litthauer et al., 2015), it seems plausible that redox status of the chloroplast is associated with F_q'/F_m' rhythms. As such, we also investigated the effects of loss of function mutants related to

the regulation of redox states in the chloroplast (Figure 3.4). While none of the mutants observed had any a significant influence upon F_q'/F_m' rhythms, this suggests that either this pathway is being influenced via another redox related gene in the chloroplast (Allen et al., 2011, Edgar et al., 2012, Diaz et al., 2018), or the significant disruption to redox state caused by the application of exogenous Qo is not directly connected to rhythms of F_q'/F_m', and rather is causing plant wide stress response which is cascading into disruption of processes within the chloroplast including F_q'/F_m' rhythms and the interactions between phototropins and F_q'/F_m' rhythms are not based directly upon the redox state of the chloroplast.

3.3.2. Phototropin internalisation does not influence circadian rhythms of F_q'/F_m' in *Arabidopsis thaliana*

Phototropins are known to localise to the plasma membrane, internalising in response to blue light (Preuten et al., 2015). phot1 moves to the endoplasmic reticulum while phot2 re-localises to the Golgi apparatus (Kaiserli et al., 2009, Kong et al., 2013, Suetsugu and Wada, 2013), both phototropins have also been shown to internalise to the chloroplast outer membrane (Kong et al., 2013). Phototropins are also known to be involved in chloroplast relocalisation responses, with phot1 regulating chloroplast accumulation under low fluence rates of blue light and phot2 regulating chloroplast avoidance responses to high intensity blue light (Jarillo et al., 2001b**,** Christie et al., 2007), although the mechanism by which this occurs is not well understood it is now known to be unrelated to the internalisation of phot1 as it still occurs in *farn* mutants (Preuten et al., 2015). As phototropins are known to be required to maintain circadian rhythms of prompt chlorophyll fluorescence (Litthauer et al., 2015), it was hypothesised

that the internalisation of phot1 to the cytoplasm may be part of the mechanism by which phototropins interact with the circadian clock. In order to test this hypothesis, *phot1 phot2* double mutants transformed with a construct expressing a farnesylated phot1::GFP fusion protein (*farn*) which is anchored to the lipid bilayer of the outer membrane (Preuten et al., 2015), were imaged using prompt fluorescence imaging techniques (Figure 3.5). Under 20 µmol m^{-2} s^{-1} of blue actinic light, circadian periods of rhythms of prompt fluorescence in *farn* mutants were similar to those of both wild type and *phot1phot2* double mutants. The rhythmicity of *Fq'/Fm'* rhythms in *phot1phot2* double mutants however was significantly reduced when compared to wild type (p <0.001), a phenotype which was recovered in *farn* mutants (p =0.935). This suggests that farnesylated phot1 is sufficient to recover the loss of *Fq'/Fm'* rhythmicity seen in *phot1phot2* double mutants, suggesting that phot1 internalisation is not involved in the interaction between phototropins and the circadian clock. However, it should be noted that the previously observed loss of rhythmicity in *phot1phot2* mutants under these conditions was mostly seen between ZT96 and ZT120 (Litthauer et al., 2015) and this test failed to complete a full 120 hour testing period, as such, loss of rhythmicity of *phot1phot2* mutants, while statistically significant, was not as pronounced as has previously been seen (Figure 3.5.B.) and as such it cannot be discounted that a greater loss of rhythmicity may still occur in *farn* mutants imaged for a longer duration. From what has been observed, it seems most likely that phototropins influence the circadian clock indirectly via the chloroplast circadian clock, by preventing damage to the chloroplasts under blue light, phototropins enable the continued function of interactions between the chloroplast and nuclear circadian clocks. In the absence of phototropins, chloroplast movement is inhibited and chloroplast damage occurs damaging chloroplast-nuclear circadian clock interactions.

3.3.3. Different luciferase reporter genes influence the accuracy of measurement of circadian rhythms of luciferase bioluminescence

Due to the circadian regulation of around 30% of expressed genes in the *Arabidopsis* genome (Covington et al., 2008), a wide range of promoters are available to be utilised in circadian reporter constructs (Millar et al., 1992, Harmer and Kay, 2005, Matsuo et al., 2006). As different circadian genes cycle with different phases and regulate each other in a complex and interconnected series of feedback loops, the phase, amplitude and robustness of rhythms observed with one reporter gene may differ significantly from those seen using another (Michael and McClung, 2002). Furthermore, many circadian functions are controlled by multiple genes working redundantly, meaning that a loss of function in one peripheral clock gene or clock genes in a specific tissue may not have any effect on the circadian clock as a whole (Harmer et al., 2000, Haydon et al., 2013b). In a healthy, wild type plant, regardless of the circadian gene being observed using a reporter construct, circadian rhythms should fluctuate with a similar period (Figure 3.6.), although the brightness and amplitude of the luciferase gene incorporated into the reporter fusion protein, as well as the location of the reporter gene within the genome can lead to variations in brightness and clarity of luciferase bioluminescence rhythms (Jones et al., 2015) and potentially introduce inaccuracies into these measurements. To counteract this loss of clarity due to reporter brightness, circadian rhythms are often measured using groups of seedlings grown tightly together in order to increase the brightness of luciferase bioluminescence measured within a single data point. While this methodology is generally useful and produces brighter measurements, due to the natural variation of individual plants (Maloof et al., 2001, Malpas and Jones, 2016) this too can potentially introduce irregularities into a dataset as if one or more

grouped plants are not synchronised with the rest of the group the RAE of the data point can be increased. In order to more accurately measure circadian rhythms, many circadian reporter constructs make use of the brighter LUC+ or LUC2 in place of LUC when possible, reducing the need to grow seedlings in groups or with supplemental exogenous sucrose. Alternatively, seedlings are often grown on media containing exogenous metabolic sugars such as sucrose, which increase the brightness and stability of luciferase bioluminescence emissions (Harmer et al., 2000, Haydon et al., 2013a). However, sugar treatments have been shown to alter circadian rhythms (Haydon et al., 2013a) and as such this can skew data away from a representation of the 'real world' conditions which the experiment is trying to portray.

In order to identify which of the circadian reporter genes available to us would produce the most accurate measurements of circadian rhythms in phototropin mutants; we used luciferase imaging to measure circadian rhythms in a range of wild type plants, each expressing a different circadian luciferase reporter gene. *CCA1::LUC2* seedlings differed from the other plants tested in that due to the brightness of LUC2 bioluminescence, these seedlings were grown individually rather than in groups of 5-10. Of the reporter genes tested, *CAB::LUC* produced the brightest luciferase bioluminescence with a clear, stable rhythms and a period of around 25 hours (Figure 3.6.). However, as individual *CCA1::LUC2* seedlings also produced a clear, bright rhythm along with CCA1 being a core gene of the circadian system the *CCA1::LUC2* reporter was chosen to use in production of our phototropin mutant luciferase reporter lines.

3.3.4. Phototropins do not influence circadian rhythms of *CCA1* in *Arabidopsis thaliana* under blue light

Unlike other photoreceptors, phototropins are not known to act as an input to the circadian system in *Arabidopsis*. Development of prompt fluorescent imaging as a tool for imaging circadian rhythms in *Arabidopsis* has revealed that phototropins are required to maintain circadian rhythms in the chloroplast, as represented by a loss of rhythmic variations in photosynthetic efficiency of PSII after several days (Litthauer et al., 2015). Later analysis using RT-qPCR revealed that phototropins do not delay the phase of circadian transcript accumulation in the evening-phased circadian genes; *GI*, *TOC1* or *CCR2* (Litthauer et al., 2016).

In order to further assess the significance of phototropins in the circadian system, mutant plants lacking functional phototropins were crossed to introduce a circadian luciferase reporter gene utilising the promoter from the morning phased core clock gene CCA1 (*phot1 CCA1::LUC2; phot2 CCA1::LUC2; p1p2 CCA1::LUC2*). These mutants were then used to measure circadian rhythms of *CCA1* expression under blue and red light of a range of low intensities from 7 μmol m^{-2} s^{-1} to 40 μmol m^{-2} s^{-1}. Under red light, predictably, all phototropin mutants behave similarly to wild type under all intensities, however, under blue light *phot2* single mutants and *phot1phot2* double mutants both present a subtle but not significant long period phenotype under all intensities of light (around 0.5h longer than wild type or *phot1* single mutants, *p values* = >0.5). While not significantly longer period than wild type under blue light of 7 to 40 μmol m^{-2} s^{-1}, these data suggest that phot2 may play a subtle role in the maintenance of circadian rhythms of *CCA1* expression in *Arabidopsis*, further testing is required to determine whether this

effect is significant at lower light intensities, although a general loss of rhythmicity is likely to be apparent under much lower light conditions.

In this chapter, we have characterised rhythms of F_q'/F_m' in the chloroplast under blue light and further examined the interactions between F_q'/F_m' rhythms and phototropins. Our data suggests that while altering the redox state of the plant using exogenous Qo causes disruption to rhythms of F_q'/F_m' this may not be a direct causal link to this system and may rather be impacting photosynthetic efficiency as a whole rather than simply the circadian controlled aspects thereof. This is further supported by evidence that many chloroplast redox regulation mutants have F_q'/F_m' rhythms similar to those seen in wild type. Additionally, we have examined the influence of phototropins upon the morning phased circadian clock gene CCA1 under blue and red light. While phototropins are required to maintain rhythms of F_q'/F_m', this process is not mechanistically linked to the internalisation of phototropins in response to blue light. Furthermore, phototropins do not influence the morning phased elements of the circadian clock under red or blue light of 7 to 40 μmol m^{-2} s^{-1} and we have not observed any significant influence of phototropins upon the circadian system. In order to further analyse the role of phototropins in the regulation of the circadian system, further fluence rates of blue light, both lower and higher than those tested here, could be observed. Additionally, observation of further photoreceptor mutants, especially those with mutations in the phototropins alongside other photoreceptors may reveal as of yet unknown interactions between phototropins and other photoreceptors which are required to maintain circadian rhythms.

Chapter 4- Understanding the effects of green light upon the circadian system in *Arabidopsis thaliana*

4.1. Introduction

As sessile photoautotrophs, plants are acutely sensitive to and wholly dependent upon their surrounding light conditions. Plant photoperception ranges from the broad sensitivity associated with photosynthesis to the more subtle and specific responses of photoreceptors (Koussevitzky et al., 2007, Christie et al., 2015, Dodd et al., 2015). In *Arabidopsis thaliana*, five families of photoreceptor proteins have been identified; the red and far-red light sensing phytochromes, the blue light sensitive cryptochromes, phototropins, and zeitlupes, as well as the UV-B receptive UVR8 (Christie et al., 2015, Millar, 2016). Notably, of these known photoreceptors, none are specific to green light, one of the most prevalent spectral ranges in sunlight (Deitzer, 1994, Smith et al., 2017). The green colouration of most plant leaves leads to much of the green spectrum being reflected by the leaf surface (Nishio, 2000, Smith et al., 2017), although the green light which is absorbed is used remarkably efficiently for photosynthesis (Terashima et al., 2009). A variety of green light responses in plants have been observed, ranging from stomatal opening to low-light avoidance and hypocotyl elongation (Zhang et al., 2011, Folta, 2004). However, largely due to the lack of a specific green-light responsive photoreceptor, the mechanisms underlying these responses are poorly understood (Smith et al., 2017, Wang et al., 2013, Wang and Folta, 2013, Folta, 2004, Lin et al., 1995). While cryptochromes have long been suggested to be situationally responsive to green light (Lin et al., 1995, Bouly et al., 2007), they are not widely considered to be a green light photoreceptor. Additionally, some reported green light responses have been found to instead be caused by responses to the low intensity blue wavelengths found in

many green light sources (Wang and Folta, 2013). In this section, we will investigate responses of photoreceptor mutants in *Arabidopsis* to green light and explore the interactions between green light and the circadian clock.

4.2. Results

4.2.1. Spectra of light sources used for plant growth and experiments

In order to understand how green light was influencing the circadian system we first had to document the wavelengths our lights were emitting. Spectra of light emitting diode (LED) (Figure 4.1.A.) and fluorescent (Figure 4.1.B.) lights were measured using a SR9910-V7 Double Monochromator Spectroradiometer (Macam Photometrics Ltd, Livingston, UK). Testing performed under constant light conditions utilised either; red (~600-700 nm, peaking at ~660 nm), blue (~420-510 nm, peaking at ~450 nm) or green (~465-590 nm, peaking at ~510 nm) LED lights (Bright Technology Industrial Ltd., Shenzhen City, China; Figure 4.1.A.) or a combination of these lights with or without additional light filters. Green LEDs filtered with #312 Canary yellow filters were used in a range of tests and the spectra is included here (Figure 4.1.A.; ~490-575 nm, peaking at ~520 nm). Standard growth conditions (Methods 2.3.1.) made use of white fluorescent lights (Figure 4.1.B.) within controlled growth environments.

The spectrum of the green LEDs used during our testing is wide, with wavelengths ranging from around 465 nm to 590 nm and peaking at 510 nm. Of this spectrum, around 11% of the relative intensity is below 500 nm, typically described as blue wavelengths. This leads to around 2.2 μmol m^{-2} s^{-1} in every 20 μmol m^{-2} s^{-1} of light from these LEDs being within the blue range of the visible light spectrum (Figure 4.6.A. and

4.6.B.). By filtering this light using a #312 Canary Yellow filter, a filtered green (fGreen) spectrum can be achieved. fGreen light ranged from around 490 nm to 575 nm and peaked at 520 nm. Around 3% of this fGreen spectrum is within the blue wavelengths, around 0.6 μmol m^{-2} s^{-1} of blue in every 20 μmol m^{-2} s^{-1} of fGreen light.

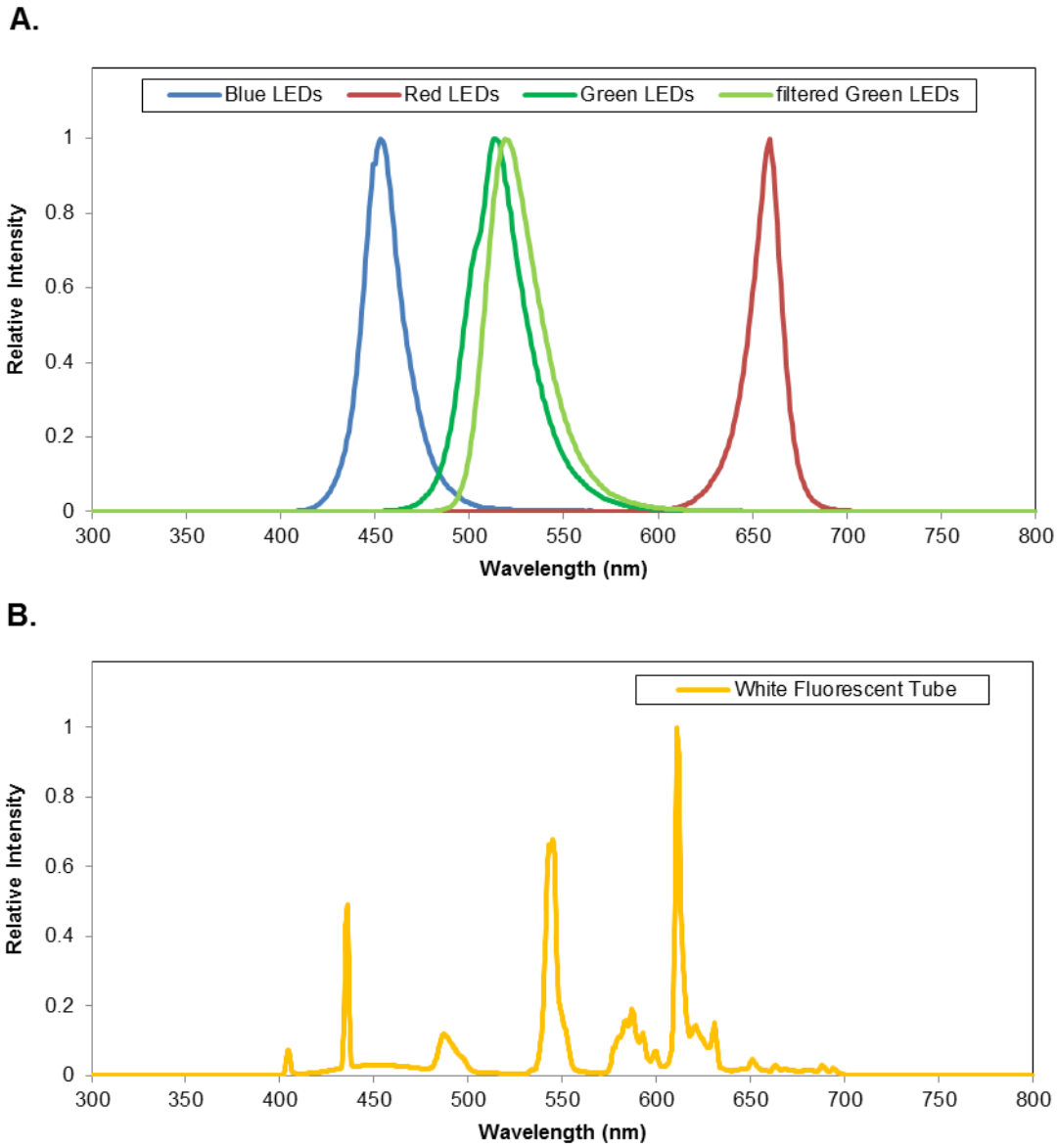

Figure 4.1. Spectra of light sources used in this study. Waveforms of electromagnetic spectra emitted by (**A**) blue, red and green Light Emitting Diodes (LEDs; Bright Technology Industrial Ltd., Shenzhen, China) along with the spectrum of green LEDs as viewed through a #312 Canary yellow filter (Stage Depot Ltd., Bristol, UK) and (**B**) cool white fluorescent tubes (Conviron Europe Ltd., Isleham, UK). (**A**) LEDs were used to provide constant light conditions during many tests throughout this study and (**B**) white fluorescent lights were used during growth and entrainment of many plants for tests throughout this study. Waveforms are presented as intensity of light as a proportion of maximum intensity at a given wavelength for each light source plotted against wavelength of emission.

4.2.2. Circadian rhythms of *CCA1* under different light qualities

In order to assess the effects of the different light qualities provided by our LED lights upon circadian rhythms in *Arabodipsis*, wild type (Col-0) seedlings expressing a *CCA1::LUC2* reporter were entrained individually for 6 days under standard growth conditions (Methods 2.6.1) before transferring to 15 μmol m^{-2} s^{-1} of constant light from either red (cR), blue (cB), green (cG) or filtered green (cfG) LEDs or constant darkness (cD) for luciferase imaging (Figures 4.2A-E; Methods 2.6.2.). Waveforms of luciferase bioluminescence from each test were used to estimate circadian periods which were plotted against the RAE of luciferase bioluminescence (Figure 4.2.F.).

In darkness, waveforms of luciferase bioluminescence are arrhythmic and no circadian period estimates could be calculated. Under blue and unfiltered green light, a similar (p =0.58; student's t-test) circadian period of around 24h was observed, significantly lower (p <0.046) than the period of around 27h seen in seedlings image under both red and filtered green light which were also similar to each other (p =0.7). The rhythmicity of wavelengths under red and filtered green light were also similar (RAE around 0.25; p =0.14) while the rhythmicity under blue light was similar to that seen under filtered green light (RAE =0.2; p =0.69) but significantly more rhythmic than under red (p =0.0093) or unfiltered green (RAE = 0.36; p <0.0001). Unfiltered green produced the least rhythmic rhythms beside constant darkness with an RAE of around 0.36, significantly less rhythmic than waveforms under blue or filtered green (p <0.012) but not significantly less rhythmic than rhythms under red (p =0.1177).

These data suggest that green light induces circadian rhythms similar to those seen under blue light whilst filtered green light produces more rhythmic rhythms which are both significantly different to those seen under unfiltered green light and similar to

those seen under red light. Both green and unfiltered green are sufficient to maintain circadian rhythms, unlike darkness, showing that these wavelengths of light are sufficient to maintain circadian rhythms. Furthermore, whilst not novel data (see also Somers et al, 1998), it should be noted that different qualities of light are sufficient to produce significantly different circadian rhythms in *Arabidopsis* independent of fluence rate.

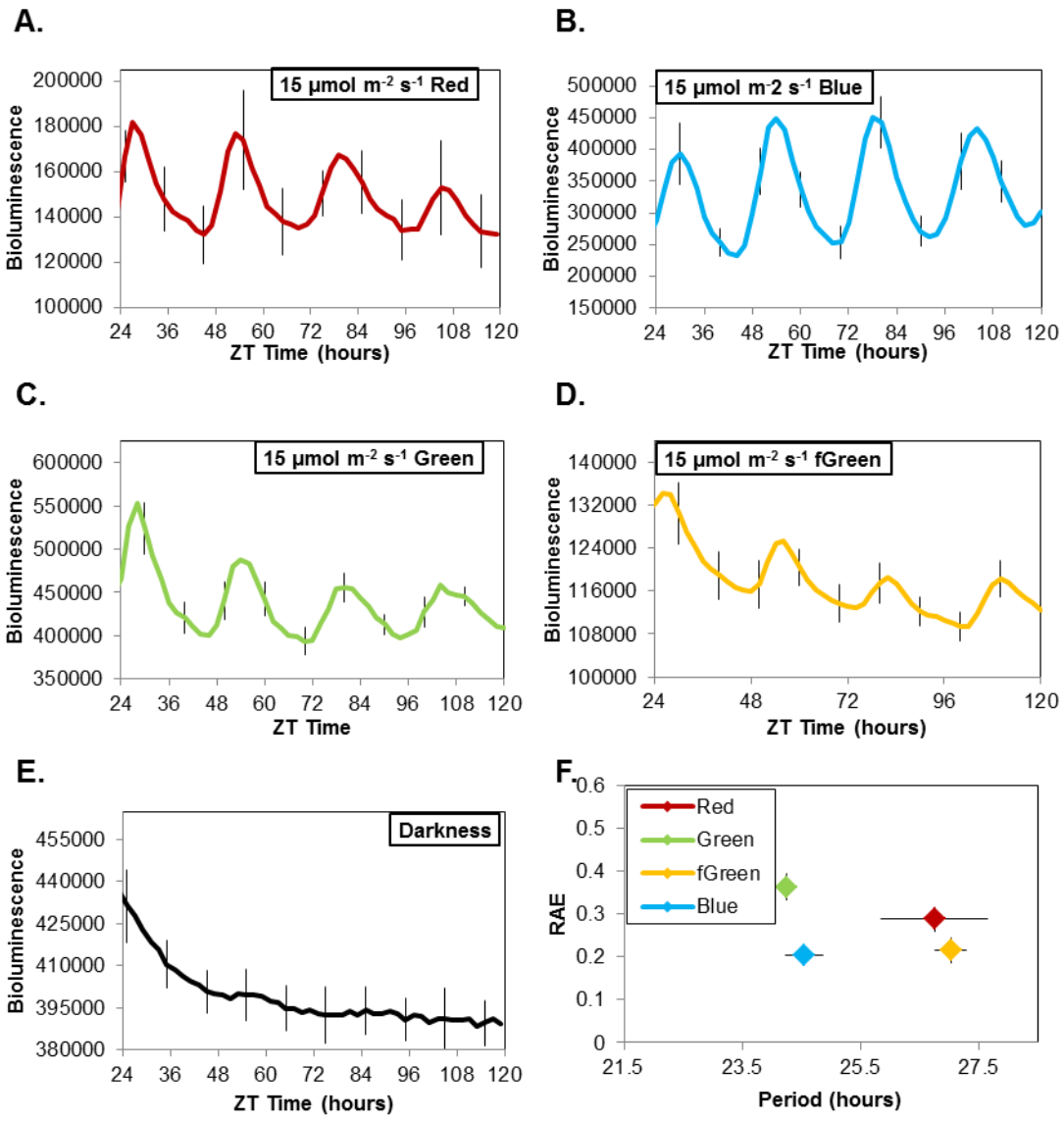

Figure 4.2. Comparison of circadian rhythms of *CCA1* in *Arabidopsis thaliana* under different light qualities. Waveforms of luciferase activity in 6 day old Col-0 *CCA1::LUC2* seedlings under 15 µmol m^{-2} s^{-1} of either (**A**) red Light Emitting Diodes (LEDs), (**B**) blue LEDs, (**C**) green LEDs or (**D**) green LEDs filtered with a #312 Canary yellow filter (fGreen; Stage Depot Ltd., Bristol, UK) or (**E**) in constant darkness. (**F**) Circadian period estimates plotted against Relative Amplitude Error (RAE) calculated for each waveform shown previously, excluding (**E**) complete darkness, for which no circadian period could be calculated. Seedlings were grown under 12:12 light:dark cycles of 60 µmol m^{-2} s^{-1} white light before imaging. Error bars indicate standard error of the mean with n=4-10. Waveforms are an average of time series data for seedlings used in analysis, with error bars shown every 5-10 hours for clarity. Data from one of 1-4 independent experiments are shown.

4.2.3. Hypocotyl elongation responses in *Arabidopsis* seedlings to light of different qualities and intensities

The circadian clock is known to regulate hypocotyl elongation in *Arabidopsis* seedlings (Nozue et al., 2007) and as such, irregularities in hypocotyl elongation responses can be indicative of irregularities in circadian rhythms. Plants begin development in an etiolated state, in which hypocotyl elongation is rapid and leaf development is delayed. De-etiolation, the transition from this etiolated state as part of photomorphogenesis, is triggered when plants first encounter light and is regulated by photoreceptors in order to allow plants to locate more ideal light conditions before developing mature leaves for better light harvesting (Ma et al., 2001, Zhang et al., 2011, Casal, 2013). De-etiolation responses are a highly studied area of plant development and responses to both red and blue light have been well documented (Sullivan and Deng, 2003, Wang and Folta, 2014, Su et al., 2015), responses to green light however are less well understood and are still being described (Zhang, et al. 2011).

In order to further assess the effects of green light and other light qualities upon *Arabidopsis thaliana*, mutant seedlings presenting a loss of function in one or more photoreceptors were grown under constant light of one of a range of qualities and intensities for five days (Methods 2.5.2.). Col-0 wild type seedlings, along with *phot1*, *phot2* and *phyB* single mutants and *cry1cry2* and *phot1phot2* double mutants were grown for 5 days on 0.5x MS agar plates under 1 or 10 μmol m^{-2} s^{-1} of red, blue or green light or green light filtered through a #312 Canary filter alongside an additional plate grown in constant darkness.

The average hypocotyl length at the end of testing under each light quality and intensity was normalised to the length of seedlings grown in darkness (with average length of

seedlings grown in darkness presented as a value of 1). Relative hypocotyl lengths were used to conduct a Dunnet's test comparing the interaction between fluence rate of light under each condition and the relative hypocotyl length in each genotype to that seen in wild type Col-0 seedlings (Figure 4.3).

Under red light in (Figure 4.3.A.), *phyB* single mutants presented a significantly reduced response to the change in light intensity relative to that seen in wild type (p <0.001) whereas *cry1cry2* and all *phot* mutants did not show a significantly different level of responsiveness to Col-0 wild type (p >0.58).

Under blue light (Figure 4.3.B.), all *phot* mutant lines along with *phyB* single mutants responded to blue light in a comparable way to that seen in Col-0 (p >0.07). The response of *cry1cry2* seedlings to increasing blue light intensities however, was significantly less than that seen in wild type (p <0.001).

Under green light (Figure 4.3.C.), all seedlings, *cry1cry2*, *phot* mutants and *phyB*, show similar reactions to changing light intensity as is seen in wild type (p >0.16). Filtered green light however (Figure 4.3.D.) causes a significantly different response to the increasing light intensity in *cry1cry2* (p <0.001), *phot1phot2* (p =0.012) and *phyB* (p =0.011) mutant seedlings when compared to wild type. *phot1* and *phot2* single mutants do not show a significantly different response to increasing filtered green light intensities than Col-0 (p >0.12).

These data suggest, as has been previously reported (Folta and Spalding, 2001), that hypocotyl elongation responses under red light are less pronounced in *phyB* mutants and under blue light are less pronounced in *cry1cry2* mutants. Under green LED light without the addition of filters none of the observed mutants presented a significantly

greater response to the changing light intensity than was observed in wild type, however the introduction of a #312 Canary filter (removing some of the blue light wavelengths from the light) was sufficient to induce a significantly different response to wild type in *cry1cry2*, *phot1phot2* and *phyB* mutants. This may suggest that the blue wavelengths present in our unfiltered green LED light are sufficient to allow detection of this light in these mutants but that these mutants may be less sensitive to green light once these blue wavelengths are removed, or that these photoreceptors contribute to the perception of the blue:green light ratio.

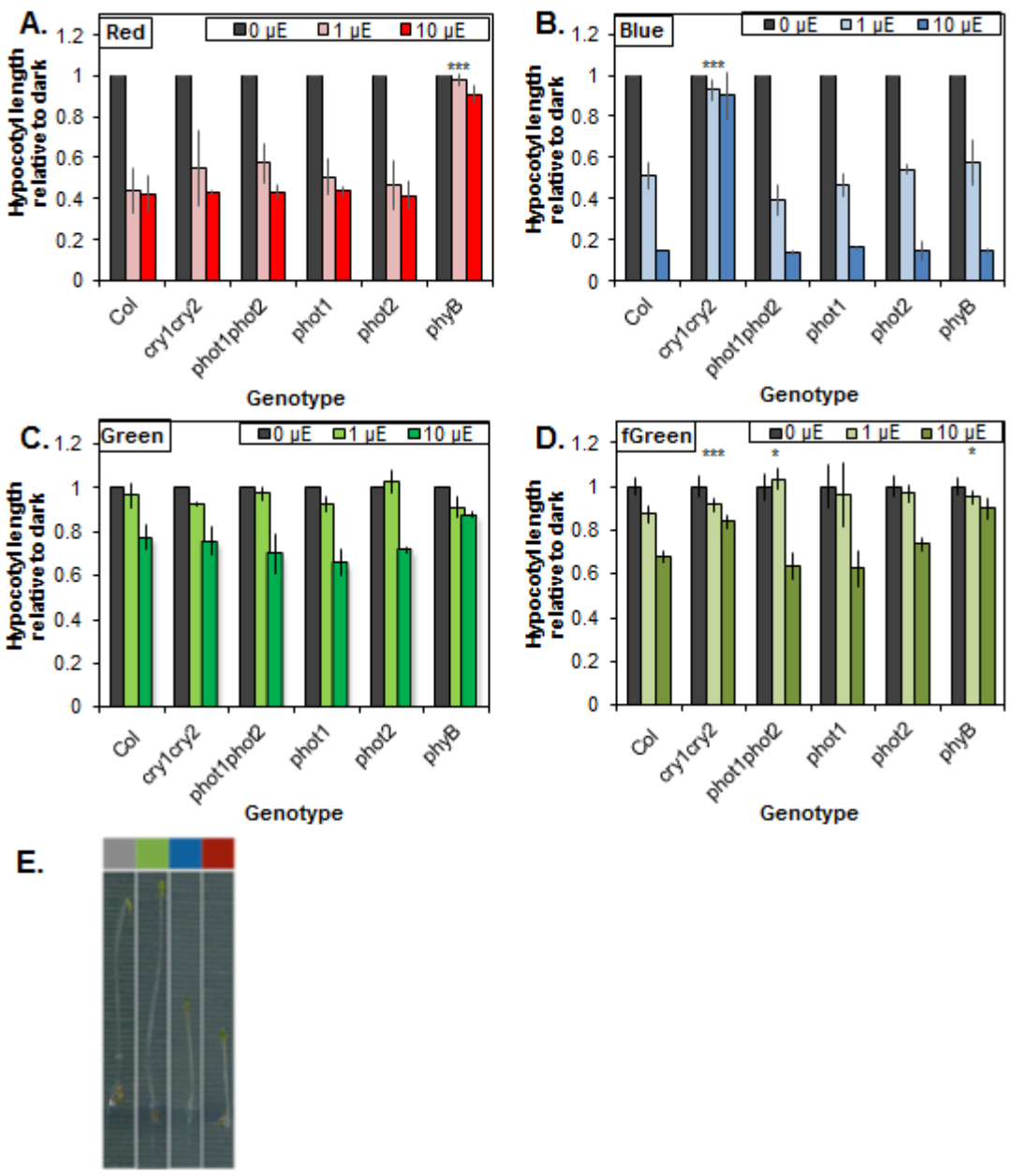

Figure 4.3. Hypocotyl elongation responses to light quality and intensity. Average hypocotyl length of Col wild type and *cry1 cry2*, *phot1 phot2*, *phot1*, *phot2* and *phyB* photoreceptor knockout mutant seedlings grown for 5 days on 0.5x MS agar plates under 1 or 10 µmol m^{-2} s^{-1} (µE) of (**A**) red, (**B**) blue, (**C**) green or (**D**) green filtered through a #312 canary filter (Stage Depot Ltd., UK) and in darkness with hypocotyl length presented as relative to the average length of seedlings of the same genotype grown in darkness (Average length of this genotype in darkness = 1). Data points represent the average hypocotyl length of seedlings from one of 3-4 independent experiments. Error bars indicate standard error of the mean where n= 2-18. Asterisks indicate a statistically significant change in hypocotyl length relative to fluence rate relative to the change seen in wild type seedlings (* $p<0.05$; *** $p<0.001$; Dunnet's test). (**E**) Wild type seedlings grown on 0.5x MS agar plates in darkness or under 1 µmol m^{-2} s^{-1} of green, blue or red light showing pronounced elongated hypocotyls in dark and green grown seedlings.

4.2.4. Effects of exogenous sucrose on hypocotyl elongation responses in *Arabidopsis thaliana*

As green light is readily used for photosynthesis (Terashima et al., 2009) we examined whether the provision of sucrose altered hypocotyl responses to green light. Wild type (Col-0) seedlings, along with the *cry1cry2* double mutant, *phyB* single mutant, *phot1* and *phot2* single mutants and *phot1phot2* double mutant seedlings were exposed to white fluorescent light (120 μmol m^{-2} s^{-1}) for 4-6h in order to enhance germination before being transferred to constant light and grown vertically on 0.5x MS agar plates with 3% supplemental sucrose for 5 days (Methods 2.5.2.). The constant light conditions used were either red (cR), blue (cB) or green (cG) LED light with an intensity of either 1 or 10 μmol m^{-2} s^{-1}, a further plate of seedlings per test were grown in darkness. Data was analysed as previously described, Section 4.2.3.

Under red light in combination with exogenous sucrose (Figure 4.4.A.), *phot2* and *phyB* mutants both presented a significantly different response to the change in light intensity relative to that seen in wild type (*phot2* p= 0.0392 ; *phyB* p= 0.0104) whereas all other mutants did not show a significantly different level of responsiveness (p >0.97). It should be noted that the responses observed in *phot2* mutants under red light was unexpected and may be due to poor germination of the *phot2* under these conditions limiting the number of samples under each light intensity.

Under blue light (Figure 4.4.B.), all lines excluding *cry1cry2* showed similar response to the change in intensity as that seen in wild type (p >0.53). *cry1cry2* mutant seedlings showed a significantly reduced responsiveness to blue light (p <0.001) with hypocotyl lengths under both 1 and 10 μmol m^{-2} s^{-1} blue light similar to but greater than those seen when grown in darkness.

Under green light (Figure 4.4.C.), all seedlings show similar reactions to changing light intensity as is seen in wild type (p >0.44).

These data suggest that exogenous sucrose is sufficient to reduce the light-induced hypocotyl de-etiolation response in *Arabidopsis* seedlings. However, the response is not completely suppressed, as is most clearly seen in mutant lines which are unresponsive to red or blue light continuing to be significantly less responsive to the increase in light intensity than wild type or responsive mutant lines.

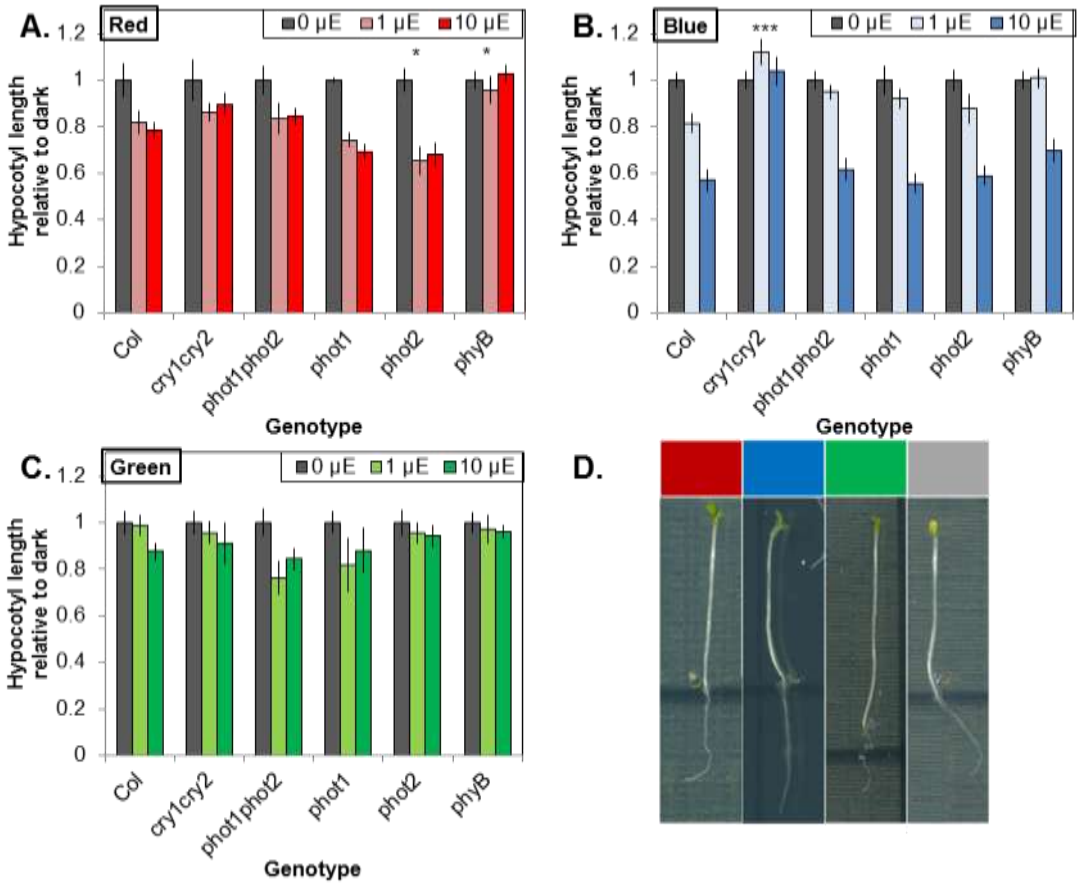

Figure 4.4. Hypocotyl elongation responses to light quality and intensity in the presence of exogenous sucrose. Average hypocotyl length of Col-0 wild type and *cry1 cry2*, *phot1 phot2*, *phot1*, *phot2* and *phyB* photoreceptor knockout mutant seedlings grown for 5 days on 0.5x MS agar plates with 3% supplemental sucrose under 1 or 10 µmol m^{-2} s^{-1} (µE) of (**A**) red, (**B**) blue or (**C**) green and in darkness with hypocotyl length presented as relative to the average length of seedlings of the same genotype grown in darkness (Average length of this genotype in darkness = 1). Data points represent the average hypocotyl length of seedlings from one of 3-4 independent experiments. Error bars indicate standard error of the mean where n= 8-15. Asterisks indicate a statistically significant change in hypocotyl length relative to fluence rate relative to the change seen in wild type seedlings (* $p<0.05$; *** $p<0.001$; Dunnet's test). (**D**) Wild type seedlings grown on 0.5x MS agar plates with 3% supplemental sucrose in darkness or under 1 µmol m^{-2} s^{-1} of green, blue or red light showing pronounced elongated hypocotyls in dark and green grown seedlings.

4.2.5. Low-light responses of hypocotyl elongation under complex light regimes

It has previously been observed that under complex light regimes containing mixed PAR wavelengths including green wavelengths that green light can produce low-light avoidance responses and alter or oppose otherwise seen responses to red or blue light (Zhang, et al. 2011). The exact mechanism behind these responses is unknown although they have been suggested to be evidence of green light responses in the cryptochromes and phytochromes (Zhang, et al. 2011). In order to characterise these low-light avoidance responses in *Arabidopsis*, we observed hypocotyl elongation responses in Col-0 and photoreceptor mutant seedlings under a mix of constant red and blue light (3.0:2.0 ratio) and again under constant red, green and blue light (3.0:2.5:2.0 ratio) at 1 and 10 μmol m^{-2} s^{-1} of intensity, these were again assessed relative to the length of seedlings grown in constant darkness.

Wild type (Col-0) seedlings, along with the *cry1cry2* double mutant, *phyB* single mutant, *phot1* and *phot2* single mutants and *phot1phot2* double mutant were tested for hypocotyl elongation responses (Methods 2.5.2.) under 1 or 10 μmol m^{-2} s^{-1} of constant red:blue (cRB; Figure 4.5.A.) or red:green:blue (cRGB; Figure 4.5.B.) light or in constant darkness. Average hypocotyl length for each genotype under each light condition were normalised to seedlings of the same genotype grown in darkness. Relative hypocotyl lengths were used to conduct a Dunnet's test comparing the interaction between fluence rate of light under each condition and the relative hypocotyl length in each genotype to that seen in wild type Col-0 seedlings.

Under cRB light (Figure 4.5.A.) all combinations of *phot* mutants showed similar hypocotyl elongation response to light intensity to that seen in wild type (p >0.17) while

cry1cry2 seedlings presented a significantly reduced responsiveness to light intensity (p <0.001) as did *phyB* seedlings (p= 0.0264).

cRGB light (Figure 4.5.B.) induces similar responses to cRB light with all *phot* mutants responding similarly to Col-0 wild type (p >0.21) and *cry1cry2* and *phyB* mutants showing a significantly less pronounced response to increasing light intensity (*cry1cry2* p <0.001; *phyB* p=0.002).

A post-hoc Bonferroni adjusted students t-test was also performed in order to compare the relative hypocotyl length of each genotype under 1 μmol m^{-2} s^{-1} of cRB light to that seen under 1 μmol m^{-2} s^{-1} of cRGB light. This test showed that the length of Col-0 wild type hypocotyls was significantly longer under 1 μmol m^{-2} s^{-1} of cRGB light than under cRB light (p <0.0001), the same was true for *phot1*(p <0.0001) and *phyB* (p <0.0001) single mutants. In *cry1cry2*, *phot1phot2* and *phot2* mutants however there was no significant change in hypocotyl length between 1 μmol m^{-2} s^{-1} of cRB and cRGB light (p >0.08) .

These data suggest that *cry1cry2* and *phyB* mutants are less sensitive to changing intensities of these complex regimes of light than Col-0 wild type or *phot* mutants, in line with their established roles in photomorphogenesis (Whitelam et al., 1993, Folta and Spalding, 2001, Wu and Spalding, 2007, Wang et al., 2013). We were also able to induce a 'low-light avoidance response' using very low intensities of cRGB light. This low-light response was not seen in *cry1cry2*, *phot1phot2* or *phot2* mutants. This could indicate that cryptochromes or phot2 are required to induce shade avoidance responses to green light under complex light regimes.

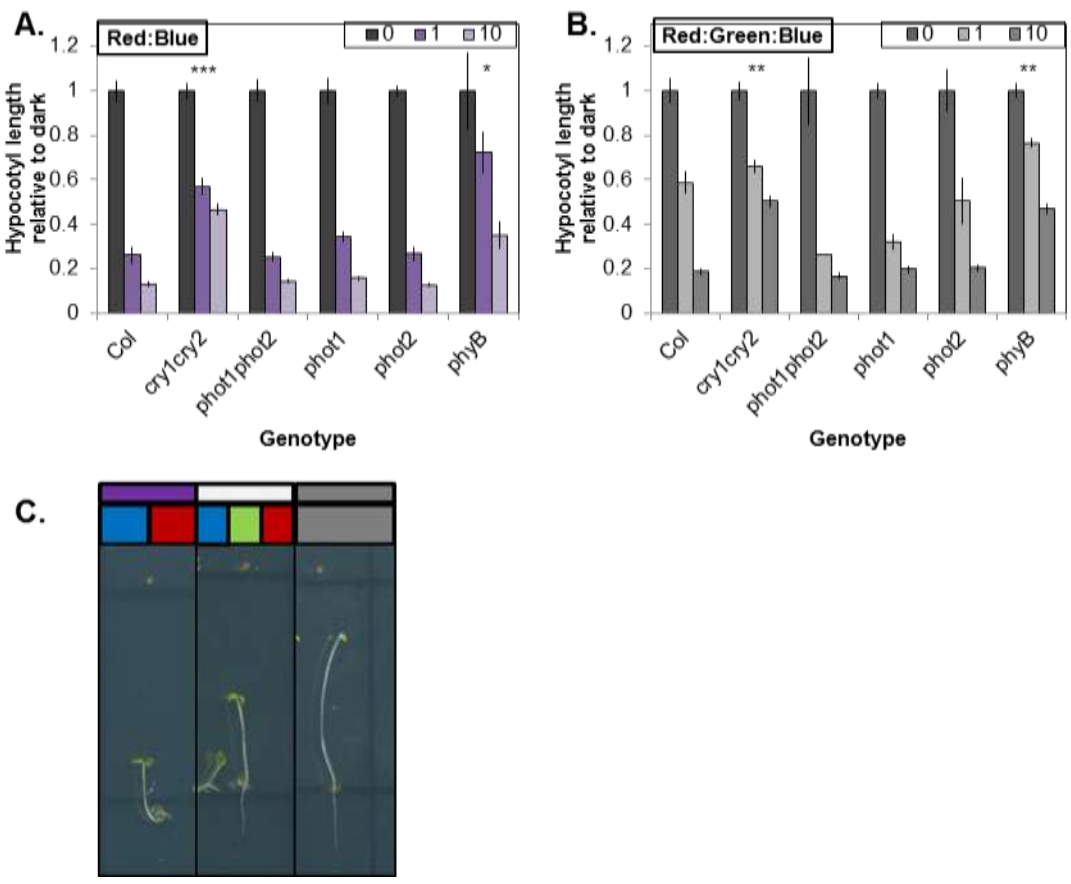

Figure 4.5. Hypocotyl elongation responses to quality and intensity under complex light regimes. Average hypocotyl length of Col-0 wild type and *cry1 cry2*, *phot1 phot2*, *phot1*, *phot2* and *phyB* photoreceptor knockout mutant seedlings grown for 5 days on 0.5x MS agar plates in darkness or under 1 or 10 µmol m^{-2} s^{-1} (µE) of; (**A**) a 3.0:2.0 mix of red:blue LED light or (**B**) a 3.0:2.5:2.0 mix of red:green:blue LED light. Hpocotyl length presented as relative to the average length of seedlings of the same genotype grown in darkness (Average length of this genotype in darkness = 1). Data points represent the average hypocotyl length of seedlings from one of three independent experiments. Error bars indicate standard error of the mean where n= 4-18. Asterisks indicate a statistically significant change in hypocotyl length relative to fluence rate relative to the change seen in wild type seedlings (* $p<0.05$; ** $p<0.01$; *** $p<0.001$; Dunnet's test). (**C**) Wild type seedlings grown on 0.5 MS agar plates under 1 µmol m^{-2} s^{-1} of a 3.0:2.0 mix of red:blue LED light, a 3.0:2.5:2.0 mix of red:green:blue or in darkness.

4.2.6. Effects of very low intensities of blue light upon the circadian system in *Arabidopsis thaliana*

In order to test whether the intensity of blue light wavelengths present in our green and filtered green LED light was enough to maintain circadian rhythms in absence of the green wavelengths, Col-0 *CCA1::LUC2* were entrained individually for 6 days under standard growth conditions (Methods 2.6.1.) before transferring to constant blue LED light for 5 days for luciferase imaging (Methods 2.6.2).

One group of entrained seedlings were transferred to 25 μmol m^{-2} s^{-1} of blue LED light with half of the tested seedlings being covered by a neutral density filter in order to reduce the blue light intensity to 3 μmol m^{-2} s^{-1} for luciferase imaging (Figure 4.6.C.). Under 25 μmol m^{-2} s^{-1} of blue light, seedlings presented a circadian period of around 23.1h and an RAE of 0.24. Seedlings imaged under 3 μmol m^{-2} s^{-1} of blue light produced waveforms with a significantly lengthened period of around 23.8h (p =0.0061) but no significant loss of rhythmicity (RAE =0.28; p = 0.39).

A separate group of similarly entrained seedlings were transferred to 20 μmol m^{-2} s^{-1} of blue LED light with half of the seedlings covered by a filter to expose them to 0.8 μmol m^{-2} s^{-1} of blue LED light (Figure 4.6.D.). Under 20 μmol m^{-2} s^{-1} of blue light, waveforms were imaged with a period of around 23.8h, while in the same experiment, under 0.8 μmol m^{-2} s^{-1} of blue light, waveforms produced were arrhythmic and no period estimates could be calculated.

These data demonstrate that rhythmicity can be maintained under as little as 3 μmol m^{-2} s^{-1} of blue light but is lost entirely under 0.8 μmol m^{-2} s^{-1} of blue. These intensities of blue light were used in order to be comparable to the quantity of μmol m^{-2} s^{-1} of blue

wavelengths found in our green LED light spectra before and after filtration with a #312 Canary filter. This indicates that the quantity of blue wavelengths in unfiltered green light is sufficient to maintain circadian rhythms in the absence of the green wavelengths present although the same is not true for filtered green light.

A.

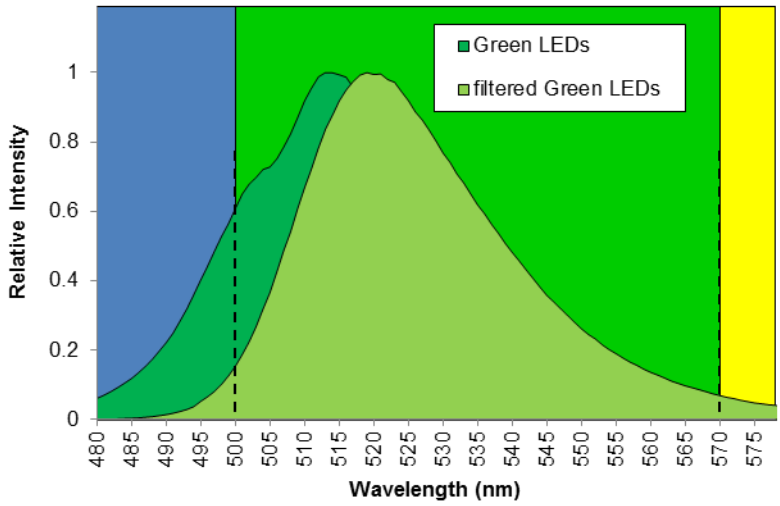

B.

Colour	Wavelength (nm)	Proportion of light in 20 µmol m^{-2} s^{-1} of light from this source within this spectral range (µmol m^{-2} s^{-1})	
		filtered Green LEDs	**Green LEDs**
Blue	450-500	**0.665**	**2.254**
Green	500-570	**18.76**	**17.39**
Yellow	570-590	**0.372**	**0.229**

C. D.

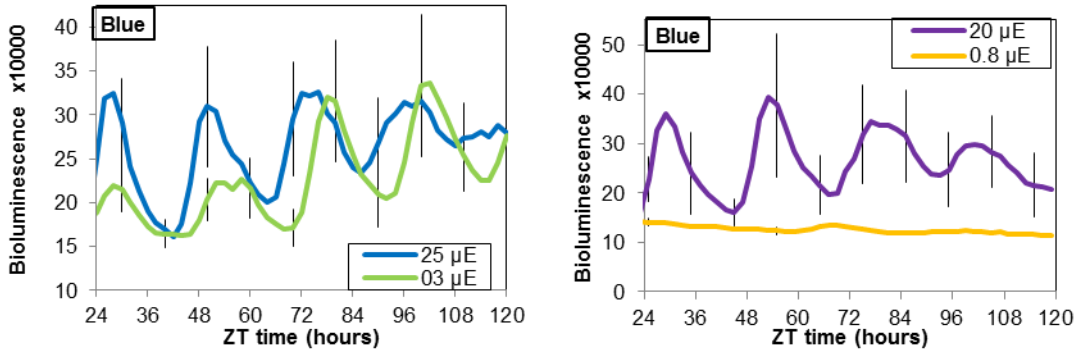

Figure 4.6. Effects of low intensities of blue wavelengths found in green LED light on circadian rhythms in *Arabidopsis thaliana*. (**A**) Spectra of light emissions from green Light Emitting Diodes (LEDs; Bright Technology Industrial Ltd., Shenzhen, China) and green LED light filtered with a #312 Canary Filter (filtered green LEDs; Stage Depot Ltd., Bristol, UK) highlighting the regions of these spectra in the blue, green and yellow regions of the visible light spectrum. (**B**) Table indicating the spectral ranges of blue, yellow and green light along with the quantity of light (µmol m^{-2} s^{-1}) in each range produced within 20 µmol m^{-2} s^{-1} of light from filtered or unfiltered green LEDs. (**C**, **D**) Waveforms of luciferase bioluminescence in Col-0 *CCA1::LUC2* seedlings entrained for 6 days under 12h:12h light:dark cycles before transfer to constant conditions for imaging under blue light of various intensities; either (**C**) 25 (blue line), 3 (green line), (**D**) 20 (purple line) or 0.8 µmol m^{-2} s^{-1} (yellow line).

4.2.7. Circadian responses to different intensities of filtered green light in *Arabidopsis thaliana*

We had observed that hypocotyls responded differently to different intensities of filtered green light but had not yet observed circadian rhythms under these conditions. Additionally, we have shown that by filtering green LED light through a #312 Canary filter we can produce a filtered green spectrum lacking sufficient intensities of blue wavelengths to maintain circadian rhythms in wild type seedlings. In order to assess the effects of filtered green light upon the *Arabidopsis* circadian system, Col-0 *CCA1::LUC2* seedlings were observed under constant filtered green of various intensities. Individual seedlings were entrained for 6 days under standard conditions (Methods 2.6.1.) before being transferred to either 4, 8, 13 or 22 μmol m^{-2} s^{-1} of constant green light filtered through a #312 Canary filter of for luciferase imaging (Methods 2.6.2.).

Waveforms of luciferase bioluminescence from each group of plants were generated (Figure 4.7.A.) and used to calculate periods which were plotted against LOG_{10} fluence rate (Figure 4.7.B.) and circadian amplitudes (Figure 4.7.C.). Rhythms of luciferase bioluminescence were produced with a period significantly longer under 4 and 8 μmol m^{-2} s^{-1} of filtered green light than under 13 and 22 μmol m^{-2} s^{-1} (p <0.003). Likewise, the amplitude and RAE of these rhythms was significantly higher under 13 and 22 μmol m^{-2} s^{-1} than under 4 and 8 μmol m^{-2} s^{-1} of filtered green light (Amplitude p <0.0002; RAE p <0.028).

These data show that wild type plants can maintain circadian rhythmicity under green light filtered with #312 Canary filters, through which less blue light than is required to maintain rhythmicity is emitted, even under as little as 4 μmol m^{-2} s^{-1} of light. Suggesting

that green light alone is sufficient to maintain circadian rhythms, even in the absence of blue wavelengths.

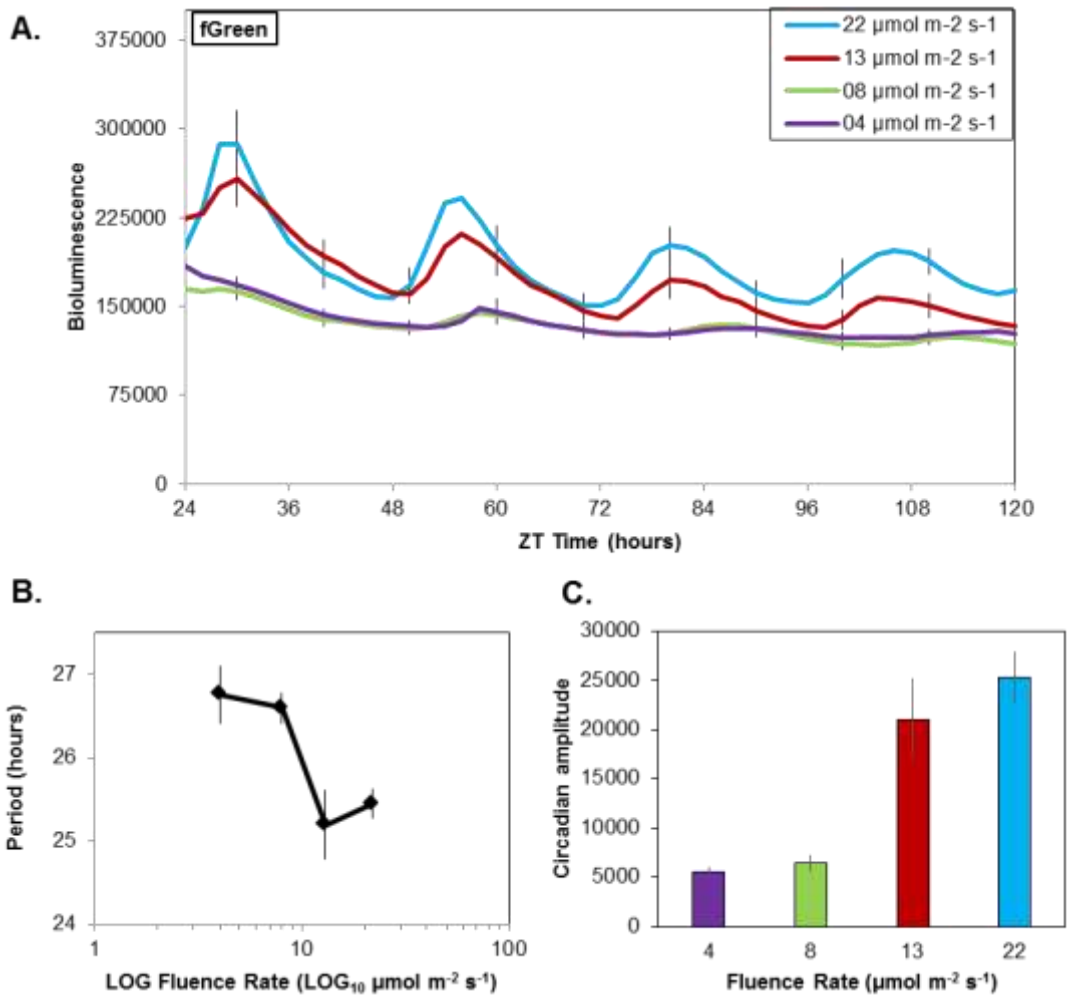

Figure 4.7. Fluence rate responses of *CCA1* to filtered green light. (**A**) Waveforms, (**B**) circadian period estimates plotted against LOG fluence rate and (**C**) circadian amplitude plotted against fluence rate of luciferase bioluminescence rhythms in Col-0 *CCA1::LUC2* entrained for 6 days under 12h:12h light:dark cycles on 0.5x MS agar plates and imaged under 4, 8, 13 or 22 µmol m^{-2} s^{-1} of green LED light filtered through a #312 Canary filter (Stage Depot Ltd., UK). Error bars indicate standard error of the mean with n=6-11. For waveforms, error bars are shown every 10 hours for clarity.

4.2.8. Effects of DCMU upon circadian rhythms in *Arabidopsis thaliana*

While circadian rhythms could be observed in plants under filtered green light it was not clear as to whether these rhythms were being caused by photoreceptor or photosynthetic inputs to the circadian system, or by a combination of these factors. In order to test the effects of photosynthesis based biochemical inputs to the circadian system on rhythms under filtered green light, PSII electron flow was inhibited by the application of DCMU prior to imaging of circadian rhythms.

Col-0 *CCA1::LUC2* seedlings were entrained individually for 5 days under standard growth conditions (Methods 2.6.1.) before being transferred to fresh 0.5x MS agar plates with or without 3% exogenous sucrose and being treated with either 20 µmol DCMU in DMSO or a control treatment of DMSO only and returned to standard growth conditions for a further day. Seedlings were then transferred to either 20 µmol m^{-2} s^{-1} of constant blue (Figure 4.8.A. and 4.8.B.) or filtered green (Figure 4.8.C. and 4.8.D.) light for luciferase imaging (Methods 2.6.2.). Wavelengths of luciferase bioluminescence (Figure 4.8.A. and 4.8.C.) were generated and used to calculate circadian period estimates (Figure 4.8.B and Figure 4.8.D.) which were plotted against RAE of luciferase bioluminescence.

Under both blue and filtered green light and in the absence of sucrose, DCMU is sufficient to suppress circadian rhythms of luciferase bioluminescence, producing arrhythmicity in generated waveforms and no calculable circadian period estimates. The addition of exogenous sucrose alongside DCMU recovers rhythms of luciferase bioluminescence under both light conditions tested, producing no significant change in circadian period compared to a DMSO treated control (p= 0.25 under blue; p= 0.79 under filtered green). Under blue light, all sucrose treated plants, with or without the

addition of DCMU, showed a significantly increased RAE compared to a control treated with DMSO only, with an RAE of around 0.5 compared to the control RAE of around 0.2 (p <0.0001), it should be noted however that this loss of rhythmicity may be due to poor germination under these conditions and further investigation would be necessary to confirm these findings. No significant loss of rhythmicity was observed in sucrose treated plants under filtered green light (p >0.38).

These data suggest that inhibiting photosynthesis using DCMU is sufficient to inhibit circadian rhythms of luciferase bioluminescence under either blue or green light. However, the recovery of these rhythms through the introduction of exogenous sucrose suggests that this loss of rhythmicity may be due to a starvation response rather than due to a photosynthetic circadian input.

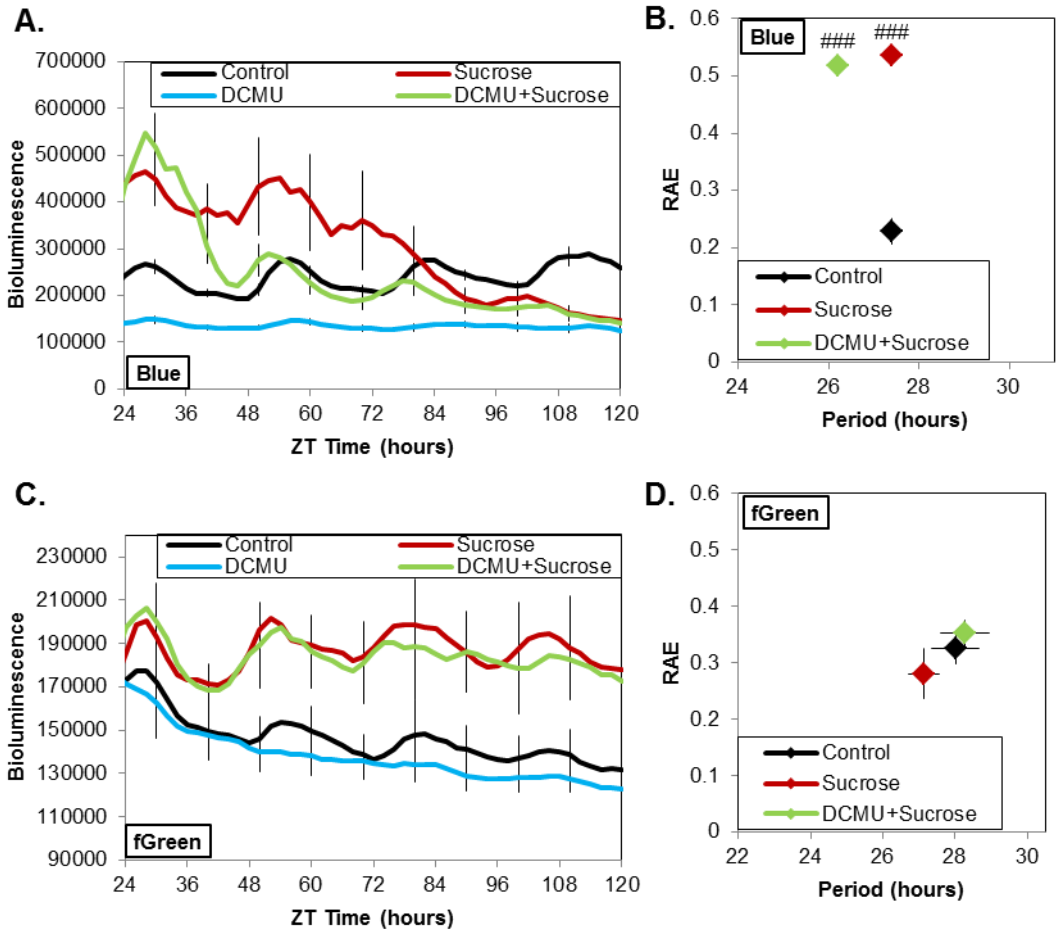

Figure 4.8. Effects of DCMU on circadian rhythms in *Arabidopsis thaliana*. (**A, C**) Waveforms of luciferase bioluminescence rhythms and (**B**, **D**) circadian period estimates plotted against relative amplitude error (RAE) in Col-0 *CCA1::LUC2* seedlings treated with either; 3% exogenous sucrose (red lines), 20 µmol DCMU (blue lines), both sucrose and DCMU (green lines) or an untreated control (black lines) under (**A, B**) 20 µmol m^{-2} s^{-1} blue light or (**C, D**) 20 µmol m^{-2} s^{-1} filtered green light. Seedlings were grown for 6 days on 0.5x MS agar plates with or without exogenous sucrose and entrained in 12h:12h light:dark cycles under 60 µmol m^{-2} s^{-1} white light before imaging. DCMU was applied 1 day before imaging by spray treatment of DCMU dissolved in DMSO, all plants not treated with DCMU were treated with a spray of DMSO only. Error bars indicate standard error of the mean with n=2-10. For waveforms, error bars are shown every 10 hours for clarity. Hashes indicate a statistically significant difference in RAE relative to control seedlings (### $p<0.001$; student's t-test).

4.2.9. Cryptochrome dependant circadian responses to different qualities of light in *Arabidopsis thaliana*

As cryptochromes have previously been reported to respond to green light (Zhang and Folta, 2012, Banerjee et al., 2007) we examined the involvement of cryptochromes in the green light responses observed in *Arabidopsis*. The cryptochrome double mutant line, *cry1cry2* was transformed with a *CCA1::LUC2* circadian luciferase reporter gene to produce a *cry1cry2 CCA1::LUC2* reporter line. Wild type Col-0 and *cry1cry2* mutant seedlings, both expressing the *CCA1::LUC2* reporter, were entrained individually for 6 days under standard growth conditions before being transferred to either darkness or 20 µmol m^{-2} s^{-1} of constant blue or #312 Canary filtered green light for luciferase imaging (Methods 2.6.2., Figures 4.9A-D)). Plants transferred to darkness were grown on 0.5x MS with (Figure 4.9.A.) or without (Figure 4.9.B) 3% exogenous sucrose in order to allow rhythms of luciferase bioluminescence to be observed in the absence of light. Waveforms of luciferase bioluminescence were used to generate circadian period estimates (Figure 4.9.E. and 4.9.F.) which were plotted against RAE of circadian bioluminescence.

Under blue light, waveforms of luciferase bioluminescence in *cry1cry2* mutants were arrhythmic, with no calculable circadian period. Under filtered green light, there was no significant difference in the period of the *cry1cry2* mutant and wild type (p= 0.58) although there was a significant loss of rhythmicity with *cry1cry2* mutants (RAE= 0.48) showing a significantly higher RAE than in wild type (RAE= 0.32; p=0.0038). In darkness, both mutant and wild type plants were arrhythmic in the absence of exogenous sucrose, and with exogenous sucrose there was no significant difference between the wild type and *cry1cry2* rhythms (circadian period p= 0.99; RAE p= 0.24).

These data suggest that, cryptochromes are required to maintain circadian rhythms of *CCA1* expression under blue light. Furthermore, while cryptochromes are unlikely to be the only factor in maintaining circadian rhythms under filtered green light, the absence of cryptochromes does lead to a significant loss of robustness of circadian rhythms. In darkness, circadian rhythms of luciferase bioluminescence are not present without the addition of exogenous sucrose, which may suggest that the loss of rhythms is a starvation response due to the loss of photosynthetically produced sugars when grown in darkness, although no specific photoreceptor is required to maintain circadian rhythms if exogenous sucrose is present.

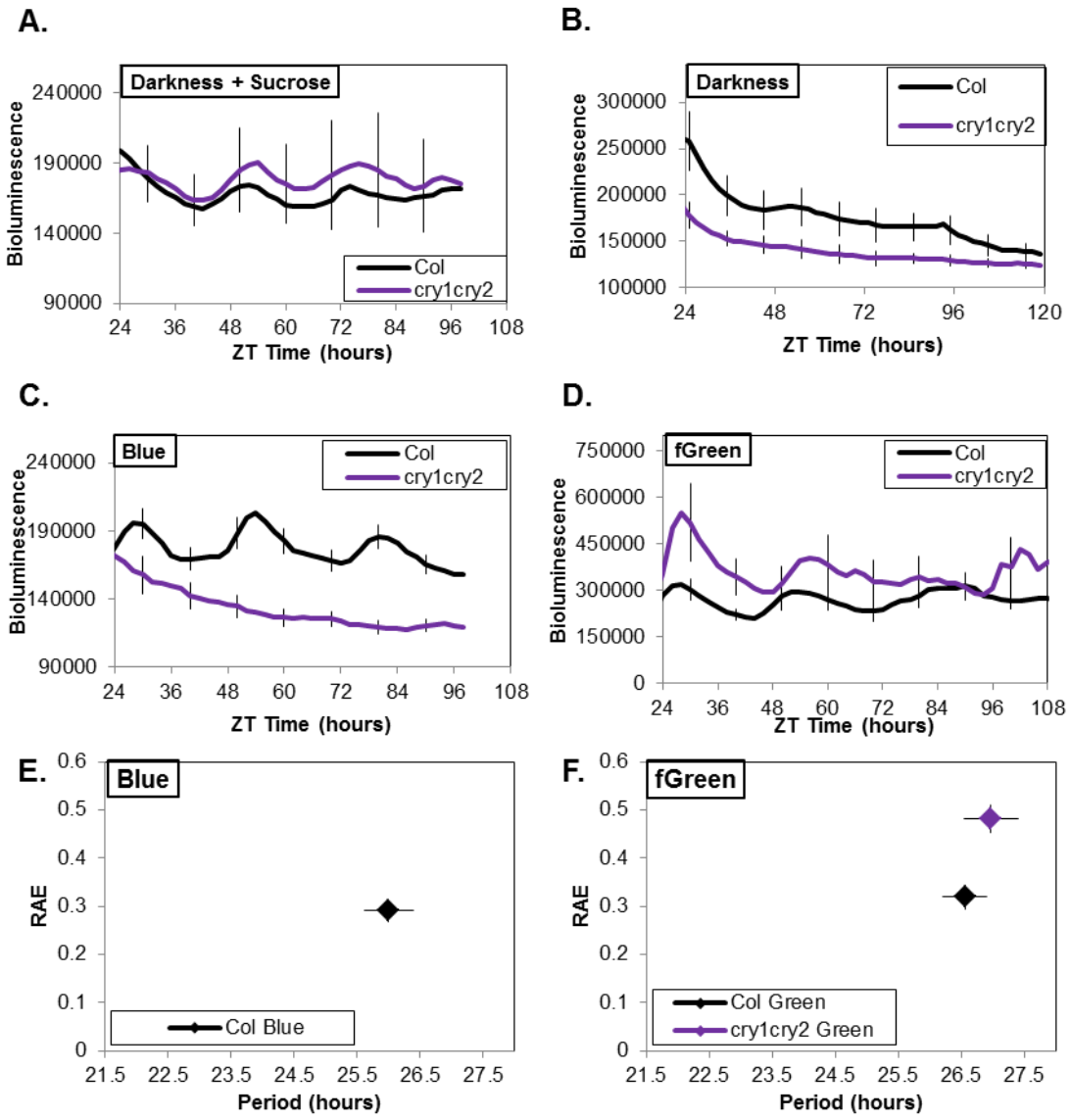

Figure 4.9. Circadian rhythms of *CCA1* in cryptochrome knockout mutants. (**A**) Waveforms of luciferase bioluminescence rhythms in Col-0 *CCA1::LUC2* (black) and *cry1cry2 CCA1::LUC* (purple) seedlings entrained for 6 days under 12h:12h light:dark cycles on 0.5x MS agar plates with 3% supplemental sucrose and imaged in darkness before imaging in darkness or (**B**-**D**) grown on 0.5x MS agar without supplemental sucrose in (**B**) darkness or under (**C**) 20 µmol m^{-2} s^{-1} blue LED light or (**D**) 20 µmol m^{-2} s^{-1} green LED light filtered through a #312 Canary filter (Stage Depot Ltd., UK). Circadian period estimates plotted against relative amplitude error (RAE) of luciferase bioluminescence in Col-0 *CCA1::LUC2* (black) and *cry1cry2 CCA1::LUC* (purple) seedlings entrained for 6 days under 12h:12h light:dark cycles on 0.5x MS agar plates before imaging under (**E**) 20 µmol m^{-2} s^{-1} blue LED light or (**F**) 20 µmol m^{-2} s^{-1} green LED light filtered through a #312 Canary filter (Stage Depot Ltd., UK). No circadian period could be calculated from *cry1cry2 CCA1::LUC2* luciferase bioluminescence under blue light. Error bars indicate standard error of the mean with n=8-16. For waveforms, error bars are shown every 10 hours for clarity.

4.2.10. Circadian rhythms under OG515 filtered green light

In order to further assess the influence of the blue wavelengths found in our green and filtered green light sources an optical glass filter with a cut-off wavelength of 515 nm (OG515) was used to further filter our green LED lights. While this limited the potential light intensity of experiments to 17 μmol m^{-2} s^{-1} it also removed more of the blue wavelengths of light than our previously utilised filters (Figure 4.10.A.) allowing us to further test how the blue wavelengths found in green lights influence circadian photoperception in *Arabidopsis*.

Col-0 *CCA1::LUC2* and *cry1cry2 CCA1CCA1::LUC2* seedlings were entrained for 6 days (Methods 2.6.1.) before transferring to constant conditions under 17 μmol m^{-2} s^{-1} of green light filtered with OG515 filters. Waveforms of luciferase bioluminescence (Figure 4.10.B.) were generated and used to calculate circadian period estimates which were plotted against RAE of luciferase bioluminescence (Figure 4.10.B.). *cry1cry2* seedlings tested under these light conditions were arrhythmic, producing no calculable circadian period, while wild type seedlings presented a circadian period of around 26h with an RAE of around 0.35.

These data suggest that circadian rhythms under these light conditions require cryptochromes in order to maintain rhythmicity. This further suggests that rhythms observed in *cry1cry2* seedlings under green light filtered with #312 Canary filters (Figure 3.9.D.) may be due to the blue wavelengths present in these light conditions rather than the much greater intensities of green light. This further implicates the potential role of other, photoreceptors in *Arabidopsis* in the maintenance of circadian rhythms under #312 Canary filtered green light but not in maintaining rhythms under OG515 filtered green light.

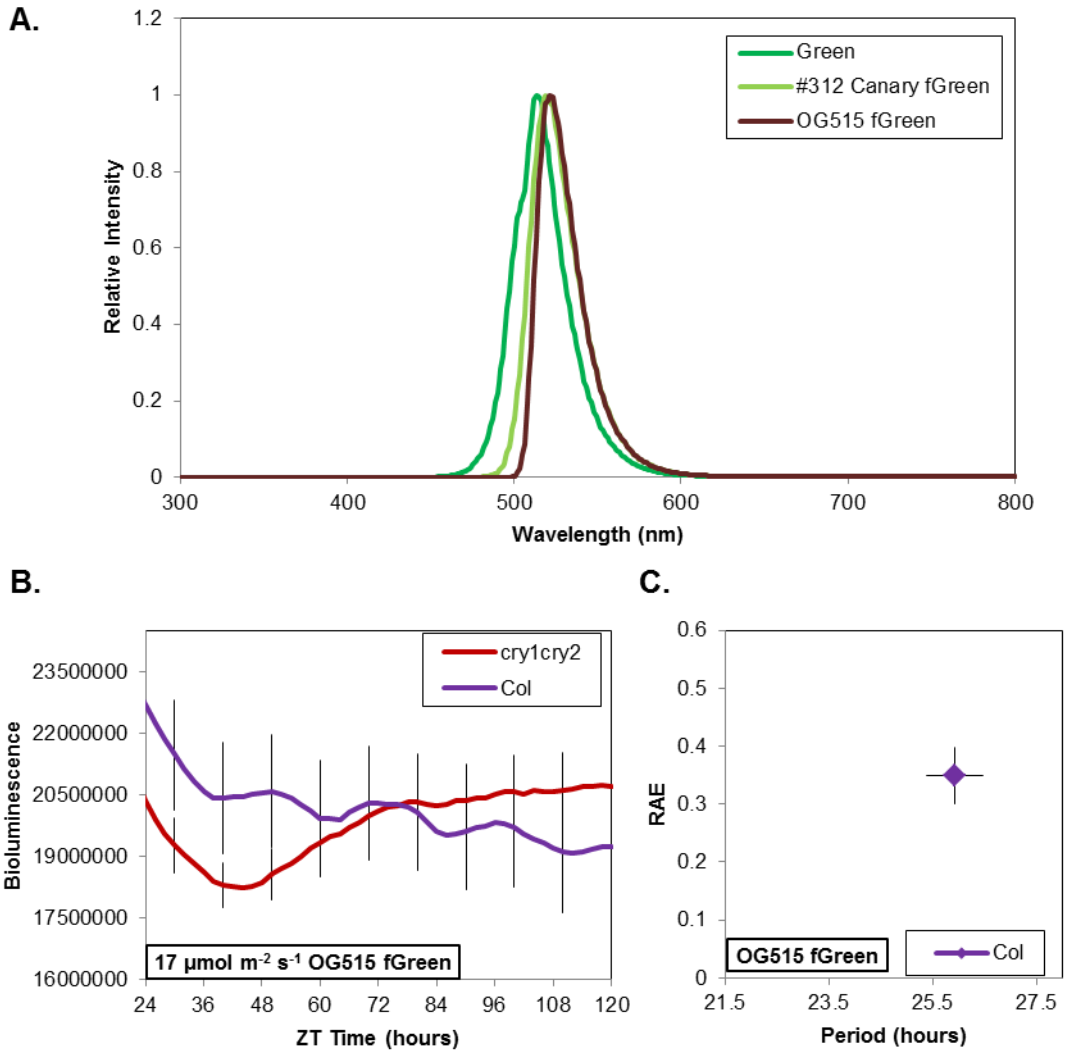

Figure 4.10. Circadian responses to OG515 filtered green light in cryptochrome double mutants. (**A**) Waveforms of spectra emitted by green LEDs without filters (dark green line) and filtered with a #312 canary filter (light green line; Stage Depot Ltd., UK) or an OG515 optical glass filter (brown line; Galvoptics Ltd., UK). (**B**) Waveforms and (**C**) circadian period estimates plotted against relative amplitude error (RAE) in Col-0 *CCA1::LUC2* (purple line) and *cry1cry2 CCA1::LUC2* (red line) seedlings entrained for 6 days under 12h:12h light:dark cycles on 0.5x MS agar plates and imaged under 17 µmol m^{-2} s^{-1} of green LED light filtered through an OG515 filter (Galvoptics Ltd., UK). Error bars indicate standard error of the mean with n=3-11. For waveforms, error bars are shown every 10 hours for clarity. No circadian period estimates could be generated from waveforms of *cry1cry2* seedlings.

4.3. Discussion

4.3.1. The role of green light in plant photobiological studies

The role of green light in plant development is poorly understood. Many commercial organisations have switched from fluorescent white growth lights to mixed blue and red LED growth lights in order to minimise energy costs whilst maintaining crop yield (Massa et al., 2008), eliminating green light from the crop growth spectra. Additionally, plants have no known photoreceptors with absorbance peaks found within green-light wavelengths, while families of established photoreceptors are specifically responsive to red, blue and UV light (Sullivan and Deng, 2003, Franklin and Whitelam, 2004, Briggs et al., 2001, Liu et al., 2016, Kim et al., 2007, Christie et al., 2012a), further encouraging the belief that plants are not responsive to green light in any meaningful way. Roles have been identified for green light in low-light avoidance, stomatal opening and hypocotyl elongation (Folta, 2004, Zhang et al., 2011), although some green light responses have been shown to in fact be mis-attributed responses to very low intensities of blue light present in many green light sources which can be detected by blue light photoreceptors in plants (see Figure 4.5. for examples of plant responses to very low intensities of blue light) (Wang and Folta, 2013, Wang et al., 2013, Zhang et al., 2011). Therefore, in order to study the effects of green light on plants we must first identify a green light which lacks interfering blue or red wavelengths.

LEDs are becoming available in a wide range of light qualities for an increasingly lower price. While affordable LEDs with a narrow enough spectrum for use in plant studies of the effects of green light are difficult to source, the combination of broader spectrum green LEDs with yellow or orange filters can help to produce a spectrum lacking many of the blue wavelengths which would otherwise cause interference when testing

responses *in planta*. Our study therefore made use of green LEDs with and without the addition of yellow filters (Figure 4.2.) to examine the effects of the blue wavelengths found in the unfiltered green light upon plants compared to the green light lacking these wavelengths produced by the addition of a filter.

4.3.2. Hypocotyl elongation under green light is regulated by both cryptochromes and phytochromes

Seedlings grown in partial or complete darkness undergo etiolation, a process by which cotyledon development is suppressed and the hypocotyl extends rapidly until a sufficiently intense light source is reached (Josse and Halliday, 2008, Alabadi et al., 2008). Upon exposure to light, de-etiolation begins, reducing the rate at which hypocotyl elongation occurs and beginning leaf development from the cotyledons to true leaves (Quail, 2002, Folta et al., 2003, Lu et al., 2009a, Nusinow et al., 2011). The rate at which de-etiolation occurs is dependent upon the quality and intensity of light to which the plant is exposed, this rate can be estimated by measuring the hypocotyl length of seedlings grown under specific light conditions and is an indicator of the level to which a seedling is sensitive to such a light condition (Ma et al., 2001). Both photosynthesis and photoreceptors are involved in the regulation of de-etiolation (Wang and K, 2014, Lu et al., 2014). De-etiolation can also be partially induced in the absence of light via a range of metabolic substrates such as nitric oxide (Beligni and Lamattina, 2000). Hypocotyl elongation responses to red, blue and white light are well documented (Aukerman et al., 1997, Somers et al., 2004, Yu et al., 2010) although the responses to green light are less well understood (Folta, 2004, Zhang et al., 2011).

In order to identify the involvement of green light in the de-etiolation process, mutant seedlings lacking function in one or more photoreceptors were grown under a range of light qualities and intensities, plants grown under each condition were compared to seedlings grown simultaneously in complete darkness (Figure 4.3.; Figure 4.4.; Figure 4.7.). As has been previously reported, under red light *phyB* mutants lack a significant de-etiolation response (Figure 4.3.A.; Hennig et al., 1999) and a similar response can be seen in *cry1cry2* double mutants under blue light (Figure 4.3.B.; Yu et al., 2010). Under unfiltered green light (Figure 4.3.C.), *cry1cry2* double mutants, all combinations of *phot* mutants and *phyB* mutants all show similar responsiveness to Col-0 wild type, suggesting that de-etiolation in response to green light is not being regulated by any of the specific photoreceptors being tested. Under green light filtered through a #312 Canary filter however, significant loss of responsiveness relative to wild type can be observed in *cry1cry2*, *phot1phot2* and *phyB* mutants (Figure 4.3.D.), suggesting that the removal of a proportion of the blue wavelengths and potentially the increased proportion of yellow wavelengths seen in filtered green light are sufficient to produce observable phenotypes in these mutants.

The response to filtered green light seen in the *phot1phot2* double mutant, along with the lack of significantly different response from wild type seen in either the *phot1* or *phot2* single mutant suggest that this response is normally regulated by both phot1 and phot2 redundantly and the loss of both photoreceptors is required to see any change in responsiveness. The responses seen in both *phyB* and *cry1cry2* mutants in these data are particularly interesting as they suggest that both blue and red photoreceptors are involved in the regulation of plant responses to green light. This could also suggest that a greater response to filtered green light would be observed in a *cry1cry2phyB* triple

mutant, although this mutant would most likely be unhealthy even without the potential stresses caused by testing conditions. Future testing using mutant lines lacking one or more of the ZEITLUPE family of blue light photoreceptors would allow for a broader assessment of photoreceptor responses to green light, as would testing of *cry1* and *cry2* single mutants and mutants lacking function of phytochromes other than phyB or multiple phytochromes.

We also assessed the effects of exogenous sucrose upon hypocotyl elongation responses to red, blue and green light by performing the tests seen in Figure 4.4. with the addition of 3% sucrose to the growth media. The addition of exogenous sucrose is known to induce de-etiolation responses in seedlings, even when grown in darkness (Stewart et al, 2011), and as such, all seedlings showed a reduced hypocotyl elongation response (Figure 4.4.) to that seen in plants grown without exogenous sucrose (Figure 4.3.), masking much of the light response observed. Under red light with exogenous sucrose, *phyB* mutants continue to show a significantly reduced response to increasing intensities of red light relative to the response seen in wild type (Figure 4.4.A.) and under of blue light *cry1cry2* mutants are similarly unresponsive even with exogenous sucrose (Figure 4.4.B.). Additionally, a significantly different response to wild type was seen in *phot2* mutants under red light with sucrose (Figure 4.4.A.), although this response may be due to poor germination of our *phot2* line under these conditions and additional testing would be required to confirm this phenotype. The response to green light in the presence of exogenous sucrose (Figure 4.4.C.) is more pronounced under 10 μmol m^{-2} s^{-1} of green light than it is in the absence of sucrose (Figure 4.3.C.), a difference which may suggest that photosynthetically produced sugars play a significant role in regulating de-etiolation under green light. However, there is still no significant

difference in responsiveness to increasing green light fluence rates between wild type and tested *cry1cry2*, *phot* and *phyB* mutants further suggesting the lack of significant involvement of photoreceptors in de-etiolation responses to these light conditions.

Additionally, in order to test whether the presence of green light within the wavelengths observed by a seedling is sufficient to stimulate low-light avoidance responses (Zhang et al. 2011), hypocotyl elongation responses to complex regimes of combined red and blue or red, green and blue LED lights were tested (Figure 4.7.). *phyB* and *cry1cry2* mutants are both less responsive to both of these light conditions than wild type, and *phot* mutants continued to present no significantly different responsiveness under either condition, suggesting that, like with green light, cryptochromes and phytochromes play a dominant role in regulating de-etiolation in response to these complex light regimes. However, hypocotyl lengths under 1 μmol m^{-2} s^{-1} of cRGB light in Col-0, *phot1* and *phyB* seedlings were visibly longer relative to dark grown seedlings than similar plants grown under cRB were relative to dark grown seedlings. This response, which was not seen in *cry1cry2*, *phot2* or *phot1phot2* mutants, suggesting that a low-light avoidance response is being stimulated by the addition of green light to the cRGB light regime and that cryptochromes and phot2 may be involved in order to maintain or regulate this response to green light in the presence of blue or red light. Furthermore, these data suggest that phytochrome B and phot1 are not required in order to maintain this low-light avoidance response.

4.3.3. Green light is sufficient to maintain circadian rhythms in wild type *Arabidopsis* seedlings

Another aspect of photobiology which has focussed primarily upon darkness or red, blue or white light is the interaction of light with the circadian clock. In the absence of light, the circadian clock can maintain rhythms, although extended periods of darkness will lead to a lengthening of circadian period and arrhythmia (Millar et al., 1995). The loss of robustness of circadian rhythms in plants grown in constant darkness can be remedied by the addition of a metabolic sugar such as sucrose to the growth media of the plants being tested (Haydon et al., 2013b), although this causes further inaccuracies in measurements as metabolic sugars have a distinct effect upon circadian rhythms (Dalchau et al., 2011). Under red light, all phytochromes act as an input to the circadian clock (Somers et al., 1998, Jones et al., 2015), although the dominant phytochrome, phyB, is primarily required to maintain stable circadian rhythms (Somers et al., 1998). The higher the intensity of red light a wild type plant is exposed to the shorter the period of the circadian clock will become. The same is true for increasing the intensity of blue light, although rhythms under blue light require cryptochromes to maintain them (Somers et al., 1998; Figure 4.9.) and are further influenced by members of the ZEITLUPE family of photoreceptors (Baudry et al., 2010). Circadian responses to green light however, are largely undocumented.

In order to assess the effects of green light upon circadian rhythms, wild type seedlings expressing a *CCA1::LUC2* reporter were imaged under constant green light filtered through a #312 Canary filter at various intensities (Figure 4.6.). As with other light qualities, increased intensities of filtered green light lead to a reduction in circadian period in wild type plants and at lower intensities a significant loss of robustness of

circadian rhythms was observed. These data suggest that while plants are able to use green light to maintain circadian rhythms, low fluence rates induce a loss of rhythmicity. This is consistent with our observations of hypocotyl responses to green light which also suggest that wild type plants, while responsive to green light, are less able to respond to low fluence rates of green light than to higher fluence rates (Figure 4.3.).

4.3.4. Cryptochromes are required to maintain robust circadian rhythms under green light

Cryptochromes are the primary blue-light photoreceptors in *Arabidopsis*(Lin et al., 1995, Folta and Maruhnich, 2007, Sellaro et al., 2010). They are known to be required to maintain circadian rhythms under blue light(Harmer et al., 2000, Toth et al., 2001) and have previously been suggested to potentially act as a green-light photoreceptor under a range of different conditions (Banerjee et al., 2007, Wang et al., 2013, Zhang and Folta, 2012), although this is a point of contention within the photobiology community, in part because the definition of 'green light' has been so poorly defined (Steinitz et al., 1985, Zhang et al., 2011, Herbel et al., 2013). In order to test whether cryptochromes are required to maintain circadian rhythms under green light in *Arabidopsis*, circadian reporter lines of a mutant lacking function in both cryptochromes (*cry1cry2 CCA1::LUC2*) were imaged (Figure 4.9.) under constant blue LED light or green LED light filtered through a #312 Canary filter to remove many of the blue regions of the spectrum (fGreen; Figure 4.5.). Under both light conditions, wild type plants expressing the same *CCA1::LUC2* reporter maintained robust circadian rhythms of LUC bioluminescence whereas *cry1cry2* seedlings showed complete arrhythmicity under

blue light and a loss of robustness of rhythms of luciferase bioluminescence under fGreen light (Figure 4.9.). The loss of rhythmicity seen under blue light in *cry1cry2 CCA1:LUC2* plants is seen throughout testing (Figure 4.9.C.) whereas under fGreen light, loss of rhythmic robustness is not apparent until after 60 hours of imaging (Figure 4.9.D.), suggesting that while cryptochromes are required to maintain robustness of rhythms under fGreen light they are less dominant in this role than they are under blue light. This could suggest that there may be other photochemical processes involved in the maintenance of circadian rhythms under these light conditions. It should be noted however that *cry1cry2* mutants are noticeably smaller than wild type seedlings, a phenotype which can cause a loss of amplitude of circadian rhythms of luciferase bioluminescence which can in turn produce a reduction in robustness of rhythms.

Finally, by filtering green light through an OG515 filter a spectrum can be achieved lacking more blue wavelengths than can be removed using a #312 Canary filter (Figure 4.10.). This further filtration creates a green light spectrum with a range beginning at around 500 nm and peaking at around 525 nm rather than the spectrum through our original filters which began at around 490 nm. Filtering green LED light through an OG515 filter produces a spectrum which is not sufficient to maintain circadian rhythms of luciferase bioluminescence in *cry1cry2 CCA1::LUC2* mutants under 17 µmol m^{-2} s^{-1} of light while wild type seedlings are still capable of producing rhythms with a periodicity of around 26 hours (Figure 4.10.) while under 20 µmol m^{-2} s^{-1} of #312 Canary filtered green light *cry1cry2 CCA1::LUC2* seedlings are still capable of producing rhythms of luciferase bioluminescence with a period of around 27 hours, albeit with a relatively low rhythmicity (RAE= 0.48; Figure 4.9.). This data suggests that while cryptochromes are not required to maintain rhythmicity in the presence of miniscule intensities of blue

light, total removal of these blue wavelengths along with loss of function in the cryptochromes is sufficient to induce arrhythmicity. This may indicate that cryptochromes are required to maintain circadian rhythms under green light but also suggests that another photoreceptor or photo-responsive mechanism is capable of maintaining rhythms under the wavelengths produced by green LEDs filtered through a #312 Canary filter but not through an OG515 filter. It should be noted that data in Figure 4.10. is taken from a single test however, and further testing is required to confirm these findings.

4.3.5. Exogenous sugars are sufficient to counteract circadian period lengthening in plants with inhibited photosynthetic electron transport under blue and green light

In order to assess the involvement of photosynthesis in green light responses observed in *Arabidopsis* seedlings, plants were grown on media with or without exogenous sucrose and treated with DCMU, an inhibitor of photosynthetic electron transport in photosystem II (PSII). The addition of exogenous sucrose is known to recover many phenotypes seen in plants treated with DCMU (Haydon et al., 2013b) and as such was used as a control treatment in this test. Circadian rhythms in these plants were then measured using luciferase imaging under blue (Figure 4.8.A) or #312 Canary filtered green light (Figure 4.8.C). Under both light conditions, circadian rhythms were significantly lengthened in seedlings treated with DCMU in the absence of sucrose although the addition of sucrose recovered the rhythms in plants treated with sucrose and DCMU under green light. Under blue light, plants treated with sucrose and DCMU presented a shortened circadian period although the high relative amplitude error

(RAE) of the rhythms seen in plants grown on sucrose under blue light, which could be attributed to stress caused by increased fungal infection on plates containing sucrose, reduces the reliability of these period measurements. Previously documented experiments have shown that under blue light, DCMU increases circadian period and that plants treated with both DCMU and sucrose lose this long period phenotype (Haydon et al., 2013b), as was seen in our plants tested under green light. This suggests that while photosynthesis is required to maintain circadian rhythms of luciferase bioluminescence under both blue and green light, this may be due to the requirement of energy to maintain these rhythms, which can be produced under any photosynthetically active wavelength of sufficient intensity, rather than the direct, non-metabolic involvement of photoperception with the circadian clock.

In this chapter, we have characterised hypocotyl elongation responses and circadian rhythms in wild type and photoreceptor mutant lines in *Arabidopsis*. Our data suggests that green light responses are regulated by a combination of cryptochrome, phototropin and phytochrome photoreceptors along with photosynthetic regulation, most likely via metabolic sugars. Hypocotyl de-etiolation can be induced by green light in wild type plants, although under filtered green light spectra responsiveness is reduced in *cry1cry2, phot1phot2* and *phyB* mutants. Additionally, wild type Col-0 plants are capable of maintaining circadian rhythms under constant green light, even with the removal of low intensity blue wavelengths from the green spectra, although in the absence of cryptochromes these rhythms become less robust or arrhythmic. While circadian rhythms of luciferase bioluminescence can be disrupted under both blue and green light by inhibiting PSII electron transport using DCMU, the application of exogenous sucrose is sufficient to recover these rhythms, suggesting that they may be being suppressed by

energy starvation. qRT-PCR could be used to determine whether circadian rhythms persist in the presence of DCMU in *cry1cry2* mutants without the need for luciferase reporters.

Chapter 5- Engineering green-light specific photoresponses in plants

5.1. Introduction

The ability to induce gene expression on command in a rapid, non-invasive, chemical-free manner is useful for both research, where the observation of specific genes under specific conditions can provide insight into the gene interactions and processes, and industry, where chemical-free induction of gene expression can aid in providing ideal conditions for the production of therapeutics and other biologically synthesised products. Optogenetic constructs have been used for some time in bacterial and mammalian systems to allow for rapid, non-invasive initiation of gene expression for both research and industry (Levskaya et al., 2005, Stein and Alexandrov, 2014). In plants, optogenetic approaches are limited by the interference of the activating light with endogenous photoreceptors which are present in all plant cells. Recently however, developments have been made in the form of optogenetic systems in plant protoplasts, with the engineering of both red/far-red and green/dark switching mechanisms in protoplasts from *Arabidopsis thaliana* and *Nicotiana benthamiana* (Ochoa-Fernandez et al., 2016, Chatelle et al., 2018).

Photosensitivity is integral to all plant life. In *Arabidopsis* the photoreceptor activity peaks in the red, blue and UV-B regions of the PAR spectrum but is notably lower in green wavelengths (Sullivan and Deng, 2003, Franklin and Whitelam, 2004, Briggs et al., 2001, Liu et al., 2016, Kim et al., 2007, Christie et al., 2012a). Optogenetic systems have been developed for plants using both plant and bacterial photoreceptors (Müller et al., 2014, Chatelle et al., 2018) but are far more limited than the range of systems tested in mammalian and bacterial cells (Moglich and Moffat, 2007, Ryu and Gomelsky, 2014, Tabor et al., 2011, Schmidl et al., 2014). Although plants are responsive to green light,

these responses are limited and can often be counteracted by the presence of even low intensities of red or blue light (Smith et al., 2017, Wang et al., 2013, Wang and Folta, 2013, Zhang and Folta, 2012). It has therefore been suggested that green light could be used to create an optogenetic system for use in plants.

In order to produce a green light activated optogenetic system, a photoreceptor with absorbance peaks in green wavelengths must be utilised. Due to the absence of such a photoreceptor in plants, we chose to make use of cyanobacteriochromes, a group of phytochrome-like photoreceptors naturally occurring in cyanobacteria known for their atypical absorbance spectra (Ikeuchi and Ishizuka, 2008). The aquatic environment of many cyanobacteria lacks the full spectrum of light which is made use of by terrestrial photosynthetic organisms, with the red spectrum being especially limited due to absorbance by water (Kehoe, 2010). CcaS is a green/red light cyanobacteriochrome which allows *Synechocystis* sp. PCC 6803 (*Synechocystis*) to respond to an abundance of green-light wavelengths and produce antenna proteins to better harvest light from the green spectral range when required (Hirose et al., 2008).

In *Synechocystis*, CcaS functions alongside CcaR in a typical prokaryotic two component regulatory system (Ikeuchi and Ishizuka, 2008). CcaS and CcaR have already been engineered and refined as a two-component light-switching control mechanism for gene expression in Escherichia coli (Tabor et al., 2011, Schmidl et al., 2014). In this chapter, the process undertaken to produce a similar system which functions within *Arabidopsis thaliana* and *Nicotiana benthamiana* is described. The testing of this Green Light Activated Synthetic System (GLASSys), transiently expressed in *Nicotiana benthamiana* leaves is also described along with the complications faced with the utilisation of this system in *Arabidopsis*.

5.2. Results

5.2.1. Designing a promoter for green light activated gene expression in plants

In *Synechocystis* sp. PCC 6803, the genomic cluster *ccaS-ccaR-cpcG2* allows for green light regulated expression of the cpcG2 antenna protein, which allows more efficient absorption of green wavelengths for use in photosynthesis (Hirose et al., 2008). Upon green light exposure, the green/red photoreceptor, CcaS, autophosphorylates and then phosphorylates the response regulator, CcaR, which changes conformation into an active state capable of binding to the G-box of the cpcG2 promoter region (Figure 5.1.A.). While this native promoter region has been successfully used to engineer green light switching constructs in both cyanobacteria (Abe et al., 2014) and *E. coli* (Tabor et al., 2011), the native promoter has been shown to be leaky when expressed in *E. coli* (Schmidl et al., 2014). Furthermore, the native G-box, from the cpcG2 promoter of *Synechocystis* sp. PCC 6803 which acts as a binding site for active CcaR, has been used to produce a synthetic promoter which has been shown to improve expression of the downstream gene in *E.coli* (Schmidl et al., 2014).

In order to adapt this pathway for use in plants we applied the methodology for plant promoter design found in Harmer and Kay (2005) in which, the binding region of the promoter for the desired input gene was connected to a Nopaline synthase (NOS) minimal promoter which then drove expression of a firefly luciferase gene. As such, we designed our promoter for green light expression (pGLE; Figure 5.1.B.) using four repeats of the *Synechocystis* sp. PCC 6803 G-box separated by spacer sequences of around 16 random bases and connected to a NOS minimal promoter (Harmer and Kay, 2005). We also designed this promoter with overhangs containing the recognition sequence for the Type IIS restriction enzyme *BsaI* at the 5' and 3' ends allowing the

promoter to be used as a Level 0 module for golden gate cloning without further adjustment.

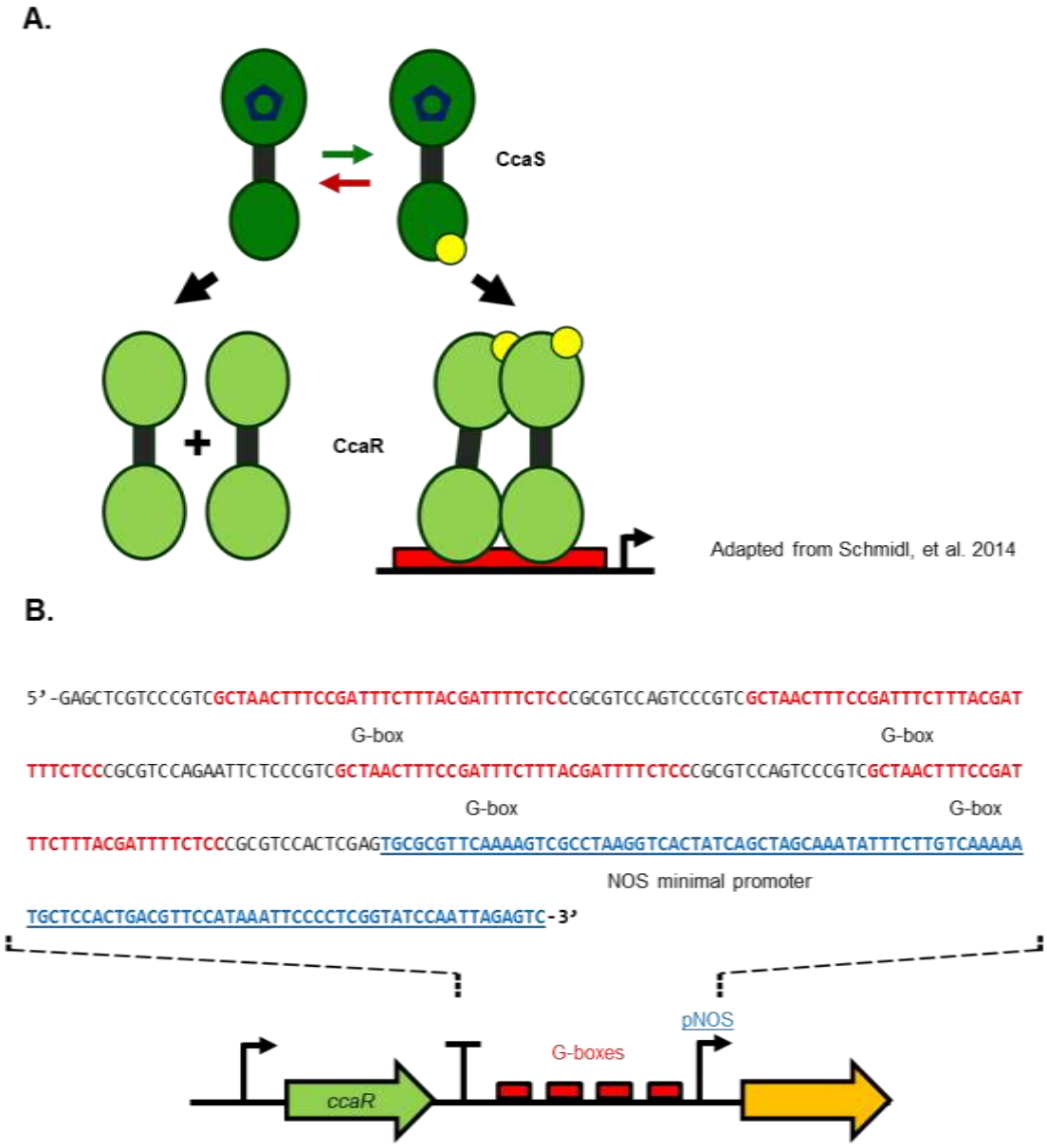

Figure 5.1. Design methodology for a promoter for green light expression for plants. (**A**) Diagram describing the green/red photoconversion of CcaS between dephosphorylated and auto-phosphorylated states along with the state of CcaR before and after phosphorylation by active CcaS. When exposed to red light or in the absence of sufficient green light, CcaS remains in an inactive, dephosphorylated state, as does CcaR. Upon exposure to green light, CcaS changes conformation to an active state and auto-phosphorylates. In turn, active CcaS phosphorylates CcaR which changes conformation to an active state in which two CcaR proteins can collectively bind to a single G-box found in the promoter region of *CPCG2* (Schmidl et al., 2014) or *pGLE*. (**B**) Sequence of the synthetic *PROMOTER FOR GREEN LIGHT EXPRESSION* (*pGLE*) designed to integrate the CcaS-CcaR green light sensing pathway into plants, showing sequences for 'spacer' regions (black text), *CPCG2* promoter G-boxes (red text) and NOS minimal promoter (blue underlined text), along with a diagram indicating the location of this promoter sequence within a synthetic construct; downstream of *ccaR* and upstream of a targeted output gene.

5.2.2. Designing Level 0 modules for Golden Gate assembly of multi-gene constructs

Constructs were assembled in three main stages using Golden Gate assembly (as per Weber et al., 2011). Firstly, Level 0 (L0) modules were selected from a wide range of available sequences or designed (if the required sequence is currently unavailable). Newly created sequences were deposited in a central of available level 0 modules for future use. For this study, most sequences, including all promoters and terminators were taken from the plant Golden Gate toolbox (Engler et al., 2014). Non-standardised modules were either produced synthetically or using PCR. If using PCR, overhangs were added to primer sequences in order to produce a sequence containing the gene of interest flanked by the required Type IIS restriction enzyme sites (Patron et al., 2015). Where possible, non-standardised modules were also 'domesticated', removing any internal *BsaI* sites and *BpiI* sites. In order to produce our Green Light Activated Synthetic System (GLASSys), Level 0 modules containing *ccaS* and *ccaR* coding sequences were synthesised (L0-*ccaS*; L0- *ccaR*; Table 5.1.), these sequences were codon optimised to function within *Arabidopsis* and included the necessary overhangs to produce Level 0 modules. We also produced a Level 0 module containing a firefly luciferase (*LUC*) gene using PCR (L0-*luc*; Table 5.1.) and then inserted into a L0 universal acceptor vector using digestion-ligation reaction cycles (Methods 2.4.4.; Figure 5.2.).

Module Name	Sequence in Module	Sequence Type	Relevant References
L0-*p35S*	Cauliflower Mosaic Virus RNA 35S (35S) promoter	Promoter	Engler et al. 2014
L0-*pFMV*	Figwort Mosaic Virus 35S (FMV) promoter	Promoter	Engler et al. 2014
L0-*pGLE*	Synthetic promoter, contains Nopaline Synthase (NOS) minimal promoter and G-boxes from *Synechocystis sp.* PC 6803	Promoter	Harmer and Kay, 2005, Schmidl et al. 2014
L0-*pUBI*	Ubiquitin promoter derived from *Zea mays*	Promoter	Engler et al. 2014
L0-*pMAS*	Mannopine synthase (MAS) promoter derived from *Agrobacterium tumefaciens*	Promoter	Engler et al. 2014
L0-*pACT*	Actin (ACT) promoter derived from *Arabidopsis thaliana*	Promoter	Engler et al. 2014
L0-*ccaS*	*ccaS* photoreceptor sequence derived from *Synechocystis sp.* PC 6803 and codon optimised for expression in *Arabidopsis thaliana*	CDS	Schmidl et al. 2014
L0-*ccaR*	*ccaR* response regulator derived from *Synechocystis sp.* PC 6803 and codon optimised for expression in *Arabidopsis thaliana*	CDS	Schmidl et al. 2014
L0-*luc*	Luciferase (*LUC*) gene from *Photinus pyralis*	CDS	Millar et al. 1995
L0-*bar*	*bar* gene for Basta herbicide resistance derived from *Streptomyces hygroscopicus*	CDS	Engler et al. 2014
L0-*p19*	RNA silencing suppressor *p19* (*p19*) *gene* derived from tomato bushy stunt virus (TBSV)	CDS	Engler et a. 2014
L0-*tHSP18*	Heat shock protein 18.2 (HSP18) terminator derived from *Arabidopsis thaliana*	Terminator	Engler et al. 2014
L0-*tACT2*	Actin2 (ACT2) terminator derived from *Arabidopsis thaliana*	Terminator	Engler et al. 2014
L0-*tNOS*	Nopaline synthase (NOS) terminator	Terminator	Engler et al. 2014

Table 5.1. Golden Gate Level 0 Modules utilised in this study. Level 0 Modules (L0) utilised in this study for assembly of Golden Gate multi-gene constructs listing the name of each module alongside the sequence contained within the module, the type of sequence this is (promoter, coding sequence (CDS) or terminator) and any reference relevant to the source, contents or construction and design of each module.

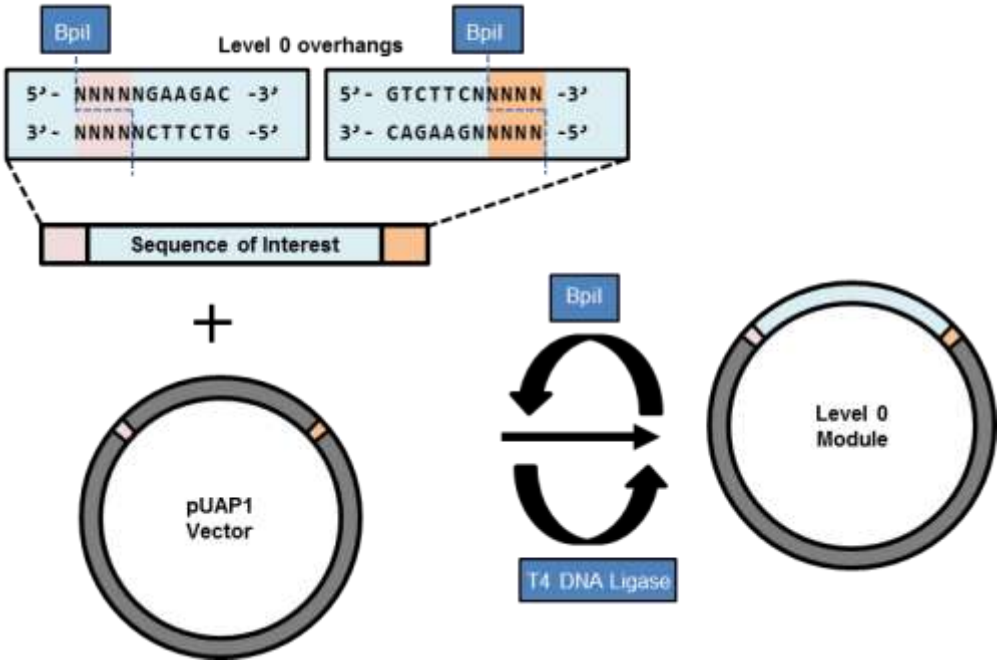

Figure 5.2. Producing Golden Gate Level 0 modules. Diagram representing the process for production of a Level 0 module (L0) for use in Golden Gate assembly of a modular multi-gene construct. Sequence overhangs containing a recognition sequence for the Type IIS restriction enzyme BpiI along with specific 4 bp overhangs designed to produce sticky ends with a specific 4 bp sequence appropriate to the module type are added to the 3' and 5' end of a sequence of interest; either during gene synthesis or using PCR. A Golden Gate digestion-ligation reaction with BpiI (Methods 2.4.4.) is then performed upon the sequence of interest together with an empty L0 Universal Acceptor Plasmid (pUAP1). Correct insertion into the pUAP1 vector aligns the sequence with new overhangs which produce a complete L0 module containing the gene of interest with appropriate overhangs for the production of a Level 1 gene cassette.

5.2.3. Assembling Level 1 cassettes from Level 0 modules

Level 0 modules were next assembled into Level 1 (L1) cassettes by performing a single digestion-ligation reaction (Methods 2.4.4.) in which three L0 modules; a promoter module, coding sequence module and a terminator module, were assembled into L1 vector backbone using T4 DNA ligase and *BsaI* restriction enzyme (Figure 5.3.). Once assembled, Level 1 constructs were transformed into *E. coli* and grown on selective media before being tested using colony PCR with appropriate primers (Methods 2.4.3.).

The L1 vector backbone adds *BpiI* restriction sites, required for Level 2 assemblies, to the 3' and 5' end of the L1 cassette sequence. L1 backbones are numbered 1 to 7 and can be either forward or reverse oriented in order to produce the intended positioning and orientation of L1 cassettes when assembled into a Level 2 construct. When producing the original GLASSys construct we produced four cassettes; a position 1 *ccaS* cassette containing a *p35S* promoter and a *tHSP18* terminator, a position 2 *ccaR* cassette containing a *pFMV* promoter and a *tACT2* terminator, a position 3 *LUC* cassette in reverse orientation containing the *pGLE* promoter and a *tNOS* terminator and a position 4 Glufosinate-ammonium (Basta; Bayer, Germany) herbicide resistance cassette containing *bar*, *pNOS* and *tNOS*. Additional L1 cassettes were produced later during the study for the production of further L2 constructs, all L1 cassettes used in this study are listed in Table 5.2.

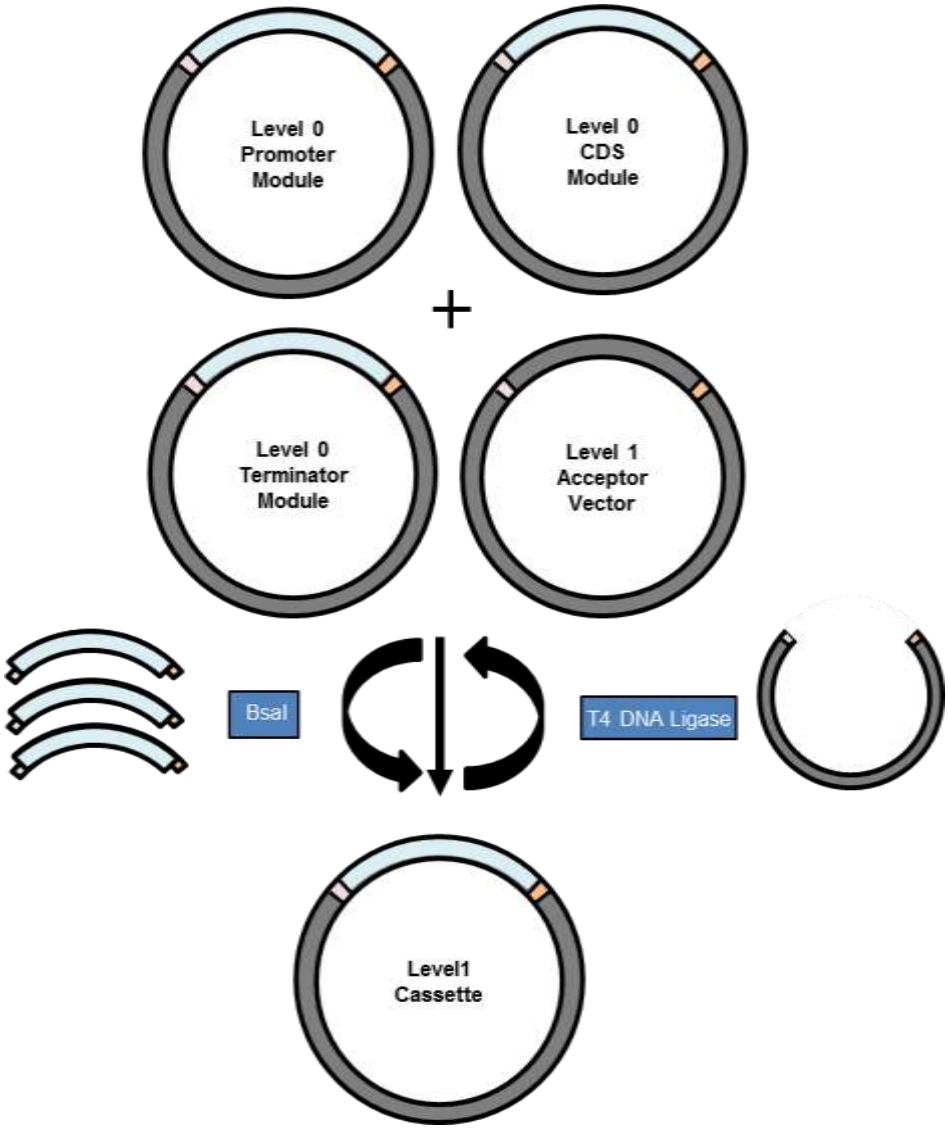

Figure 5.3. Producing Golden Gate Level 1 gene cassettes. Diagram representing the process for production of a Level 1 cassette (L1) from three Level 0 modules (L0) for use in Golden Gate assembly of a modular multi-gene construct. A promoter, coding sequence (CDS) and terminator L0 module along with an appropriate, empty L1 acceptor vector are combined using a Golden Gate digestion-ligation reaction with BsaI (Methods 2.4.4.) in order to produce a single L1 cassette containing a promoter, CDS and terminator with appropriate overhangs for the production of a Level 2 (L2) multi-gene construct. 14 primary L1 acceptor vectors can be used (F1-F7 and R1-R7); the L1 acceptor vector used will designate the position (position 1-7) within a L2 construct and the direction (Forward or Reverse) which the L1 cassette will take when used to assemble an L2 construct. This is done by aligning a properly assembled sequence within the L1 acceptor vector with new overhangs which produce specific sticky ends when digested with BpiI and align with the left and right bordering L1 cassettes when performing L2 assembly.

Cassette Name	Promoter module	CDS Module	Terminator module
F1-CcaS	L0-*p35S*	L0-*ccaS*	L0-*HSP18*
F2-p35S.CcaR	L0-*p35S*	L0-*ccaR*	L0-*tACT2*
F2-pFMV.CcaR	L0-*pFMV*	L0-*ccaR*	L0-*tACT2*
F2-pUBI.CcaR	L0-*pUBI*	L0-*ccaR*	L0-*tACT2*
F2-pMAS.CcaR	L0-*pMAS*	L0-*ccaR*	L0-*tACT2*
R3-LUC	L0-*pGLE*	L0-*luc*	L0-*tNOS*
F4-BAR	L0-*pNOS*	L0-*bar*	L0-*tNOS*
F5-p35S.P19	L0-*p35S*	L0-*p19*	L0-*HSP18*
F5-pACT.P19	L0-*pACT*	L0-*p19*	L0-*HSP18*

Table 5.2. Golden Gate Level 1 cassettes produced for this study. Level 1 Cassettes (L1) produced for this study for assembly of Golden Gate multi-gene constructs listing the name of each cassette alongside the promoter, coding sequence (CDS) and terminator Level 0 Modules (L0) used in their construction.

5.2.4. Generation of the original GLASSys Level 2 construct

Level 2 (L2) constructs use a number of L1 cassettes along with a L2 vector backbone and an end linker sequence to produce a complete multigene construct. Like L1 construction, all required pieces were assembled by combining in a single tube and running through digestion-ligation cycles in a thermal cycler (Methods 2.4.4.; Figure 5.4.A.).

The original GLASSys construct was built using the L1 cassettes; F1-CcaS, F2-pFMV.CcaR, R3-LUC and F4-BAR (Figure 5.4.B.). This was designed to introduce the CcaS-CcaR two component system, attached to a luciferase reporter gene, into plants, along with the *bar* herbicide resistance gene to act as a selection marker when transformed into *Arabidopsis thaliana.*

Once assembled and transformed into *E. coli*, GLASSys Level 2 constructs were tested using colony PCR (Figure 5.4.C.), cultures were then grown to obtain plasmid DNA (Methods 2.4.5). Prepared plasmids were then transformed into *Agrobacterium tumefaciens* (*Agrobacterium*) for transformation into *Arabidopsis* or *Nicotiana Benthamiana* (Methods 2.3.4, Methods 2.3.6.).

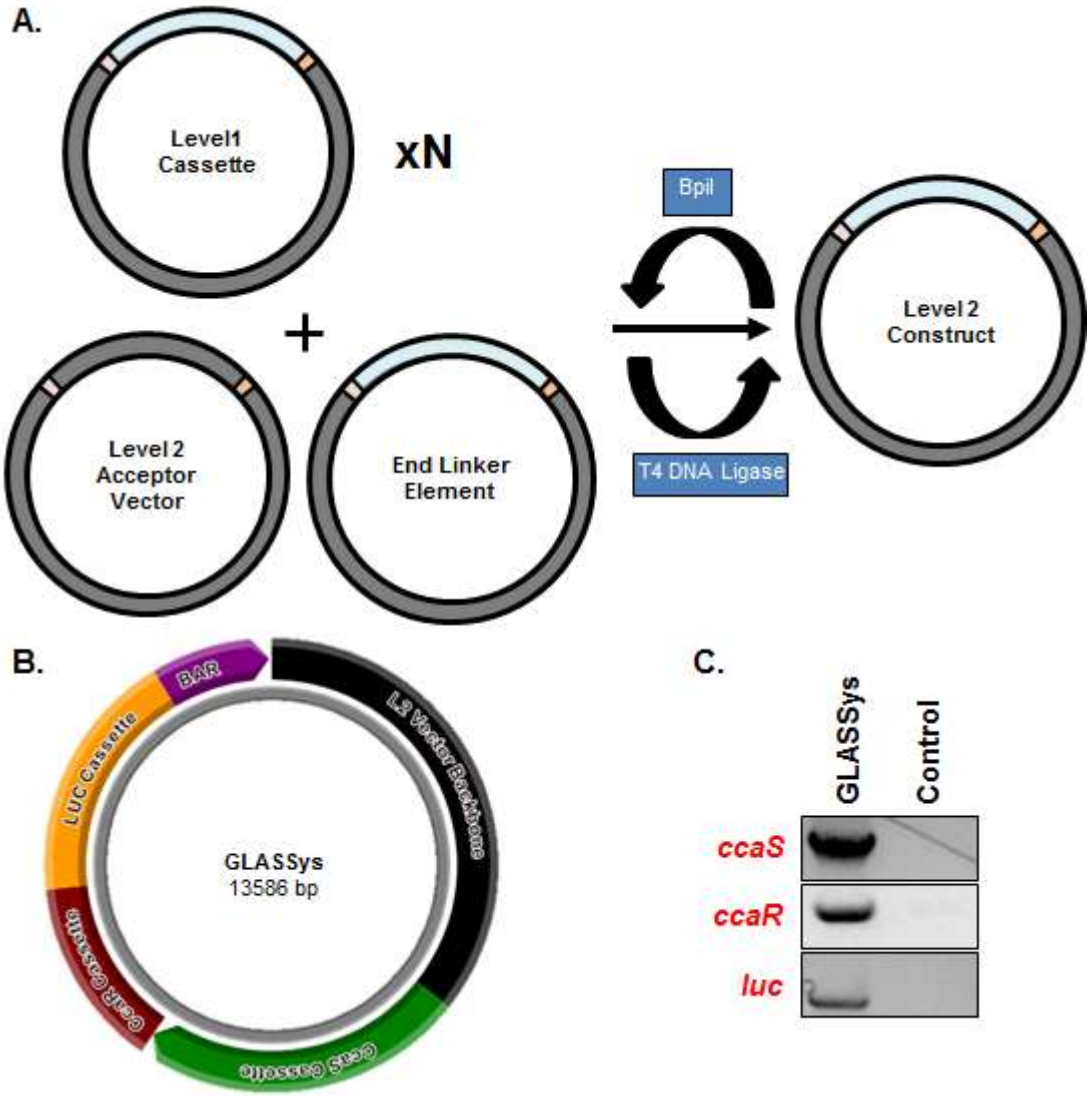

Figure 5.4. Producing Golden Gate Level 2 multi-gene constructs. (**A**) Diagram representing the process for production of a Level 2 multi-gene construct (L2) from multiple Level 1 cassettes (L1) using Golden Gate assembly. Between 1 and 7 L1 cassettes and an appropriate End Linker Element (ELE) are assembled into an empty L2 acceptor vector in a single pot digestion-ligation reaction with BpiI (Methods 2.4.4.). L1 cassettes used must begin at position 1 and run sequentially without repeat positions from position 1-7, as designated by the L1 acceptor vectors into which they were constructed, until the final cassette, the position number of the last cassette used will correspond to the ELE needed (1-6) for assembly with no ELE required for construction with a complete set of 7 L1 cassettes. The direction (Forward or Reverse) of sequence insertion for each L1 cassette is determined by the L1 vector into which they have been assembled and different cassette directions can be combined into the same L2 construct. (**B**) Vector map of the original GLASSys multi-gene construct, built from the F1-CcaS, F2-FMV.CcaR, R3-LUC and F4-BAR L1 cassettes. (**C**) Gel electrophoresis from quality control PCR run on the GLASSys construct confirming the presence of *ccaS*, *ccaR* and *LUC* in the construct. Template tested is indicated above (black) and primers used are indicated to the left (red) of the gel.

5.2.5. Preliminary testing of the GLASSys construct in plants

In order to test whether the GLASSys construct was functioning before *Arabidopsis* T3 stable transgenic lines were generated we tested its expression in transiently transformed *Nicotiana benthamiana*. *Agrobacterium tumefaciens* (GV3101) cells were transformed with the GLASSys plasmid and infiltrated into the leaves of *Nicotiana benthamiana* plants (Methods 2.3.6.) which were then imaged for luciferase bioluminescence under various combinations of LED lights (Methods 2.6.2).

As ccaS is a reversible green/red photosensor we first assessed luciferase activity in response to red and green light. Infiltrated *Nicotiana benthamiana* leaves were imaged under 20 μmol m^{-2} s^{-1} red light for 2.5 hours before transferring to either green and red light (1:1 ratio, 40 μmol m^{-2} s^{-1} total) or blue and red light (1:1 ratio, 40 μmol m^{-2} s^{-1} total) (Figure 5.5.). Luciferase expression under each lighting condition was measured and used to produce an average luciferase bioluminescence per 2.5 hours of light exposure. These tests showed increased luciferase expression in plants imaged under red and green light when compared to those grown under red light only (Figure 5.5.A.) and plants grown under red and blue light were not brighter than those grown under red light only (Figure 5.5.B.). These data suggest that the GLASSys construct was successfully switching from an inactive state under red light to an active state once green light was introduced and that blue light was not sufficient to cause a similar switching behaviour. It should be noted however that these tests also indicated that the GLASSys construct was leaky under red light, with relatively high luciferase expression in what was expected to be an inactive state. Additionally, the introduction of green light, even for 5 hours, was only sufficient to produce a less than 2 fold increase in

luciferase bioluminescence, much lower than the greater than 100 fold increase which had been reported with similar constructs in *E. coli* (Schmidl et al., 2014).

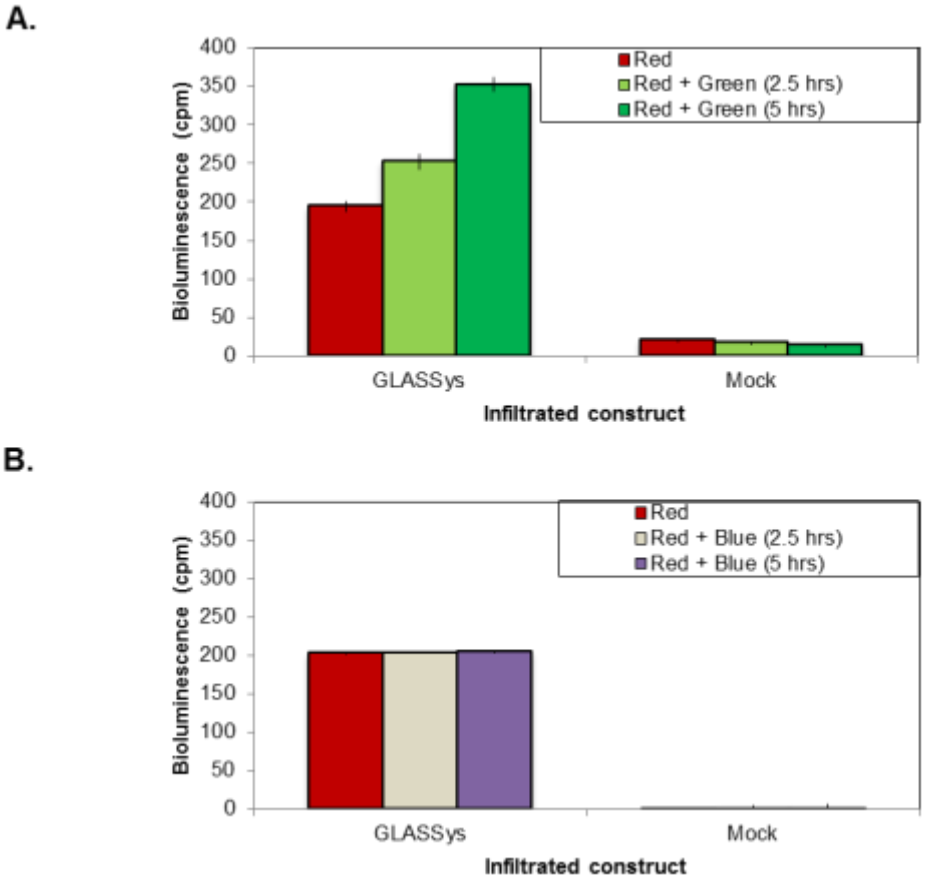

Figure 5.5. Luciferase bioluminescence under different light qualities in the original GLASSys construct expressed transiently in *Nicotiana benthamiana.* Average luciferase bioluminescence in *Nicotiana benthamiana* leaves transiently expressing the GLASSys multi-gene construct plotted against the detectable light from an untransformed mock leaf. Bars indicate the average bioluminescence from three images taken over 2.5 hours under 20 µmol m^{-2} s^{-1} red light followed a further 2.5 hours of exposure to 40 µmol m^{-2} s^{-1} of a 1:1 ratio of (**A**) red:green light or (**B**) red:blue light and then a further 2.5 hours of exposure to the latter light regime.

Alongside these tests, *Arabidopsis* seedlings were transformed with the GLASSys construct by floral inoculation (Methods 2.3.4.). Successfully transformed T0 seed was identified by Basta herbicide selection on 0.5x MS agar. Plates with resistant seedlings were imaged briefly for luciferase expression before transplanting to soil to grow for the next generation of seed. This luciferase imaging showed that around two seedlings per plate (around 1000 T0 seeds) were Basta resistant and around one seedling per plate was expressing luciferase, showing that not all transformants were expressing the complete GLASSys construct, or that the luciferase expression levels were too low for detectable bioluminescence. Additionally, many Basta resistant seedlings grown on soil were sickly and did not grow to produce seed.

15 Basta-resistant T1 seed lines were isolated and around 50-100 seeds from each line were screened using Basta on 0.5x MS agar plates. One of these 15 lines was found to not be resistant to Basta with the remaining 14 lines expressing resistance in around 75% of seedlings (Table 5.3.).

The next generation of seed lines (T2) were also screened using Basta and resistant seedlings were grown to the next generation. Of the 18 seed lines tested, 2 presented homozygous resistance to Basta and 5 presented homozygous Basta sensitivity. Luciferase screening of these lines also identified two lines which weakly expressed luciferase bioluminescence, although neither of these lines also presented homozygous Basta resistance.

The final generation of seed lines (T3) were screened with Basta and also imaged for luciferase expression. Of the 48 seed lines tested, 6 presented homozygous Basta resistance, 2 presented homozygous Basta sensitivity and none were indentified with visible luciferase expression.

These data suggest that gene silencing may have been occurring in these transformant lines, suppressing expression of one or more of the genes in the GLASSys construct and preventing visible luciferase expression from being produced. This is reinforced by the sickly nature of many of the seedlings of earlier transformant generations.

Transformant generation	Total seed lines	Tested seed lines	B^R lines	B^S lines	*luc* lines	*luc*.B^R lines
T1	15	15	N/A	1	-	-
T2	57	18	2	5	2	0
T3	185	48	6	2	0	0

B^R and B^S: homozygous Basta-resistant and Basta-sensitive phenotypes respectively
luc: possible luciferase bioluminescence observed
luc.B^R : homozygous Basta-resistant lines with possible luciferase bioluminescence observed

Table 5.3. *Arabidopsis thaliana* GLASSys transformants. Arabidopsis transformants containing GLASSys constructs showing number of lines per generation, number of lines tested and, of these tested lines, number of lines found to be homozygous for basta resistance or sensitivity along with number of lines with possible observed luciferase bioluminescence and number of homozygous basta resistant lines with possible observed luciferase bioluminescence by generation. T1 generation was not screened for luciferase expression.

5.2.6. Altering GLASSys constructs to reduce gene silencing

In order to counteract the loss of luciferase expression seen in transgenic *Arabidopsis* expressing the GLASSys construct we produced a new group of constructs expressing the basic components of the original GLASSys constructs along with a cassette for *RNA silencing suppressor P19* (*P19*). As *P19* was already being co-transformed in a separate plasmid when testing in transiently transformed tobacco it was hoped that this would also improve expression for these tests by removing the need to infiltrate with a second *Agrobacterium* culture. A second generation of L2 GLASSys constructs (GLA2) containing an additional position 5, L1 cassette containing *P19* driven by either a *pACT* or a *p35S* promoter was produced. These GLA2 constructs were transiently transformed into *Nicotiana benthamiana* leaves along with the original GLASSys both without *P19* and co-transformed with an independent L1-*p35S.P19* cassette in order to test the expression levels of luciferase bioluminescence in each *P19* variant under 20 μmol m^{-2} s^{-1} red light (Figure 5.6.).

These data suggest that luciferase expression under red light was highest in constructs either containing or co-transformed with L1-*p35S.P19* cassettes and lowest in the absence of *p19*. Expression in the GLA2 construct containing L1-*pACT.P19* was around 10 fold lower than that seen in the GLA2 construct containing L1-*p35S.P19* and as such the *L1-p35S.P19* cassette was used in all further production of second generation GLASSys constructs (GLA2).

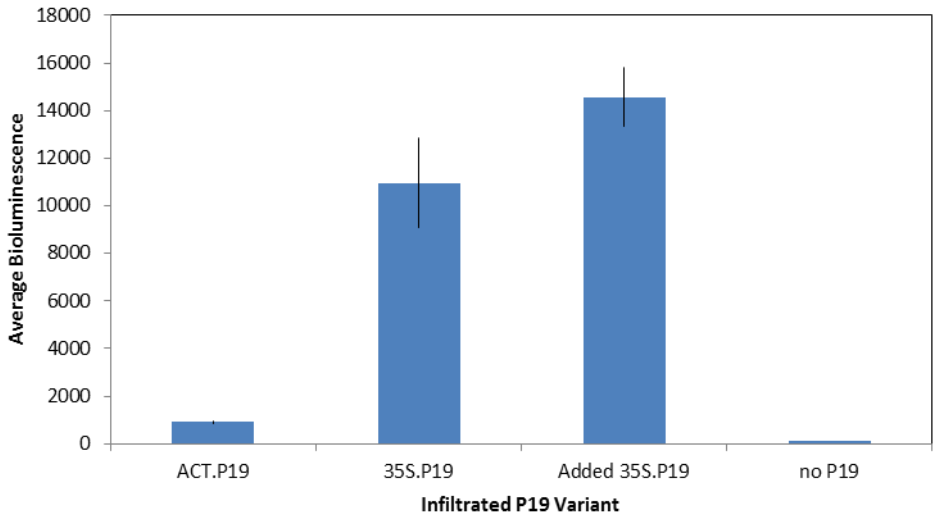

Figure 5.6. Luciferase bioluminescence of GLASSys constructs with differently expressed P19 silencing suppressors transiently expressed in *Nicotiana benthamiana*. Average luciferase bioluminescence from three images taken over 2.5 hours under 20 µmol m^{-2} s^{-1} red light in *Nicotiana benthamiana* leaves transiently expressing GLASSys construct variants containing the F5-pACT.P19 or F5-p35S.P19 Level 1 cassettes or GLASSys co-transformed with an independent F5-p35S.P19 cassette along with a control without P19.

5.2.7. Altering GLASSys constructs to improve expression and responsiveness

Once a *p19* cassette had been selected for updating the GLASSys construct, a range of GLA2 variants containing L1 cassettes expressing *ccaR* under the control of different promoters were produced. The promoter for *ccaR* was specifically chosen as the variation in these constructs as it has previously been shown in *E. coli* that variation of expression of a downstream gene controlled by the *ccaS/ccaR* genomic cluster is more strongly altered by the strength of the promoter for *ccaR* than the promoter for *ccaS* (Schmidl et al., 2014). The promoters used were; the strong promoter, cauliflower mosaic virus 35S RNA (CaMV35S, *p35S*); a medium strength promoter, ubiquitin (*pUBI*); and a weak promoter, mannopine synthase (*pMAS*). These, along with the original cassette containing a medium strength promoter, Figwort mosaic virus (*pFMV*) were all used to produce Level 1 cassettes with *ccaR* and an ACTIN2 terminator (*tACT2*). These cassettes were each used to produce a separate L2 construct containing one *ccaR* cassette variant along with L1-*ccaS,* L1-*luc,* L1-*bar* and L1-*p35S.P19* cassettes (example vector map found in Figure 5.7.A.). Collectively these second generation GLASSys constructs were called GLA2, individually they were identified by the promoter controlling *ccaR*, and as such they were referred to as; p35S.GLA2, pUBI.GLA2, pMAS.GLA2 and pFMV.GLA2 (Figure 5.7.B.). A control construct containing no *ccaR* cassette was also produced at this stage as a negative control, this construct was named noR.GLA2.

All of these GLA2 constructs were used to transform *Arabidopsis thaliana* plants by floral inoculation (Methods 2.3.4.). None of the T0 transgenic seeds tested emitted any observable luciferase bioluminescence and the sickliness seen in original GLASSys *Arabidopsis* transformants continued in GLA2 transformants. While these *Arabidopsis*

transformants were being produced and identified however, testing of the GLA2 constructs was undertaken in transiently transformed *Nicotiana benthamiana* leaves.

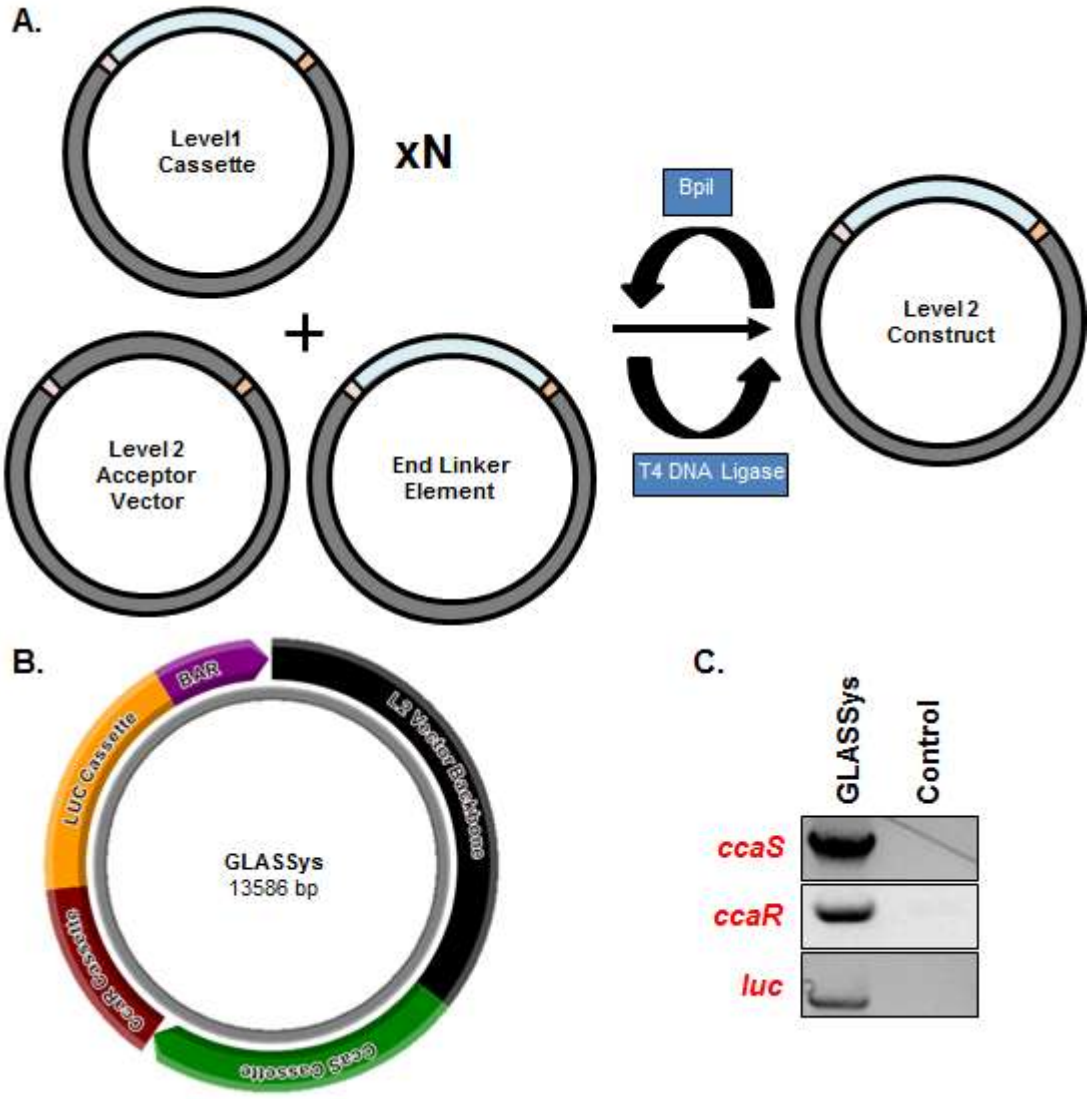

Figure 5.7. Updating and redesigning the GLASSys construct. (**A**) Vector map of an example of the improved GLASSys multi-gene construct updated to contain a cassette for the P19 silencing suppressor. This example, p35S.GLA2 was built from the F1-CcaS, F2-p35S.CcaR, R3-LUC, F4-BAR and F5-p35S.P19 Level 1 cassettes. (**B**) Table of GLASSys Level 2 constructs produced during this study listing the name of each construct alongside the names of the Level 1 cassettes containing the CcaR response regulator and the P19 silencing suppressor which were used to produce each construct.

5.2.8. Preliminary testing of the GLA2 constructs in *Nicotiana benthamiana*

Preliminary tests of the GLA2 *ccaR* promoter variant constructs were performed in transiently transformed *Nicotiana benthamiana* leaves. These tests were performed to identify which *ccaR* promoter variant of the GLA2 construct produced the clearest luciferase expression and least leakiness under red light. Tests were initially performed by imaging plants for luciferase bioluminescence under red light for 7.5 hours (Figure 5.8.A.). These tests showed that the construct containing *ccaR* controlled by the strong 35S promoter (p35S.GLA2) gave the clearest luciferase expression under red light followed by pFMV.GLA2 and pUBI.GLA2. Luciferase expression in the pMAS.GLA2 construct was very weak under red light, comparably as dim as the noR.GLA2 control construct. A further test on the p35S.GLA2 and pUBI.GLA2 construct was performed under red light for 7.5 hours followed by 7.5 hours under green light (Figure 5.8.B.), this test showed that luciferase bioluminescence in both constructs was higher under green light than under red light. Expression in the p35S.GLA2 construct was brighter than in the pUBI.GLA2 construct although leakiness was also greater under red light.

Finally, all GLA2 *ccr2* promoter variant constructs were imaged in *Nicotiana benthamiana* under 20 μmol m^{-2} s^{-1} of blue light for 17 days (Figure 5.8.C.). This imaging revealed that the expression of luciferase in all of these constructs was oscillating with a rhythm of around 30 hours, suggesting that some part of the system may somehow be being influenced weakly by the circadian clock. This also showed that luciferase expression under the GLA2 constructs naturally contained peaks and troughs, suggesting that previously observed switching behaviours could have been caused by these oscillations rather than by the application of green light. At around 12 days after infiltration of the leaf, luciferase expression in all GLA2 constructs lost rhythmicity.

However, at this stage, leaves had also begun to die. At around 60 hours after infiltration however, all leaves had reached their first peak of rhythmicity. As such, the natural variation in luciferase expression trended down after this period until around 15 hours later, presenting a potential testing period in which natural oscillations would not provide a false positive response to light treatments.

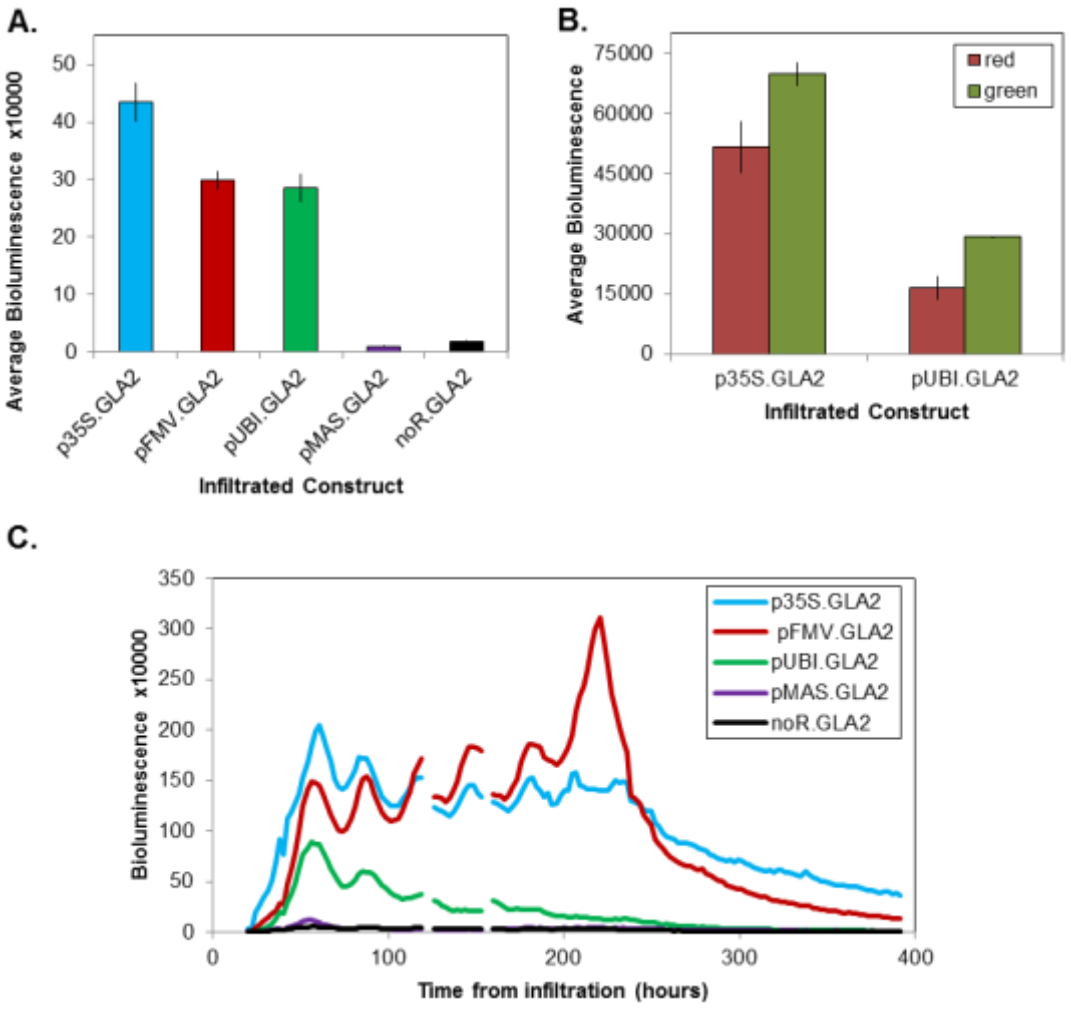

Figure 5.8. Luciferase bioluminescence of GLA2 construct variants expressed transiently in *Nicotiana benthamiana*. (**A**) Average luciferase bioluminescence from nine images taken over 7.5 hours under 20 µmol m^{-2} s^{-1} red light in *Nicotiana benthamiana* leaves transiently expressing either p35S.GLA2 (blue), pFMV.GLA2 (red), pUBI.GLA2 (green), pMAS.GLA2 (purple) or noR.GLA2 (black). (**B**) Average luciferase bioluminescence from 3 images taken over 7.5 hours under 20 µmol m^{-2} s^{-1} red light (red bar) followed by another 7.5 hours (and 3 images) under 20 µmol m^{-2} s^{-1} green light (green bar) in *Nicotiana benthamiana* leaves transiently expressing either p35S.GLA2 or pUBI.GLA2 construct variants. Error bars indicate standard error of the mean (n=3 or 9). (**C**) Waveforms of luciferase bioluminescence plotted over time from time of infiltration in *Nicotiana benthamiana* leaves transiently expressing either p35S.GLA2 (blue), pFMV.GLA2 (red), pUBI.GLA2 (green), pMAS.GLA2 (purple) or noR.GLA2 (black).

5.2.9. Optimisation of protocols for analysing light switching behaviours in *Nicotiana benthamiana* leaves transiently expressing GLA2 constructs

In order to optimise a protocol for testing GLA2 constructs in tobacco we began by finding the lowest duration of 40 μmol m^{-2} s^{-1} green light treatment which would reliably lead to an increase in luciferase expression (Figure 5.9.A., Figure 5.9.B.), and the lowest intensity of green light treatment which would reliably lead to an increase in luciferase expression after a 1 hour treatment (Figure 5.9.C., Figure 5.9.D.). These tests were performed in *Nicotiana benthamiana* leaves transiently expressing either the p35S.GLA2 construct (Figure 5.9.A, Figure 5.9.C.) and the noR.GLA2 control construct (Figure 5.9.B., Figure 5.9.D.).

These tests were performed specifically after a peak of luciferase expression had been reached in order to limit the chance that any increase in expression observed was due to a natural peak of expression being reached during testing. Firstly, plants were imaged for 7.5 hours in darkness followed by a green light treatment and then imaged for a further 7.5 hours in darkness. Average luciferase duration over each 7.5 hour imaging period, before and after light treatment, was plotted for each light treatment variant (Figure 5.9.).

When varying durations of light treatment were being tested, plants were exposed to 40 μmol m^{-2} s^{-1} green light for 0, 20, 40 or 60 minutes. p35S.GLA2 showed a small increase in luciferase expression after both 20 and 40 minute light treatments (Figure 5.9.A.). Whilst the noR.GLA2 control construct presented little luciferase expression both before and after green light treatments of any duration (Figure 5.9.B.).

When given a 1 hour treatment of decreasing intensities of green light, p35S.GLA2 showed an increase in luciferase expression after a green light treatment of any of the tested intensities but little increase after a control treatment in darkness (Figure 5.9.C.). No clear change in luciferase expression could be seen in the noR.GLA2 construct under any intensity of green light (Figure 5.9.D.).

These data suggested that the GLA2 construct switched in response to all tested green light treatments but did not switch without a green light treatment. However, it should be noted that this switching behaviour was not reliable in transiently transformed *Nicotiana benthamiana* leaves (Appendix Figure A1). Additionally, the GLA2 system continued to be leaky when imaged in darkness and the magnitude of the bioluminescence change was less than twofold.

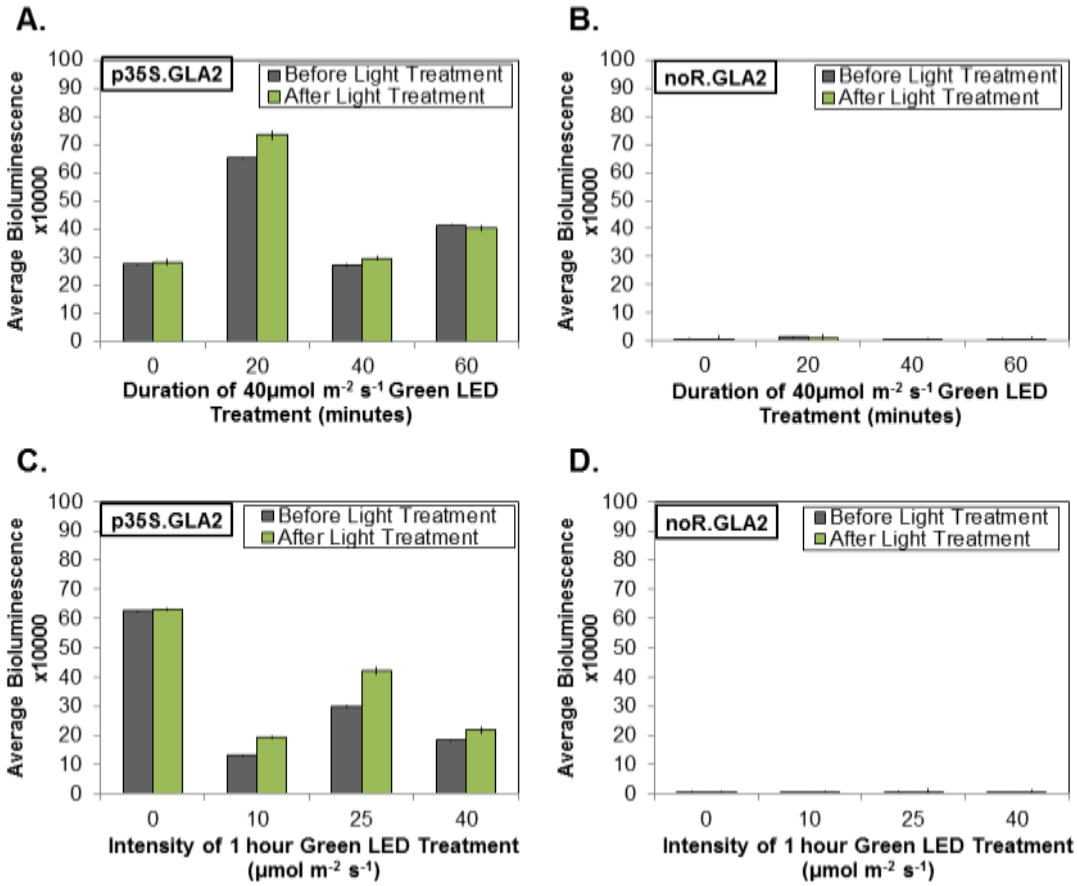

Figure 5.9. Optimising test conditions for GLA2 constructs transiently expressed in *Nicotiana benthamiana*. Average luciferase bioluminescence in *Nicotiana benthamiana* leaves transiently expressing (**A**, **C**) p35S.GLA2 or (**B**,**D**) noR.GLA2. Bars indicate average luciferase bioluminescence from nine images taken in darkness over 7.5 hours before a light treatment period under green light followed by the average bioluminescence over the subsequent 7.5 hours, also imaged in darkness. (**A**, **B**) Light treatments periods were under 40 µmol m^{-2} s^{-1} green light for 0, 20, 40 or 60 minute durations. (**C**, **D**) Light treatment periods were 60 minute duration exposures to 0, 10, 25 or 40 µmol m^{-2} s^{-1} green light. Error bars indicate standard error of the mean (n=9).

5.2.10. Specificity of switching behaviour of GLA2 transiently expressed in *Nicotiana benthamiana* under different light qualities

In order to test how the p35S.GLA2 construct responded to different qualities of light, *Nicotiana benthamiana* leaves were infiltrated with *Agrobacterium tumefaciens* containing either the p35S.GLA2 construct or a *CCA1::LUC2* circadian luciferase reporter construct co-infiltrated with an L1-*p35S.P19*. *CCA1::LUC2* was used to allow comparison with well understood light responses. Testing was performed specifically after a peak of luciferase expression had been reached in order to limit the chance that any increase in expression observed was due to a natural peak of expression being reached during testing. Plants were then imaged in darkness for 7.5 hours before being given a 3 hour treatment of either darkness (Figure 5.9.A.) or 40 μmol m^{-2} s^{-1} of blue light, green light or red light (Figure 5.9.B.-5.9.D.). Plants were then returned to darkness for a further 7.5 hours of imaging. After no light treatment or a blue light treatment, no increase in luciferase expression could be observed.

After a red or a green light treatment, luciferase expression can be seen to increase (Figure 5.9.C.-5.9.D.). When treated with blue light or given no light treatment, luciferase expression decreases after the treatment period (Figure 5.9.A.-5.9.B.), probably due to the rhythmic variation of luciferase bioluminescence previously observed in GLA2 constructs under blue light (Figure 5.8.C.). Regardless of the light quality of the treatment given, luciferase bioluminescence increases were small, with a less than 2 fold increase after both green and red light treatments. Luciferase bioluminescence in leaves expressing *CCA1::LUC2* responded as expected, increasing after a red light treatment, due to the previously reported red light mediated expression

of *CCA1* (Más et al., 2003b), decreasing after a long duration in darkness, and remaining stable under blue and green light.

These data suggest that the p35S.GLA2 construct becomes active in response to both red and green light, rather than being active under green and inactive under red light, the construct is not however responsive to blue light. This may suggest that CcaS functions differently in plants than in cyanobacteria or *E. coli*, or more likely, that the p35S.GLA2 construct is being interfered with by endogenous photoreceptors, possibly phytochromes which belong to the same superfamily of photoreceptors as the cyanobacteriochrome (CcaS) used in the GLASSys constructs and therefore may share similar structures and binding sites to native phytochromes allowing for possible interaction with native phytochrome targets and phytochrome targeting proteins. Assessment of homology between CcaS and native phytochromes should be performed before future studies are undertaken.

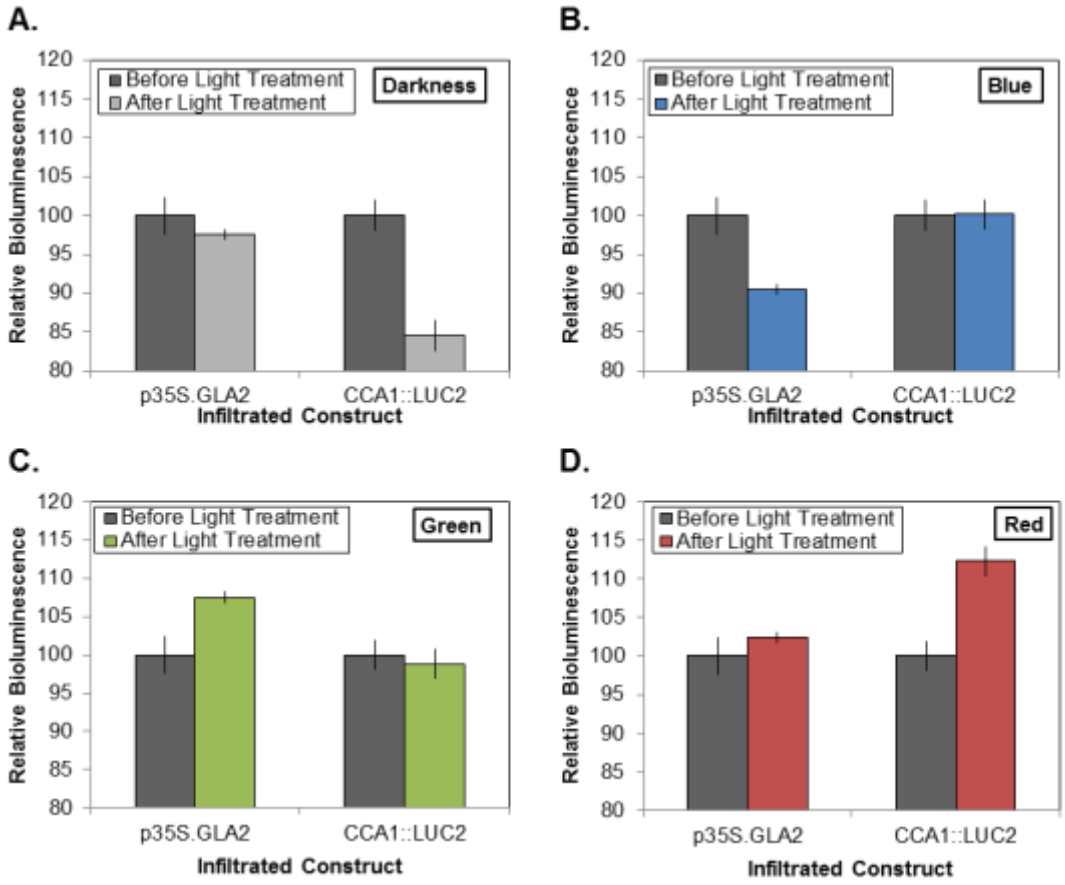

Figure 5.10. Comparison of switching behaviours of p35S.GLA2 expressed transiently in *Nicotiana benthamiana* leaves under different light qualities. Average luciferase bioluminescence in *Nicotiana benthamiana* leaves transiently expressing p35S.GLA2 or *CCA1::LUC2*. Bars indicate average luciferase bioluminescence from nine images taken in darkness over 7.5 hours before a 1 hour period (**A**) in darkness or under 40 µmol m^{-2} s^{-1} of (**B**) blue light, (**C**) green light or (**D**) red light, followed by the average bioluminescence over the subsequent 7.5 hours, also imaged in darkness. Error bars indicate standard error of the mean (n=9).

5.3. Discussion

5.3.1. Design, construction and transformation of GLASSys multigene constructs

The green-light activated gene cluster on which the GLASSys multi-gene construct was based, *ccaS-ccaR-cpcG2*, is found naturally in *Synechocystis* sp. PCC6803 (*Synechocystis*), where it allows for green-light induced expression of the *cpcG2* gene via the green/red cyanobacteriochrome photoreceptor histidine kinase, CcaS, and its cognate response regulator, CcaR (Hirose et al., 2008). In previously designed optogenetic constructs, *ccaS* and *ccaR* have been used alongside either the native promoter region of *cpcG2* (Hirose et al., 2008, Tabor et al., 2011) or a synthetic promoter based upon a putative constitutive promoter taken from the host organism and fused to G-boxes from the *cpcG2* promoter region (Schmidl et al., 2014, Milias-Argeitis et al., 2016) fused to a gene of interest such as a reporter gene. This second approach has been shown to reduce leakiness and increase the observed increase of expression under green light in *E. coli* (Schmidl et al., 2014). Expression level and leakiness has also been improved in *E. coli* by replacing the native, *Synechocystis*, promoter and terminator regions of *ccaS* and *ccaR* with sequences found in the host organism's genome (Schmidl et al., 2014). As such, when designing the GLASSys construct to function in *Arabidopsis* we applied a similar technique, adding promoter and terminator sequences known to function in *Arabidopsis* to coding sequences for *ccaS* and *ccaR* codon optimised for *Arabidopsis* and designing a synthetic promoter, *pGLE*, based upon the G-boxes from the *cpcG2* promoter and a *NOS* minimal promoter sequence (Figure 5.1.).

The *pGLE* promoter was designed using four repeats of the G-box taken from the promoter region of *cpcG2*, which have been shown to act as binding sites for CcaR (Schmidl, et al. 2014), separated by spacer sequences and fused to a *NOS* minimal

promoter as previously used in a similar synthetic plant promoter (Harmer and Kay, 2005). The *pGLE* promoter was used to allow CcaS regulated expression of a *LUC* reporter gene in response to light when transiently expressed in *Nicotiana benthamiana*. However, some alterations could have been made to the *pGLE* promoter in order to optimise the GLASSys construct. Firstly, reducing the number of G-boxes may have prevented non-specific binding and improved fold-increase of expression by reducing leakiness of the system. Secondly, replacing the *NOS* minimal promoter region with a different promoter region may have been more effective in this construct both due to the nature of the *NOS* promoter as a weak promoter. Finally, the spacer sequences used between each G-box in the pGLE promoter were based upon those found in Harmer and Kay (2005), which were fragments of a circadian gene, replacing these spacers with truly random spacer sequences or removing the spacer sequences entirely may have improved binding and could potentially have prevented some of the unusual rhythmic *LUC* activity observed in *N. benthamiana* (Figure 5.8.C.).

Another concern with the GLASSys construct which we were unable to address was a pair of recognition sites for the type IIS restriction enzyme *BpiI* which is a key part of Golden Gate assembly of multigene constructs (Engler et al., 2014). Proper protocol dictates that sequences should be domesticated by removing these internal sites before using them in Golden Gate cloning although the location of these recognition sites along with the G-C rich nature of the *LUC* gene made this difficult to achieve and ultimately led to us using an undomesticated *LUC* sequence to produce our constructs. While this did not prevent us from producing the GLASSys constructs, it did slow down and reduce the reliability of the process and if further work were to be done on the GLASSys construct it would be far quicker if a domesticated *LUC* sequence were used.

While the p35S.GLA2 construct did produce an increase in *LUC* expression under green light when transiently expressed in *Nicotiana benthamiana* (Figure 5.9.), the observed increase in expression of targeted genes under green light using our construct was, highly varied between experiments (Appendix Figure A1) and far lower (less than 2-fold increase; Figure 5.9.) than what has previously been observed in *E. coli* expressing similar CcaS/CcaR constructs (over 100-fold increase; Schmild, et al. 2014). In order to improve this expression level in future constructs a range of approaches could be taken. Firstly, the addition of fluorescent protein tags to each protein in the GLASSys construct would have allowed us to more directly observe expression *in planta* and identify whether expression was localised to any specific organelles. While both the codon optimised *ccaS* and *ccaR* sequences used did include the sequence for a nuclear localisation signal, without tagging the protein we could not observe whether this localisation had occurred.

5.3.2. Preliminary analysis in tobacco suggests that CcaS acts as a green/red activated switch in tobacco

While the GLASSys constructs were initially designed to function in *Arabidopsis*, the majority of the testing *in planta* occurred in transiently transformed *Nicotiana benthamiana* leaves. The original GLASSys construct was tested in this way to ensure that the construct functioned and to observe whether the expected switching characteristics were present in transgenic plants (Figure 5.5.). As ccaS has previously been reported to be a green/red photoreversible switch we used red light to minimize luciferase bioluminescence observed in these leaves after the transient transformation protocol was performed, before the first image was taken. The addition of green light to

this light treatment was shown to increase LUC bioluminescence by a noticeable but low level, an increase of expression which became greater after further exposure to green light (Figure 5.5.A.). While this shows that the construct was functioning as intended, there was more leakiness and a smaller increase in expression under green light that had been expected. Further tests demonstrated that blue light was insufficient to produce an increase in LUC bioluminescence (Figure 5.5.B.). These tests suggested that the construct was green-light specific but that the time required for complete switching under green light could be as long as 7.5 hours or longer. These initial experiments suggested that GLASSys was responsive to green light but the magnitude of induction was less than had been expected based upon similar constructs functioning in *E. coli* (Schmidl et al., 2014). Furthermore, simultaneous testing of *Arabidopsis* transformant lines suggested that the construct was been being silenced, we sought to minimise silencing effects by integrating *P19* into the construct.

After producing the GLA2 construct, which was designed to address a potential gene silencing issue in *Arabidopsis* transformants, further tests were performed in *N. benthamiana*. Firstly, the effects of different types of *P19* were assessed (Figure 5.6.), leaves transiently transformed with either GLA2 constructs containing integrated *P19* driven by a *pACT* promoter or a *p35S* promoter or the original GLASSys construct, co-transformed with a separate *p35S.P19* plasmid were imaged under red light. This test showed that integrated *P19* allowed for transient expression of GLASSys constructs in *N. benthamiana* leaves and that greater expression could be observed using *p35S.P19* than *pACT.P19* as the integrated cassette. While co-transformation of the *p35S.P19* cassette produced slightly higher expression than the integrated *p35S.P19* construct, this was not a practical option when producing stable transgenic *Arabidopsis* lines and

therefore further tests made use of integrated *P19* rather than co-transformation. Further GLA2 constructs were then produced using integrated *p35S.P19* cassettes along with *ccaR* cassettes containing a range of different strength promoters. These constructs were imaged under red light for 7.5 hours in order to test luciferase expression levels in each construct (Figure 5.8.A.). This test showed that p35S.GLA2 produced the brightest luciferase bioluminescence of this range of GLA2 constructs followed by pFMV.GLA2 and pUBI.GLA2, with pMAS.GLA2 producing very little luciferase bioluminescence. The p35S.GLA2 and pUBI.GLA2 constructs were then tested similarly to the original GLASSys construct, reducing background LUC bioluminescence under red light before taking imaging and then exposing the leaf to green light and imaging again (Figure5.8.B.). This test showed that both constructs had an increased level of bioluminescence after a green light treatment. While the p35S.GLA2 construct showed greater levels of LUC bioluminescence under both conditions, the pUBI.GLA2 construct had a slightly greater fold increase under green light and was less leaky under red light.

Further testing of the GLA2 constructs with alternative *ccaR* promoters, was performed under blue light with multiple images taken over 400 hours in order to judge the baseline expression of the transiently expressed constructs and to find an ideal time point after transient transformation had begun to perform tests in the future (Figure 5.8.C.). These tests showed that all GLA2 constructs, which were expected to express LUC at a relatively constant level under the constant blue light, produced LUC bioluminescence with an oscillating expression rhythm of around 30 hours under these conditions. This confined the observation period during which future testing could occur to a far smaller window, only after expression had peaked, in order to prevent

observed bioluminescence increases from being due to expression rhythms rather than CcaS activation.

Furthermore, this test showed that leakiness in the GLA2 construct could be linked to the strength of the promoter driving *ccaR* as the constructs containing stronger promoters for *ccaR* all showed greater levels of expression under blue light than those with weaker promoters. The pMAS.GLA2 construct was also shown to either not function or produce such low levels of *ccaR* expression that LUC bioluminescence in this construct was comparable to the noR.GLA2 construct (Figure 5.8.C.). Although p35S.GLA2 was shown to be the most leaky construct, we chose 35S.GLA2 for initial examination due to its increased luminescence, it will be of interest however, to examine the other GLA2 constructs in future to see if lines with reduced luminescence produce a greater difference in light-induced activation.

With the new window for test timing in mind, future testing set start point for imaging of LUC bioluminescence by observing the leaves over time in darkness and waiting for expression to peak before giving light treatments in the period when LUC expression would typically be dropping. Tests were performed to identify the duration (Figure 5.9.A.-5.9.B.) and intensity (Figure 5.9.C.-5.9.D.) of green light required to produce the greatest increase in LUC bioluminescence with the intention of finding the shortest duration and lowest intensity which would produce a measurable, reliable increase of LUC bioluminescence. This testing was made difficult due the inconsistent bioluminescence observed in separate transiently transformed leaves (Appendix Figure A1). While an increase in LUC bioluminescence was normally observable after a green light treatment, intensity of LUC bioluminescence varied greatly between different samples. In order to address this, leaves with the observably highest levels of

bioluminescence were used as control samples and remained untreated, reducing the likeliness of observed increases in LUC bioluminescence being due to an unseen oscillation in LUC expression. Light intensity was observed to generally have a greater effect on LUC bioluminescence than duration of light treatment (Figure 5.9), although it was considered that this could have been due to a greater availability of photosynthetically produced sugars after a full hour long light treatment.

In order to test the effect of different light qualities upon the p35S.GLA2 construct, leaves were acclimated in darkness and an imaging start point was selected after expression peaked. Leaves were then given a 3 hour treatment of darkness, blue light, green light or red light (Figure 5.10.). Plants treated with green light showed the greatest fold-increase of expression (Figure 5.10.C.), although plants exposed to red light, the condition which should inactivate the GLASSys sensor, also showed an increase in expression (Figure 5.10.D.). When kept in darkness (Figure 5.10.A.) or exposed to blue light (Figure 5.10.B.), no increase in expression was observed, indicating that observed changes in expression were a green/red specific response, although the green/red switching behaviour expected from CcaS was not present. This is contrary to previously published work in cyanobacteria and *E. coli* (Hirose et al., 2008, Tabor et al., 2011). This could be due to crosstalk between the cyanobacteriochrome pathway introduced by the GLA2 construct and endogenous phytochrome pathways or due to another, yet unclear, process found in plant cells which does not occur in cyanobacteria or bacteria.

5.3.3. Possible causes underlying the inability to isolate stable GLASSys *Arabidopsis* transformant lines

While the GLASSys construct was designed for use in *Arabidopsis*, attempts at producing stable transgenic *Arabidopsis* lines were unsuccessful (Table 5.3.). While limited LUC bioluminescence was observed in seedlings grown from T0 seed, these seedlings were sickly and most died before growing to maturity and producing T1 seed. Luciferase bioluminescence was also observed in two T2 seed lines although neither of these lines was homozygous for the Basta herbicide resistance gene found in the GLASSys construct. Stable T3 lines produced were homozygous for Basta resistance but did not produce any detectable luciferase bioluminescence.

In the original GLASSys construct, this loss of expression was thought to have potentially been being caused by silencing of one or more genes in the GLASSys multigene construct. In order to address this, the GLA2 constructs were produced including a *P19* silencing suppressor gene cassette. This construct proved to be useful for transient transformation of *Nicotiana benthamiana* but did not produce any improvements in stable *Arabidopsis* transformants, which did not produce clear luciferase bioluminescence in seedlings grown from T0 seed. This suggests that either the lack of expression in the original GLASSys construct at T3 was not caused by silencing, the *P19* gene was not functioning in *Arabidopsis*, or the *P19* gene was causing additional issues when expressed in *Arabidopsis*, further preventing healthy expression of the GLASSys construct. If the lack of luciferase expression was not caused by silencing, it may have been due to one of several potential reasons including; inhibition of the *pGLE* G-boxes, inhibition of CcaS or CcaR expression or phosphorylation by a native *Arabidopsis* protein, loss of function due to nuclear localisation of CcaS and CcaR

or possible toxicity of CcaS or CcaR in *Arabidopsis.* If *P19* was not functioning in *Arabidopsis* then gene silencing may still have been preventing GLA2 from functioning. It is also possible that *P19* was making the seedlings overly vulnerable to external pathogens, as silencing makes up a large part of the plant immune system (Voinnet, 2001); this could have led to the only healthy plants being those which produced low levels of the P19 protein, allowing for continued silencing. Alternatively, P19 induced pathogen vulnerability could have led to all plants being too unhealthy to express significant levels of each GLA2 component to observe LUC bioluminescence. Although the GLA2 seedlings were unhealthy, the original GLASSys seedlings were also sickly, suggesting that if *P19* was the cause of some of the issues with GLA2 it was not the only problem with this construct.

Chapter 6- General Discussion

6.1. Introduction

As sessile photoautotrophs, plants are acutely sensitive to and wholly dependent upon their surrounding light conditions. Plant photoperception ranges from the broad sensitivity associated with photosynthesis to the more subtle and specific responses of photoreceptors. In *Arabidopsis thaliana*, five families of photoreceptor proteins have been identified; the red and far-red light sensing phytochromes, the blue light sensitive cryptochromes, phototropins and ZEITLUPEs and the UV-B receptive UVR8 proteins (Sullivan and Deng, 2003, Franklin and Whitelam, 2004, Briggs et al., 2001, Liu et al., 2016, Kim et al., 2007, Christie et al., 2012a). All of these photoreceptors have also been associated to varying degrees with the circadian clock in *Arabidopsis* (Millar, 2003, Hsu and Harmer, 2014, Galvao and Fankhauser, 2015, Jones, 2018), the internal timekeeping mechanism of interlinked transcriptional and metabolic feedback loops by which plants and other organisms predict and adapt to cyclic environmental changes in light, temperature and other stimuli. Of these, the blue light sensitive phototropins are the most recent to be identified as playing a role in the maintenance of circadian rhythms in *Arabidopsis* (Litthauer et al., 2015) and as such their involvement in the circadian system is the least well documented. By extension of our understanding of these photoreceptors, our understanding of the mechanisms by which plants respond to red and blue light are well documented (Sullivan and Deng, 2003, Wang and Folta, 2014, Su et al., 2015), green light responses however, are less well understood (Wang and Folta, 2013, Zhang et al., 2011). During this project, plant photoresponses, including the circadian functions of the phototropins and the developmental and circadian functions of green light within *Arabidopsis* were examined. We have shown that phototropins do

not regulate expression of the morning phased circadian gene *CCA1* under blue light (Chapter 3.2.8-3.2.9). Additionally, we have identified cryptochrome and phytochrome regulated hypocotyl de-etiolation under green light (Chapter 4.2.3-4.2.5), suggesting roles for both of these photoreceptor families in green light photoperception. We have also observed a loss of circadian rhythmicity in *cry1cry2* double mutants under green light (Chapter 4.2.9-4.2.10.), further suggesting that cryptochromes are required for proper regulation of responses to green light in *Arabidopsis*. In addition to this we have engineered a light-inducible multigene construct utilising cyanobacterial green light photoreceptor proteins which functions as a green/red light activated gene expression switch in transiently transformed *Nicotiana benthamiana* leaves (Chapter 5.2.10.). In this final chapter, the data from previous chapters are discussed, along with potential avenues for future investigation.

6.2. The mechanism behind circadian rhythms of prompt fluorescence remains illusive

While the mechanisms underlying prompt fluorescence is relatively well understood, being caused by photochemical quenching of energy absorbed by the pigment antennae of PSII (Gould et al., 2009, Litthauer et al., 2015), the mechanisms causing this fluorescence to cycle with a circadian rhythm is still unknown (Litthauer et al., 2015). Initial studies into circadian rhythms of prompt fluorescence in *Arabidopsis* have shown that phototropins are required to maintain the robustness of these rhythms in constant blue light (Litthauer et al., 2015). In order to further our understanding of prompt fluorescence rhythms, we further examined the effects of phototropin mutants upon prompt fluorescence. We have shown that *Arabidopsis* mutants lacking either phot1 or

phot2 have comparable rhythms of prompt fluorescence to wild type (Figure 3.8.C.-3.8.D.), although due to the subtlety of previously observed effects (Litthauer et al., 2015), it is possible that further loss of rhythmicity in phototropin mutants would be observable if imaging had been continued for another day or more.

As prompt fluorescence is known to originate in the chloroplast (Goltsev et al., 2003, Gould et al., 2009), and we had observed a loss of prompt fluorescence rhythmicity after the application of exogenous oxidised quinone (Figure 3.3.), we also observed the effects of a range of mutants lacking function of various different chloroplast proteins associated with regulation of the redox state of the chloroplast upon prompt fluorescence rhythms (Figure 3.4.). However, none of the observed mutants had any measurable effect upon prompt fluorescence rhythms relative to wild type suggesting that pathways regulated by these proteins are unlikely to be involved in maintaining rhythms of F_q'/F_m'. With this in mind, and due to the wide range of potential mechanisms by which oxidised quinones could be influencing the redox status of the quinone pool in the chloroplast, further work will be required to understand how the application of exogenous Qo effects prompt chloroplast fluorescence rhythms.

6.3. Green light responses in plants are mediated by both cryptochromes and phytochromes and green light acts as an input to the circadian clock via the cryptochromes

The limited responsiveness of plants to green light is well reported but poorly understood (Smith et al., 2017, Wang et al., 2013, Wang and Folta, 2013, Folta, 2004, Lin et al., 1995). While it has been suggested that the cryptochromes may act as a green-

light responsive photoreceptor (Lin et al., 1995, Bouly et al., 2007), they are not widely considered to be a green light photoreceptor. We have shown that cryptochromes have a limited but significant involvement in maintaining circadian rhythms of *CCA1* under green light (Figure 4.9.-4.10.) and that both cryptochromes and phytochrome B are required to maintain de-etiolation responses under green light in *Arabidopsis* (Figure 4.3.-4.5.).

Whilst this observed hypocotyl elongation response suggests that cryptochromes and phyB are both independently required for hypocotyl de-etiolation to occur fully under green light, it does not discount the further involvement of other photoreceptors including the other four phytochromes, phyA and phyC-phyE, which were not examined in this study. It is also possible that the phyB response is not caused directly but by interactions between phyB and cryptochromes as have been previously reported to be involved in hypocotyl elongation and low-light avoidance responses (Kang et al., 2009, Fankhauser and Batschauer, 2016, Pedmale et al., 2016, Xu et al., 2016). In order to test this, further studies using mutants lacking function of phyA, phyC, phyD and phyE as well as mutants lacking function in multiple phytochromes or both phytochromes and cryptochromes would allow a more complete model of photoreceptor based green light photoperception in *Arabidopsis* to be formed. Furthermore, it is possible that subtle underlying roles for other photoreceptors in green light perception may be being masked by the more dominant roles of the cryptochromes and phytochromes. Although phototropin mutants did not appear to respond differently to wild type under green light (Figure 4.3.-4.4.) the phototropins may play a subtle role, hinted at by the lack of responsiveness to green wavelengths seen when observing phototropin mutants under complex light regimes with and without green wavelengths (Figure 4.5.). This response

could be further examined by observing mutants lacking functional phototropins and cryptochromes or phytochromes under green light. Additionally, no testing of the ZEITLUPE family of blue light photoreceptors has been performed and this could provide further insight into green-light photoperception in *Arabidopsis*. Lastly, it is still possible that an as of yet unknown green light receptor may be present in plants and a broader understanding of green light responses and the specific conditions in which they occur in *Arabidopsis* could help to unveil conditions in which this hypothetical photoreceptor is more dominant than other known photoreceptors, as of yet however, these conditions have not been observed.

The observed requirement of cryptochromes to maintain circadian rhythms under specific wavelengths of green light (Figure 4.9.-4.10.) suggest that while the absorption peak of cryptochromes is in the blue wavelengths, they still have sufficient functional photoreceptive properties in green wavelengths to act as an input to the circadian clock under even low intensities of green light. It should be noted however, that under wider spectrums of green light circadian rhythms persist even in absence of functional cryptochromes, although with a longer circadian period and loss of rhythmicity (Figure 4.9.), suggesting that other photoreceptors may be capable of assisting in the maintenance of circadian rhythms under green light or that photosynthesis alone may be sufficient to maintain these rhythms. Further removal of blue light wavelengths from test conditions (Figure 4.10) have also been shown to cause arrhythmicity in *cry1cry2* double mutants but not in wild type, suggesting that under these specific green light conditions and in the absence of blue wavelengths, cryptochromes are required to maintain circadian rhythms. These findings suggest that the sensitivity of plants to green light is sufficient to stimulate a wide range of processes as the circadian clock is

involved in the regulation of around one third of the *Arabidopsis* genome (Covington et al., 2008). By extension, while the introduction of green light to a growth environment containing sufficient blue and red light wavelengths is unlikely to have a significant effect upon wild type plant growth (Wang and Folta, 2013), it is probable that it would have a broad range of subtle effects upon the plant which may provide a competitive advantage in a natural environment. With this in mind, while green light is required for ideal growth conditions, plants are capable of growing somewhat healthily in its absence, something which cannot be said for blue or red wavelengths, and as such greens are the best wavelengths of light available for the introduction of optogenetic systems into plants.

6.4. Future utilisation of cyanobacteriochromes to engineer optogenetic systems for plants

When expressed in *Arabidopsis*, the GLASSys construct produced early generation transgenic seedlings with a range of sickly phenotypes suggesting that one or more parts of the construct may have been toxic when expressed in plants. Additionally later generations were more healthy but presented a loss of luciferase bioluminescence activity indicating that gene silencing had most likely suppressed expression of one or more genes within the GLASSys construct in these seedlings, further indicating that part of the construct may have been toxic to *Arabidopsis* (Chapter 5.2.4., Table 5.3.). Due to this toxicity, future iterations of the construct may need to include alternative photoreceptor proteins in place of the CcaS photoreceptor used in GLASSys. Cyanobacteriochromes continue to be a major source of photoreceptors with atypical absorbance peaks and spectra and are therefore of particular interest when seeking a

green-light responsive photoreceptor. Cyanobacteriochromes functionally differ from phytochromes in that the linear tetrapyrrole molecules bound in their cGMP phosphodiesterase/adenylyl cyclase/FhlA (GAF) domains have distinct amino acid sequences from the GAF of phytochromes, resulting in phytochrome-like photoconversion properties with atypical spectral absorbance ranges (Rockwell et al., 2012). While phytochromes typically photoconvert reversibly between red/far-red or far-red/red (Galvao and Fankhauser, 2015), cyanobacteriochromes have been identified which photoconvert reversibly under spectral ranges including violet/yellow, blue/green, green/red and red/green (Hirose et al., 2008, Yoshihara et al., 2004, Narikawa et al., 2008b).

Green-sensitive cyanobacteriochromes are of particular interest in the development of optogenetic systems for plants due to their lack of native, green-light specific photoreceptors and relative lack of sensitivity to green light seen in plants (Wang and Folta, 2013, Zhang et al., 2011), potentially providing a light quality which can activate an optogenetic system without acting as an invasive input to native photoperceptors. The red-light induced photoreversibility of green/red and red/green type cyanobacteriochromes also provides a switching characteristic which could be utilised to provide tighter control of construct-induced gene expression. CcaS, the green/red type cyanobacteriochrome used in the original GLASSys construct design was therefore ideal from a spectral perspective but, upon further examination of the system in *Arabidopsis*, may not have been the ideal photoreceptor for a system designed for use in plants.

Two types of green/red cyanobacteriochrome have been identified; CcaS and RcaE. CcaS has been identified in both *Synechocystis* sp. PCC 6803 (*Synechocystis*) and *Nostoc*

punctiforme ATCC 29133 (*N. punctiforme*) (Hirose et al., 2010) and RcaE is naturally expressed in *Fremyella diplosiphon* (*F. diplosiphon*) (Hirose et al., 2013). The *Synechocystis CcaS* gene was used in the original GLASSys design (Figure 5.1., Figure 5.4.), although both CcaS and RcaE act as the green-light inducible photoreceptor input for a complementary chromatic adaptation response to an abundance of green light in the environment, inducing expression of pigmented phycobiliproteins in order to optimise light-harvesting for photosynthesis (Hirose et al., 2010, Hirose et al., 2013). The GAF domains of CcaS and RcaE are homologous, providing similar spectral absorbance mechanisms under green and red light (Hirose et al., 2010). However, CcaS autophosphorylates under green light and directly phosphorylates a response regulator protein (CcaR), whereas RcaE autophosphorylates under red light, passing this phosphoryl group to RcaF which then phosphorylates RcaC in a three-part phosphorelay system (Hirose et al., 2010). Despite these differing mechanisms, both of these proteins perform similar roles and function under similar conditions (Hirose et al., 2013). Both RcaE (Gottlieb et al., 2014) and CcaS (Tabor et al., 2011) have previously been used to produce optogenetic switching systems. *Synechocystis* CcaS has also been optimised to function in *Eschericia coli* (Schmidl et al., 2014), showing its functionality outside of cyanobacteria, which was the reason it was chosen for the GLASSys construct.

Due to its optimisation outside of the native species along with the relative simplicity of its two-component histidine kinase system over the three-component system of RcaE, we chose to use CcaS in the production of our green/red light-switching system. However, due to the observed toxicity of our *Synechocystis* CcaS-based GLA system in *Arabidopsis*, and lack of green/red photoreversability in *N. benthamiana, N. punctiforme* CcaS or *F. diplosiphon* RcaE could prove to be a functional alternative in a similar, future

optogenetic system for plants. Alternatively, a red/green type cyanobacteriochrome such as AnPixJ, from *Anabaena* (*Nostoc*) sp. PCC 7120 (Narikawa et al., 2008), or a blue/green type such as SyPixJ, from *Synechocystis* (Song et al., 2011), could be utilised to produce a green-light inhibited switching mechanism as a possible alternative to the current GLASSys construct. Before further use of cyanobacteriochromes in constructs for use in plants however, each cyanobacteriochrome being considered for use should be used as bait in a yeast two-hybrid (Y2H) screen against plant phytochromes and a range of plant proteins known to interact with plant phytochromes (Phee et al., 2006), such as the phytochrome interacting factors (PIFs), in order to judge whether native proteins are likely to be interfering with the cyanobacteriochrome systems when expressed in plants.

6.5. Future iterations of GLASSys

Further research into and iterations of the GLASSys construct would require a stable transgenic line in order to conclusively test the efficiency and effectiveness of the construct before further improvements could be worked on. To begin this, transformation of *Arabidopsis* plants with the individual parts of the construct would allow us to identify whether any individual component of the GLASSys construct is toxic to Arabidopsis, with CcaS, CcaR and P19 all being potentially problematic in stable transformants. If this was found to be the case a different, fast-growing model plant such as *Marchantia polymorphia* (Ishizaki et al., 2008) could potentially be usable in place of *Arabidopsis*. If the toxicity of CcaS and CcaR is discounted as an issue, replacement of all promoter and terminator sequences in the GLASSys construct with differing sequences could prevent any potential issues caused by the repeated use of

these sequences in the current constructs. Once stable, homozygous transgenic plants expressing a CcaS/CcaR construct have been produced, assessment of whether the oscillations seen in transiently transformed *N. benthamiana* occur in stable transgenic lines would be a high priority. Adjustments to the spacer regions between G-boxes of the *pGLE* promoter are the most likely method by which these could be eliminated, although testing whether any native *Arabidopsis* proteins, especially phytochromes, can interact with the G-boxes of *pGLE* would also be a priority. Identifying protein-protein interactions between CcaS/CcaR and native proteins, especially those under the control of the circadian clock, would be the next priority if *pGLE* was found to not be the source of these rhythms. Once stable expression is achieved the system could be optimised for expression and leakiness by adjusting the promoter and terminator regions of each cassette in the GLASSys construct before further testing under specific light conditions could be performed. This finalised GLASSys construct could then be combined with different genes of interest, replacing the LUC reporter gene, under the control of the pGLE promoter to allow for green-light induced expression of the selected genes, allowing for quick, deliberate induction of gene expression in GLASSys transgenic plants.

Overall, we have shown that while the use of optogenetic constructs to control gene expression *in planta* is promising, a CcaS/CcaR based, specifically green-light responsive system may not be functional in *Arabidopsis*, or at least requires further work to refine the design and methodology behind this system. Additionally, the observed green/red activated switching seen in *Nicotiana benthamiana* leaves transiently transformed with GLASSys and GLA2 constructs was greatly less effective (Figure 5.4., Figure 5.9.) than the upward of 100-fold increase of expression under green light reported in similar

systems optimised for use in *E. coli* (Schmidl et al., 2014). This suggests that, even once issues of stability were alleviated, substantial future work would be required to optimise this system for use in plants in order to produce an effective and functional system for research and industry. In spite of this, recently reported success in producing functional green-light specific optogenetic system utilising light-sensitive bacterial transcription factors in *Arabidopsis* protoplasts (Chatelle et al., 2018), suggest that a functional, green-light specific optogenetic system in stable transgenic plants will not be a distant and inaccessible goal for future research.

References

Abe, K., Sakai, Y., Nakashima, S., Araki, M., Yoshida, W., Sode, K. & Ikebukuro, K. 2014. Design of riboregulators for control of cyanobacterial (Synechocystis) protein expression. *Biotechnol Lett,* **36,** 287-94.

Ahmad, M., Jarillo, J. A., Smirnova, O. & Cashmore, A. R. 1998. Cryptochrome blue-light photoreceptors of Arabidopsis implicated in phototropism. *Nature,* **392,** 720-3.

Alabadi, D., Gallego-Bartolome, J., Orlando, L., Garcia-Carcel, L., Rubio, V., Martinez, C., Frigerio, M., Iglesias-Pedraz, J. M., Espinosa, A., Deng, X. W. & Blazquez, M. A. 2008. Gibberellins modulate light signaling pathways to prevent Arabidopsis seedling de-etiolation in darkness. *Plant J,* **53,** 324-35.

Alabadi, D., Oyama, T., Yanovsky, M. J., Harmon, F. G., Mas, P. & Kay, S. A. 2001. Reciprocal regulation between TOC1 and LHY/CCA1 within the Arabidopsis circadian clock. *Science,* **293,** 880-3.

Allen, J. F., Santabarbara, S., Allen, C. A. & Puthiyaveetil, S. 2011. Discrete redox signaling pathways regulate photosynthetic light-harvesting and chloroplast gene transcription. *PLoS One,* **6,** e26372.

Arabidopsis Genome, I. 2000. Analysis of the genome sequence of the flowering plant Arabidopsis thaliana. *Nature,* **408,** 796-815.

Aukerman, M. J., Hirschfeld, M., Wester, L., Weaver, M., Clack, T., Amasino, R. M. & Sharrock, R. A. 1997. A deletion in the PHYD gene of the Arabidopsis Wassilewskija ecotype defines a role for phytochrome D in red/far-red light sensing. *Plant Cell,* **9,** 1317-26.

Bacchus, W. & Fussenegger, M. 2012. The use of light for engineered control and reprogramming of cellular functions. *Curr Opin Biotechnol,* **23,** 695-702.

Badary, A., Abe, K., Ferri, S., Kojima, K. & Sode, K. 2015. The development and characterization of an exogenous green-light-regulated gene expression system in marine cyanobacteria. *Mar Biotechnol (NY),* **17,** 245-51.

Baker, N. R. 2008. Chlorophyll fluorescence: a probe of photosynthesis in vivo. *Annu Rev Plant Biol,* **59,** 89-113.

Balasubramanian, S., Sureshkumar, S., Agrawal, M., Michael, T. P., Wessinger, C., Maloof, J. N., Clark, R., Warthmann, N., Chory, J. & Weigel, D. 2006. The PHYTOCHROME C photoreceptor gene mediates natural variation in flowering and growth responses of Arabidopsis thaliana. *Nat Genet,* **38,** 711-5.

Banerjee, R., Schleicher, E., Meier, S., Viana, R. M., Pokorny, R., Ahmad, M., Bittl, R. & Batschauer, A. 2007. The signaling state of Arabidopsis cryptochrome 2 contains flavin semiquinone. *J Biol Chem,* **282,** 14916-22.

Barber, J. 2009. Photosynthetic energy conversion: natural and artificial. *Chem Soc Rev,* **38,** 185-96.

Baudry, A., Ito, S., Song, Y. H., Strait, A. A., Kiba, T., Lu, S., Henriques, R., Pruneda-Paz, J. L., Chua, N. H., Tobin, E. M., Kay, S. A. & Imaizumi, T. 2010. F-box

proteins FKF1 and LKP2 act in concert with ZEITLUPE to control Arabidopsis clock progression. *Plant Cell,* **22,** 606-22.

Beligni, M.V. & Lamattina, L. 2000. Nitric oxide stimulates seed germination and de-etiolation, and inhibits hypocotyl elongation, three light-inducible responses in plants. *Planta,* **210,** 215-221.

Beyer, H. M., Juillot, S., Herbst, K., Samodelov, S. L., Muller, K., Schamel, W. W., Romer, W., Schafer, E., Nagy, F., Strahle, U., Weber, W. & Zurbriggen, M. D. 2015. Red Light-Regulated Reversible Nuclear Localization of Proteins in Mammalian Cells and Zebrafish. *ACS Synth Biol,* **4,** 951-8.

Boccalandro, H. E., Rugnone, M. L., Moreno, J. E., Ploschuk, E. L., Serna, L., Yanovsky, M. J. & Casal, J. J. 2009. Phytochrome B enhances photosynthesis at the expense of water-use efficiency in Arabidopsis. *Plant Physiol,* **150,** 1083-92.

Bohn, A., Geist, A., Rascher, U. & Lüttge, U. 2001. Responses to different external light rhythms by the circadian rhythm of Crassulacean acid metabolism in Kalanchoe daigremontiana. *Plant, Cell & Environment,* **24,** 811-820.

Bordage, S., Sullivan, S., Laird, J., Millar, A. J. & Nimmo, H. G. 2016. Organ specificity in the plant circadian system is explained by different light inputs to the shoot and root clocks. *New Phytol,* **212,** 136-49.

Bouly, J. P., Schleicher, E., Dionisio-Sese, M., Vandenbussche, F., Van Der Straeten, D., Bakrim, N., Meier, S., Batschauer, A., Galland, P., Bittl, R. & Ahmad, M. 2007. Cryptochrome blue light photoreceptors are activated through interconversion of flavin redox states. *J Biol Chem,* **282,** 9383-91.

Brautigam, C. A., Smith, B. S., Ma, Z., Palnitkar, M., Tomchick, D. R., Machius, M. & Deisenhofer, J. 2004. Structure of the photolyase-like domain of cryptochrome 1 from Arabidopsis thaliana. *Proc Natl Acad Sci U S A,* **101,** 12142-7.

Briggs, W. R. & Christie, J. M. 2002. Phototropins 1 and 2: versatile plant blue-light receptors. *Trends Plant Sci,* **7,** 204-10.

Briggs, W. R., Christie, J. M. & Salomon, M. 2001. Phototropins: a new family of flavin-binding blue light receptors in plants. *Antioxid Redox Signal,* **3,** 775-88.

Butler, W. L. 1978. Energy Distribution in the Photochemical Apparatus of Photosynthesis. *Annual Review of Plant Physiology,* **29,** 345-378.

Camsund, D., Lindblad, P. & Jaramillo, A. 2011. Genetically engineered light sensors for control of bacterial gene expression. *Biotechnol J,* **6,** 826-36.

Capra, E. J. & Laub, M. T. 2012. Evolution of two-component signal transduction systems. *Annu Rev Microbiol,* **66,** 325-47.

Carter, G. A. & Knapp, A. K. 2001. Leaf optical properties in higher plants: linking spectral characteristics to stress and chlorophyll concentration. *Am J Bot,* **88,** 677-84.

Casal, J. J. 2013. Photoreceptor signaling networks in plant responses to shade. *Annu Rev Plant Biol,* **64,** 403-27.

Cashmore, A. R., Jarillo, J. A., Wu, Y. J. & Liu, D. 1999. Cryptochromes: blue light receptors for plants and animals. *Science,* **284,** 760-5.

Casson, S. A., Franklin, K. A., Gray, J. E., Grierson, C. S., Whitelam, G. C. & Hetherington, A. M. 2009. phytochrome B and PIF4 regulate stomatal development in response to light quantity. *Curr Biol,* **19,** 229-34.

Chatelle, C., Ochoa Fernandez, R., Engesser, R., Schneider, N., Beyer, H., Jones, A., Timmer, J., Zurbriggen, M.D. and Weber, W. 2018. A green light-responsive system for the control of transgene expression in mammalian and plant cells. *ACS synthetic biology*. **7,** 1349-1358

Chaves, I., Pokorny, R., Byrdin, M., Hoang, N., Ritz, T., Brettel, K., Essen, L. O., Van Der Horst, G. T., Batschauer, A. & Ahmad, M. 2011. The cryptochromes: blue light photoreceptors in plants and animals. *Annu Rev Plant Biol,* **62,** 335-64.

Chen, M., Chory, J. & Fankhauser, C. 2004. Light signal transduction in higher plants. *Annu Rev Genet,* **38,** 87-117.

Cho, H. Y., Tseng, T. S., Kaiserli, E., Sullivan, S., Christie, J. M. & Briggs, W. R. 2007. Physiological roles of the light, oxygen, or voltage domains of phototropin 1 and phototropin 2 in Arabidopsis. *Plant Physiol,* **143,** 517-29.

Christie, J. M. 2007. Phototropin blue-light receptors. *Annu Rev Plant Biol,* **58,** 21-45.

Christie, J. M., Arvai, A. S., Baxter, K. J., Heilmann, M., Pratt, A. J., O'hara, A., Kelly, S. M., Hothorn, M., Smith, B. O., Hitomi, K., Jenkins, G. I. & Getzoff, E. D. 2012a. Plant UVR8 photoreceptor senses UV-B by tryptophan-mediated disruption of cross-dimer salt bridges. *Science,* **335,** 1492-6.

Christie, J. M., Blackwood, L., Petersen, J. & Sullivan, S. 2015. Plant flavoprotein photoreceptors. *Plant Cell Physiol,* **56,** 401-13.

Christie, J. M. & Briggs, W. R. 2001. Blue light sensing in higher plants. *J Biol Chem,* **276,** 11457-60.

Christie, J. M., Hitomi, K., Arvai, A. S., Hartfield, K. A., Mettlen, M., Pratt, A. J., Tainer, J. A. & Getzoff, E. D. 2012b. Structural tuning of the fluorescent protein iLOV for improved photostability. *J Biol Chem,* **287,** 22295-304.

Christie, J. M., Reymond, P., Powell, G. K., Bernasconi, P., Raibekas, A. A., Liscum, E. & Briggs, W. R. 1998. Arabidopsis NPH1: a flavoprotein with the properties of a photoreceptor for phototropism. *Science,* **282,** 1698-701.

Christie, J. M., Salomon, M., Nozue, K., Wada, M. & Briggs, W. R. 1999. LOV (light, oxygen, or voltage) domains of the blue-light photoreceptor phototropin (nph1): binding sites for the chromophore flavin mononucleotide. *Proc Natl Acad Sci U S A,* **96,** 8779-83.

Christie, J. M., Swartz, T. E., Bogomolni, R. A. & Briggs, W. R. 2002. Phototropin LOV domains exhibit distinct roles in regulating photoreceptor function. *Plant J,* **32,** 205-19.

Chun, L., Kawakami, A. and Christopher, D.A., 2001. Phytochrome A mediates blue light and UV-A-dependent chloroplast gene transcription in green leaves. *Plant physiology,* **125,** 1957-1966.

Clarke, J. D. 2009. Cetyltrimethyl ammonium bromide (CTAB) DNA miniprep for plant DNA isolation. *Cold Spring Harb Protoc,* **2009,** pdb prot5177.

Clough, R. C. V., R.D. 1997. Phytochrome degradation. *Plant, cell and Environment,* **20,** 713-721.

Conrad, K. S., Manahan, C. C. & Crane, B. R. 2014. Photochemistry of flavoprotein light sensors. *Nat Chem Biol,* **10,** 801-9.

Covington, M. F., Maloof, J. N., Straume, M., Kay, S. A. & Harmer, S. L. 2008. Global transcriptome analysis reveals circadian regulation of key pathways in plant growth and development. *Genome Biol,* **9,** R130.

Dalchau, N., Baek, S. J., Briggs, H. M., Robertson, F. C., Dodd, A. N., Gardner, M. J., Stancombe, M. A., Haydon, M. J., Stan, G. B., Goncalves, J. M. & Webb, A. A. 2011. The circadian oscillator gene GIGANTEA mediates a long-term response of the Arabidopsis thaliana circadian clock to sucrose. *Proc Natl Acad Sci U S A,* **108,** 5104-9.

De Mairan, J. J. O. 1729. Observation Botanique. *Histoire de l'Academie Royale des Sciences, Paris*, 35-36.

De Souza, A., Wang, J. Z. & Dehesh, K. 2017. Retrograde Signals: Integrators of Interorganellar Communication and Orchestrators of Plant Development. *Annu Rev Plant Biol,* **68,** 85-108.

Deitzer, G. Spectral comparisons of sunlight and different lamps. International Lighting in Controlled Environments Workshop, 1994.

Devlin, P. F., Halliday, K. J., Harberd, N. P. & Whitelam, G. C. 1996. The rosette habit of Arabidopsis thaliana is dependent upon phytochrome action: novel phytochromes control internode elongation and flowering time. *Plant J,* **10,** 1127-34.

Devlin, P. F. & Kay, S. A. 2000. Cryptochromes are required for phytochrome signaling to the circadian clock but not for rhythmicity. *Plant Cell,* **12,** 2499-2510.

Devlin, P. F. & Kay, S. A. 2001. Circadian photoperception. *Annu Rev Physiol,* **63,** 677-94.

Diaz, M. G., Hernandez-Verdeja, T., Kremnev, D., Crawford, T., Dubreuil, C. & Strand, A. 2018. Redox regulation of PEP activity during seedling establishment in Arabidopsis thaliana. *Nat Commun,* **9,** 50.

Dodd, A. N., Belbin, F. E., Frank, A. & Webb, A. A. 2015. Interactions between circadian clocks and photosynthesis for the temporal and spatial coordination of metabolism. *Front Plant Sci,* **6,** 245.

Dodd, A. N., Parkinson, K. & Webb, A. a. R. 2004. Independent circadian regulation of assimilation and stomatal conductance in the ztl-1 mutant of Arabidopsis. *New Phytologist,* **162,** 63-70.

Dodd, A. N., Salathia, N., Hall, A., Kevei, E., Toth, R., Nagy, F., Hibberd, J. M., Millar, A. J. & Webb, A. A. 2005. Plant circadian clocks increase photosynthesis, growth, survival, and competitive advantage. *Science,* **309,** 630-3.

Edelstein, A., Amodaj, N., Hoover, K., Vale, R. & Stuurman, N. 2010. Computer control of microscopes using microManager. *Curr Protoc Mol Biol,* **Chapter 14,** Unit14 20.

Edgar, R. S., Green, E. W., Zhao, Y., Van Ooijen, G., Olmedo, M., Qin, X., Xu, Y., Pan, M., Valekunja, U. K., Feeney, K. A., Maywood, E. S., Hastings, M. H., Baliga, N. S., Merrow, M., Millar, A. J., Johnson, C. H., Kyriacou, C. P., O'neill, J. S. & Reddy, A. B. 2012. Peroxiredoxins are conserved markers of circadian rhythms. *Nature,* **485,** 459-64.

Edwards, K. D. & Millar, A. J. 2007. Analysis of circadian leaf movement rhythms in Arabidopsis thaliana. *Methods Mol Biol,* **362,** 103-13.

Endo, M., 2016. Tissue-specific circadian clocks in plants. *Current opinion in plant biology,* **29,** 44-49.

Endo, M., Shimizu, H., Nohales, M. A., Araki, T. & Kay, S. A. 2014. Tissue-specific clocks in Arabidopsis show asymmetric coupling. *Nature,* **515,** 419-22.

Engelhard, C., Wang, X., Robles, D., Moldt, J., Essen, L. O., Batschauer, A., Bittl, R. & Ahmad, M. 2014. Cellular metabolites enhance the light sensitivity of Arabidopsis cryptochrome through alternate electron transfer pathways. *Plant Cell,* **26,** 4519-31.

Engelke, D. R., Krikos, A., Bruck, M. E. & Ginsburg, D. 1990. Purification of Thermus aquaticus DNA polymerase expressed in Escherichia coli. *Anal Biochem,* **191,** 396-400.

Engler, C., Kandzia, R. & Marillonnet, S. 2008. A one pot, one step, precision cloning method with high throughput capability. *PLoS One,* **3,** e3647.

Engler, C., Youles, M., Gruetzner, R., Ehnert, T. M., Werner, S., Jones, J. D., Patron, N. J. & Marillonnet, S. 2014. A golden gate modular cloning toolbox for plants. *ACS Synth Biol,* **3,** 839-43.

Fankhauser, C. & Christie, J. M. 2015. Plant phototropic growth. *Curr Biol,* **25,** R384-9.

Fankhauser, C. & Batschauer, A., 2016. Shadow on the plant: a strategy to exit. *Cell,* **164**, 15-17.

Fankhauser, C. & Staiger, D. 2002. Photoreceptors in Arabidopsis thaliana: light perception, signal transduction and entrainment of the endogenous clock. *Planta,* **216,** 1-16.

Feher, B., Kozma-Bognar, L., Kevei, E., Hajdu, A., Binkert, M., Davis, S. J., Schafer, E., Ulm, R. & Nagy, F. 2011. Functional interaction of the circadian clock and UV RESISTANCE LOCUS 8-controlled UV-B signaling pathways in Arabidopsis thaliana. *Plant J,* **67,** 37-48.

Fogelmark, K. & Troein, C. 2014. Rethinking transcriptional activation in the Arabidopsis circadian clock. *PLoS Comput Biol,* **10,** e1003705.

Folta, K. M. 2004. Green light stimulates early stem elongation, antagonizing light-mediated growth inhibition. *Plant Physiol,* **135,** 1407-16.

Folta, K. M. & Kaufman, L. S. 2003. Phototropin 1 is required for high-fluence blue-light-mediated mRNA destabilization. *Plant Mol Biol,* **51,** 609-18.

Folta, K. M., Lieg, E. J., Durham, T. & Spalding, E. P. 2003. Primary inhibition of hypocotyl growth and phototropism depend differently on phototropin-mediated increases in cytoplasmic calcium induced by blue light. *Plant Physiol,* **133,** 1464-70.

Folta, K. M. & Maruhnich, S. A. 2007. Green light: a signal to slow down or stop. *J Exp Bot,* **58,** 3099-111.

Folta, K. M. & Spalding, E. P. 2001. Unexpected roles for cryptochrome 2 and phototropin revealed by high-resolution analysis of blue light-mediated hypocotyl growth inhibition. *Plant J,* **26,** 471-8.

Franklin, K. A., Praekelt, U., Stoddart, W. M., Billingham, O. E., Halliday, K. J. & Whitelam, G. C. 2003. Phytochromes B, D, and E act redundantly to control multiple physiological responses in Arabidopsis. *Plant Physiol,* **131,** 1340-6.

Franklin, K. A. & Quail, P. H. 2010. Phytochrome functions in Arabidopsis development. *J Exp Bot,* **61,** 11-24.

Franklin, K. A. & Whitelam, G. C. 2004. Light signals, phytochromes and cross-talk with other environmental cues. *J Exp Bot,* **55,** 271-6.

Frechilla, S., Talbott, L.D., Bogomolni, R.A. and Zeiger, E., 2000. Reversal of blue light-stimulated stomatal opening by green light. *Plant and Cell Physiology,* **41,** 171-6.

Fujiwara, S., Wang, L., Han, L., Suh, S. S., Salome, P. A., Mcclung, C. R. & Somers, D. E. 2008. Post-translational regulation of the Arabidopsis circadian clock through selective proteolysis and phosphorylation of pseudo-response regulator proteins. *J Biol Chem,* **283,** 23073-83.

Fukuda, H., Ukai, K. & Oyama, T. 2012. Self-arrangement of cellular circadian rhythms through phase-resetting in plant roots. *Phys Rev E Stat Nonlin Soft Matter Phys,* **86,** 041917.

Galperin, M. Y. 2010. Diversity of structure and function of response regulator output domains. *Curr Opin Microbiol,* **13,** 150-9.

Gao, J., Wang, X., Zhang, M., Bian, M., Deng, W., Zuo, Z., Yang, Z., Zhong, D. and Lin, C., 2015. Trp triad-dependent rapid photoreduction is not required for the function of Arabidopsis CRY1. *Proceedings of the National Academy of Sciences,* **112,** 9135-9140.

Galvao, V. C. & Fankhauser, C. 2015. Sensing the light environment in plants: photoreceptors and early signaling steps. *Curr Opin Neurobiol,* **34,** 46-53.

Gardner, L. & Deiters, A. 2012. Light-controlled synthetic gene circuits. *Curr Opin Chem Biol,* **16,** 292-9.

Gardner, T. S., Cantor, C. R. & Collins, J. J. 2000. Construction of a genetic toggle switch in Escherichia coli. *Nature,* **403,** 339-42.

Gendron, J.M., Pruneda-Paz, J.L., Doherty, C.J., Gross, A.M., Kang, S.E. and Kay, S.A., 2012. Arabidopsis circadian clock protein, TOC1, is a DNA-binding transcription factor. *Proceedings of the National Academy of Sciences,* **109,** 3167-72.

Giraud, E., Ng, S., Carrie, C., Duncan, O., Low, J., Lee, C. P., Van Aken, O., Millar, A. H., Murcha, M. & Whelan, J. 2010. TCP transcription factors link the regulation of genes encoding mitochondrial proteins with the circadian clock in Arabidopsis thaliana. *Plant Cell,* **22,** 3921-34.

Goltsev, V., Zaharieva, I., Lambrev, P., Yordanov, I. & Strasser, R. 2003. Simultaneous analysis of prompt and delayed chlorophyll a fluorescence in leaves during the induction period of dark to light adaptation. *J Theor Biol,* **225,** 171-83.

Gottlieb, S.M., Kim, P.W., Corley, S.C., Madsen, D., Hanke, S.J., Chang, C.W., Rockwell, N.C., Martin, S.S., Lagarias, J.C. and Larsen, D.S., 2014. Primary and secondary photodynamics of the violet/orange dual-cysteine NpF2164g3 cyanobacteriochrome domain from Nostoc punctiforme. *Biochemistry*, **53,** 1029-1040.

Gould, P. D., Diaz, P., Hogben, C., Kusakina, J., Salem, R., Hartwell, J. & Hall, A. 2009. Delayed fluorescence as a universal tool for the measurement of circadian rhythms in higher plants. *Plant J,* **58,** 893-901.

Goyal, A., Szarzynska, B. & Fankhauser, C. 2013. Phototropism: at the crossroads of light-signaling pathways. *Trends Plant Sci,* **18,** 393-401.

Graf, A., Schlereth, A., Stitt, M. & Smith, A. M. 2010. Circadian control of carbohydrate availability for growth in Arabidopsis plants at night. *Proc Natl Acad Sci U S A,* **107,** 9458-63.

Gyula, P., Schafer, E. & Nagy, F. 2003. Light perception and signalling in higher plants. *Curr Opin Plant Biol,* **6,** 446-52.

Halliday, K. J., Koornneef, M. & Whitelam, G. C. 1994. Phytochrome B and at Least One Other Phytochrome Mediate the Accelerated Flowering Response of Arabidopsis thaliana L. to Low Red/Far-Red Ratio. *Plant Physiol,* **104,** 1311-1315.

Harmer, S. L. 2009. The circadian system in higher plants. *Annu Rev Plant Biol,* **60,** 357-77.

Harmer, S. L., Hogenesch, J. B., Straume, M., Chang, H. S., Han, B., Zhu, T., Wang, X., Kreps, J. A. & Kay, S. A. 2000. Orchestrated transcription of key pathways in Arabidopsis by the circadian clock. *Science,* **290,** 2110-3.

Harmer, S. L. & Kay, S. A. 2005. Positive and negative factors confer phase-specific circadian regulation of transcription in Arabidopsis. *Plant Cell,* **17,** 1926-40.

Hassidim, M., Yakir, E., Fradkin, D., Hilman, D., Kron, I., Keren, N., Harir, Y., Yerushalmi, S. & Green, R. M. 2007. Mutations in CHLOROPLAST RNA BINDING provide evidence for the involvement of the chloroplast in the regulation of the circadian clock in Arabidopsis. *Plant J,* **51,** 551-62.

Hastings, J. W. 1996. Chemistries and colors of bioluminescent reactions: a review. *Gene,* **173,** 5-11.

Haydon, M. J., Hearn, T. J., Bell, L. J., Hannah, M. A. & Webb, A. A. 2013a. Metabolic regulation of circadian clocks. *Semin Cell Dev Biol,* **24,** 414-21.

Haydon, M. J., Mielczarek, O., Robertson, F. C., Hubbard, K. E. & Webb, A. A. 2013b. Photosynthetic entrainment of the Arabidopsis thaliana circadian clock. *Nature,* **502,** 689-92.

Hennig, L., Funk, M., Whitelam, G. C. & Schafer, E. 1999. Functional interaction of cryptochrome 1 and phytochrome D. *Plant J,* **20,** 289-94.

Herbel, V., Orth, C., Wenzel, R., Ahmad, M., Bittl, R. & Batschauer, A. 2013. Lifetimes of Arabidopsis cryptochrome signaling states *in vivo*. *The Plant Journal*, **74,** 583-592

Hirose, Y., Narikawa, R., Katayama, M. & Ikeuchi, M. 2010. Cyanobacteriochrome CcaS regulates phycoerythrin accumulation in Nostoc punctiforme, a group II chromatic adapter. *Proc Natl Acad Sci U S A,* **107,** 8854-9.

Hirose, Y., Rockwell, N.C., Nishiyama, K., Narikawa, R., Ukaji, Y., Inomata, K., Lagarias, J.C. and Ikeuchi, M., 2013. Green/red cyanobacteriochromes regulate complementary chromatic acclimation via a protochromic photocycle. *Proceedings of the National Academy of Sciences*, **110,** 4974-4979.

Hirose, Y., Shimada, T., Narikawa, R., Katayama, M. & Ikeuchi, M. 2008. Cyanobacteriochrome CcaS is the green light receptor that induces the expression of phycobilisome linker protein. *Proc Natl Acad Sci U S A,* **105,** 9528-33.

Hosokawa, N., Kushige, H. & Iwasaki, H. 2013. Attenuation of the posttranslational oscillator via transcription-translation feedback enhances circadian-phase shifts in Synechococcus. *Proc Natl Acad Sci U S A,* **110,** 14486-91.

Hsu, P. Y. & Harmer, S. L. 2014. Wheels within wheels: the plant circadian system. *Trends Plant Sci,* **19,** 240-9.

Hu, W., Franklin, K. A., Sharrock, R. A., Jones, M. A., Harmer, S. L. & Lagarias, J. C. 2013. Unanticipated regulatory roles for Arabidopsis phytochromes revealed by null mutant analysis. *Proc Natl Acad Sci U S A,* **110,** 1542-7.

Hua, J., Chang, C., Sun, Q. & Meyerowitz, E. M. 1995. Ethylene insensitivity conferred by Arabidopsis ERS gene. *Science,* **269,** 1712-4.

Huala, E., Oeller, P. W., Liscum, E., Han, I. S., Larsen, E. & Briggs, W. R. 1997. Arabidopsis NPH1: a protein kinase with a putative redox-sensing domain. *Science,* **278,** 2120-3.

Hussain, M. I. & Reigosa, M. J. 2015. Characterization of xanthophyll pigments, photosynthetic performance, photon energy dissipation, reactive oxygen species generation and carbon isotope discrimination during artemisinin-induced stress in Arabidopsis thaliana. *PLoS One,* **10,** e0114826.

Ihnatowicz, A., Pesaresi, P., Varotto, C., Richly, E., Schneider, A., Jahns, P., Salamini, F. & Leister, D. 2004. Mutants for photosystem I subunit D of Arabidopsis thaliana: effects on photosynthesis, photosystem I stability and expression of nuclear genes for chloroplast functions. *Plant J,* **37,** 839-52.

Ikeuchi, M. & Ishizuka, T. 2008. Cyanobacteriochromes: a new superfamily of tetrapyrrole-binding photoreceptors in cyanobacteria. *Photochem Photobiol Sci,* **7,** 1159-67.

Imaizumi, T., Tran, H. G., Swartz, T. E., Briggs, W. R. & Kay, S. A. 2003. FKF1 is essential for photoperiodic-specific light signalling in Arabidopsis. *Nature,* **426,** 302-6.

Inada, K. 1976. Action spectra for photosynthesis in higher plants. *Plant and cell physiology,* **17,** 355-365.

Inoue, S., Kinoshita, T., Matsumoto, M., Nakayama, K. I., Doi, M. & Shimazaki, K. 2008a. Blue light-induced autophosphorylation of phototropin is a primary step for signaling. *Proc Natl Acad Sci U S A,* **105,** 5626-31.

Inoue, S., Kinoshita, T., Takemiya, A., Doi, M. & Shimazaki, K. 2008b. Leaf positioning of Arabidopsis in response to blue light. *Mol Plant,* **1,** 15-26.

Ishizaki, K., Chiyoda, S., Yamato, K.T. and Kohchi, T., 2008. Agrobacterium-mediated transformation of the haploid liverwort Marchantia polymorpha L., an emerging model for plant biology. *Plant and cell physiology,* **49,** 1084-1091.

Ito, S., Nakamichi, N., Nakamura, Y., Niwa, Y., Kato, T., Murakami, M., Kita, M., Mizoguchi, T., Niinuma, K., Yamashino, T. & Mizuno, T. 2007. Genetic linkages between circadian clock-associated components and phytochrome-dependent red light signal transduction in Arabidopsis thaliana. *Plant Cell Physiol,* **48,** 971-83.

Ito, S., Song, Y. H. & Imaizumi, T. 2012. LOV domain-containing F-box proteins: light-dependent protein degradation modules in Arabidopsis. *Mol Plant,* **5,** 573-82.

James, A. B., Monreal, J. A., Nimmo, G. A., Kelly, C. L., Herzyk, P., Jenkins, G. I. & Nimmo, H. G. 2008. The circadian clock in Arabidopsis roots is a simplified slave version of the clock in shoots. *Science,* **322,** 1832-5.

Jang, S., Marchal, V., Panigrahi, K.C., Wenkel, S., Soppe, W., Deng, X.W., Valverde, F. and Coupland, G., 2008. Arabidopsis COP1 shapes the temporal pattern of CO accumulation conferring a photoperiodic flowering response. *The EMBO journal,* **27,** 1277-1288.

Jarillo, J. A., Capel, J., Tang, R. H., Yang, H. Q., Alonso, J. M., Ecker, J. R. & Cashmore, A. R. 2001a. An Arabidopsis circadian clock component interacts with both CRY1 and phyB. *Nature,* **410,** 487-90.

Jarillo, J. A., Gabrys, H., Capel, J., Alonso, J. M., Ecker, J. R. & Cashmore, A. R. 2001b. Phototropin-related NPL1 controls chloroplast relocation induced by blue light. *Nature,* **410,** 952-4.

Jeong, S. Y., Peffer, N. & Meier, I. 2004. Phosphorylation by protein kinase CKII modulates the DNA-binding activity of a chloroplast nucleoid-associated protein. *Planta,* **219,** 298-302.

Jiao, Y., Lau, O. S. & Deng, X. W. 2007. Light-regulated transcriptional networks in higher plants. *Nat Rev Genet,* **8,** 217-30.

Johnson, E., Bradley, M., Harberd, N. P. & Whitelam, G. C. 1994. Photoresponses of Light-Grown phyA Mutants of Arabidopsis (Phytochrome A Is Required for the Perception of Daylength Extensions). *Plant Physiol,* **105,** 141-149.

Jones, M. A. 2009. Entrainment of the *Arabidopsis* circadian clock. *Journal of Plant Biology,* **52,** 202-209.

Jones, M. A. 2018. Interplay of Circadian Rhythms and Light in the Regulation of Photosynthesis-Derived Metabolism. *In:* CÁNOVAS, F. M., LÜTTGE, U. & MATYSSEK, R. (eds.) *Progress in Botany Vol. 79.* Cham: Springer International Publishing.

Jones, M. A. & Christie, J. M. 2008. Phototropin receptor kinase activation by blue light. *Plant Signal Behav,* **3,** 44-6.

Jones, M. A., Covington, M. F., Ditacchio, L., Vollmers, C., Panda, S. & Harmer, S. L. 2010. Jumonji domain protein JMJD5 functions in both the plant and human circadian systems. *Proc Natl Acad Sci U S A,* **107,** 21623-8.

Jones, M. A., Hu, W., Litthauer, S., Lagarias, J. C. & Harmer, S. L. 2015. A Constitutively Active Allele of Phytochrome B Maintains Circadian Robustness in the Absence of Light. *Plant Physiol,* **169,** 814-25.

Josse, E. M. & Halliday, K. J. 2008. Skotomorphogenesis: the dark side of light signalling. *Curr Biol,* **18,** R1144-6.

Junker, A. & Junker, B. H. 2012. Synthetic gene networks in plant systems. *Methods Mol Biol,* **813,** 343-58.

Kagawa, T., Sakai, T., Suetsugu, N., Oikawa, K., Ishiguro, S., Kato, T., Tabata, S., Okada, K. & Wada, M. 2001. Arabidopsis NPL1: a phototropin homolog controlling the chloroplast high-light avoidance response. *Science,* **291,** 2138-41.

Kagawa, T. & Wada, M. 2002. Blue light-induced chloroplast relocation. *Plant Cell Physiol,* **43,** 367-71.

Kaiserli, E., Sullivan, S., Jones, M. A., Feeney, K. A. & Christie, J. M. 2009. Domain swapping to assess the mechanistic basis of Arabidopsis phototropin 1 receptor kinase activation and endocytosis by blue light. *Plant Cell,* **21,** 3226-44.

Kami, C., Lorrain, S., Hornitschek, P. and Fankhauser, C., 2010. Light-regulated plant growth and development, *Current topics in developmental biology*, **91,** 29-66

Kang, C.Y., Lian, H.L., Wang, F.F., Huang, J.R. and Yang, H.Q., 2009. Cryptochromes, phytochromes, and COP1 regulate light-controlled stomatal development in Arabidopsis. *The Plant Cell,* **21,** 2624-2641.

Kasahara, M., Kagawa, T., Oikawa, K., Suetsugu, N., Miyao, M. & Wada, M. 2002. Chloroplast avoidance movement reduces photodamage in plants. *Nature,* **420,** 829-32.

Kehoe, D. M. 2010. Chromatic adaptation and the evolution of light color sensing in cyanobacteria. *Proc Natl Acad Sci U S A,* **107,** 9029-30.

Kiba, T., Henriques, R., Sakakibara, H. & Chua, N. H. 2007. Targeted degradation of PSEUDO-RESPONSE REGULATOR5 by an SCFZTL complex regulates clock function and photomorphogenesis in Arabidopsis thaliana. *Plant Cell,* **19,** 2516-30.

Kim, B. & Lin, M. Z. 2013. Optobiology: optical control of biological processes via protein engineering. *Biochem Soc Trans,* **41,** 1183-8.

Kim, J., Geng, R., Gallenstein, R. A. & Somers, D. E. 2013. The F-box protein ZEITLUPE controls stability and nucleocytoplasmic partitioning of GIGANTEA. *Development,* **140,** 4060-9.

Kim, W. Y., Fujiwara, S., Suh, S. S., Kim, J., Kim, Y., Han, L., David, K., Putterill, J., Nam, H. G. & Somers, D. E. 2007. ZEITLUPE is a circadian photoreceptor stabilized by GIGANTEA in blue light. *Nature,* **449,** 356-60.

Kim, Y. I., Vinyard, D. J., Ananyev, G. M., Dismukes, G. C. & Golden, S. S. 2012. Oxidized quinones signal onset of darkness directly to the cyanobacterial circadian oscillator. *Proc Natl Acad Sci U S A,* **109,** 17765-9.

Kinoshita, T., Doi, M., Suetsugu, N., Kagawa, T., Wada, M. & Shimazaki, K. 2001. Phot1 and phot2 mediate blue light regulation of stomatal opening. *Nature,* **414,** 656-60.

Klar, T., Pokorny, R., Moldt, J., Batschauer, A. & Essen, L. O. 2007. Cryptochrome 3 from Arabidopsis thaliana: structural and functional analysis of its complex with a folate light antenna. *J Mol Biol,* **366,** 954-64.

Kleine, T., Lockhart, P. & Batschauer, A. 2003. An Arabidopsis protein closely related to Synechocystis cryptochrome is targeted to organelles. *Plant J,* **35,** 93-103.**Klose, C., Viczián, A., Kircher, S., Schäfer, E. and Nagy, F.,** 2015. Molecular mechanisms for mediating light-dependent nucleo/cytoplasmic partitioning of phytochrome photoreceptors. *New Phytologist,* **206,** 965-971.

Kondo, K., Geng, X. X., Katayama, M. & Ikeuchi, M. 2005. Distinct roles of CpcG1 and CpcG2 in phycobilisome assembly in the cyanobacterium Synechocystis sp. PCC 6803. *Photosynth Res,* **84,** 269-73.

Kondo, K., Ochiai, Y., Katayama, M. & Ikeuchi, M. 2007. The membrane-associated CpcG2-phycobilisome in Synechocystis: a new photosystem I antenna. *Plant Physiol,* **144,** 1200-10.

Konermann, S., Brigham, M. D., Trevino, A., Hsu, P. D., Heidenreich, M., Cong, L., Platt, R. J., Scott, D. A., Church, G. M. & Zhang, F. 2013. Optical control of mammalian endogenous transcription and epigenetic states. *Nature,* **500,** 472-476.

Kong, S. G., Suetsugu, N., Kikuchi, S., Nakai, M., Nagatani, A. & Wada, M. 2013. Both phototropin 1 and 2 localize on the chloroplast outer membrane with distinct localization activity. *Plant Cell Physiol,* **54,** 80-92.

Koussevitzky, S., Nott, A., Mockler, T. C., Hong, F., Sachetto-Martins, G., Surpin, M., Lim, J., Mittler, R. & Chory, J. 2007. Signals from chloroplasts converge to regulate nuclear gene expression. *Science,* **316,** 715-9.

Kralj, J. M., Douglass, A. D., Hochbaum, D. R., Maclaurin, D. & Cohen, A. E. 2011. Optical recording of action potentials in mammalian neurons using a microbial rhodopsin. *Nat Methods,* **9,** 90-5.

Kreps, J. A. & Simon, A. E. 1997. Environmental and genetic effects on circadian clock-regulated gene expression in Arabidopsis. *Plant Cell,* **9,** 297-304.

Levskaya, A., Chevalier, A. A., Tabor, J. J., Simpson, Z. B., Lavery, L. A., Levy, M., Davidson, E. A., Scouras, A., Ellington, A. D., Marcotte, E. M. & Voigt, C. A. 2005. Synthetic biology: engineering Escherichia coli to see light. *Nature,* **438,** 441-2.

Li, J., Li, G., Wang, H. and Deng, X.W., 2011. Phytochrome signaling mechanisms. *The Arabidopsis book/American Society of Plant Biologists,* **9.**

Li, X., Wang, Q., Yu, X., Liu, H., Yang, H., Zhao, C., Liu, X., Tan, C., Klejnot, J., Zhong, D. and Lin, C., 2011. Arabidopsis cryptochrome 2 (CRY2) functions by the

photoactivation mechanism distinct from the tryptophan (trp) triad-dependent photoreduction. *Proceedings of the National Academy of Sciences,* **108,** 20844-49.

Lin, C., Ahmad, M., Gordon, D. & Cashmore, A. R. 1995b. Expression of an Arabidopsis cryptochrome gene in transgenic tobacco results in hypersensitivity to blue, UV-A, and green light. *Proc Natl Acad Sci U S A,* **92,** 8423-7.

Lin, C., Robertson, D.E., Ahmad, M., Raibekas, A.A., Jorns, M.S., Dutton, P.L. and Cashmore, A.R., 1995a. Association of flavin adenine dinucleotide with the Arabidopsis blue light receptor CRY1. *Science,* **269,** 968-70.**Lin, C., Yang, H., Guo, H., Mockler, T., Chen, J. & Cashmore, A. R.** 1998. Enhancement of blue-light sensitivity of Arabidopsis seedlings by a blue light receptor cryptochrome 2. *Proc Natl Acad Sci U S A,* **95,** 2686-90.

Liscum, E., Askinosie, S. K., Leuchtman, D. L., Morrow, J., Willenburg, K. T. & Coats, D. R. 2014. Phototropism: growing towards an understanding of plant movement. *Plant Cell,* **26,** 38-55.

Liscum, E. & Briggs, W. R. 1995. Mutations in the NPH1 locus of Arabidopsis disrupt the perception of phototropic stimuli. *Plant Cell,* **7,** 473-85.

Litthauer, S., Battle, M. W. & Jones, M. A. 2016. Phototropins do not alter accumulation of evening-phased circadian transcripts under blue light. *Plant Signal Behav,* **11,** e1126029.

Litthauer, S., Battle, M. W., Lawson, T. & Jones, M. A. 2015. Phototropins maintain robust circadian oscillation of PSII operating efficiency under blue light. *Plant J,* **83,** 1034-45.

Liu, B., Yang, Z., Gomez, A., Liu, B., Lin, C. & Oka, Y. 2016. Signaling mechanisms of plant cryptochromes in Arabidopsis thaliana. *J Plant Res,* **129,** 137-48.

Liu, H., Liu, B., Zhao, C., Pepper, M. & Lin, C. 2011. The action mechanisms of plant cryptochromes. *Trends Plant Sci,* **16,** 684-91.

Liu, H., Yu, X., Li, K., Klejnot, J., Yang, H., Lisiero, D. and Lin, C., 2008. Photoexcited CRY2 interacts with CIB1 to regulate transcription and floral initiation in Arabidopsis. *Science,* **322,** 1535-9.

Liu, L. J., Zhang, Y. C., Li, Q. H., Sang, Y., Mao, J., Lian, H. L., Wang, L. & Yang, H. Q. 2008. COP1-mediated ubiquitination of CONSTANS is implicated in cryptochrome regulation of flowering in Arabidopsis. *Plant Cell,* **20,** 292-306.

Liu, W. & Stewart, C. N., Jr. 2016. Plant synthetic promoters and transcription factors. *Curr Opin Biotechnol,* **37,** 36-44.

Liu, X. L., Covington, M. F., Fankhauser, C., Chory, J. & Wagner, D. R. 2001. ELF3 encodes a circadian clock-regulated nuclear protein that functions in an Arabidopsis PHYB signal transduction pathway. *Plant Cell,* **13,** 1293-304.

Lu, S. X., Knowles, S. M., Andronis, C., Ong, M. S. & Tobin, E. M. 2009a. CIRCADIAN CLOCK ASSOCIATED1 and LATE ELONGATED HYPOCOTYL function synergistically in the circadian clock of Arabidopsis. *Plant Physiol,* **150,** 834-43.

Lu, T. K., Khalil, A. S. & Collins, J. J. 2009b. Next-generation synthetic gene networks. *Nat Biotechnol,* **27,** 1139-50.

Lu, Y., Gehan, J. P. & Sharkey, T. D. 2005. Daylength and circadian effects on starch degradation and maltose metabolism. *Plant Physiol,* **138,** 2280-91.

Lu, Z., Liu, Y., Zhao, L., Jiang, X., Li, M., Wang, Y., Xu, Y., Gao, L. & Xia, T. 2014. Effect of low-intensity white light mediated de-etiolation on the biosynthesis of polyphenols in tea seedlings. *Plant Physiol Biochem,* **80,** 328-36.

Ma, L., Li, J., Qu, L., Hager, J., Chen, Z., Zhao, H. & Deng, X. W. 2001. Light control of Arabidopsis development entails coordinated regulation of genome expression and cellular pathways. *Plant Cell,* **13,** 2589-607.

Maloof, J. N., Borevitz, J. O., Dabi, T., Lutes, J., Nehring, R. B., Redfern, J. L., Trainer, G. T., Wilson, J. M., Asami, T., Berry, C. C., Weigel, D. & Chory, J. 2001. Natural variation in light sensitivity of Arabidopsis. *Nat Genet,* **29,** 441-6.

Malpas, K. R. & Jones, M. A. 2016. Natural variations of circadian rhythms in Kalanchoe species. *Haseltonia,* **22,** 35-42.

Martin-Tryon, E. L., Kreps, J. A. & Harmer, S. L. 2007. GIGANTEA acts in blue light signaling and has biochemically separable roles in circadian clock and flowering time regulation. *Plant Physiol,* **143,** 473-86.

Martin, W. & Herrmann, R. G. 1998. Gene transfer from organelles to the nucleus: how much, what happens, and Why? *Plant Physiol,* **118,** 9-17.

Martin, W., Rujan, T., Richly, E., Hansen, A., Cornelsen, S., Lins, T., Leister, D., Stoebe, B., Hasegawa, M. & Penny, D. 2002. Evolutionary analysis of Arabidopsis, cyanobacterial, and chloroplast genomes reveals plastid phylogeny and thousands of cyanobacterial genes in the nucleus. *Proc Natl Acad Sci U S A,* **99,** 12246-51.

Mas, P., Kim, W. Y., Somers, D. E. & Kay, S. A. 2003. Targeted degradation of TOC1 by ZTL modulates circadian function in Arabidopsis thaliana. *Nature,* **426,** 567-70.

Más, P., Alabadí, D., Yanovsky, M.J., Oyama, T. and Kay, S.A. 2003b. Dual role of TOC1 in the control of circadian and photomorphogenic responses in Arabidopsis. *The Plant Cell*, **15**, 223-236.

Mašek, T., Vopalenský, V. & Pospíšek, M. 2013. The Luc2 gene enhances reliability of bicistronic assays. *Open Life Sciences,* **8,** 423-431.

Massa, G.D., Kim, H.H., Wheeler, R.M. & Mitchell, C.A. 2008. Plant Productivity in Response to LED Lighting. *Hort Science*, **43,** 1951-1956

Matsuo, T., Onai, K., Okamoto, K., Minagawa, J. & Ishiura, M. 2006. Real-time monitoring of chloroplast gene expression by a luciferase reporter: evidence for nuclear regulation of chloroplast circadian period. *Mol Cell Biol,* **26,** 863-70.

Mayer, G. & Heckel, A. 2006. Biologically active molecules with a "light switch". *Angew Chem Int Ed Engl,* **45,** 4900-21.

Mcclung, C. R. 2006. Plant circadian rhythms. *Plant Cell,* **18,** 792-803.

Michael, T. P. & Mcclung, C. R. 2002. Phase-specific circadian clock regulatory elements in Arabidopsis. *Plant Physiol,* **130,** 627-38.

Milias-Argeitis, A., Summers, S., Stewart-Ornstein, J., Zuleta, I., Pincus, D., El-Samad, H., Khammash, M. & Lygeros, J. 2011. In silico feedback for in vivo regulation of a gene expression circuit. *Nat Biotechnol,* **29,** 1114-6.

Milias-Argeitis, A., Rullan, M., Aoki, S.K., Buchmann, P. and Khammash, M. 2016. Automated optogenetic feedback control for precise and robust regulation of gene expression and cell growth. *Nature communications*, **7**, 12546.

Millar, A., Brown, P. E. & Rand, D. A. 2010. BRASS version 3.

Millar, A. J. 2003. A suite of photoreceptors entrains the plant circadian clock. *J Biol Rhythms,* **18,** 217-26.

Millar, A. J. 2016. The Intracellular Dynamics of Circadian Clocks Reach for the Light of Ecology and Evolution. *Annu Rev Plant Biol,* **67,** 595-618.

Millar, A. J., Carre, I. A., Strayer, C. A., Chua, N. H. & Kay, S. A. 1995. Circadian clock mutants in Arabidopsis identified by luciferase imaging. *Science,* **267,** 1161-3.

Millar, A. J., Short, S. R., Chua, N. H. & Kay, S. A. 1992. A novel circadian phenotype based on firefly luciferase expression in transgenic plants. *Plant Cell,* **4,** 1075-87.

Missra, A., Ernest, B., Lohoff, T., Jia, Q., Satterlee, J., Ke, K. & Von Arnim, A. G. 2015. The Circadian Clock Modulates Global Daily Cycles of mRNA Ribosome Loading. *Plant Cell,* **27,** 2582-99.

Mittag, M., Kiaulehn, S. & Johnson, C. H. 2005. The circadian clock in Chlamydomonas reinhardtii. What is it for? What is it similar to? *Plant Physiol,* **137,** 399-409.

Mockler, T., Yang, H., Yu, X., Parikh, D., Cheng, Y. C., Dolan, S. & Lin, C. 2003. Regulation of photoperiodic flowering by Arabidopsis photoreceptors. *Proc Natl Acad Sci U S A,* **100,** 2140-5.

Mockler, T. C., Guo, H., Yang, H., Duong, H. & Lin, C. 1999. Antagonistic actions of Arabidopsis cryptochromes and phytochrome B in the regulation of floral induction. *Development,* **126,** 2073-82.

Moglich, A. & Moffat, K. 2007. Structural basis for light-dependent signaling in the dimeric LOV domain of the photosensor YtvA. *J Mol Biol,* **373,** 112-26.

Moni, A., Lee, A. Y., Briggs, W. R. & Han, I. S. 2015. The blue light receptor Phototropin 1 suppresses lateral root growth by controlling cell elongation. *Plant Biol (Stuttg),* **17,** 34-40.

Monte, E., Alonso, J. M., Ecker, J. R., Zhang, Y., Li, X., Young, J., Austin-Phillips, S. & Quail, P. H. 2003. Isolation and characterization of phyC mutants in Arabidopsis reveals complex crosstalk between phytochrome signaling pathways. *Plant Cell,* **15,** 1962-80.

Montgomery, B. L. 2007. Sensing the light: photoreceptive systems and signal transduction in cyanobacteria. *Mol Microbiol,* **64,** 16-27.

Mouradov, A., Cremer, F. & Coupland, G. 2002. Control of flowering time: interacting pathways as a basis for diversity. *Plant Cell,* **14 Suppl,** S111-30.

Muller, K., Siegel, D., Rodriguez Jahnke, F., Gerrer, K., Wend, S., Decker, E. L., Reski, R., Weber, W. & Zurbriggen, M. D. 2014. A red light-controlled synthetic gene expression switch for plant systems. *Mol Biosyst,* **10,** 1679-88.

Muller, K. & Weber, W. 2013. Optogenetic tools for mammalian systems. *Mol Biosyst,* **9,** 596-608.

Muller, N. A. & Jimenez-Gomez, J. M. 2016. Analysis of Circadian Leaf Movements. *Methods Mol Biol,* **1398,** 71-9.

Muller, P., Li, X. P. & Niyogi, K. K. 2001. Non-photochemical quenching. A response to excess light energy. *Plant Physiol,* **125,** 1558-66.

Mullineaux, P. & Karpinski, S. 2002. Signal transduction in response to excess light: getting out of the chloroplast. *Curr Opin Plant Biol,* **5,** 43-8.

Nagel, D. H. & Kay, S. A. 2012. Complexity in the wiring and regulation of plant circadian networks. *Curr Biol,* **22,** R648-57.

Nakamichi, N., Kiba, T., Kamioka, M., Suzuki, T., Yamashino, T., Higashiyama, T., Sakakibara, H. and Mizuno, T., 2012. Transcriptional repressor PRR5 directly regulates clock-output pathways. *Proceedings of the National Academy of Sciences,* **109,** 17123-8.

Narikawa, R., Enomoto, G., Ni Ni, W., Fushimi, K. & Ikeuchi, M. 2014. A new type of dual-Cys cyanobacteriochrome GAF domain found in cyanobacterium Acaryochloris marina, which has an unusual red/blue reversible photoconversion cycle. *Biochemistry,* **53,** 5051-9.

Narikawa, R., Fukushima, Y., Ishizuka, T., Itoh, S. and Ikeuchi, M. 2008. A novel photoactive GAF domain of cyanobacteriochrome AnPixJ that shows reversible green/red photoconversion. *Journal of molecular biology*, **380**, 844-855.

Narikawa, R., Fushimi, K., Ni Ni, W. & Ikeuchi, M. 2015a. Red-shifted red/green-type cyanobacteriochrome AM1_1870g3 from the chlorophyll d-bearing cyanobacterium Acaryochloris marina. *Biochem Biophys Res Commun,* **461,** 390-5.

Narikawa, R., Nakajima, T., Aono, Y., Fushimi, K., Enomoto, G., Ni Ni, W., Itoh, S., Sato, M. & Ikeuchi, M. 2015b. A biliverdin-binding cyanobacteriochrome from the chlorophyll d-bearing cyanobacterium Acaryochloris marina. *Sci Rep,* **5,** 7950.

Narusaka, M., Shiraishi, T., Iwabuchi, M. & Narusaka, Y. 2010. The floral inoculating protocol: A simplified Arabidopsis thaliana transformation method modified from floral dipping. *Plant Biotechnol,* **27,** 349-351.

Ni, W., Xu, S.L., Tepperman, J.M., Stanley, D.J., Maltby, D.A., Gross, J.D., Burlingame, A.L., Wang, Z.Y. and Quail, P.H., 2014. A mutually assured destruction mechanism attenuates light signaling in Arabidopsis. *Science,* **344(6188),** 1160-1164.

Nishio, J. N. 2000. Why are higher plants green? Evolution of the higher plant photosynthetic pigment complement. *Plant, cell and Environment,* **23,** 539-548.

Niyogi, K. K., Grossman, A. R. & Bjorkman, O. 1998. Arabidopsis mutants define a central role for the xanthophyll cycle in the regulation of photosynthetic energy conversion. *Plant Cell,* **10,** 1121-34.

Noordally, Z. B., Ishii, K., Atkins, K. A., Wetherill, S. J., Kusakina, J., Walton, E. J., Kato, M., Azuma, M., Tanaka, K., Hanaoka, M. & Dodd, A. N. 2013. Circadian control of chloroplast transcription by a nuclear-encoded timing signal. *Science,* **339,** 1316-9.

Nozue, K., Covington, M.F., Duek, P.D., Lorrain, S., Fankhauser, C., Harmer, S.L. and Maloof, J.N., 2007. Rhythmic growth explained by coincidence between internal and external cues. *Nature,* **448,** 358.

Nusinow, D. A., Helfer, A., Hamilton, E. E., King, J. J., Imaizumi, T., Schultz, T. F., Farre, E. M. & Kay, S. A. 2011. The ELF4-ELF3-LUX complex links the circadian clock to diurnal control of hypocotyl growth. *Nature,* **475,** 398-402.

O'neill, J. S., Van Ooijen, G., Dixon, L. E., Troein, C., Corellou, F., Bouget, F. Y., Reddy, A. B. & Millar, A. J. 2011. Circadian rhythms persist without transcription in a eukaryote. *Nature,* **469,** 554-8.

Oakenfull, R.J. and Davis, S.J., 2017. Shining a light on the Arabidopsis circadian clock. *Plant, cell & environment,* **40,** 2571-2585.

Ochoa-Fernandez, R., Samodelov, S.L., Brandl, S.M., Wehinger, E., Müller, K., Weber, W. and Zurbriggen, M.D., 2016. Optogenetics in plants: red/far-red light control of gene expression. *Optogenetics* (125-139). Humana Press, New York, NY.

Ogrzewalla, K., Piotrowski, M., Reinbothe, S. & Link, G. 2002. The plastid transcription kinase from mustard (Sinapis alba L.). A nuclear-encoded CK2-type chloroplast enzyme with redox-sensitive function. *Eur J Biochem,* **269,** 3329-37.

Ohgishi, M., Saji, K., Okada, K. & Sakai, T. 2004. Functional analysis of each blue light receptor, cry1, cry2, phot1, and phot2, by using combinatorial multiple mutants in Arabidopsis. *Proc Natl Acad Sci U S A,* **101,** 2223-8.

Padidam, M. 2003. Chemically regulated gene expression in plants. *Curr Opin Plant Biol,* **6,** 169-77.

Pal, S. K., Liput, M., Piques, M., Ishihara, H., Obata, T., Martins, M. C., Sulpice, R., Van Dongen, J. T., Fernie, A. R., Yadav, U. P., Lunn, J. E., Usadel, B. & Stitt, M. 2013. Diurnal changes of polysome loading track sucrose content in the rosette of wild-type arabidopsis and the starchless pgm mutant. *Plant Physiol,* **162,** 1246-65.

Parks, B. M., Quail, P. H. & Hangarter, R. P. 1996. Phytochrome A regulates red-light induction of phototropic enhancement in Arabidopsis. *Plant Physiol,* **110,** 155-62.

Patron, N. J., Orzaez, D., Marillonnet, S., Warzecha, H., Matthewman, C., Youles, M., Raitskin, O., Leveau, A., Farre, G., Rogers, C., Smith, A., Hibberd, J., Webb, A. A., Locke, J., Schornack, S., Ajioka, J., Baulcombe, D. C., Zipfel, C., Kamoun, S., Jones, J. D., Kuhn, H., Robatzek, S., Van Esse, H. P., Sanders, D., Oldroyd, G., Martin, C., Field, R., O'connor, S., Fox, S., Wulff, B., Miller, B., Breakspear, A., Radhakrishnan, G., Delaux, P. M., Loque, D., Granell, A., Tissier, A., Shih, P., Brutnell, T. P., Quick, W. P., Rischer, H., Fraser, P. D., Aharoni, A., Raines, C., South, P. F., Ane, J. M., Hamberger, B. R., Langdale, J., Stougaard, J., Bouwmeester, H., Udvardi, M., Murray, J. A., Ntoukakis, V., Schafer, P., Denby, K., Edwards, K. J., Osbourn, A. & Haseloff, J. 2015. Standards for plant synthetic biology: a common syntax for exchange of DNA parts. *New Phytol,* **208,** 13-9.

Pedmale, U.V., Huang, S.S.C., Zander, M., Cole, B.J., Hetzel, J., Ljung, K., Reis, P.A., Sridevi, P., Nito, K., Nery, J.R. and Ecker, J.R., 2016. Cryptochromes interact directly with PIFs to control plant growth in limiting blue light. *Cell,* **164**, 233-245.

Peschke, F. & Kretsch, T. 2011. Genome-wide analysis of light-dependent transcript accumulation patterns during early stages of Arabidopsis seedling deetiolation. *Plant Physiol,* **155,** 1353-66.

Phee, B.K., Shin, D.H., Cho, J.H., Kim, S.H., Kim, J.I., Lee, Y.H., Jeon, J.S., Bhoo, S.H. and Hahn, T.R., 2006. Identification of phytochrome-interacting protein candidates in Arabidopsis thaliana by co-immunoprecipitation coupled with MALDI-TOF MS. *Proteomics*, **6,** 3671-3680.

Piques, M., Schulze, W. X., Hohne, M., Usadel, B., Gibon, Y., Rohwer, J. & Stitt, M. 2009. Ribosome and transcript copy numbers, polysome occupancy and enzyme dynamics in Arabidopsis. *Mol Syst Biol,* **5,** 314.

Plautz, J. D., Straume, M., Stanewsky, R., Jamison, C. F., Brandes, C., Dowse, H. B., Hall, J. C. & Kay, S. A. 1997. Quantitative analysis of Drosophila period gene transcription in living animals. *J Biol Rhythms,* **12,** 204-17.

Pluthero, F. G. 1993. Rapid purification of high-activity Taq DNA polymerase. *Nucleic Acids Res,* **21,** 4850-1.

Preuten, T., Blackwood, L., Christie, J. M. & Fankhauser, C. 2015. Lipid anchoring of Arabidopsis phototropin 1 to assess the functional significance of receptor internalization: should I stay or should I go? *New Phytol,* **206,** 1038-50.

Puerto-Galan, L., Perez-Ruiz, J. M., Guinea, M. & Cejudo, F. J. 2015. The contribution of NADPH thioredoxin reductase C (NTRC) and sulfiredoxin to 2-Cys peroxiredoxin overoxidation in Arabidopsis thaliana chloroplasts. *J Exp Bot,* **66,** 2957-66.

Purnick, P. E. & Weiss, R. 2009. The second wave of synthetic biology: from modules to systems. *Nat Rev Mol Cell Biol,* **10,** 410-22.

Puthiyaveetil, S., Ibrahim, I. M. & Allen, J. F. 2013. Evolutionary rewiring: a modified prokaryotic gene-regulatory pathway in chloroplasts. *Philos Trans R Soc Lond B Biol Sci,* **368,** 20120260.

Puthiyaveetil, S., Kavanagh, T. A., Cain, P., Sullivan, J. A., Newell, C. A., Gray, J. C., Robinson, C., Van Der Giezen, M., Rogers, M. B. & Allen, J. F. 2008. The ancestral symbiont sensor kinase CSK links photosynthesis with gene expression in chloroplasts. *Proc Natl Acad Sci U S A,* **105,** 10061-6.

Quail, P. H. 2002. Phytochrome photosensory signalling networks. *Nat Rev Mol Cell Biol,* **3,** 85-93.

Rao, C. V. 2012. Expanding the synthetic biology toolbox: engineering orthogonal regulators of gene expression. *Curr Opin Biotechnol,* **23,** 689-94.

Rascher, U., Hutt, M. T., Siebke, K., Osmond, B., Beck, F. & Luttge, U. 2001. Spatiotemporal variation of metabolism in a plant circadian rhythm: the biological clock as an assembly of coupled individual oscillators. *Proc Natl Acad Sci U S A,* **98,** 11801-5.

Raven, J. A. & Allen, J. F. 2003. Genomics and chloroplast evolution: what did cyanobacteria do for plants? *Genome Biol,* **4,** 209.

Robson, P., Whitelam, G. C. & Smith, H. 1993. Selected Components of the Shade-Avoidance Syndrome Are Displayed in a Normal Manner in Mutants of Arabidopsis thaliana and Brassica rapa Deficient in Phytochrome B. *Plant Physiol,* **102,** 1179-1184.

Robson, P. R. & Smith, H. 1996. Genetic and transgenic evidence that phytochromes A and B act to modulate the gravitropic orientation of Arabidopsis thaliana hypocotyls. *Plant Physiol,* **110,** 211-6.

Rockwell, N. C., Martin, S. S. & Lagarias, J. C. 2012. Red/green cyanobacteriochromes: sensors of color and power. *Biochemistry,* **51,** 9667-77.

Rockwell, N.C., Su, Y.S. and Lagarias, J.C., 2006. Phytochrome structure and signaling mechanisms. *Annu. Rev. Plant Biol.,* **57**, 837-858.

Rugnone, M. L., Faigon Soverna, A., Sanchez, S. E., Schlaen, R. G., Hernando, C. E., Seymour, D. K., Mancini, E., Chernomoretz, A., Weigel, D., Mas, P. & Yanovsky, M. J. 2013. LNK genes integrate light and clock signaling networks at the core of the Arabidopsis oscillator. *Proc Natl Acad Sci U S A,* **110,** 12120-5.

Ryu, M. H. & Gomelsky, M. 2014. Near-infrared light responsive synthetic c-di-GMP module for optogenetic applications. *ACS Synth Biol,* **3,** 802-10.

Sakai, T., Kagawa, T., Kasahara, M., Swartz, T. E., Christie, J. M., Briggs, W. R., Wada, M. & Okada, K. 2001. Arabidopsis nph1 and npl1: blue light receptors that mediate both phototropism and chloroplast relocation. *Proc Natl Acad Sci U S A,* **98,** 6969-74.

Sakamoto, K. & Briggs, W. R. 2002. Cellular and subcellular localization of phototropin 1. *Plant Cell,* **14,** 1723-35.

Samol, I., Shapiguzov, A., Ingelsson, B., Fucile, G., Crevecoeur, M., Vener, A. V., Rochaix, J. D. & Goldschmidt-Clermont, M. 2012. Identification of a photosystem II phosphatase involved in light acclimation in Arabidopsis. *Plant Cell,* **24,** 2596-609.

Sawa, M., Nusinow, D. A., Kay, S. A. & Imaizumi, T. 2007. FKF1 and GIGANTEA complex formation is required for day-length measurement in Arabidopsis. *Science,* **318,** 261-5.

Schaffer, R., Landgraf, J., Accerbi, M., Simon, V., Larson, M. & Wisman, E. 2001. Microarray analysis of diurnal and circadian-regulated genes in Arabidopsis. *Plant Cell,* **13,** 113-23.

Schmidl, S. R., Sheth, R. U., Wu, A. & Tabor, J. J. 2014. Refactoring and optimization of light-switchable Escherichia coli two-component systems. *ACS Synth Biol,* **3,** 820-31.

Schmidt, D. & Cho, Y. K. 2015. Natural photoreceptors and their application to synthetic biology. *Trends Biotechnol,* **33,** 80-91.

Schneider, C. A., Rasband, W. S. & Eliceiri, K. W. 2012. NIH Image to ImageJ: 25 years of image analysis. *Nat Methods,* **9,** 671-5.

Scholl, R. L., May, S. T. & Ware, D. H. 2000. Seed and molecular resources for Arabidopsis. *Plant Physiol,* **124,** 1477-80.

Schultz, T. F., Kiyosue, T., Yanovsky, M., Wada, M. & Kay, S. A. 2001. A role for LKP2 in the circadian clock of Arabidopsis. *Plant Cell,* **13,** 2659-70.

Selby, C. P. & Sancar, A. 2006. A cryptochrome/photolyase class of enzymes with single-stranded DNA-specific photolyase activity. *Proc Natl Acad Sci U S A,* **103,** 17696-700.

Sellaro, R., Crepy, M., Trupkin, S. A., Karayekov, E., Buchovsky, A. S., Rossi, C. & Casal, J. J. 2010. Cryptochrome as a sensor of the blue/green ratio of natural radiation in Arabidopsis. *Plant Physiol,* **154,** 401-9.

Sharrock, R.A. and Clack, T., 2002. Patterns of expression and normalized levels of the five Arabidopsis phytochromes. *Plant Physiology*, **130**, 442-456.

Smith, A. M. & Stitt, M. 2007. Coordination of carbon supply and plant growth. *Plant Cell Environ,* **30,** 1126-49.

Smith, H. L., Mcausland, L. & Murchie, E. H. 2017. Don't ignore the green light: exploring diverse roles in plant processes. *J Exp Bot,* **68,** 2099-2110.

Somers, D. E., Devlin, P. F. & Kay, S. A. 1998a. Phytochromes and cryptochromes in the entrainment of the Arabidopsis circadian clock. *Science,* **282,** 1488-90.

Somers, D. E., Kim, W. Y. & Geng, R. 2004. The F-box protein ZEITLUPE confers dosage-dependent control on the circadian clock, photomorphogenesis, and flowering time. *Plant Cell,* **16,** 769-82.

Somers, D. E., Schultz, T. F., Milnamow, M. & Kay, S. A. 2000. ZEITLUPE encodes a novel clock-associated PAS protein from Arabidopsis. *Cell,* **101,** 319-29.

Somers, D. E., Webb, A. A., Pearson, M. & Kay, S. A. 1998b. The short-period mutant, toc1-1, alters circadian clock regulation of multiple outputs throughout development in Arabidopsis thaliana. *Development,* **125,** 485-94.

Song, C., Velazquez Escobar, F., Xu, X. L., Narikawa, R., Ikeuchi, M., Siebert, F., Gartner, W., Matysik, J. & Hildebrandt, P. 2015. A Red/Green Cyanobacteriochrome Sustains Its Color Despite a Change in the Bilin Chromophore's Protonation State. *Biochemistry,* **54,** 5839-48.

Song, J. Y., Cho, H. S., Cho, J. I., Jeon, J. S., Lagarias, J. C. & Park, Y. I. 2011. Near-UV cyanobacteriochrome signaling system elicits negative phototaxis in the cyanobacterium Synechocystis sp. PCC 6803. *Proc Natl Acad Sci U S A,* **108,** 10780-5.

Song, Y. H., Ito, S. & Imaizumi, T. 2013. Flowering time regulation: photoperiod- and temperature-sensing in leaves. *Trends Plant Sci,* **18,** 575-83.

Stein, V. & Alexandrov, K. 2014. Protease-based synthetic sensing and signal amplification. *Proc Natl Acad Sci U S A,* **111,** 15934-9.

Steinitz, B., Ren, Z. & Poff, K.L. 1985. Blue and green light-induced phototropism in *Arabidopsis thaliana* and *Lactuca sativa* L. seedlings. *Plant Physiol*, **77**, 248-251

Stewart, J.L., Maloof, J.N. & Nemhauser, J.L. 2011. *PIF* genes mediate the effect of sucrose on seedling growth dynamics. *PLoS ONE*, **6**, p.e19894

Stock, A. M., Robinson, V. L. & Goudreau, P. N. 2000. Two-component signal transduction. *Annu Rev Biochem,* **69,** 183-215.

Strasser, B., Sanchez-Lamas, M., Yanovsky, M. J., Casal, J. J. & Cerdan, P. D. 2010. Arabidopsis thaliana life without phytochromes. *Proc Natl Acad Sci U S A,* **107,** 4776-81.

Su, L., Hou, P., Song, M., Zheng, X., Guo, L., Xiao, Y., Yan, L., Li, W. & Yang, J. 2015. Synergistic and Antagonistic Action of Phytochrome (Phy) A and PhyB during Seedling De-Etiolation in Arabidopsis thaliana. *Int J Mol Sci,* **16,** 12199-212.

Suetsugu, N. & Wada, M. 2013. Evolution of three LOV blue light receptor families in green plants and photosynthetic stramenopiles: phototropin, ZTL/FKF1/LKP2 and aureochrome. *Plant Cell Physiol,* **54,** 8-23.

Sullivan, J. A. & Deng, X. W. 2003. From seed to seed: the role of photoreceptors in Arabidopsis development. *Dev Biol,* **260,** 289-97.

Sullivan, S., Hart, J. E., Rasch, P., Walker, C. H. & Christie, J. M. 2016. Phytochrome A Mediates Blue-Light Enhancement of Second-Positive Phototropism in Arabidopsis. *Front Plant Sci,* **7,** 290.

Sun, J. N., J.N.; Vogelmann, T.C. 1998. Green light drives CO_2 fixation deep within leaves. *Plant and cell physiology,* **39,** 1020-1026.

Tabor, J. J., Levskaya, A. & Voigt, C. A. 2011. Multichromatic control of gene expression in Escherichia coli. *J Mol Biol,* **405,** 315-24.

Takahashi, N., Hirata, Y., Aihara, K. & Mas, P. 2015. A hierarchical multi-oscillator network orchestrates the Arabidopsis circadian system. *Cell,* **163,** 148-59.

Takemiya, A., Inoue, S., Doi, M., Kinoshita, T. & Shimazaki, K. 2005. Phototropins promote plant growth in response to blue light in low light environments. *Plant Cell,* **17,** 1120-7.

Tepperman, J. M., Hwang, Y. S. & Quail, P. H. 2006. phyA dominates in transduction of red-light signals to rapidly responding genes at the initiation of Arabidopsis seedling de-etiolation. *Plant J,* **48,** 728-42.

Terashima, I., Fujita, T., Inoue, T., Chow, W. S. & Oguchi, R. 2009. Green light drives leaf photosynthesis more efficiently than red light in strong white light: revisiting the enigmatic question of why leaves are green. *Plant Cell Physiol,* **50,** 684-97.

Thain, S. C., Murtas, G., Lynn, J. R., Mcgrath, R. B. & Millar, A. J. 2002. The circadian clock that controls gene expression in Arabidopsis is tissue specific. *Plant Physiol,* **130,** 102-10.

Tilbrook, K., Arongaus, A. B., Binkert, M., Heijde, M., Yin, R. & Ulm, R. 2013. The UVR8 UV-B Photoreceptor: Perception, Signaling and Response. *Arabidopsis Book,* **11,** e0164.

Timmis, J. N., Ayliffe, M. A., Huang, C. Y. & Martin, W. 2004. Endosymbiotic gene transfer: organelle genomes forge eukaryotic chromosomes. *Nat Rev Genet,* **5,** 123-35.

Tindall, A. J., Waller, J., Greenwood, M., Gould, P. D., Hartwell, J. & Hall, A. 2015. A comparison of high-throughput techniques for assaying circadian rhythms in plants. *Plant Methods,* **11,** 32.

Tischer, D. & Weiner, O. D. 2014. Illuminating cell signalling with optogenetic tools. *Nat Rev Mol Cell Biol,* **15,** 551-8.

Toth, R., Kevei, E., Hall, A., Millar, A. J., Nagy, F. & Kozma-Bognar, L. 2001. Circadian clock-regulated expression of phytochrome and cryptochrome genes in Arabidopsis. *Plant Physiol,* **127,** 1607-16.

Untergasser, A., Nijveen, H., Rao, X., Bisseling, T., Geurts, R. & Leunissen, J. A. 2007. Primer3Plus, an enhanced web interface to Primer3. *Nucleic Acids Res,* **35,** W71-4.

Usami, T., Mochizuki, N., Kondo, M., Nishimura, M. and Nagatani, A., 2004. Cryptochromes and phytochromes synergistically regulate Arabidopsis root greening under blue light. *Plant and Cell Physiology*, **45,** 1798-1808.

Van Ooijen, G. & Millar, A. J. 2012. Non-transcriptional oscillators in circadian timekeeping. *Trends Biochem Sci,* **37,** 484-92.

Voinnet, O. 2001. RNA silencing as a plant immune system against viruses. *Trends in Genetics*, **17**, 449-459.

Walter, A., Silk, W. K. & Schurr, U. 2009. Environmental effects on spatial and temporal patterns of leaf and root growth. *Annu Rev Plant Biol,* **60,** 279-304.

Wang, L., Fujiwara, S. & Somers, D. E. 2010. PRR5 regulates phosphorylation, nuclear import and subnuclear localization of TOC1 in the Arabidopsis circadian clock. *EMBO J,* **29,** 1903-15.

Wang, Y. & Folta, K. M. 2013. Contributions of green light to plant growth and development. *Am J Bot,* **100,** 70-8.

Wang, Y. & Folta, K, M. 2014. Phototropin 1 and dim-blue light modulate the red light de-etiolation response. *Plant Signal Behav,* **9,** e976158.

Wang, Y., Maruhnich, S. A., Mageroy, M. H., Justice, J. R. & Folta, K. M. 2013. Phototropin 1 and cryptochrome action in response to green light in combination with other wavelengths. *Planta,* **237,** 225-37.

Wang, H. and Wang, H., 2015. Phytochrome signaling: time to tighten up the loose ends. *Molecular plant,* **8,** 540-551.

Webb, A. A. & Satake, A. 2015. Understanding circadian regulation of carbohydrate metabolism in Arabidopsis using mathematical models. *Plant Cell Physiol,* **56,** 586-93.

Weber, E., Gruetzner, R., Werner, S., Engler, C. and Marillonnet, S. 2011. Assembly of designer TAL effectors by Golden Gate cloning. *PloS one,* **6**, 19722.

Wenden, B., Kozma-Bognar, L., Edwards, K. D., Hall, A. J., Locke, J. C. & Millar, A. J. 2011. Light inputs shape the Arabidopsis circadian system. *Plant J,* **66,** 480-91.

Werner, S., Engler, C., Weber, E., Gruetzner, R. & Marillonnet, S. 2012. Fast track assembly of multigene constructs using Golden Gate cloning and the MoClo system. *Bioeng Bugs,* **3,** 38-43.

Whitelam, G. C., Johnson, E., Peng, J., Carol, P., Anderson, M. L., Cowl, J. S. & Harberd, N. P. 1993. Phytochrome A null mutants of Arabidopsis display a wild-type phenotype in white light. *Plant Cell,* **5,** 757-68.

Whitelam, G. C. D., P.F. 1997. Roles of different phytochromes in Arabidopsis photomorphogenesis. *Plant, cell and Environment,* **20,** 752-758.

Wood, N. T., Haley, A., Viry-Moussaid, M., Johnson, C. H., Van Der Luit, A. H. & Trewavas, A. J. 2001. The calcium rhythms of different cell types oscillate with different circadian phases. *Plant Physiol,* **125,** 787-96.

Wu, D., Hu, Q., Yan, Z., Chen, W., Yan, C., Huang, X., Zhang, J., Yang, P., Deng, H., Wang, J., Deng, X. & Shi, Y. 2012. Structural basis of ultraviolet-B perception by UVR8. *Nature,* **484,** 214-9.

Wu, G. & Spalding, E. P. 2007. Separate functions for nuclear and cytoplasmic cryptochrome 1 during photomorphogenesis of Arabidopsis seedlings. *Proc Natl Acad Sci U S A,* **104,** 18813-8.

Wyka, T. P., Duarte, H. M. & Luttge, U. E. 2005. Redundancy of stomatal control for the circadian photosynthetic rhythm in Kalanchoe daigremontiana Hamet et Perrier. *Plant Biol (Stuttg),* **7,** 176-81.

Xu, P.B., Lian, H.L., Wang, W.X., Xu, F. and Yang, H.Q., 2016. Pivotal roles of the phytochrome-interacting factors in cryptochrome signaling. *Molecular plant,* **9,** 496-497.

Xu, X., Paik, I., Zhu, L. and Huq, E., 2015. Illuminating progress in phytochrome-mediated light signaling pathways. *Trends in plant science,* **20(10),** 641-650.

Yakir, E., Hassidim, M., Melamed-Book, N., Hilman, D., Kron, I. & Green, R. M. 2011. Cell autonomous and cell-type specific circadian rhythms in Arabidopsis. *Plant J,* **68,** 520-31.

Yakir, E., Hilman, D., Kron, I., Hassidim, M., Melamed-Book, N. & Green, R. M. 2009. Posttranslational regulation of CIRCADIAN CLOCK ASSOCIATED1 in the circadian oscillator of Arabidopsis. *Plant Physiol,* **150,** 844-57.

Yang, X., Montano, S. and Ren, Z., 2015. How Does Photoreceptor UVR8 Perceive a UV-B Signal?. *Photochemistry and photobiology,* **91,** 993-1003.

Yang, X., Tang, J., Mustard, J. F., Lee, J. E., Rossini, M., Joiner, J., Munger, J. W., Kornfeld, A. & Richardson, A. D. 2015. Solar-induced chlorophyll fluorescence that correlates with canopy photosynthesis on diurnal and seasonal scales in a temperate deciduous forest. *Geophysical research letters,* **42,** 2977-2987.

Yanovsky, M. J. & Kay, S. A. 2001. Signaling networks in the plant circadian system. *Curr Opin Plant Biol,* **4,** 429-35.

Ye, J., Coulouris, G., Zaretskaya, I., Cutcutache, I., Rozen, S. & Madden, T. L. 2012. Primer-BLAST: a tool to design target-specific primers for polymerase chain reaction. *BMC Bioinformatics,* **13,** 134.

Yeom, M., Kim, H., Lim, J., Shin, A. Y., Hong, S., Kim, J. I. & Nam, H. G. 2014. How do phytochromes transmit the light quality information to the circadian clock in Arabidopsis? *Mol Plant,* **7,** 1701-1704.

Yoshihara, S., Katayama, M., Geng, X. and Ikeuchi, M., 2004. Cyanobacterial phytochrome-like PixJ1 holoprotein shows novel reversible photoconversion between blue-and green-absorbing forms. *Plant and cell physiology*, **45,** 1729-1737.

Yu, X., Liu, H., Klejnot, J. & Lin, C. 2010. The Cryptochrome Blue Light Receptors. *Arabidopsis Book,* **8,** e0135.

Zeugner, A., Byrdin, M., Bouly, J.P., Bakrim, N., Giovani, B., Brettel, K. and Ahmad, M., 2005. Light-induced electron transfer in Arabidopsis cryptochrome-1 correlates with in vivo function. *Journal of Biological Chemistry,* **280,** 19437-40.

Zhang, T. & Folta, K. M. 2012. Green light signaling and adaptive response. *Plant Signal Behav,* **7,** 75-8.

Zhang, C., Mallery, E., Reagan, S., Boko, V.P., Kotchoni, S.O. and Szymanski, D.B., 2013. The endoplasmic reticulum is a reservoir for WAVE/SCAR regulatory complex signaling in the Arabidopsis leaf. *Plant physiology,* 113.

Zhang, T., Maruhnich, S. A. & Folta, K. M. 2011. Green light induces shade avoidance symptoms. *Plant Physiol,* **157,** 1528-36.

Zhu, J. Y., Oh, E., Wang, T. & Wang, Z. Y. 2016. TOC1-PIF4 interaction mediates the circadian gating of thermoresponsive growth in Arabidopsis. *Nat Commun,* **7,** 13692.

Zhu L, Xin R, Bu Q, Shen H, Dang J, Huq E. A, 2016. Negative Feedback Loop between PHYTOCHROME INTERACTING FACTORs and HECATE Proteins Fine-Tunes Photomorphogenesis in Arabidopsis. *The Plant Cell,* **28(4),** 855-874.

Appendix I

Primer Name	Primer Sequence
cpCK2-A LP	TGCCATTCACGTGGAATCAT
cpCK2-A RP	TCATTCCATTACAGCTTAAACCAAGTT
csk 074 rep F	TCCCTGCGGGTCTACG
csk074 rep R	CCAACAAAGACGGTCAAGC
phot2-101_F	GTTTCTGCAAGGGCCAGAC
phot2-101_R	GCCTCAATGCTTTATCATTTACC
scr_lectin_F	ACCTTGCTGGACGTGACCTTACTGAT
scr_lectin_R	GTTGTCTCGTGGATTCCAGCAGCTT
scr_NTRC_F	TGAGCAACACCAAGGGACA
scr_NTRC_R	GATGGGGACACGGAGGAT
scr_phot1-5_F	GAACGTATCGAGAAGAATTTCG
scr_phot1-5_R	GTTCACCACTTTCCAACACC
scr_phot2-1_F	CAAGGAAATTGTTGGAAGAAAC
scr_phot2-1_R	TTGCTAACTTCAACCTGCATC
scr_SRX_F	CAAATATACGAGTTCCCTTCGAGT
scr_SRX_R	CAGCTTCTTCATCCAACGGTAA

Table A1. Primers used for PCR reactions screening and genotyping *Arabidopsis* mutants. DNA oligonucleotides used to prime PCR and DNA sequencing reactions in this study are listed. All primer sequences are given in the 5'-3' orientation.

Appendix II

Primer Name	Primer Sequence
F_Dom_LUC_BpiI2	CTGAAGACCTCGGGCGCACCTCTTTC
F_Dom_LUC_BpiI3	CTGAAGACCTGATGAACACTTCTTCATAGTTGACC
F_UAP_LUC	CTGAAGACCTCTCAAATGGAGGACGCCAAAAACAT
FDom_ccaS_BpiI1	CTGAAGACCTCGTAGACGTATCGAAATTTCCA
FDom_ccaS_BpiI2	CTGAAGACCTAGGCGAACTGAGGAGGTGA
FDom_ccaS_BpiI3	CTGAAGACCTCGAGGACGAACTGAGGAGGT
Fwd_UAP_ccaS/R	CTGAAGACCTCTAAATGTTACAACCAAAGAAGAAAAGGA
L0_gg_R	CACTTCGTGGTCTCAAAGCCTAA
pCCA1_gg_F	TAGAAGACATCTCAGGAGGTCTTCTACCCTTCATGCATGG
pCCA1_gg_R	TAGAAGACTACTCGGTAACACTAAGCTCCTCTACACAACTTCAG
R_Dom_LUC_BpiI2	CTGAAGACCTCCCGGAAGCAATTTCGTG
R_Dom_LUC_BpiI3	CTGAAGACCTCATCTTCGTCCCAGTAAGCTATGT
R_UAP_ccaS	CTGAAGACCTCTCGAAGCCTAAGCCCTTGGCAAGTGG
R_UAP_LUC	CTGAAGACCTCTCGAAGCTTACAATTTGGACTTTCCGCC
R_UAP_ccaR	CTGAAGACCTCTCGAAGCCTAATTTTTCCCCTGACAAAGAGA
RDom_ccaS_BpiI1	CTGAAGACCTTACGTTCCTGATTTTGTCGACC
RDom_ccaS_BpiI2	CTGAAGACCTGCCTTCGCTCGGTGACAT
RDom_ccaS_BpiI3	CTGAAGACCTCTCGCTCGGTGACATCTCTT

Table A2. Primers used for producing and screening Level 0 modules. DNA oligonucleotides used to prime PCR and DNA sequencing reactions in this study are listed. All primer sequences are given in the 5'-3' orientation.

Appendix III

Primer Name	Primer Sequence
scr_CCA1_L1check	ATGGAGGATGCAGCAGAGAG
scr_CcaS_L1check	GATTGTTGATCACGCACCA
scr_L1bb_F	AAACCTTTTCACGCCCTTTT
scr_L2_ccaR-BB3	AACGTGGAAAAGAGCTGTCC
scr_L2_F	GTCGCCTGAAGTTTTGACAG
scr_L2_Insert_Fwd	CAGCTTGGCATCAGACAAAC
scr_L2_Insert_Fwd	CAGCTTGGCATCAGACAAAC
scr_L2_R	CGAACGGATAAACCTTTTCAC

Table A3. Primers used for screening Level 1 cassettes and Level 2 constructs. DNA oligonucleotides used to prime PCR and DNA sequencing reactions in this study are listed. All primer sequences are given in the 5'-3' orientation.

Appendix IV

Primer Name	Primer Sequence
LUC_F_sc	CTGTGGTCTCAAATGGAAGACGCC
LUC_R_sc	TCGTGGTCTCAAAGCTTACAATTTGGACTTT
scr_ccaR_BpiI	AACGTGGAAAAGAGCTGTCC
scr_ccaR_F	TCCCGTCTCGAGTACGATCT
scr_ccaR_R	TCAAAGCCTAATTTTTCCCC
scr_ccaR_R2	GACTTCTCGGTGAGGTTTGC
scr_ccaS_F	ATATGGCAAGACGGAACAGG
scr_ccaS_R	TCAAAGCCTAAGCCCTTGG
scr_ccaS_R2	GAATTTGATCGGCGAGGTTA
scr_LUC_BpiI_1_R	GCCTTATGCAGTTGCTCTCC
scr_LUC_BpiI_2+3	TCCAGGGATACGACAAGGAT
scr_LUC_L1check	ATGGGAAGTCACGAAGGTGT
scr_NLS_F	ATGTTACAACCAAAGAAGAAAAGGA
seq_LUC_2	GGGCTGAATACAAATCACAGA
seq_LUC_3	CCTAAGGGTGTGGCCCTTC
seq_LUC_4	ACAAGGATATGGGCTCACTG

Table A4. Primers used for further screening and sequencing of GLASSys constructs. DNA oligonucleotides used to prime PCR and DNA sequencing reactions in this study are listed. All primer sequences are given in the 5'-3' orientation.

Appendix V

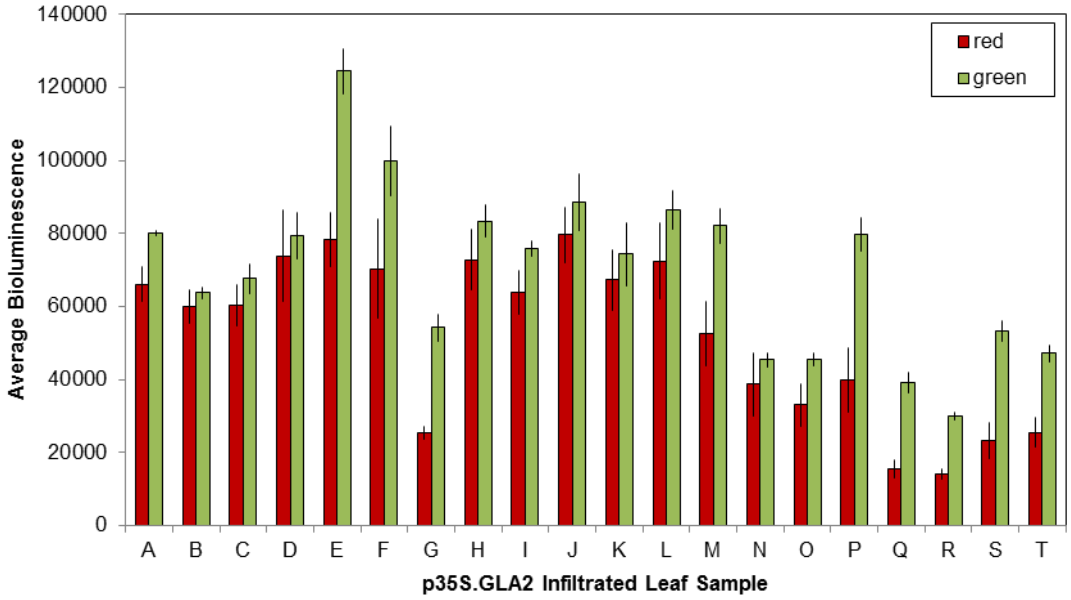

Figure A1. Variation of luciferase bioluminescence in transiently transformed *Nicotiana benthamiana* leaves. Average luciferase bioluminescence in leaf disks taken from 20 separately infiltrated *Nicotiana benthamiana* leaves transiently expressing p35S.GLA2. Bars indicate average luciferase bioluminescence from three images taken under 20 µmol m^{-2} s^{-1} of red light over 7.5 hours (red bars) followed by the average bioluminescence over the subsequent 7.5 hours under 20 µmol m^{-2} s^{-1} of green light (green bars). Error bars indicate standard error of the mean (n=3).